



ADULT DELTA SMELT ENTRAINMENT

Study 2 – Distribution Estimates for Hypothesized
Swimming Behaviors and Statistical Evaluation of
Particle-Tracking Models Predicting Proportional
Entrainment Loss

Prepared by:

Edward Gross
Benjamin Saenz
Richard Rachiele
Stacie Grinbergs
Lenny Grimaldo
Josh Korman
Pete Smith
Michael MacWilliams
Aaron Bever

With a summary prepared by Eva Bush from the Delta
Science Program

Prepared for:

The Collaborative Science and Adaptive Management Program's
Collaborative Adaptive Management Team

September 2020

Table of Contents

Preface	i
Executive Summary	ii
Policy Science Forum Summary	iii
Estimation of Adult Delta Smelt Distribution for Hypothesized Swimming Behaviors Using Hydrodynamic Suspended Sediment and Particle Tracking Models.....	1
Executive Summary.....	3
Introduction.....	5
Simulation Periods	6
Hydrodynamic and Turbidity Modeling.....	13
Particle Tracking Scenarios	14
Swimming Behavior Formulation	17
Evaluation of Predicted Distribution	20
Results	24
Behavior Ranking.....	40
Discussion	52
Conclusions.....	55
References	56
Statistical Examination of Particle-Tracking Models Predicting Proportional Entrainment Loss for Adult Delta Smelt in the Sacramento-San Joaquin Delta.....	1
Abstract.....	2
Introduction	5
Methods.....	9
Results and Discussion	21
Conclusions	30
Acknowledgments.....	38
References	39
Tables	44
Figures.....	62
Appendix A: Supplemental Tables	100

Preface for Entrainment Study 2

Prepared by CAMT Delta Smelt Scoping Team

This Preface was prepared by the CAMT Delta Smelt Scoping Team (DSST) to provide context for the study presented herein (Entrainment Study 2) which was commissioned by the Collaborative Science and Adaptive Management Program (CSAMP) and overseen by the Collaborative Adaptive Management Team (CAMT) and the CAMT DSST from June 2016 to May 2019. The scope of work for the study was developed in collaboration with the DSST and subjected to an independent peer review organized by the Delta Science Program in 2014. The DSST was provided regular updates during the conduct of Study 2 over a 3-year period and provided feedback on modeling inputs and initial results. The DSST also provided written comments on draft versions of various study deliverables produced which the investigators responded to in writing.

This study is one of a series of four separate but related investigations intended to examine factors affecting the entrainment of adult Delta Smelt at the Central Valley Project (CVP) and State Water Project (SWP) pumping facilities in the south Delta, and the consequences of that entrainment on the Delta Smelt population. The studies' respective subjects are as follows:

- Study 1 – determined factors predicting salvage;
- Study 2 – developed a behavior model that best explains Delta Smelt movements and entrainment into the interior Delta and SWP and CVP facilities; determined behavior-based proportional entrainment losses;
- Study 3 - estimated historical (1981-2016) adult Delta Smelt proportional entrainment loss; and
- Study 4 - intended to assess the population effects of various levels of adult Delta Smelt proportional entrainment loss.

The study yielded two separate reports, one on behavioral modeling and one on statistical fitting. The study also resulted in two manuscripts that will ultimately be submitted for publication.

Results from Study 2 were presented to CAMT and the CSAMP Policy Group in October 2019. The information presented herein represents the work of the independent investigators and does not necessarily reflect the positions of CSAMP member entities.

Executive Summary

CAMT Entrainment Study 2

Prepared by Lenny Grimaldo – Principal Investigator

In response to federal litigation from the 2008 USFWS Delta Smelt Biological Opinion on SWP and CVP operations, the Collaborative Adaptive Management Team (CAMT) solicited proposals from our investigator team to address two key uncertainties (See CAMT Progress Report and Entrainment Workplan) underlying salvage and entrainment: 1) Factors affecting salvage and entrainment; and 2) Population consequences of entrainment. In collaboration with the Delta Smelt Scoping Team (DSST), we reviewed conceptual models and hypotheses underlying these uncertainties and held several discussions to recommend priorities to most effectively meet management objectives. The ultimate goal of these recommendations is to support a more confident assessment of Delta Smelt entrainment in order to better evaluate the efficacy of management actions used to operate the water projects in a manner that is consistent with the Endangered Species Act (ESA).

Our investigator team developed the following studies: 1) An examination of factors affecting salvage at the SWP and CVP; 2) An individual-based modeling (IBM) study examining behavior and movement of adult Delta Smelt in the south Delta to better understand entrainment timing and population losses; 3) A re-examination of the historical time series of annual proportional loss estimates; and 4) A re-examination of factors affecting population growth rate using updated environmental covariates and proportional loss estimates in a published Delta Smelt life cycle model. The last study was not completed by the investigator team due to competing professional commitments of key investigators.

For Study 2, the investigator team developed an adult Delta Smelt behavior model to investigate potential water quality and hydrodynamic cues that best explained timing and magnitude of landward Delta Smelt movements during first flush events. Through an application of a particle tracking model (PTM), candidate adult Delta Smelt behaviors were examined through statistical fitting of California Department of Fish and Wildlife Spring Kodiak Trawl (CDFW SKT) and SWP/CVP salvage data over consecutive survey increments. Turbidity values, used as input to the PTM, were estimated through a separate 3d UNTRIM modeling effort using empirical observations for calibration. Four historical water years were selected for a depth-averaged modeling analysis (2002, 2004, 2005, 2010) to evaluate predictions and fit over a range of inflow and pumping conditions and 2002 was used for a three-dimensional modeling analysis. Due to limitations in the data, the modeling approach did not resolve a single behavior that best explained Delta Smelt movement during first flush. However, the modeling demonstrated that Delta Smelt behavior is more complex than previously thought as simple behaviors that relied on single covariates like salinity or turbidity provided poor fits to the data. The statistical fitting model predicted that proportional entrainment losses (PEL) were approximately two-fold higher than previously reported estimates for the POD period. This occurred because the model estimated that pre-screen loss was higher than previous estimates. Additional field-based estimates of pre-screen loss would be very helpful to determine if model-based estimates of salvage expansion factors and PEL are more accurate than past estimates or are an artefact driven by error in movement predicted by the PTM. Evaluation of alternate behavior models and resulting PEL predictions will be limited by an absence of direct information on trawl catch efficiencies and very low abundance of Delta Smelt leading to very low catch and high sampling error. Of the PEL estimates completed to date, all were highly correlated with past estimates, indicating that population losses were indeed higher during the POD years, but were reduced significantly by more restrictive pumping implemented after the 2008 Biological Opinion.

Policy Science Forum Summary
Behavioral and Statistical Models of Adult Delta Smelt Entrainment
Prepared by the Delta Science Program

Background: This memo is a summary of the results of Study 2 of 4 in the series “Investigations on Understanding Population Effects and Factors that Affect Entrainment of Delta Smelt at State Water Project (SWP) and Central Valley Project (CVP) Export Facilities” commissioned by CAMT. Study 2 was contracted to build upon the original salvage model used in the 2008 USFWS Biological Opinion, which a) did not include fine-scale variability, b) did not scale salvage to population size, and c) and considered flow at Old and Middle Rivers (OMR) as the only predictor variable. Study 1 in the series updated Delta Smelt salvage models by adding the most recent eight years of data (now spanning 1993-2016), tested alternative conceptual models and included a new type of analysis (Boosted Regression Tree) to assess the conditions associated with salvage of adult Delta Smelt. This second study resulted in two reports; a hydrodynamic and particle tracking study “Estimation of Adult Delta Smelt Distribution for Hypothesized Swimming Behaviors Using Hydrodynamic, Suspended Sediment and Particle Tracking Models” and a study using a particle tracking model in conjunction with a population dynamics model “Statistical Evaluation of Particle-Tracking Models Predicting Proportional Entrainment Loss for Adult Delta Smelt in the Sacramento-San Joaquin Delta”. This briefing summarizes report findings and subsequent related discussions by the Delta Smelt Scoping Team.

Model Insights

Behavioral Modeling has Improved our Understanding of Spawning Movements

The first part of Entrainment Study 2 is the first study of Delta Smelt to add behavior to a particle tracking model (PTM), which is a considerable methodological achievement. By adding behavior to the PTM, the investigators were able to contrast predicted distribution and entrainment resulting from different hypothesized behaviors. The study examined seven different behavior types (passive, turbidity seeking, freshwater seeking, horizontal tidal migration, vertical tidal migration, holding and random movements). For distribution and entrainment predictions, PTM runs which simulated complex fish movement behaviors that included lagged responses to multiple cues performed best. This confirmed that simple hypothesized adult Delta Smelt behaviors produced unrealistic projections of movement and distribution, validating that adult Delta Smelt do not behave like passive particles. The combination of factors giving the “best fit” to observed distribution varied from year to year. Movement triggers representing the surrounding conditions (e.g. salinity, turbidity and/or tide) explained the observed data the best. This confirms that Delta Smelt distribution and abundance depend on complex interactions of multiple factors. The modeling in this study has

increased our understanding of Delta Smelt movement and entrainment and what tools to use to improve our understanding further.

Calculating Proportional Entrainment is Challenging

Limitations of existing data make it challenging to examine the proportional entrainment loss (PEL) on the population with current analytical tools. The estimates of the Delta Smelt population abundance carry large scientific uncertainty as they are based on expanding catches from a very limited number of fish samples with low catch rates. Due to unavoidable assumptions made while calculating the expansion factors and proportional entrainment loss estimates currently available, they provide an uncertain baseline for comparison with the PTM population modeled expansion factor and proportional entrainment loss (PEL) estimates from this study. The authors of the study suggest field-based estimates of expansion factors avoid uncertain assumptions and would be beneficial upstream of both the CVP and the SWP, since entrainment varies by facility. Developing a model to reliably estimate proportional entrainment in all types of water years and thereby guide flow management decisions will require considerable effort of further refining current models. The uncertainties in all PEL estimates are driven by uncertainties in estimating both abundance and entrainment: the lack of data for SKT expansion factors used to translate catch to abundance and very limited data on expansion factors for translating salvage data to entrainment.

Further evaluation and discussion by DSST

Proportional Entrainment Varies

Proportional entrainment varies greatly from year to year based on the conditions in the upper estuary, including those affected by operations of the CVP and SWP. Due to the limitations of the existing data discussed above, the confidence is low in the absolute PEL values. However, values from analyses done using varying, but similar methods are highly correlated. This correlation suggests that the wide year-to-year variation in PEL is real. Hindcast PEL estimates for years pre 2002 from Entrainment Study 3 (*in prep.*) show similar large year-to-year variations. Additional mark-recapture experiments upstream of state and federal fish collection facilities to estimate salvage expansion factors and relationships with covariates are needed to resolve the uncertainties in the high estimated entrainment losses. Using the PTMs most consistent with the observed data, the estimated PEL of adult Delta Smelt was 35% for WY 2002, 50% for WY2004, 15% for WY 2005 and 3% for WY 2011, though values varied slightly across different population models. These values are higher than previous estimates (calculated for WY 2002, 2004 and 2005), in part due to this PTM incorporating movement predictions rather than assuming all fish are spatially evenly distributed in all habitats and using a volumetric population expansion. Additionally, they may be higher due to the model assumption that fish may be entrained from any location in their range. This may positively bias movement probability to the South Delta, resulting in positive bias in entrainment and PEL.

Even so, estimates are highly correlated with previous entrainment studies by Kimmerer (2008, 2011) and Miller (2011).

Entrainment has Declined

Using preliminary data from Entrainment Study 3 by Pete Smith et al. (*in prep.*) and salvage and survey data for Delta Smelt, the DSST discussed entrainment decline and possible reasons for the decline. The salvage and survey data were correlated to the data from Study 3, both showing a decline from 2006 on, and the DSST reached the consensus that entrainment has declined from 2006 to present. Reasons for the decline discussed include the declining population of Delta Smelt and a reduction in proportional entrainment due to a change in water operation management. The use of the salvage and survey data allows, in part, for the accounting of the population decline; the lower salvage in 2006 points to more positive flows at OMR due to its being a wet year. In 2007 a change in water operation management occurred, providing more positive flows at OMR. To what extent either of these are responsible for the decline in entrainment has not been fully established, but the relatively low entrainment in the high Delta Smelt abundance year of 2011 suggests that water operation management actions via the 2008 RPA reduced entrainment in a year where the population index suggested it should be higher.

How much progress was made on the 2013 questions raised in the study plan?

Below are the questions from the original proposal to CAMT and how much progress has been made answering them. In general, they were addressed to the extent the current data permit.

1. *What are the environmental conditions that “trigger” spawning migration of Delta Smelt?*

Note: Recognizing that the biological changes leading to spawning migrations are separate from environmental conditions, the “triggers” mentioned below are reflective of Delta Smelt response to environmental as opposed to biological changes. Study 2 describes factors that influence behavior during their spawning period, not biological triggers of spawning.

From study reports and DSST discussions: The study examined seven different behavior types (passive, turbidity seeking, freshwater seeking, horizontal tidal migration, vertical tidal migration, holding and random). No single factor used in the model explained behavior, but instead a combination of factors was a better fit for the observed data. Triggers representing the surrounding conditions such as salinity, turbidity and tide explained the observed data most accurately. Strongest triggers for initiation of movement were salinity and turbidity and strongest type of movement behaviors were tidal surfing and holding behavior. This confirms that Delta Smelt distribution is

influenced by behavior and abundance depends on complex interactions of multiple factors.

2. *How does the distribution of adult Delta Smelt vary at time scales not resolved by surveys? In particular how does the distribution evolve during the spawning migration?*

From principal investigators' presentations and DSST discussions: This question was not directly addressed by the study. Real time behavior happens at a much smaller time scale than was modeled here and the study provides a more granular look at movements on gross time scales. To answer the question in general terms, animations shown by the researchers gave the DSST a sense of the complexity of estimating Delta Smelt distribution. The particle tracking results does not provide a great depiction of distribution and more can be done to examine distributions based on available survey data.

3. *Which environmental conditions lead to adults entering the south Delta?*

Answers from the author final presentation: Net flow toward South Delta, landward movement due to increasing salinity in the western Delta, possible influence of substantial turbidity

From report and DSST discussions: The particle tracking models for 2002 and 2004 show a very strong statistical support for turbidity-based variation in salvage efficiency. In 2005 the best fitting model allowed for survival variability based on water temperature. Water year 2011 showed no turbidity or temperature connection, likely due to low Delta Smelt abundance and high flows.

4. *Which environmental conditions lead to adult Delta Smelt exiting the central and south Delta to regions with lower entrainment risk?*

From principal investigators' presentations and DSST discussions: Similar to question 2, this was addressed by viewing and discussing general modeling results, but not at the fine scale necessary to resolve the question in detail.

5. *To what degree has implementation of the RPA reduced adult Delta Smelt entrainment?*

Answers from the author final presentation: Substantial to large drops in entrainment. Using conditional tidal migration behavior in the PTM showed up to 60% decrease.

From report and DSST discussions: Using preliminary data from Study 3 by Pete Smith et al. (*in prep.*), salvage and survey data for Delta Smelt, as well as flow data from OMR, the DSST discussed entrainment decline and the possible reasons for the decline. The salvage and survey data were correlated to the data from Study 3, both showing a decline from 2006 on, and the DSST reached the consensus that entrainment has declined from 2006 to present. Reasons for the decline discussed include the declining

population of Delta Smelt and a reduction in proportional entrainment due to a change in water operation management actions via the 2008 RPA.

6. What are the salvage efficiencies of the major water export facilities?

Answers from the author final presentation: Salvage efficiencies are uncertain and possibly related to turbidity or other abiotic or biotic conditions.

From report and DSST discussions: PEL values are somewhat higher in this study than previous estimates as this particle tracking model incorporates movement predictions instead of assuming all fish are spatially evenly distributed with an equal possibility of entrainment. The results from this study shows the dynamics are similar to previous estimates by Kimmerer and Miller.

Author suggested future studies:

Additional mark-recapture experiments upstream of both state and federal fish collection facilities to estimate salvage expansions (and relationships with covariates) to resolve uncertainties about entrainment loss estimates.

Currently Planned Next Steps:

The third study in the series, "*Estimating Adult Delta Smelt Proportional Losses to State Water Project and Central Valley Project Entrainment*" is in draft report form and requires further analysis by the authors.

The fourth study, "*Determining Sensitivity of Delta Smelt Life Cycle Model Results to Revised Model Assumptions and Covariate Selection*" is pending completion of Study 3.

References:

- Kimmerer, W. J. 2008. Losses of Sacramento River Chinook Salmon and Delta Smelt to Entrainment in Water Diversions in the Sacramento-San Joaquin Delta. *San Francisco Estuary and Watershed Science* **6**.
- Kimmerer, W. J. 2011. Modeling Delta Smelt Losses at the South Delta Export Facilities. *San Francisco Estuary and Watershed Science* **9**.
- Miller, W. J. 2011. Revisiting Assumptions that Underlie Estimates of Proportional Entrainment of Delta Smelt by State and Federal Water Diversions from the Sacramento-San Joaquin Delta. *San Francisco Estuary and Watershed Science* **9**.

Estimation of Adult Delta Smelt Distribution for Hypothesized Swimming Behaviors Using Hydrodynamic, Suspended Sediment and Particle- Tracking Models

Prepared by:
Resource Management Associates
1840 San Miguel Dr., Suite 102
Walnut Creek, CA 94596
Contact: Edward Gross
925-300-3387



Prepared for

Collaborative Adaptive Management Team

US Fish and Wildlife Service

Investigators

Edward Gross (RMA)

Benjamin Saenz (RMA)

Richard Rachiele (RMA)

Stacie Grinbergs(RMA)

Lenny Grimaldo (ICF)

Josh Korman (Ecometric)

Pete Smith (USGS retired)

Michael MacWilliams (Anchor QEA)

Aaron Bever (Anchor QEA)

Executive Summary

This hydrodynamic and particle-tracking study was tasked by the Delta Smelt Scoping Team (DSST) of the Collaborative Adaptive Management Team (CAMT) as part of the Investigations on Understanding Population Effects and Factors that Affect Entrainment of Delta Smelt at State Water Project (SWP) and Central Valley Project (CVP) Export Facilities. Additional funding was provided by US Fish and Wildlife Service for preparation of this report which documents a portion of the CAMT study entitled Modeling Delta Smelt Movement into the South Delta: Linking Behavior, Habitat Suitability and Hydrodynamics to Better Understand Entrainment at the State Water Project and Central Valley Project. This report documents a subset of the CAMT work funded by USFWS, focusing on contrasting distribution resulting from hypothesized behaviors of adult delta smelt during their spawning migration.

This report documents particle-tracking model (PTM) results for different hypothesized swimming behavior rules. The hypothesized behaviors were developed after consultation with the Delta Smelt Scoping Team, the Independent Review Panel and other experts. This report is limited to simulations in which both the release time and release distribution of particles are specified a priori. In contrast, additional work documented in Korman et al. (2018) includes statistical fitting of initial distribution most consistent with observations including catch in Spring Kodiak Trawl. Because the PTM simulations for the next phase of work track particles released in 15 different regions through time they are computationally intensive relative to the simulations documented here which involve only a single release region, located on the lower Sacramento River.

Two periods were chosen for this evaluation of behavior rules. Water year 2002 was chosen as a year with a clear signal in salvage of delta smelt, and was simulated both with two-dimensional (2D) and three-dimensional (3D) modeling tools. Water year 2004 was chosen due to a double peak in observed salvage which is particularly challenging to reproduce with particle-tracking modeling. This report explores not only the relative performance of different behavior rules but also documents application of two independent sets of modeling tools, 2D and 3D, for 2002. The predicted distribution and entrainment during an additional water year (2004) is also estimated for each set of behavior rules using the 2D tools.

A set of 3D modeling tools have been applied in this study. The UnTRIM 3D hydrodynamic model (Casulli and Walters 2000) was applied with the SediMorph sediment transport model (BAW 2005) to predict water level, current speed, salinity, suspended sediment and turbidity in December 2010 and January 2011 and December 2001 through April 2002. The SWAN model (2009) was used to estimate wind wave period and height for use in bed shear stress estimates. The hydrodynamic calibration of this model is documented by MacWilliams et al (2015) and the sediment transport model is documented in Bever and MacWilliams (2013). The calibration for this project is documented in a CAMT report (Anchor QEA 2017). The hydrodynamic and turbidity predictions are used in a particle-tracking model (Ketefian et al. 2016) with an individual-based model of fish, involving swimming rules that describe delta smelt swimming responses to environmental stimuli. Broadly, the hypothesized swimming behavior rules represented possible delta smelt swimming responses to different environmental stimuli.

An independent set of 2D modeling tools were used to model depth-averaged hydrodynamics, salinity and suspended sediment, and particle tracking. Similar to a previous study concerning the spawning migration of Delta smelt (RMA 2009), the RMA2 finite element model (King, 1986) and associated tools simulated hydrodynamics and sediment transport and the RMA PTRK particle-tracking model was used

to represent delta smelt. The calibration of the hydrodynamic and sediment transport modeling tools is documented in a separate report to CAMT (RMA 2017).

For both the 3D and 2D particle-tracking models, a new swimming behavior module was developed as part of this project. The codes are distinct for each of the two particle tracking models, but they share a common input file and permit identical modeled swimming behavior in 2D and 3D. The sets of behavior rules that can be explored using these tools is described in detail.

The delta smelt distribution is predicted using different sets of behavior rules through each winter-spring simulation period, and evaluated using both qualitative and quantitative metrics. Qualitative metrics include retention in the Delta and quantitative metrics include consistency of the predicted delta smelt distribution with observed patterns of distribution in the Spring Kodiak Trawl data and the timing of salvage. In this report, we assume a fixed initial particle/fish distribution in order to better isolate differences between behaviors (all behaviors have the same initial distribution) and provide comparisons between observations and predicted distributions and entrainment.

Introduction

Delta smelt is an endangered fish species endemic to the upper San Francisco Estuary whose population has declined rapidly, particularly as part of the “pelagic organism decline” starting in the early 2000s (Thompson et al. 2010). Although several factors have been implicated in its decline, including a diminished food supply (Sommer et al. 2007), contaminants (Hammock et al. 2016) loss of habitat (Feyrer et al. 2007) and other changes to the environment (Moyle et al 2016), entrainment losses at the State Water Project (SWP) and Central Valley Project (CVP) garner significant attention because they are one factor that can be directly managed through water export reductions to minimize direct mortality to the Delta Smelt population. A greater understanding of factors that contribute to entrainment losses is desired to improve both management of the species and water export supplies (Brown et al. 2009).

One the greater sources of uncertainty in managing SWP and CVP exports to minimize entrainment impacts to delta smelt is understanding the mechanisms that attract them into the vicinity of the exports. From summer to fall, delta smelt are typically observed in turbid habitats in the low salinity zone (Feyrer et al. 2007) or in the northern freshwater region of the estuary (Cache Slough Complex; Sommer and Mejia 2013). Both these regions are situated outside substantial hydrodynamic influence of SWP and CVP exports and delta smelt are not salvaged at the SWP and CVP during these seasons. Prior to 1990, some delta smelt were found in the south Delta and were salvaged during summer and fall months. In recent decades, water clarity has substantially increased in the south Delta (Schoellhamer 2011), which may explain why delta smelt are no longer found in the south Delta from summer to fall. In contrast, during the winter, some proportion of the delta smelt population disperses into the vicinity of the SWP and CVP. These movements typically coincide with the onset of large precipitation events that transport suspended sediment (and associated turbidity) into the estuary (Grimaldo et al 2009). Also known as “first flush” periods, these events historically led to substantial salvage events within days of increased turbidity (Grimaldo et al. 2009). These salvage observations, along with targeted field studies of Delta Smelt during first flush periods (Bennett and Burau 2014), suggest that Delta Smelt behavior triggered by a change in available upstream habitat or their internal physiology (e.g., reproductive readiness) facilitates a rapid distribution shift to landward habitats not occupied during the summer and fall. Note, some delta smelt appear to remain in local tributaries and marsh habitats (Murphy and Hamilton 2013), and others appear to shift geographically seaward (i.e., to Napa River) depending on the amount of freshwater outflow.

The purpose of the study documented here and in Korman et al. (2018) is to evaluate hypothesized adult delta smelt swimming behaviors and understand how those behaviors, driven by the environmental conditions of turbidity, salinity, and Delta flows, may affect predicted adult delta smelt distribution and entrainment at the south Delta export facilities. We explore several types of behaviors guided by existing literature on delta smelt behavior, guidance from the Delta Smelt Scoping Team (DSST), and the Independent Review Panel (IRP) review of the CAMT proposal for delta smelt investigations. Our general conceptual model is that a landward migration of mature delta smelt in late fall or early winter is triggered by changes in turbidity distribution, or possibly salinity distribution. We hypothesize that delta smelt swimming may respond to the magnitude or spatial gradients of velocity, water depth, turbidity and salinity. While additional environmental cues, such as water temperature or food availability, may influence delta smelt movement, they are not explored in this work.

One hypothesized behavior is tidal migration (“tidal surfing”; Sommer et al. 2011). Bennett and Burau (2014) hypothesized a lateral tidal migration driven by tidally varying lateral turbidity gradients. In contrast, Rose et al. (2013) use salinity as the environmental cue guiding spawning migration. A previous modeling effort used a hybrid of salinity and turbidity cues to guide migration (RMA 2009). While several behaviors have been hypothesized and used in modeling studies, none of these studies contrast predicted distributions and entrainment resulting from different hypothesized behaviors. This comparison is the focus of this task of the CAMT delta smelt studies.

In this phase of modeling we aim to reproduce some general features of delta smelt distribution. One is retention in the northern estuary. Another is spatial distribution qualitatively consistent with Spring Kodiak Trawl observations. Lastly, we will compare the timing of predicted entrainment with the timing of observed salvage. The outcome of this comparison is an explanation and justification of behaviors that will be explored further in additional modeling work.

Simulation Periods

Two water years were chosen for this initial evaluation of behavior rules. Water year 2002 was chosen as a year with a clear signal in salvage and was simulated both with two-dimensional and three-dimensional modeling tools. Water year 2004 was chosen due to a double peak in observed salvage which is particularly challenging to reproduce with particle-tracking modeling. This report explores not only the relative performance of different behavior rules but also the predicted distribution by independent sets of modeling tools for 2002, a year in which both 2D and 3D tools are applied, and also the predicted distribution and entrainment during an additional water year (2004) using the 2D tools. An additional two years are considered for further evaluation of behavior rules by Korman et al. (2018).

Water year 2002 was classified as a dry year both on the Sacramento River and San Joaquin River (CDWR, 2016a). Prior to the spawning migration, delta smelt were observed primarily in the lower Sacramento River extending from Rio Vista down to the confluence in the Fall Midwater Trawl observations (Figure 1). Reported Net Delta Outflow (Figure 2) peaked at $105,892 \text{ ft}^3\text{s}^{-1}$ on Jan 6, 2002 (CDWR, 2016b). The peak in salvage was observed on January 2, 2002 with a combined expanded salvage of 882 fish, which rapidly decreased as the magnitude of negative Old and Middle River flow decreased in early January.

The habitat of delta smelt was divided into regions for the CAMT investigations, primarily for the purpose of expanding catch into abundance and those regions, shown in Figure 3, are used here for comparison of observed and predicted regional abundance. Observed catch per unit effort in the Spring Kodiak Trawl (<http://www.delta.dfg.ca.gov/data/skt>) was expanded to estimate regional abundances as described in Korman et al. (2018). Estimated regional abundance based on the Spring Kodiak Trawl observations in 2002 (Figure 4) indicates a broader distribution than the Fall Midwater Trawl observations with delta smelt observed in the confluence and in Suisun Marsh.

Water year 2004 was classified as a below normal flow year on the Sacramento River and dry year on the San Joaquin River (CDWR, 2016a). Prior to the spawning migration the distribution of delta smelt was centered on the lower Sacramento River in and above the confluence (Figure 5). The peak flow of the year, $179,947 \text{ ft}^3\text{s}^{-1}$, occurred on Feb 28, 2004, unusually late in the water year, with a smaller flow peak on January 2, 2004 of $41,319 \text{ ft}^3\text{s}^{-1}$ (Figure 6). Observed salvage also followed a dual peak with salvage ramping up at the time of each of the two flow peaks. The regional abundances estimated from

the 2004 Spring Kodiak Trawl surveys are shown in Figure 7. The possibility of variability in the sampling efficiency of the Spring Kodiak Trawl with turbidity is explored in Korman et al. (2018).

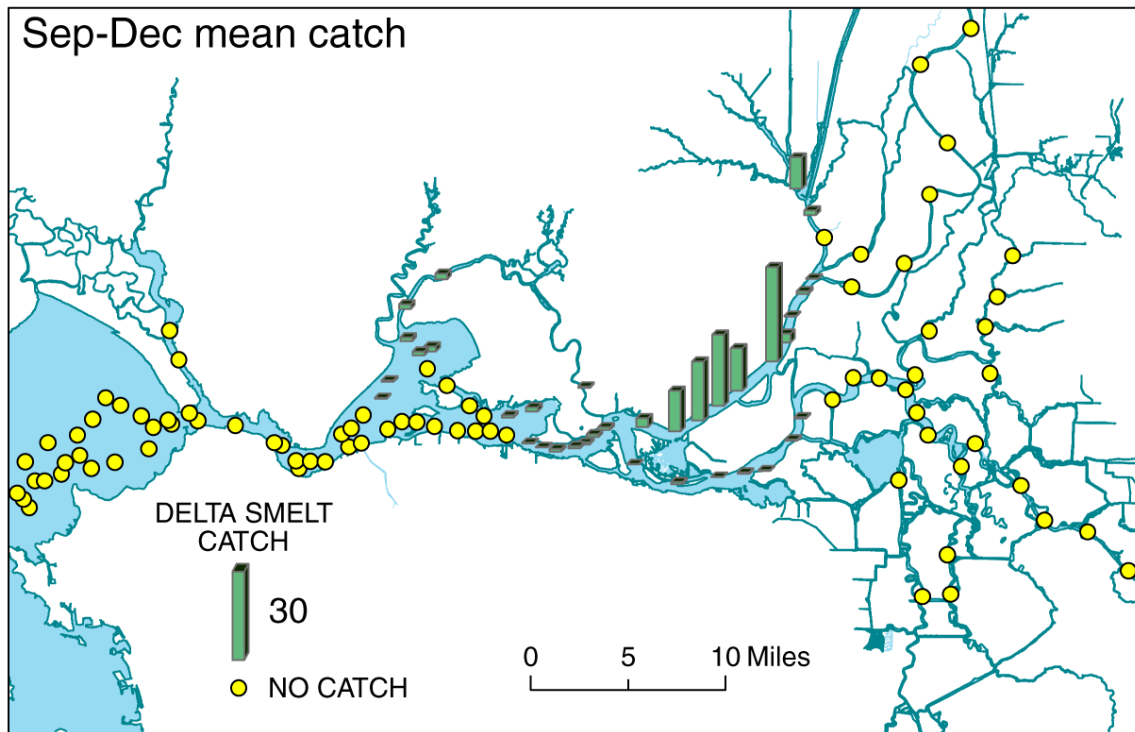


Figure 1. Observed mean catch per unit effort across all surveys of the 2001 Fall Midwater Trawl.

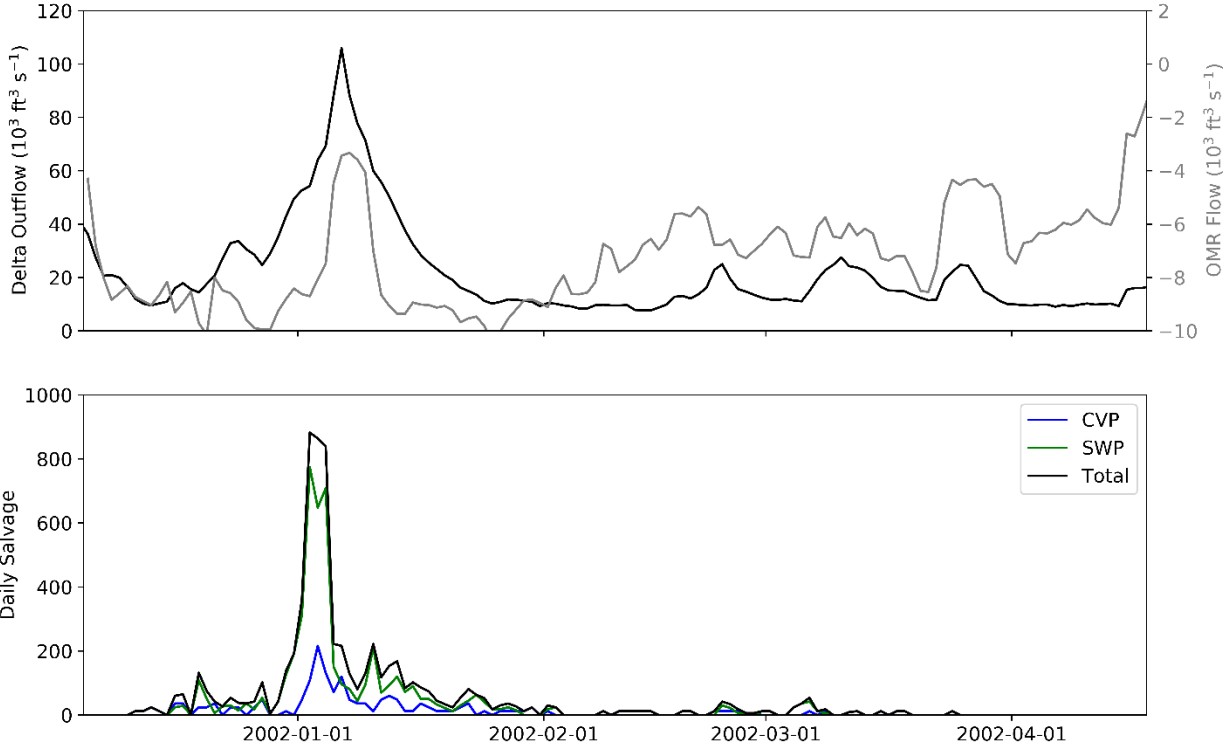


Figure 2. Net Delta outflow, OMR flow and expanded daily salvage during the water year 2002 simulation period.

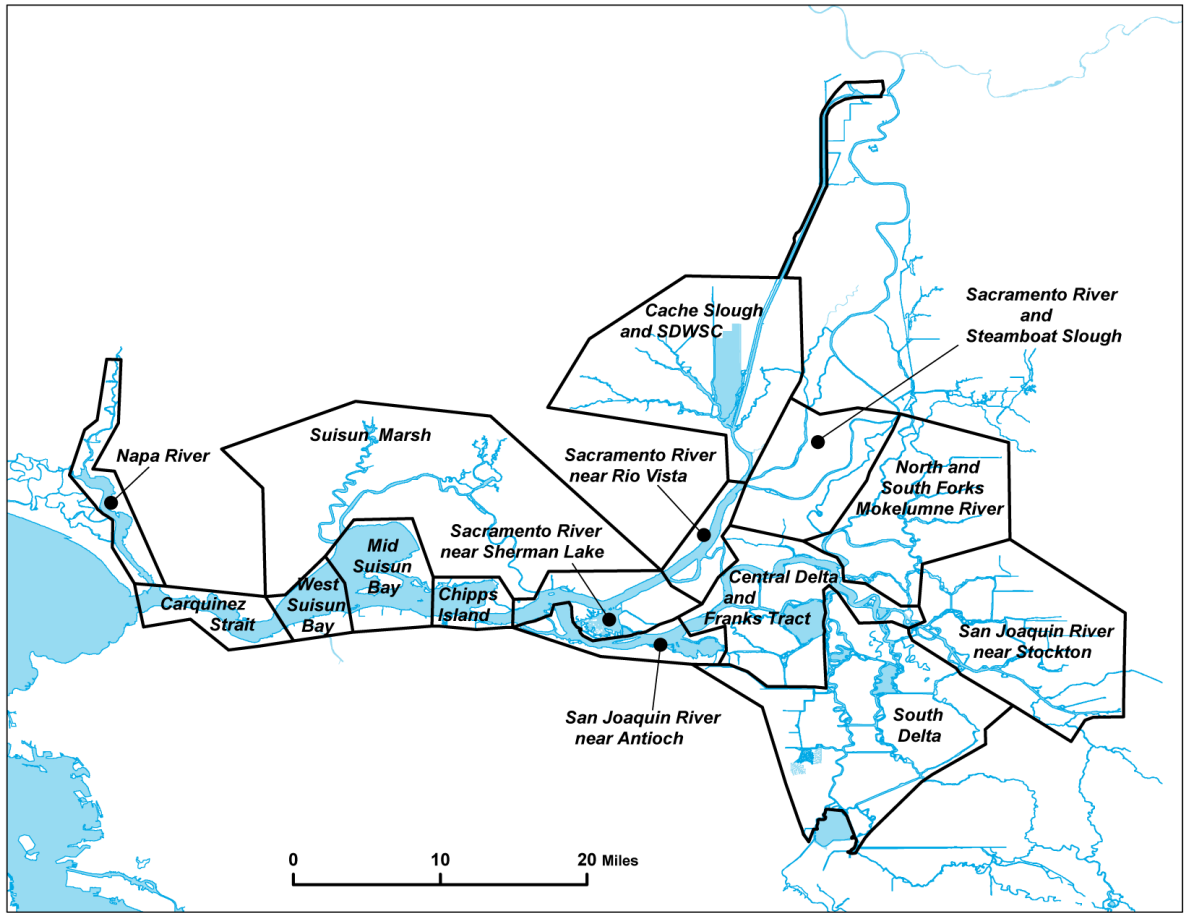


Figure 3. Regions used in CAMT delta smelt studies.

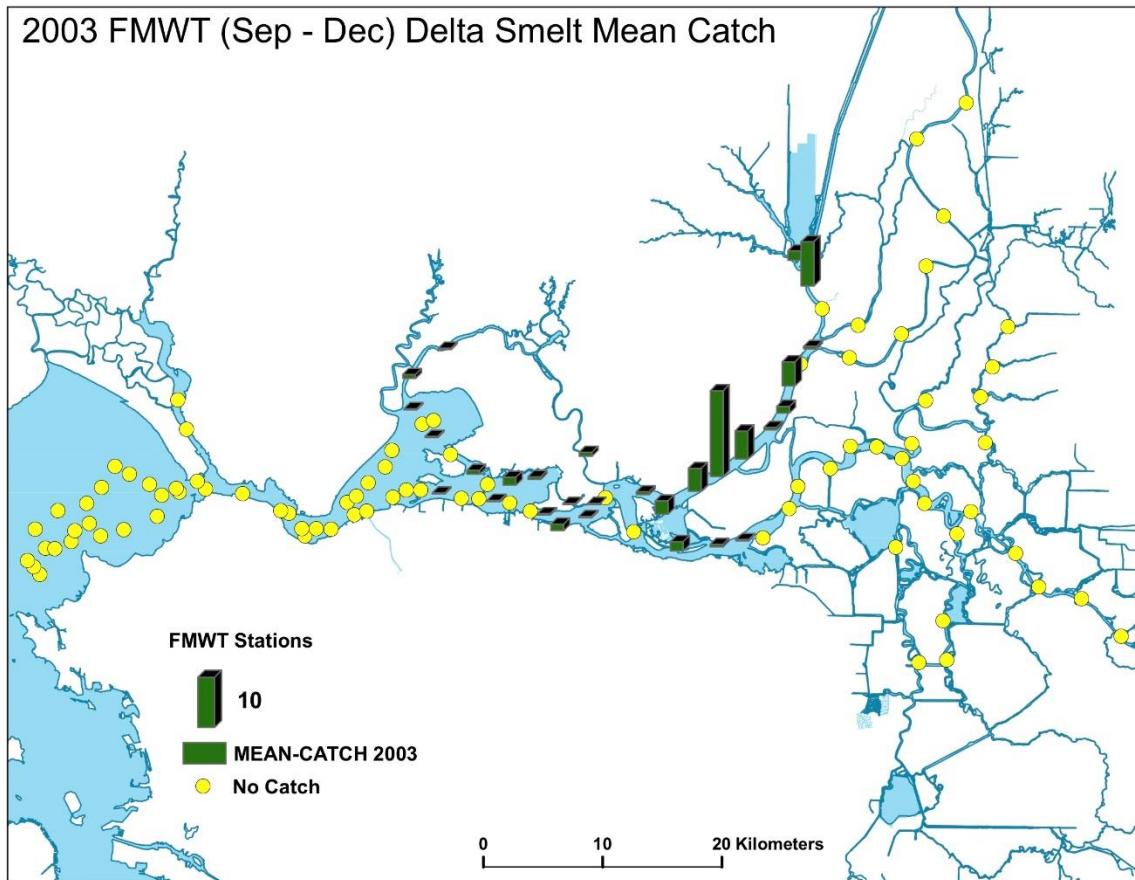


Figure 5. Observed mean catch per unit effort across all surveys of the 2001 Fall Midwater Trawl.

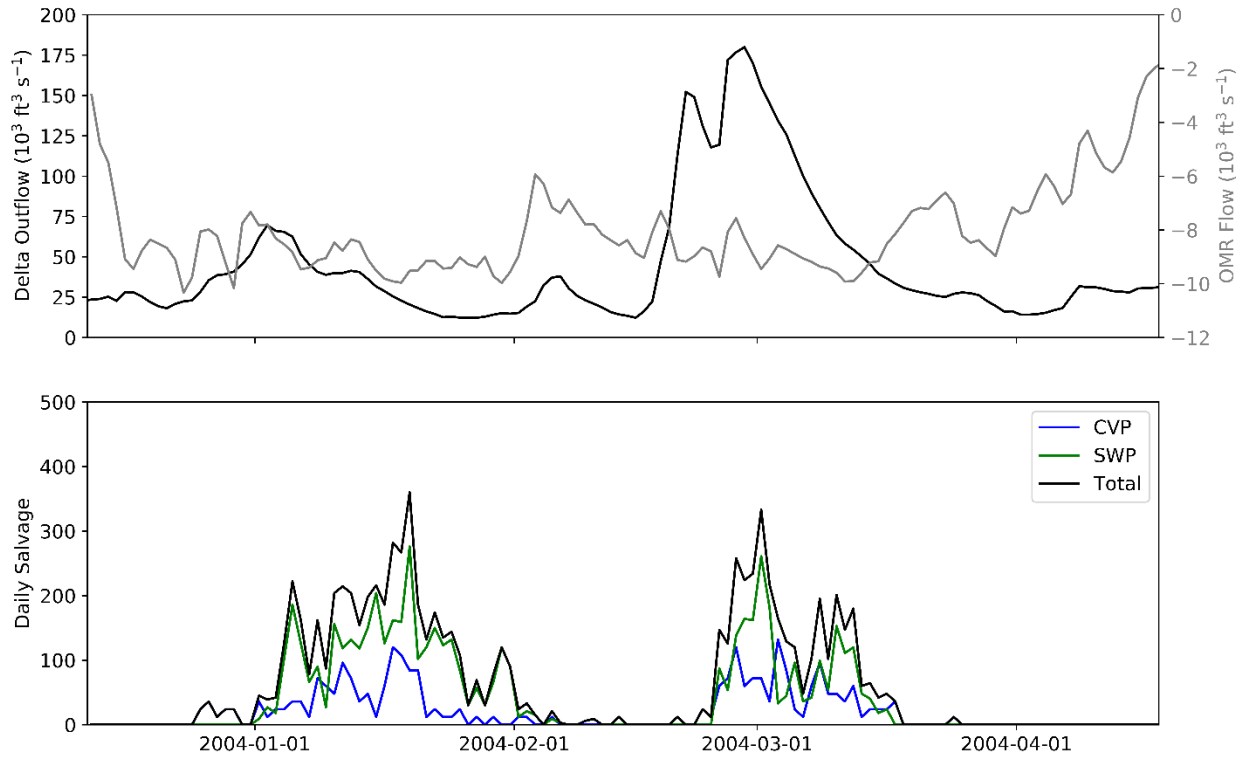


Figure 6. Net delta outflow, OMR flow and expanded daily salvage during the water year 2004 simulation period.

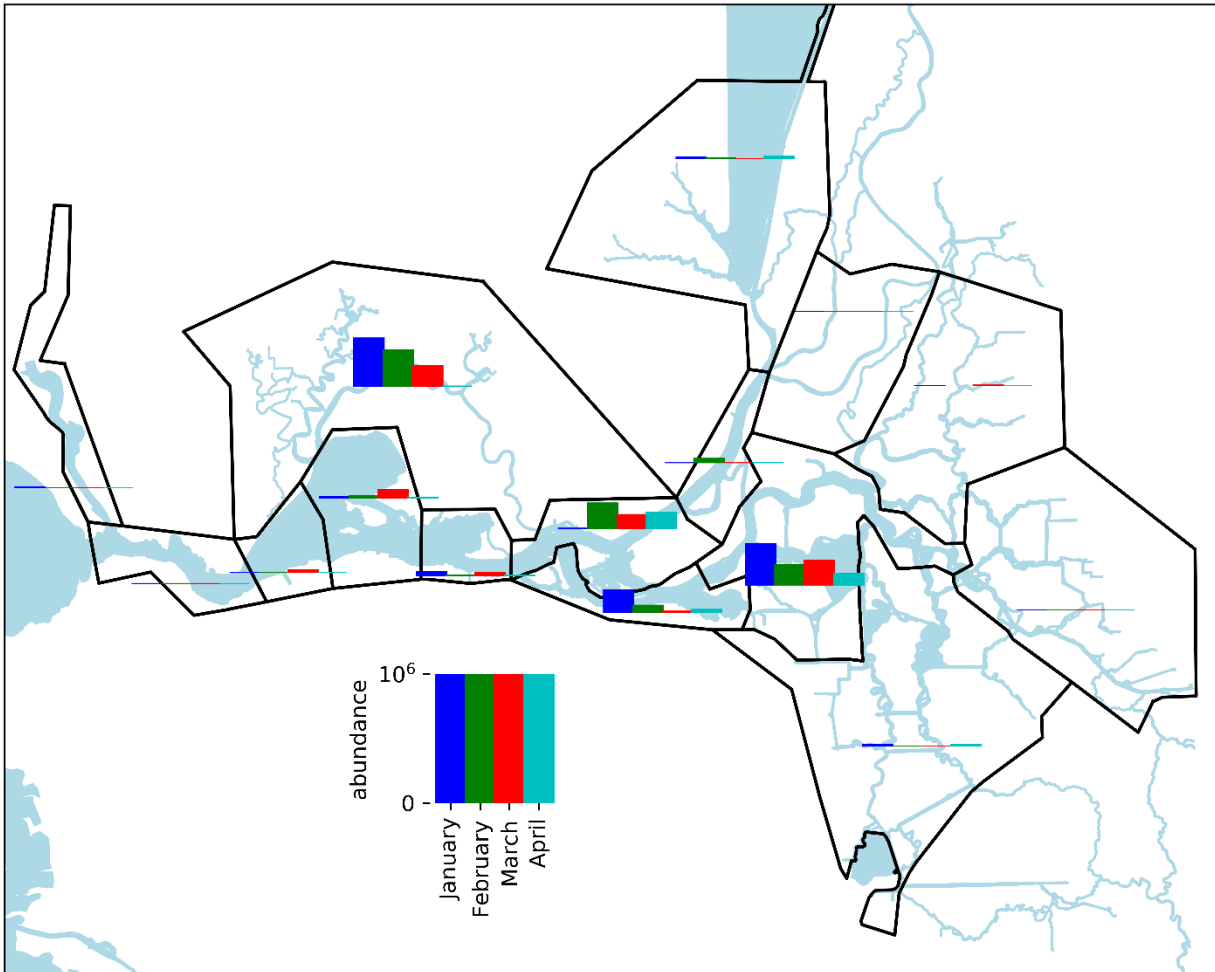


Figure 7. Estimated regional abundance for the four survey periods of the 2004 Spring Kodiak Trawl.

Hydrodynamic and Turbidity Modeling

Three-dimensional hydrodynamic, suspended sediment, and turbidity modeling was performed by Anchor QEA and builds on the hydrodynamic calibration documented in MacWilliams et al. (2015) and the suspended sediment calibration in Bever and MacWilliams (2013). The model calibration focused on water year 2011 when observations were available at several suspended sediment monitoring stations (Anchor QEA 2017).

Independent depth-averaged hydrodynamic, suspended sediment, and turbidity modeling was performed by RMA using RMA2 and associated tools. The calibration of these tools is documented in a report to CAMT (RMA 2017).

All hydrodynamic model output was written at a 15-minute output interval to be used in particle-tracking models.

Particle-Tracking Scenarios

The three-dimensional FISH-PTM model (Ketefian et al. 2016) was applied with the three-dimensional hydrodynamic output. The RMA-PTRK model (RMA 2009) was used applied with the two-dimensional hydrodynamic output. The initial particle distribution has been specified to approximate the observed 2001 Fall Midwater Trawl (FMWT) distribution shown in Figure 1. The distribution in the 2003 FMWT was similar.

Some attributes are consistent among simulations including release distribution in the lower Sacramento River and a simulation end time of the subsequent April 17 after the release time. The initial particle distribution with particles uniformly distributed through the Sacramento River near Sherman Lake and Sacramento River near Rio Vista regions is shown in Figure 8. The simulation end time of April 17 was chosen to include all Spring Kodiak Trawl surveys in both water year 2002 and 2004 and to include a period of zero salvage at the end of the simulation period. The attributes that vary among particle-tracking scenarios are:

1. Hydrodynamic modeling platform used
 - a. 3D
 - b. 2D
2. Water year of simulation period
 - a. 2002
 - b. 2004
3. Particle release time
 - a. Water year 2002
 - i. December 5, 2001
 - ii. December 20, 2001
 - b. Water year 2004
 - i. December 12, 2003
4. Categories of behavior sets
 - a. Passive
 - b. Tidal migration
 - c. Turbidity seeking
 - d. Freshwater seeking
 - e. Conditional tidal migration
 - f. Compound behaviors

The particle release time of December 5, 2001 was chosen as the approximate time when elevated turbidity water reached the particle release region in 2002 (Figure 9). December 20, 2001 was chosen as the start time consistent with Sommer et al. (2011) determined by subtracting the reported time to reach SWP after the first flush (13 days) from the peak arrival of spawners at the SWP (January 2, 2002). The December 12, 2003 release time for water year 2004 was chosen to correspond with the arrival of elevated turbidity water in the lower Sacramento (Figure 10).

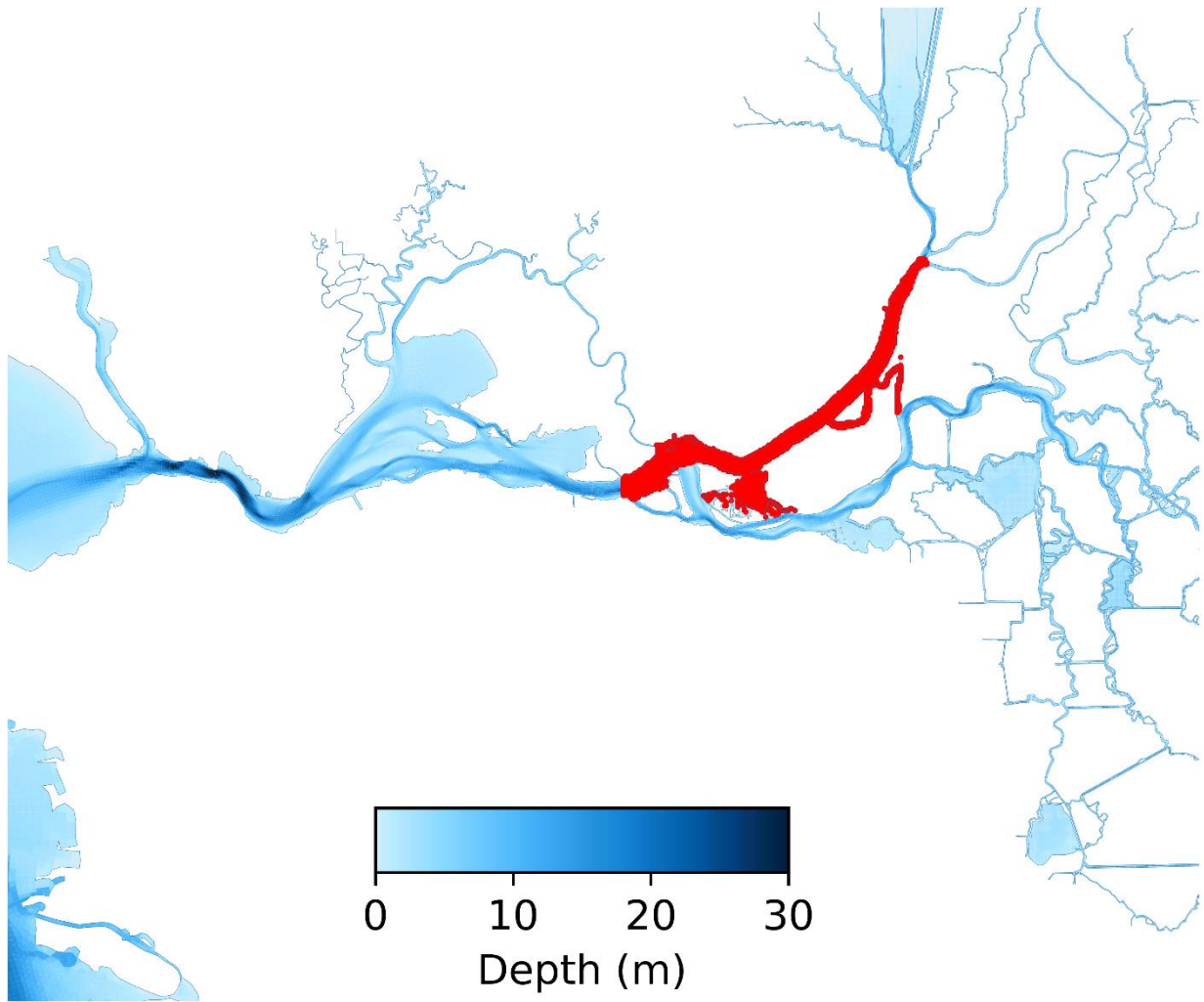


Figure 8. Initial distribution of particles at the particle release time. Each red dot indicates the horizontal position of a particle on December 5, 2001 at 00:00.

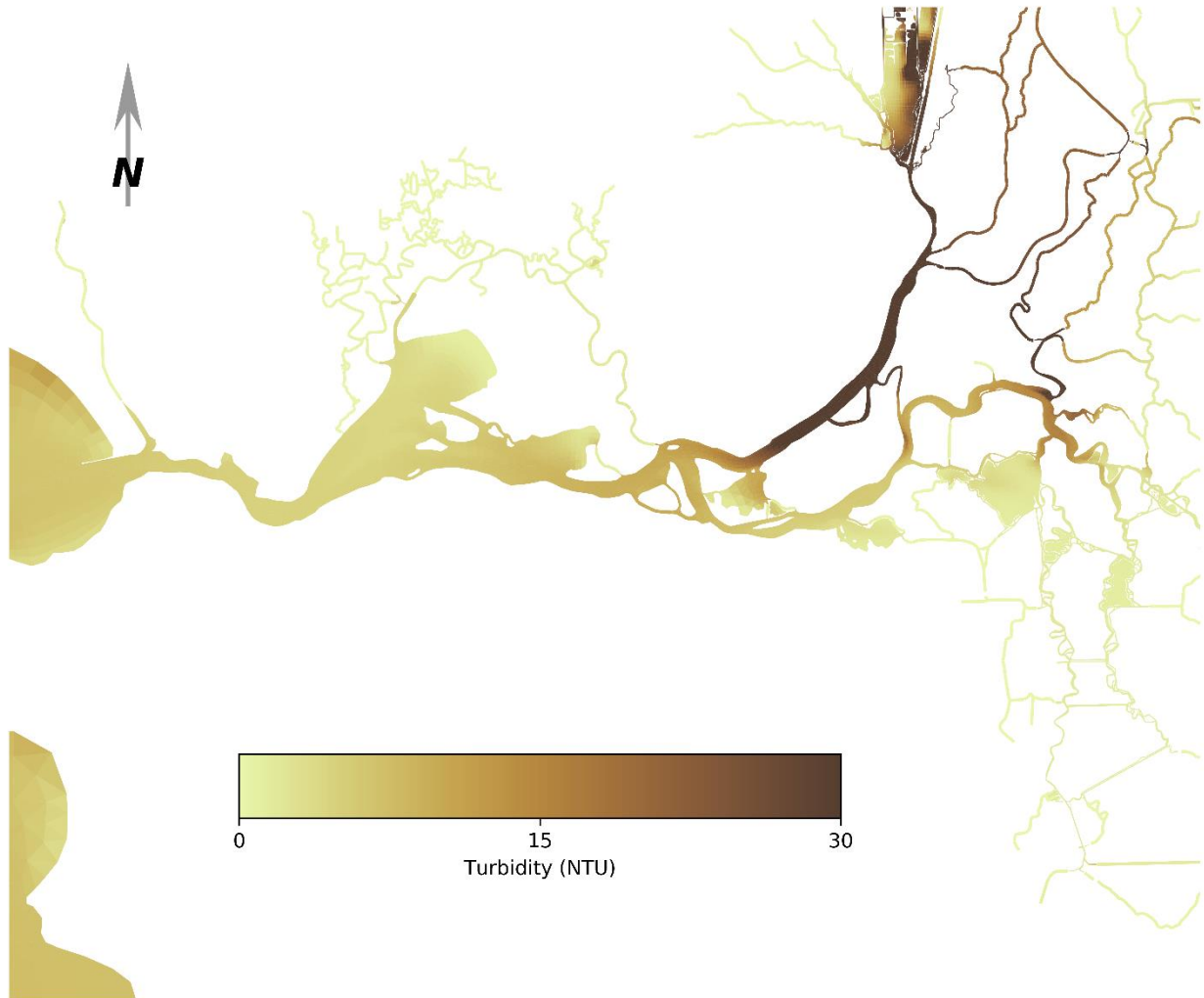


Figure 9. Depth-averaged turbidity field predicted by the 2D modeling tools on Dec 5, 2001 at 00:00.

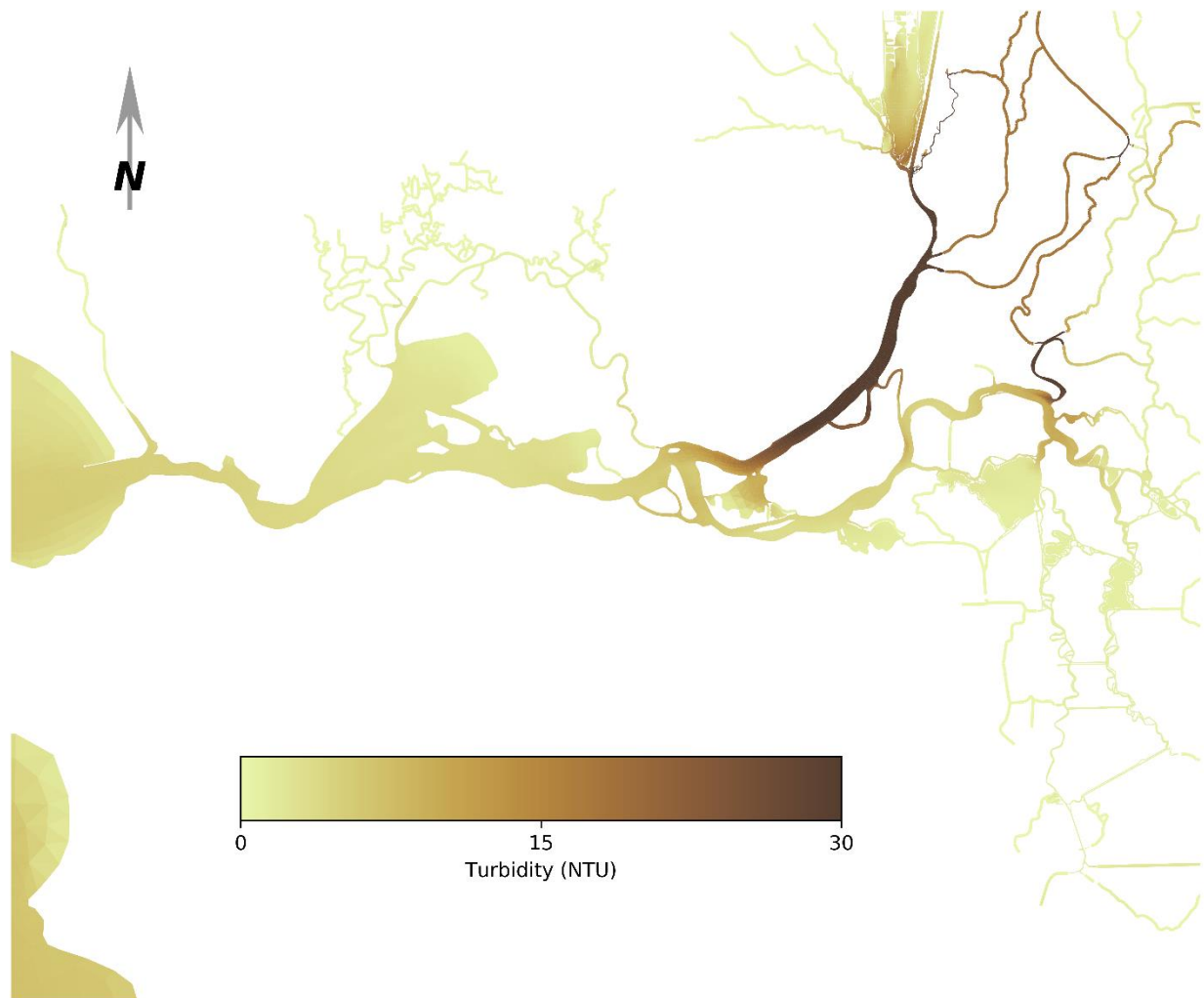


Figure 10. Depth-averaged turbidity field predicted by the 2D modeling tools on Dec 12, 2003 at 00:00.

Swimming Behavior Formulation

The hypothesized behavior rules were developed under guidance from the Delta Smelt Scoping Team (DSST) and based on review comments in the Independent Review Panel (IRP) review of the CAMT proposal for delta smelt investigations. However, given the limited observations available in this period and a potentially intractably large parameter space of a complex set of behavior rules, behaviors are explored within a specific framework. More complex variants of behavior, possibly involving additional environmental stimuli or stochasticity of responses, may be explored in the future if requested by the CAMT DSST.

Overview

All individuals (particles) are characterized by the state variables of three-dimensional position and swimming speed vector. Additional state variables associated with individuals, but only used in a subset of the behavior rules, are acclimated values of salinity and turbidity as explained below. The model proceeds in 5-minute time steps, so that state variables of each individual and the environmental stimuli

to which the individuals are exposed are updated at a 5-minute interval. The environmental stimuli are provided by the hydrodynamic models at the spatial resolution of the model grid which typically ranges from 10 meters to 100 meters through the Delta with smaller cell sizes in narrower channels. The instantaneous salinity and turbidity experienced by each individual at each time step are the turbidity and salinity in the grid cell containing the particle at that time step. Velocity is linearly interpolated through the cell according to the method of Ketefian et al. (2016). Gradients of salinity, turbidity and water depth are calculated from the values in the cell containing each particle and adjacent cells. The particle-tracking model accounts for movement of particles from the combination of hydrodynamics and swimming. The additional effect of natural mortality rate on predicted distribution is introduced in the statistical fitting subsequent to particle tracking.

Mathematical Formulation

The velocity of each particle/individual in the particle-tracking model is the summation of the hydrodynamic velocity vector and a swimming vector:

$$\vec{u} = \vec{u}_h + \vec{u}_b \quad (1)$$

where \vec{u}_h is the hydrodynamic velocity and \vec{u}_b is the swimming (behavior) velocity specified by the individual-based model.

The swimming vector is specified as the summation of three orthogonal components of velocity and a horizontal component which can be in any direction in the horizontal plane:

$$\vec{u}_b = \vec{u}_s + \vec{u}_c + \vec{u}_v + \vec{u}_{xy} \quad (2)$$

where \vec{u}_s is the streamwise swimming velocity, \vec{u}_c is the cross-stream swimming velocity, \vec{u}_v is the vertical swimming velocity, \vec{u}_{xy} is the horizontal swimming velocity. The streamwise direction is defined as the direction of the hydrodynamic velocity at the location of the particle:

$$\vec{n}_s \equiv (n_x, n_y) = \frac{\vec{u}_h}{|\vec{u}_h|} \quad (3)$$

where \vec{n}_s is the unit vector in the streamwise direction. By convention the positive cross-stream direction is to the right of the streamwise direction:

$$\vec{n}_c = (n_y, -n_x). \quad (4)$$

The direction of vertical swimming is by definition the z-coordinate direction:

$$\vec{u}_v = V(0,0,1) \quad (5)$$

where V is the vertical swimming speed and is positive for upward swimming.

Swimming speeds used vary to some extent but are generally limited to 2 body lengths per second or less. These are consistent with sustained swimming speeds reported by Swanson et al. (1998).

Behaviors are triggered by environmental stimuli at the location of each particle. Two types of environmental stimuli are considered. The first is the instantaneous and local value of an environmental property, such as turbidity or salinity. The second is a perceived change trigger based on change of an environmental property from an acclimatized condition (Goodwin et al. 2014). The acclimatized value of an environmental property is estimated based on a Pavlovian conditioning approach by an exponentially weighted moving average:

$$I_a(t) = (1 - m_a)I(t) + m_aI(t - 1) \quad (6)$$

where $I_a(t)$ is the perceived intensity of an environmental stimulus I at time t , and m_a is a parameter which determines the time scale of acclimation. The perceived change is then the difference between the instantaneous value of an environmental stimulus and the acclimatized value of the stimulus is

$$E(t) = \frac{I(t) - I_a(t)}{I_a(t)} \quad (7)$$

The environmental properties that are considered as possible stimuli are discussed in the following section.

Based partially on input from the Delta Smelt Scoping Team, the behavior rules used in this study are intentionally of limited complexity and neglect several likely attributes of actual delta smelt behavior. There is no stochasticity in thresholds that trigger behavioral responses and no variability among particles in the swimming response to a given environmental stimulus. Furthermore, the behavioral rules do not change in time with life stage of delta smelt or with light levels (no variation between day and night behavior). The lack of change with life stage could be particularly limiting to the extent that delta smelt have a distinct staging behavior prior to spawning.

Behavior Triggers

The framework of triggers and associated behaviors allows a great deal of flexibility. However, there are also limitations, including the use of fixed thresholds to trigger behaviors.

The current types of triggers used in specified behaviors are of the following general types:

1. None: No condition required, used for a default behavior
2. Instantaneous: The instantaneous value of an environmental stimulus at the location of the particle is within a specified range, for example, turbidity > 15 NTU.
3. Gradient: The instantaneous value the gradient of an environmental property at the location of the particle is within a specified range, for example, turbidity gradient > 0.001 NTU/m.
4. Acclimatized (Equation 6): The acclimatized value of an environmental property is within a specified range, for example, the acclimatized salinity > 0.5 psu.
5. Perceived change (Equation 7): The perceived change from an acclimatized value of an environmental property is within a specified range, for example a (normalized) change in turbidity of 25%.
6. Timer: Used to attribute persistence to behaviors. For example, a tidal migration behavior could be specified to be active for a minimum of 24 hours once triggered.
7. Compound: Trigger types 2-6 can be combined to form compound triggers. For example, swimming to shallower water may be triggered when turbidity > 15 NTU and the hydrodynamic velocity at the particle location is in the ebb direction.

The environmental properties that have been considered in triggers of the general types described above include

1. Hydrodynamic velocity
2. Distance to shore
3. Water depth
4. Salinity
5. Turbidity

Each of these properties, and their gradients, are evaluated at the location of each particle and through time in the particle-tracking simulations.

Behavior Types

Triggers and associated behavioral (swimming) responses are combined to form sets of behavior rules. Several general types of swimming responses have been explored. Not only are triggers deterministic but all of the responses are deterministic. While there is currently no stochasticity in swimming response (swimming speed or direction) among individuals, it has been applied in the behavior representation of salmon (e.g. Goodwin et al. 2014) and could be explored in the future. The one exception is stochasticity in swimming direction for the “random” swimming behavior listed below.

1. Passive
 - a. All swimming velocity components are zero
2. Turbidity seeking
 - a. Swim in horizontal direction of higher turbidity
3. Freshwater seeking
 - a. Swim in horizontal direction of lower salinity
4. Horizontal tidal migration
 - a. Swim in horizontal direction to shallower water on ebb
 - b. Swim in horizontal direction to deeper water on flood
5. Vertical tidal migration
 - a. Swim down during ebb
 - b. Swim up during flood
6. Holding
 - a. Oppose/resist hydrodynamic velocity in the horizontal up to some threshold speed
 - b. Swimming in horizontal direction shallow water when in deep water
7. Random
 - a. Randomly directed swimming at a fixed speed

The direction of ebb tide is determined from an analysis of a single period in which the tidal water level is transitioning from higher high water to lower low water. The direction of the strongest velocity in each cell during this period gives the ebb direction for that location. Ebb tide at any location and time occurs when the dot product of the hydrodynamic velocity at that time and location with the ebb direction vector at that location (estimated by the aforementioned analysis) is positive. It is implicitly assumed in this approach that each individual can sense the ebb direction, though the mechanism through which this information is perceived is not known.

Evaluation of Predicted Distribution

Our population dynamics model predicts the abundance, distribution, survival, and entrainment of adult delta smelt on a daily time step. The model consists of process, observation, and likelihood (fitting) components. The process component predicts the abundance of the population in each of the 15 CAMT regions for each day of the simulation. The model uses the estimates of abundance in each region and the proportion of particles in that region that are entrained, as determined by the PTM, to predict the number entrained by day. The observation component of the model translates predictions into metrics which are observed by the Spring Kodiak Trawl surveys (SKT), and daily salvage at each fish collection

facility. The likelihood component compares predictions and observations to estimate process and observation parameters by maximizing the likelihood through non-linear search.

Simulation results from the PTM are summarized in an exchange or movement matrix $\mathbf{m}_{i,d}$, which is the cumulative proportion of the original particles that are present in region i on day d , or are entrained at each pumping facility ($i=k$). This exchange matrix is treated as a large set of fixed parameters by the population dynamics model. Predictions of abundance and entrainment from the population model are translated into trends in SKT catch over space and time and trends in salvage at each facility. These predictions are compared to data, and parameters are estimated by nonlinear search using a maximum likelihood approach. In the description of the population dynamics model which follows, Greek letters denote parameters that are estimated, upper case letters denote predicted state variables, and lowercase letters denote indices (not bold), or data (bold) or fixed parameters (bold).

The process component of the population dynamics model predicts the abundance of delta smelt adults by model day and region. Regional abundance depends on the initial total abundance and cumulative survival and movement, and is calculated from,

$$N_{i,d} = e^{\gamma} \cdot \prod_d \phi_d \cdot \mathbf{m}_{i,d} \quad (8)$$

where γ is the initial abundance in log space, ϕ is the estimated survival rate on day d , with the product of those rates up to day d (denoted by the \prod symbol) being the cumulative survival from the start of the simulation to the end of day d , and $\mathbf{m}_{i,d}$ is the cumulative proportion of fish in a destination region or entrained. We do not allow survival rate to vary across regions in this analysis. However, as discussed below, additional mortality for particles that are entrained is captured in the estimate of the salvage expansion factor.

The natural survival rate of delta smelt is assumed to be constant over the duration of the simulations and is calculated from

$$\phi_d = \text{logit}(\alpha_o) \quad (9)$$

where $\text{logit}()$ denotes that the value inside the parentheses is logit-transformed so $0 \leq \phi \leq 1$.

The cumulative number of fish entrained is calculated from,

$$N_Ent_{k,d} = \sum_i N_{i,d=0} \cdot \prod_d \phi_d \cdot \mathbf{m}_{k,d} \quad (10)$$

where N_Ent is the number entrained from the start of the simulation through day d at pumping location k , and $\mathbf{m}_{k,d}$ is the cumulative proportion of fish entrained at pumping location k , as determined by the PTM. (10 scales the proportional entrainment rates from the PTM ($\mathbf{m}_{k,d}$) by accounting for initial abundance and losses due to natural mortality. The proportion of the initial population that is entrained at each pumping location up to and including day d is calculated from,

$$p_Ent_{k,d} = 1 - \prod_d \left(1 - \frac{N_Ent_{k,d} - N_Ent_{k,d-1}}{\sum_i N_{i,d-1}} \right) \quad (11)$$

(11) follows the same logic as Kimmerer (2008) and assumes natural and entrainment mortality are continuous processes over the duration of the model simulation. As a result, proportional entrainment on each day depends on the abundance at the end of the previous day, where that abundance in turn

depends on the initial abundances, and cumulative natural and entrainment losses. The ratio in Equation 11 is the proportion of fish entrained on day d from all regions relative to the total abundance (across all regions) at the end of the previous day. The term inside the product symbol (\prod) is therefore the proportion of the population surviving entrainment on day d , and that product over days is the cumulative proportion surviving from the start of the simulation through day d . Entrainment losses include both pre-screen losses and direct losses to the pumps.

The observation model predicts SKT catch for each station and survey period from,

$$\hat{C}_{SKT_{s,d}} = N_{i(s),d} \cdot \theta_{SKT_{s,d}} \quad (12)$$

where, $\hat{C}_{SKT_{s,d}}$ is the predicted SKT catch at station s on day d , $N_{i(s),d}$ is the abundance in region i where station s is located ($i(s)$), and $\theta_{SKT_{s,d}}$ is the proportion of the population in region i sampled at station s on day d . This SKT sampling efficiency term is calculated from,

$$\theta_{SKT_{s,d}} = \theta_{c_{s,d}} \frac{\mathbf{vtow}_{s,d}}{\mathbf{vreg}} \quad (13)$$

where $\theta_{c_{s,d}}$ is an estimate of the proportion of smelt within the volume towed at a station that are captured (sampling efficiency), \mathbf{vreg} is the volume of region i that delta smelt are distributed in, and \mathbf{vtow} is the volume for the tow at station s sampled on day d . We assumed that delta smelt were evenly distributed to a maximum depth of 4 m (as in Kimmerer 2008). The proportion of smelt within the volume towed ($\theta_{c_{s,d}}$) was set to 1 for the analysis here.

Salvage in the population dynamics model is calculated from,

$$\hat{C}_{SAL_{k,d}} = (N_{Ent_{k,d}} - N_{Ent_{k,d-1}}) \cdot \theta_{S_{k,d}} \cdot \mathbf{p}_{s_k} \quad (14)$$

where $\hat{C}_{SAL_{k,d}}$ is the predicted salvage on model day d at salvage location k , $\theta_{S_{k,d}}$ is the proportion of entrained fish that enter the salvage facility, and \mathbf{p}_{s_k} is the proportion of the flow in the salvage facility that is sampled per day. For consistency with past efforts, we refer to the inverse of salvage efficiency (θ_s^{-1}) as the salvage expansion factor. Time-specific values for \mathbf{p}_s for each facility were not available for all relevant time periods, thus the observed daily salvage data available to us was already expanded to account for the proportion of volume sampled each day. By using expanded salvage observations, one is assuming that $\mathbf{p}_s=1$. However, when fitting the model, using expanded salvage data would overweight the importance of the salvage data relative to other data sources (SKT). To correct for this, \mathbf{p}_s was set to a value that reflects the typical proportion of fish in the salvage facility that are sampled. Our results assume that $\mathbf{p}_s=0.08$ (sampling 10 minutes out of every two hours) for both facilities in all water years we simulated.

For the screening run evaluations, we assume salvage efficiency ($\theta_{S_{k,d}}$) can vary across facilities but does not vary over time,

$$\hat{C}_{SAL_{k,d}} = (N_{Ent_{k,d}} - N_{Ent_{k,d-1}}) \cdot \theta_{S_{k,d}} \cdot \mathbf{p}_{s_k} \quad (15)$$

where λ_0 is the proportion of entrained fish that enter the salvage facility k on day d and are counted, in logit space.

The model is fit to the data by minimizing a negative log likelihood (NLL_{TOT}) that quantifies the combined fit of the model to SKT catch (NLL_{SKT}), and salvage data (NLL_{SAL}). The total negative log likelihood (NLL_{TOT}) is,

$$NLL_{TOT} = NLL_{SKT} + NLL_{SAL} \quad (16)$$

Each likelihood component is described below. Note that the total negative log likelihood only quantifies the discrepancy between predictions and observations (observation error). There is no component that penalizes process variation in population dynamics because that variation is not modelled. For example, we could have allowed daily survival rates to be drawn from a distribution where we estimated both the mean and the extent of variation. In data-limited situations it is not possible to separate process error from observation error. Including both would increase computational time considerably and would require informative priors on the extent of process or observation error, with total variance estimates conditional on those priors. We therefore use an ‘observation error only’ model (see Ahrestani et al. 2013).

We assume that the SKT surveys provide a reliable index of abundance over both space (across regions) and time (over SKT survey periods in a year). We assume that the capture probability of the SKT survey is known and is accurately determined by the scaling factors in Equation (12). SKT catch at each station and SKT survey period is assumed to be a random variable drawn from a negative binomial distribution (negbin),

$$NLL_{SKT} = -\sum_{s,d} \log(\text{negbin}(\mathbf{C}_{SKT_{s,d}}, \hat{C}_{SKT_{s,d}}, \tau)) \quad (17)$$

where, NLL_{SKT} is the sum of negative log likelihoods across all sampling days (d) and stations (s), $\mathbf{C}_{SKT_{s,d}}$ is the observed SKT catch by station and day, $\hat{C}_{SKT_{s,d}}$ is the predicted catch from Equation (12), and τ represents the extent of overdispersion in the data. To simulate greater belief in the SKT data, τ was set to 1 for the evaluations reported here. In this case the negative binomial distribution is equivalent to the Poisson, where the variance is equal to the mean. Our approach to modelling error in the SKT data is rather ad-hoc, but as discussed in Korman et al. (2018) there is insufficient information to accurately model it.

The observed salvage at each salvage location is assumed to be Poisson-distributed (pois) random variable,

$$NLL_{SAL} = -\sum_{k,d} \log(\text{pois}(\mathbf{C}_{SAL_{k,d}} \cdot \mathbf{p}_{s_k}, \hat{C}_{SAL_{k,d}})) \quad (18)$$

where, NLL_{SAL} is the sum of the negative log likelihoods across all days, $\mathbf{C}_{SAL_{k,d}}$ is the reported expanded daily salvage at facility k on day d , \mathbf{p}_{s_k} is the average proportion of water that is sampled for fish at the salvage facility, and $\hat{C}_{SAL_{k,d}}$ is the predicted salvage computed from Equation (15). By including the proportion of water sampled for fish at the salvage facility for both observations (Equation (15)) and predictions (Equation (12)), approximately correct sample sizes are used in the likelihood.

Parameters of the model were estimated by maximum likelihood using nonlinear search in AD model-builder (ADMB, Fournier et al. 2011). We ensure convergence had occurred based on the gradients of change in parameter values relative to changes in the log likelihood and the condition of the Hessian matrix returned by ADMB. Asymptotic estimates of the standard error of parameter estimates at their maximum likelihood values were computed from the Hessian matrix within ADMB.

Results

Particle tracking results are provided for a set of scenarios. The categories of particle fate reported are entrained by exports, exited analysis region and retained in the northern estuary. Particles that are in or seaward of San Pablo are considered to have exited the analysis region.

Each set of behavior rules (“behavior set”) explored in this report is described in Appendix A. A full set of figures for 3D and 2D model results for each behavior set is provided in Appendix B.

Building from Simple to More Complex Behavior Sets

In this discussion the outcome of simple behavior rules is discussed first. For example, passive behavior is discussed as a reminder that some form of behavior is required for retention in the estuary and to quantify how quickly particles are lost out of the northern estuary without active behavior. Then active behaviors that are constant through time are explored. Next active behaviors that are only triggered under specific environmental conditions are explored. Last, behaviors with more than one possible behavioral response are discussed. The results shown here are a subset of the full set of results given in Appendix B.

Two figure types are used in the discussion of different hypothesized sets of behavior rules. Map figures have been prepared to compare the observed and predicted regional abundance at the time of the Spring Kodiak Trawl (e.g. Figure 12). Time series comparisons show the fate of the group of particles through time, classified into the categories of retained in the analysis region, which corresponds to the spatial region in which adult delta smelt are typically observed, exited from that region, or entrained into water exports (Figure 11). A time series of the proportion of particles exhibiting different categories of behavior through time (tidal migration, holding, etc.) is also shown. Next the timing of observed salvage is compared with the timing of particle entrainment. It should be noted that the particle entrainment does not consider natural mortality so this comparison is purely qualitative. Lastly, for reference, time series of Net Delta Outflow and Old and Middle River flow are shown.

For many behavior sets the two-dimensional and three-dimensional results are broadly similar, though often different in some individual regions. In the discussion below, primarily the three-dimensional results are shown but the full set of results for both 3D and 2D modeling tools are given in Appendix B. All behavior scenarios for both the 2D and 3D models for 2002 and 2D model for 2004 are included in the ranking of behaviors which will be discussed after the following discussion of results for individual behavior scenarios.

Passive Particles

Passive particles provide a useful reference of the outcome of plankton that are transported passively with the water. Figure 11 indicates that passive particles rapidly exit the northern estuary as they are

flushed to the ocean in both the 2D and 3D model results. The fitting approach selects the maximum allowable initial population of 5 million delta smelt to offset large seaward losses. Entrainment is relatively small compared with seaward losses.

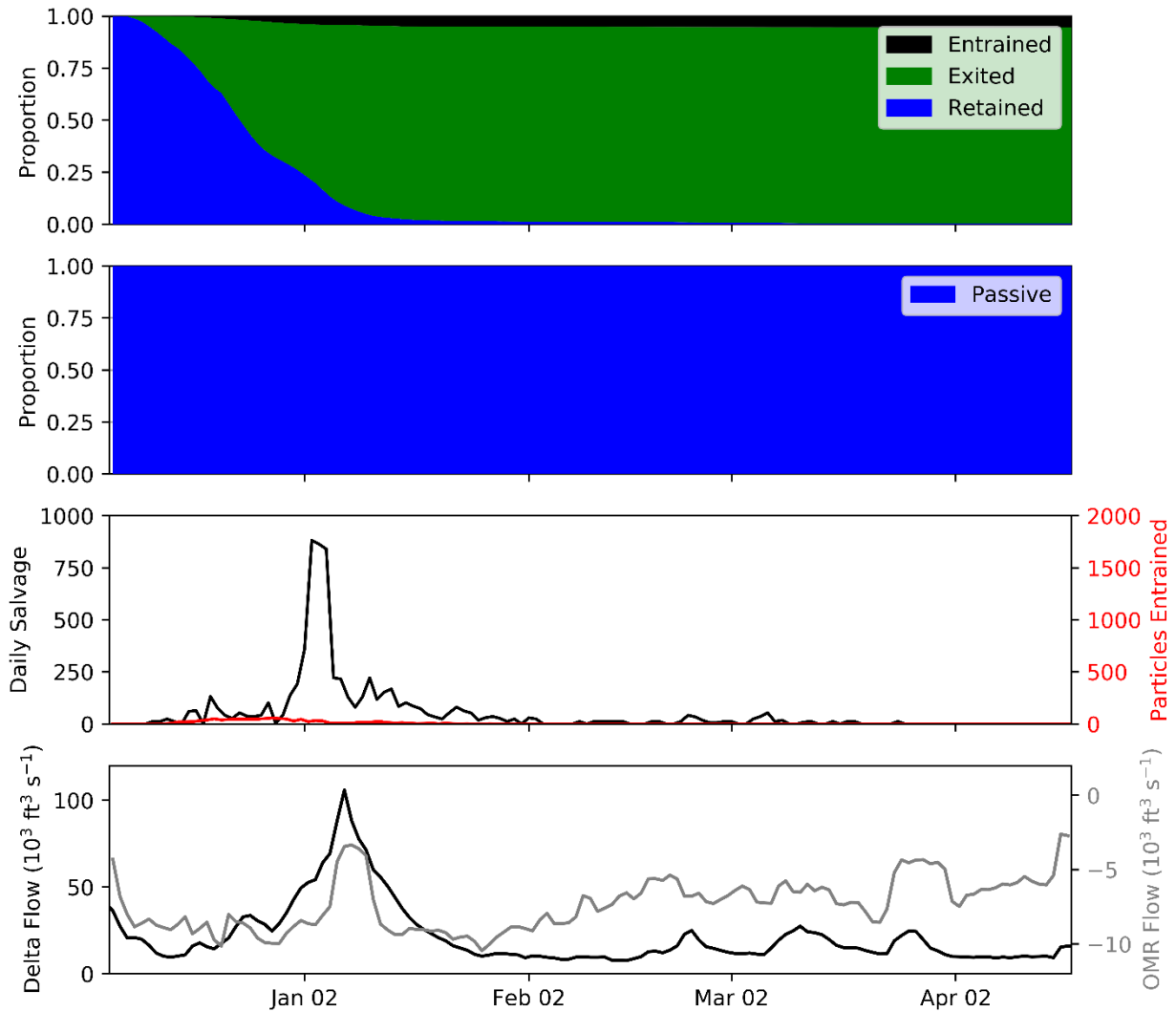


Figure 11. Passive behavior scenario results, three-dimensional model, water year 2002. The top panel shows the proportional fate of the particles through time, classified into the categories of retained in the analysis region, which corresponds to the spatial region in which adult delta smelt are typically observed, exited that region, or entrained into water exports. The second panel shows the proportion of particles exhibiting different types of behavior through time. The third panel shows daily expanded salvage and daily particle entrainment. The last panel shows daily Net Delta Outflow and Old and Middle River flow.

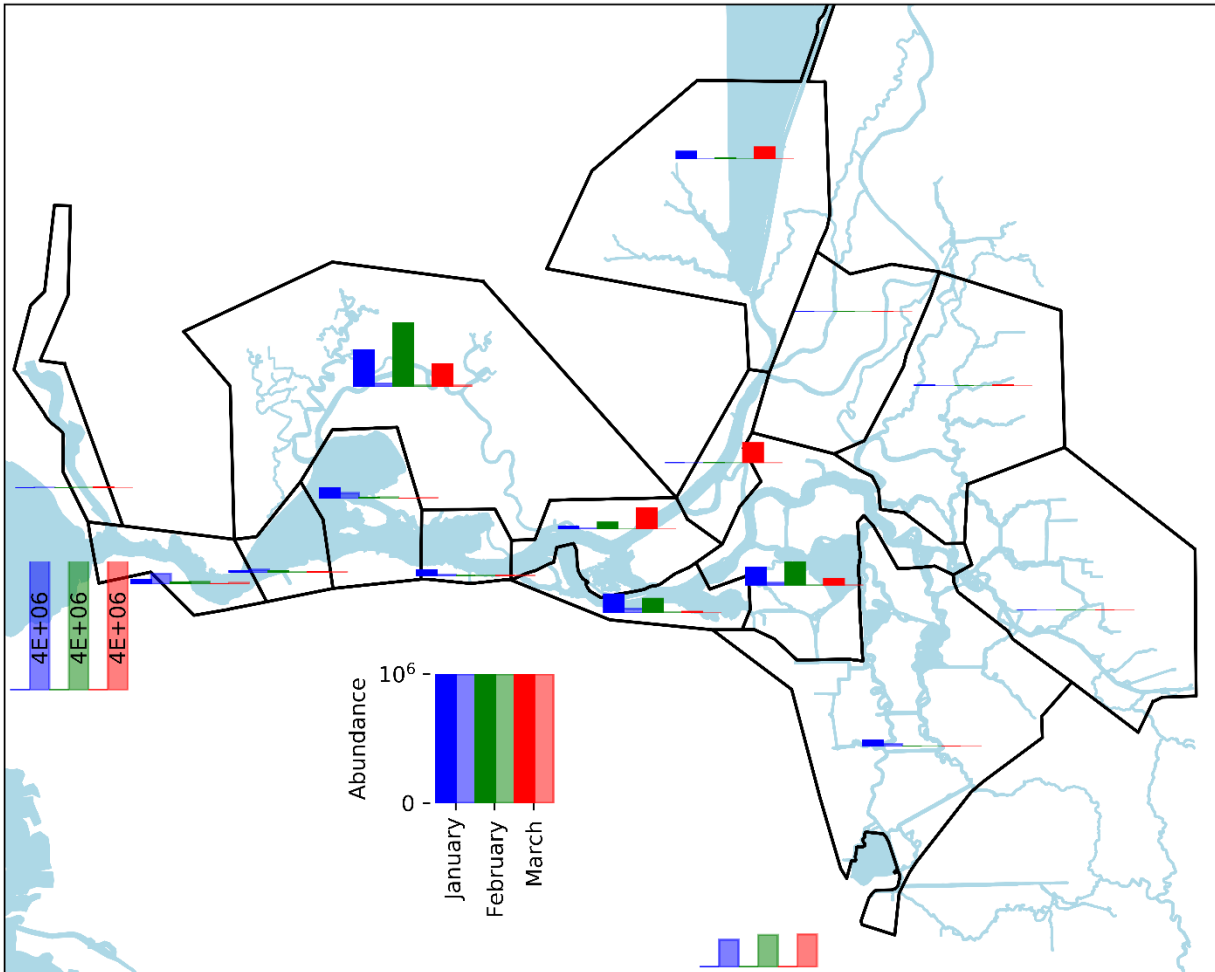


Figure 12. Comparison of predicted regional abundance for the passive behavior scenario, three-dimensional model results, water year 2002 to regional abundance estimated from the Spring Kodiak Trawl surveys. Dark colors for each month represent regional abundance estimated from each Spring Kodiak Trawl survey in 2002. Lighter colors for each month indicate model results. The predicted proportion of fish that exited the analysis region are shown to the left and below the Carquinez Strait region. Predicted cumulative entrainment is shown by the southernmost set of bars. The maximum height of each bar corresponds to a regional abundance of 10^6 delta smelt as shown in the legend. In cases where a predicted regional abundance of 10^6 delta smelt exceeded, the predicted regional abundance is annotated inside the corresponding bar.

Horizontal Tidal Migration

Tidal migration is implemented as horizontal swimming in the direction of shallow water (to the shoreline) on ebb and in the direction of deeper water (to the channel) during flood. Swimming speed for this behavior and most others is set at 8 cm s^{-1} which is approximately 1.5 body lengths per second for adult delta smelt. Vertical tidal migration was also explored using the 3D PTM, but found to be less effective at retaining particles in the freshwater (unstratified) portion of the estuary and not carried forward into the scenarios documented here.

The specified horizontal tidal migration behavior is effective at retaining particles in the estuary, as shown in Figure 13. However, it tends to move particles far landward and primarily into regions without large net river flow. This leads to large predicted entrainment losses and poor comparison to catch distribution observed in the Spring Kodiak Trawl surveys (Figure 14).

This outcome of this simple tidal migration behavior scenario can be understood to be the opposite extreme of the passive results because the passive scenario the particle distribution shifts strongly in the seaward direction while the tidal migration scenario results in a strong shift in the landward direction exposing particles to entrainment losses.

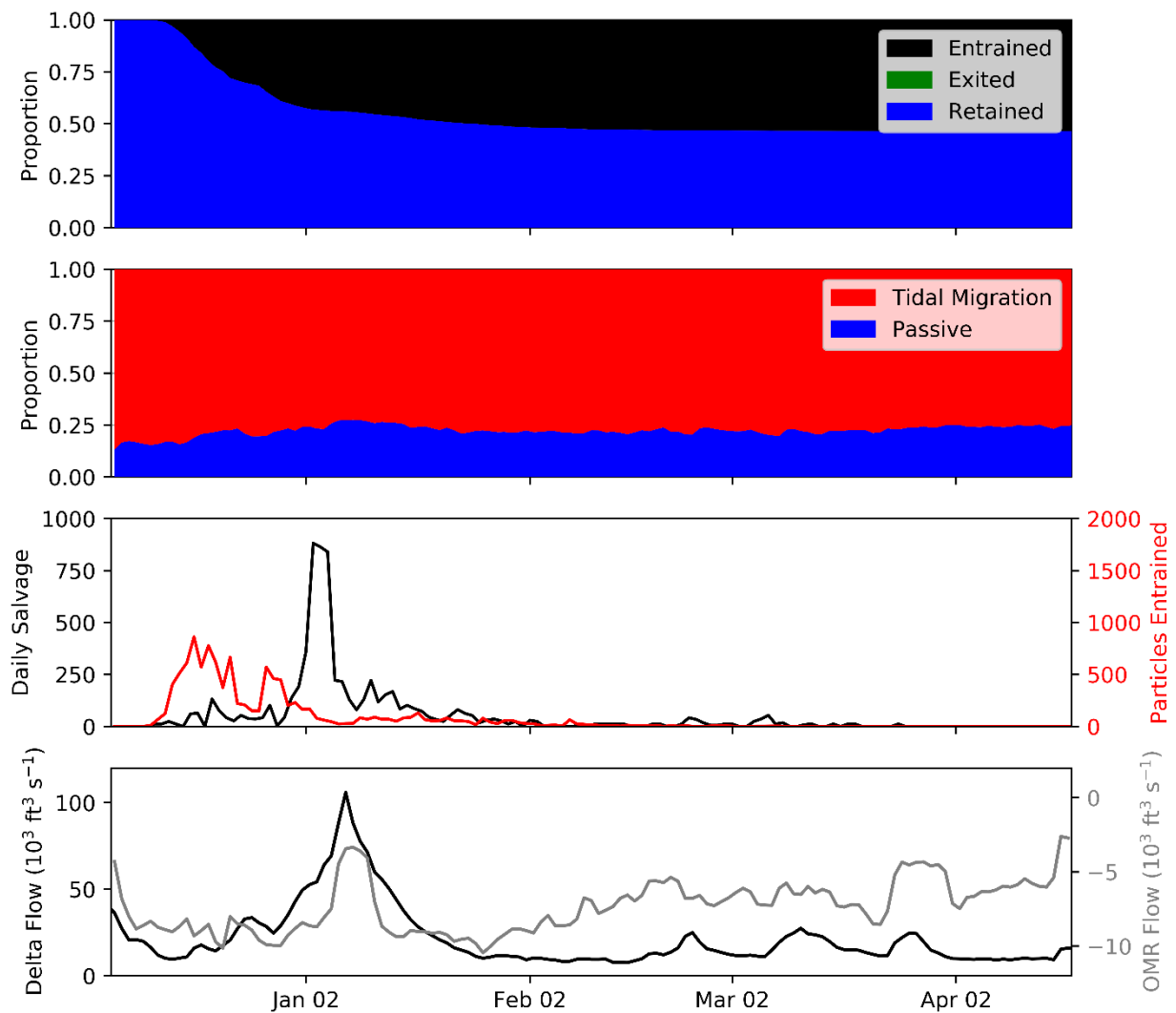


Figure 13. Tidal migration behavior scenario results, three-dimensional model, water year 2002. See caption for Figure 11.

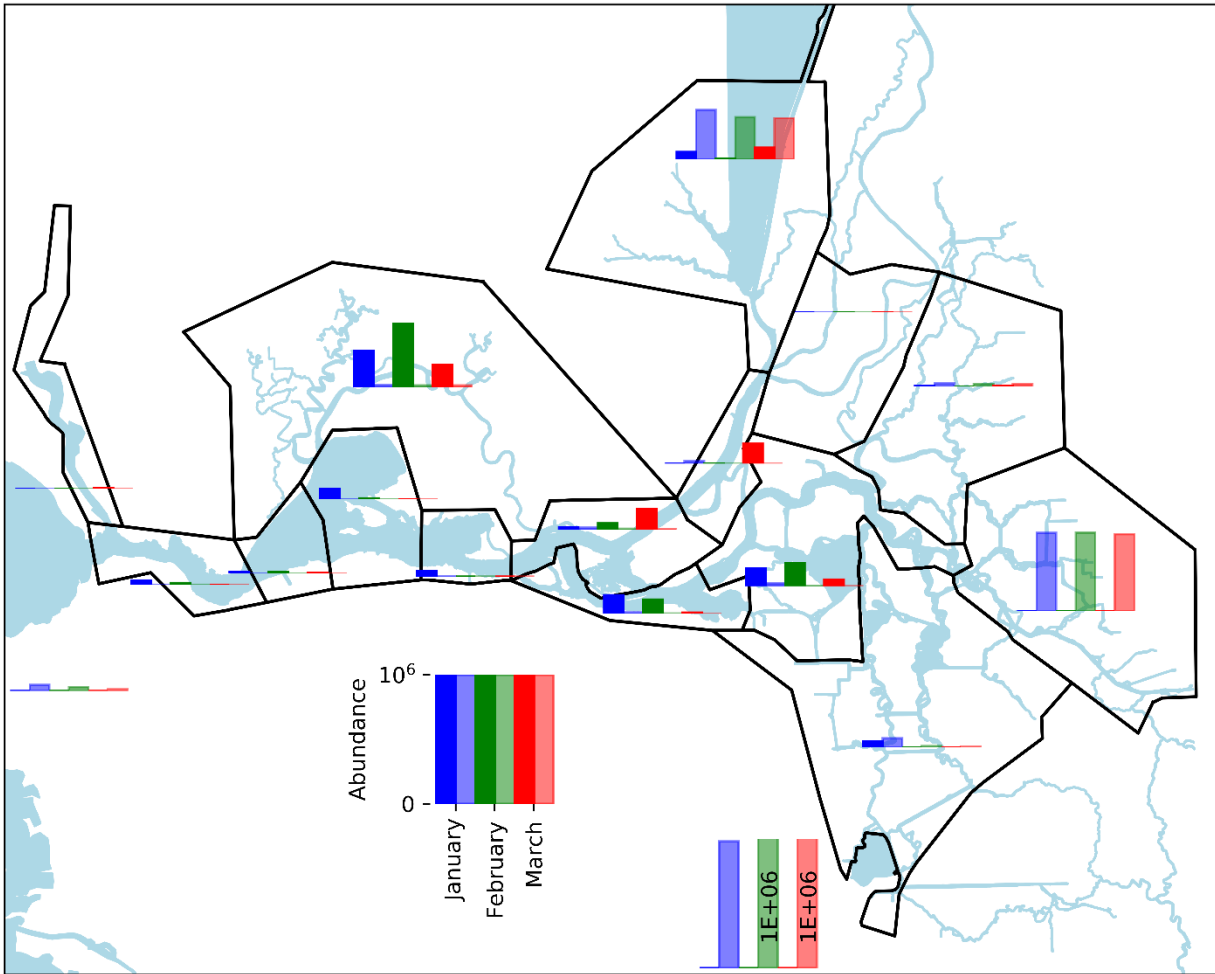


Figure 14. Comparison of predicted regional abundance for the tidal migration behavior scenario, three-dimensional model results, water year 2002 to regional abundance estimated from the Spring Kodiak Trawl surveys. See caption for Figure 12.

Turbidity Seeking

The simple turbidity seeking behavior explored is defined as horizontal swimming in the direction of the positive turbidity gradient. Turbidity seeking behavior results in poor retention, as shown in Figure 15. In the three-dimensional model results some particles are retained in Suisun Marsh (Figure 16), possibly due to weak net velocities through Suisun Marsh and a persistent orientation of turbidity increasing to the eastern (landward) side of Montezuma Slough. Fewer particles are retained in Suisun Marsh in the 2D model results (Figure 16). Turbidity seeking results in minimal entrainment for both models.

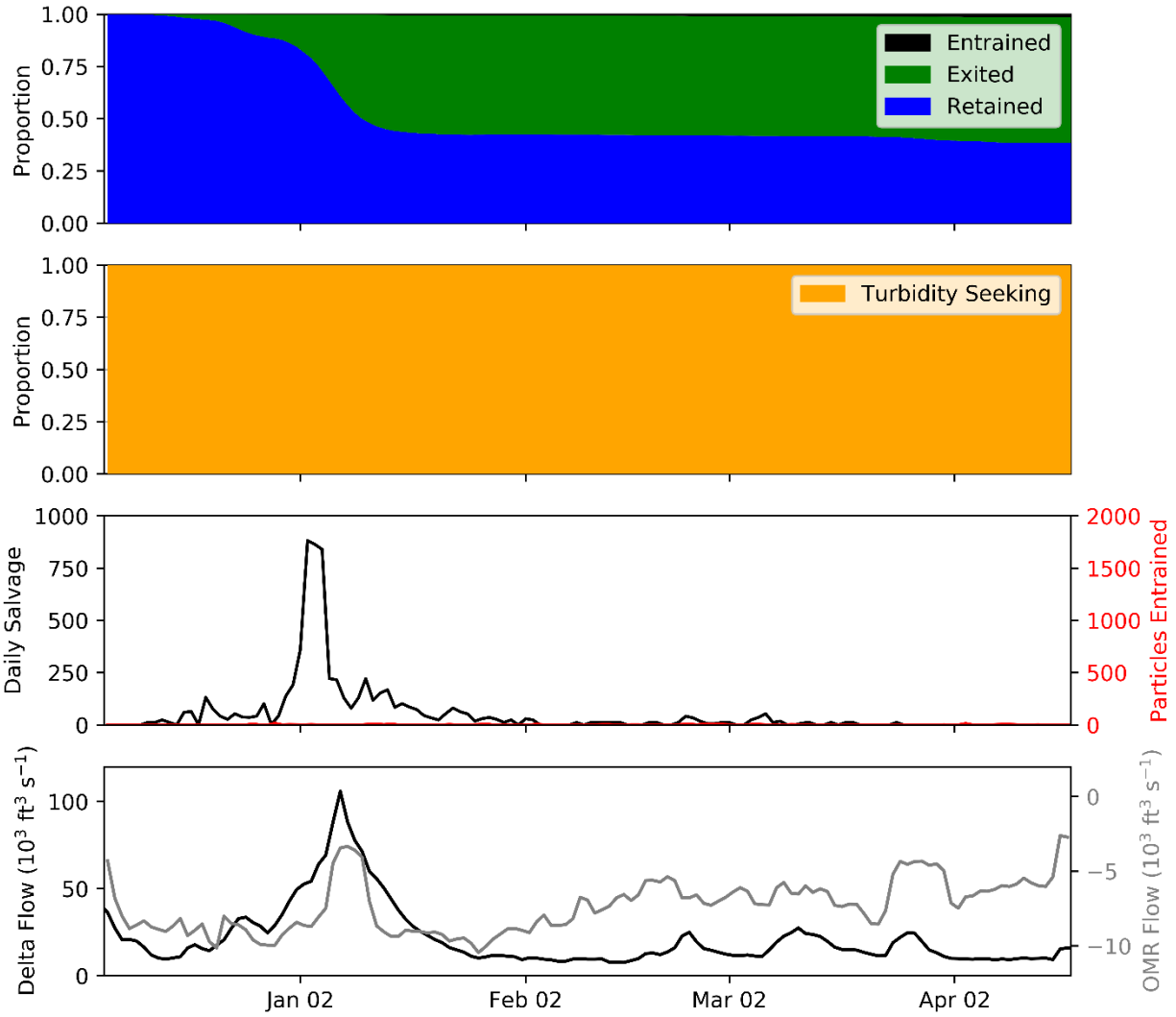


Figure 15. Turbidity seeking behavior scenario results, three-dimensional model, water year 2002. See caption for Figure 11.

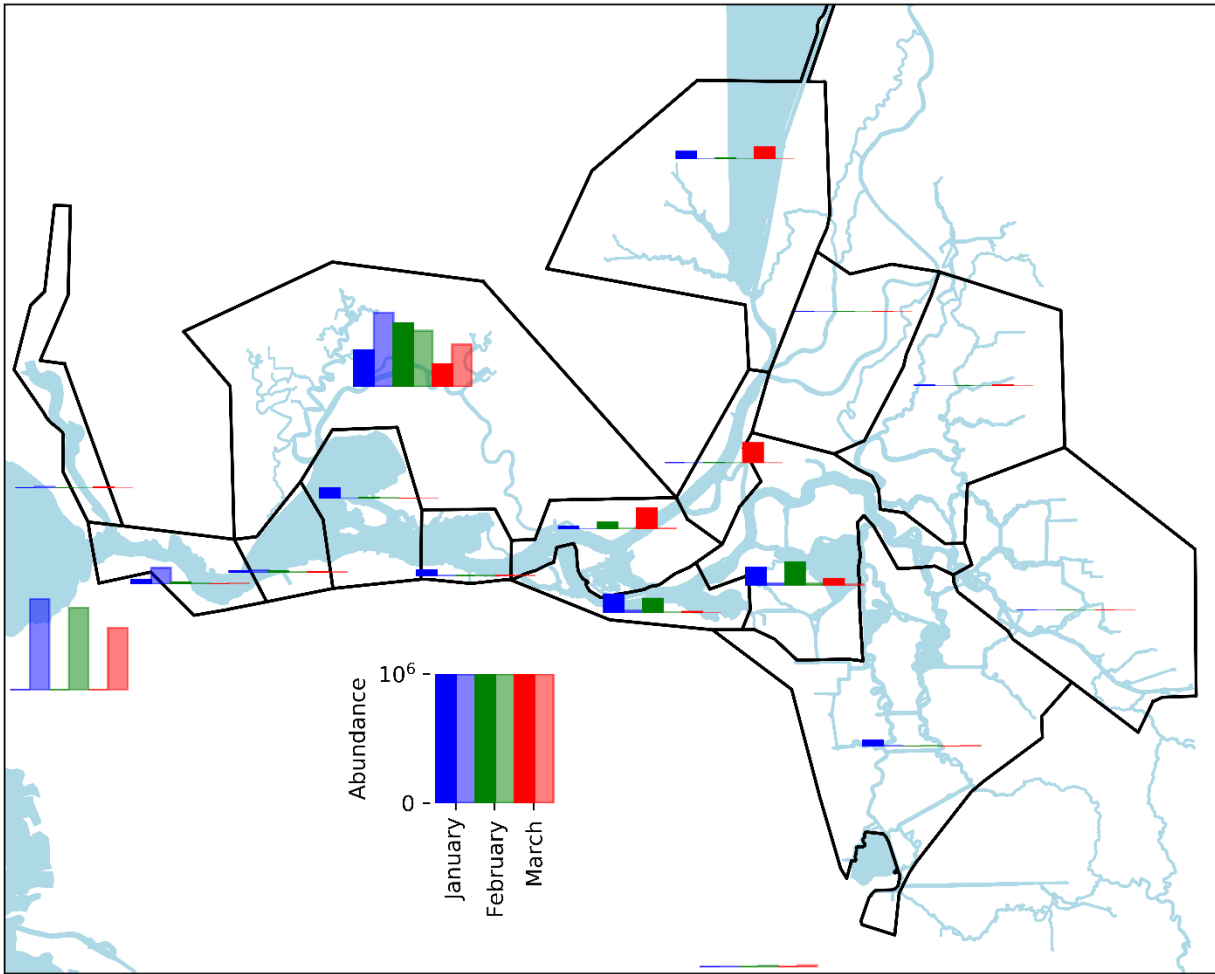


Figure 16. Comparison of predicted regional abundance for the turbidity seeking behavior scenario, three-dimensional model results, water year 2002 to regional abundance estimated from the Spring Kodiak Trawl surveys. See caption for Figure 12.

Freshwater Seeking

Freshwater seeking behavior is defined here as horizontal swimming in the opposite direction of the salinity gradient. Similar to turbidity seeking, freshwater seeking leads to poor retention and low entrainment in all simulations (Figure 17). Freshwater seeking does not retain particles as effectively in Suisun Marsh as turbidity seeking (Figure 18).

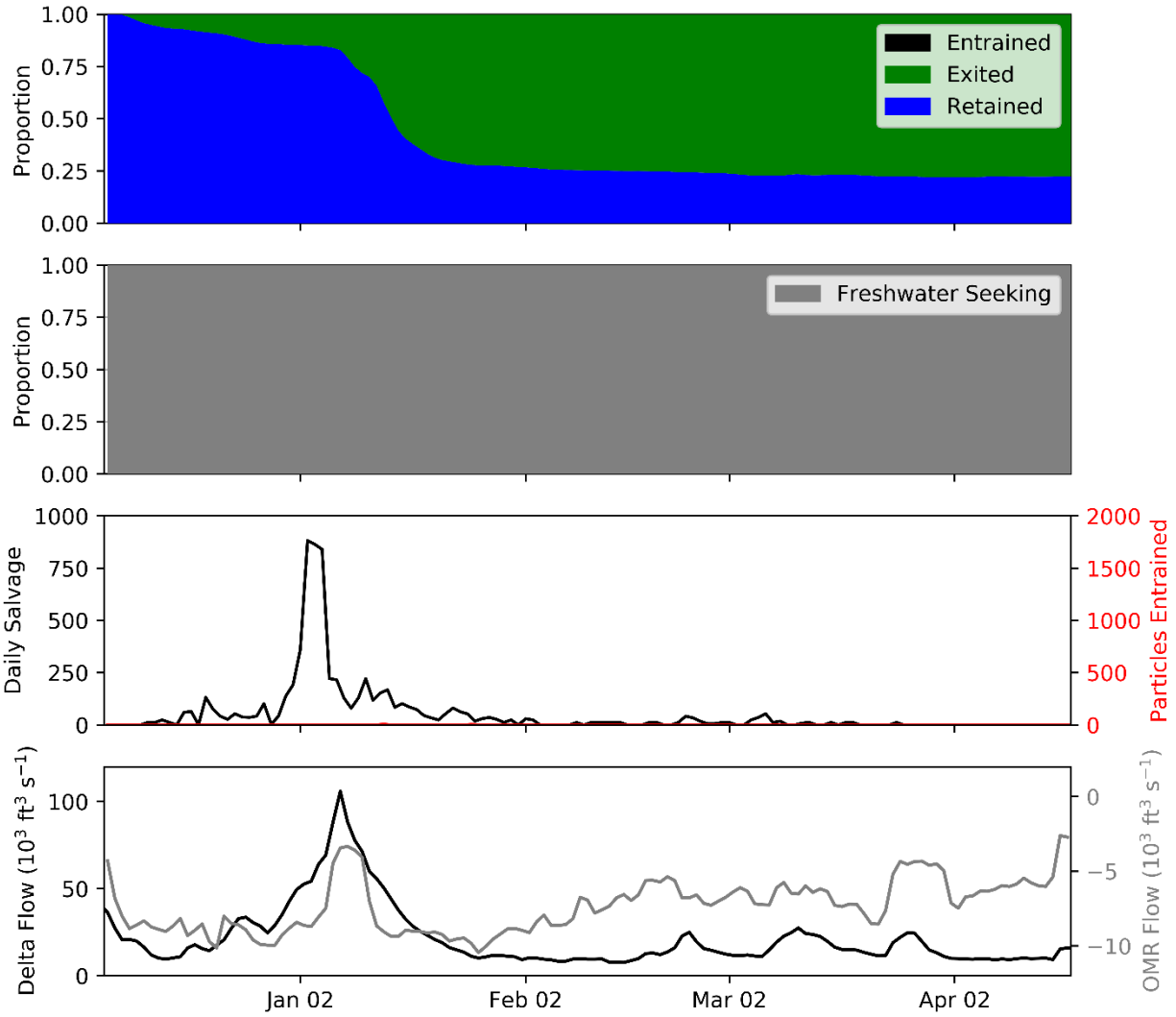


Figure 17. Freshwater seeking behavior scenario results, three-dimensional model, water year 2002. See caption for Figure 11.

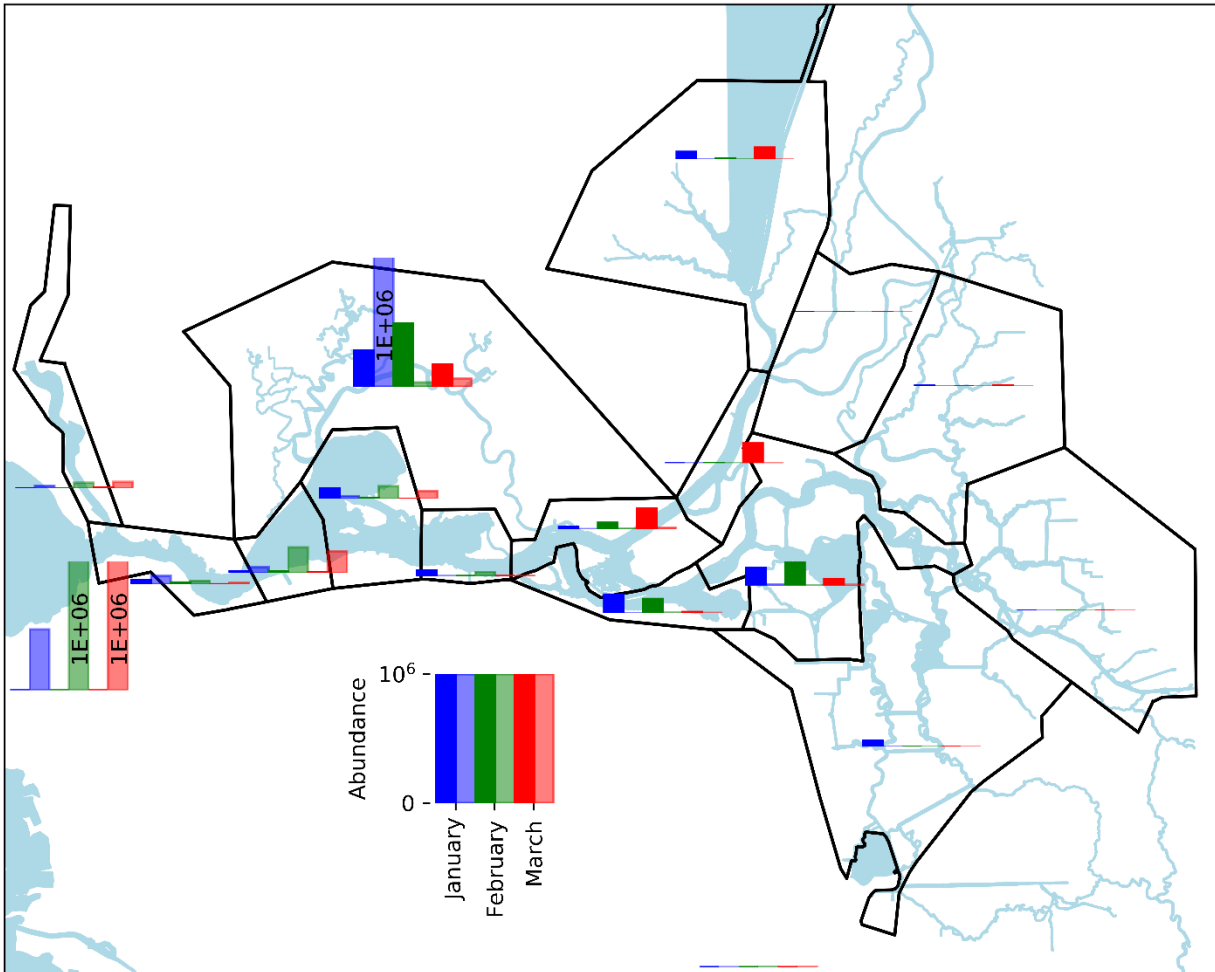


Figure 18. Comparison of predicted regional abundance for the freshwater seeking behavior scenario, three-dimensional model results, water year 2002 to regional abundance estimated from the Spring Kodiak Trawl surveys. See caption for Figure 12.

Conditional Tidal Migration

The simple behaviors explored so far are essentially continuous through the entire simulation period. Though not shown in this report, several more complex variations of these behaviors have been explored, but did not provide substantially improved results. The remaining scenarios reported all involve some form of conditional tidal migration, meaning that tidal migration is performed only under certain environmental conditions. In several cases conditional tidal migration is combined with other behaviors such as holding behaviors. A full set of figures for all behavior sets is provided in Appendix B. Here we will describe the incremental effect of several different aspects of behavior.

A conceptual model of some previous delta smelt studies was tidal migration only in turbid water and, therefore, a “turbidity bridge” would be required to move a substantial portion of delta smelt into the interior Delta against net seaward flows (RMA 2009). In Figure 19 the effect of making tidal migration conditional on turbidity with a threshold of 12 NTU is shown. The application of the turbidity threshold results in substantially less tidal migration yet a higher proportion of particles are entrained. This may be counter intuitive but can be explained by Figure 14 which shows that for continual tidal migration a

portion of the particles move to landward reaches of the domain such as Cache Slough and the San Joaquin River near Stockton. Those particles escape entrainment. However, the conditional tidal migration behavior keeps more particles in the central Delta in January where they are prone to entrainment (Figure 20). The results are not substantially changed by applying a higher turbidity threshold of 18 NTU (Figure 21).

An alternative to turbidity as the primary condition to regulate tidal migration behavior is salinity. Performing tidal migration only when salinity exceeds 1 psu results in greatly reduced entrainment relative to continuous tidal migration (Figure 22). This is understandable because high salinity did not intrude into the Delta in this period so tidal migration only in brackish water did not put many particles at risk of entrainment but was adequate to retain particles in the analysis region. A variation on this behavior is persistent tidal migration in brackish water in which tidal migration persists for at least 12 hours when triggered. The persistence results in slightly improved retention and slightly increased entrainment as shown in Figure 23.

An alternative trigger to initiate persistent tidal migration is perceived salinity change that is triggered when the salinity experienced by the particle is increasing through time. This perceived change trigger may be expected to have somewhat similar behavior to tidal migration in high salinity because it is also likely to be triggered as particles move seaward into more saline regions. However, since it is a proportional change metric in which the change is normalized by the acclimatized salinity experienced by the particle, it can also be triggered by local salinity gradients in regions with salinity less than 1 psu. Therefore, it is more likely to trigger in the interior Delta than the salinity greater than 1 psu trigger. As shown in Figure 24, both behaviors are effective at retaining particles and the trigger associated with increasing salinity leads to higher entrainment because it is more likely to be triggered in landward regions.

As will be seen in the next section on ranking particles, the best performing behaviors generally consist of conditional tidal migration with some form of salinity based trigger in conjunction with conditional holding or another additional behavior type. The effect of the addition of a holding type behavior to the tidal migration in perceived increasing salinity behavior is shown in Figure 25. The addition of holding reduced predicted entrainment in that case, though not in all cases in which holding was applied (see results in Appendix B).

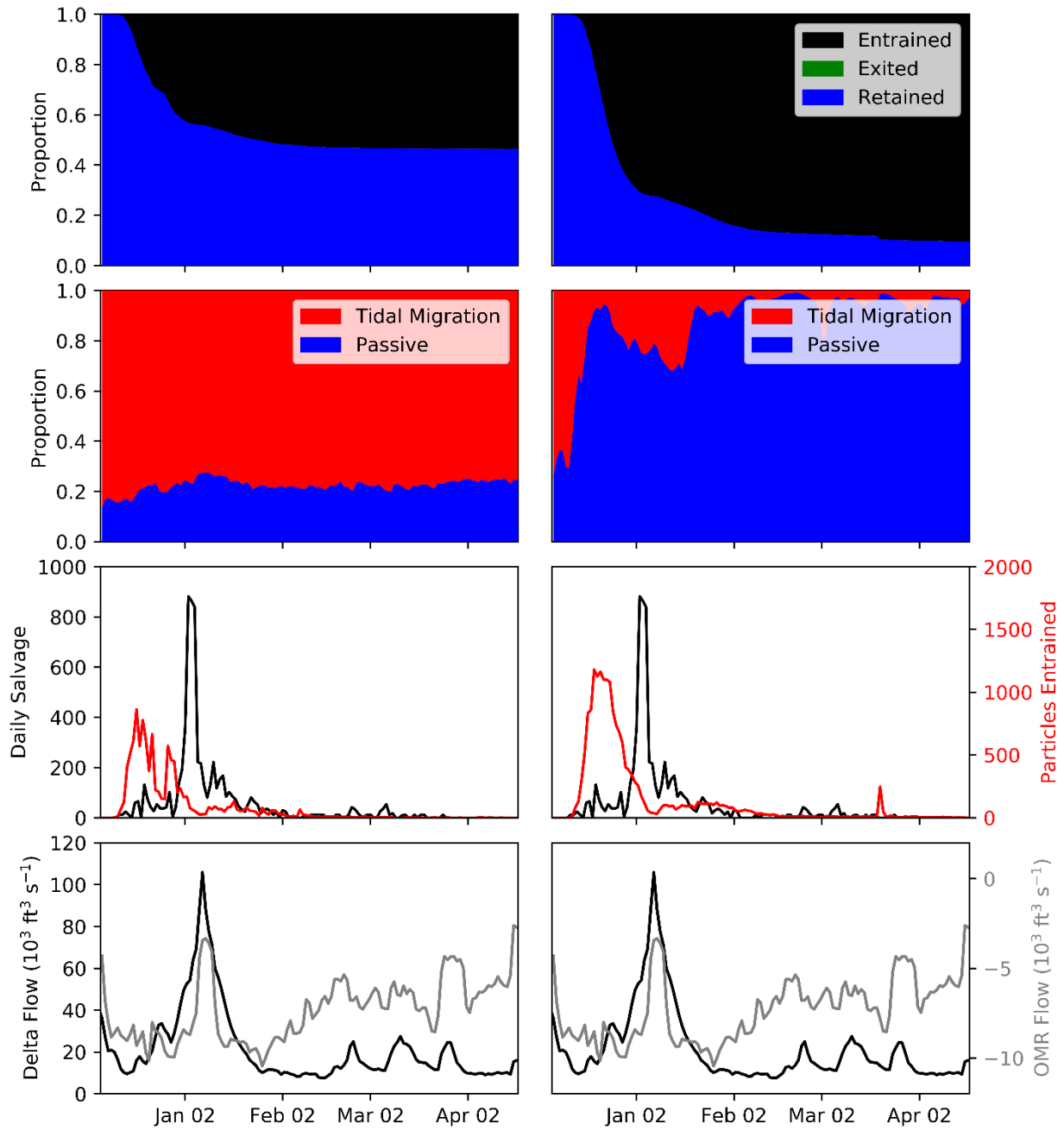


Figure 19. Results of tidal migration behavior set (left panel) and tidal migration in turbid water only behavior set (right panel) for three-dimensional model, water year 2002. See caption for Figure 11.

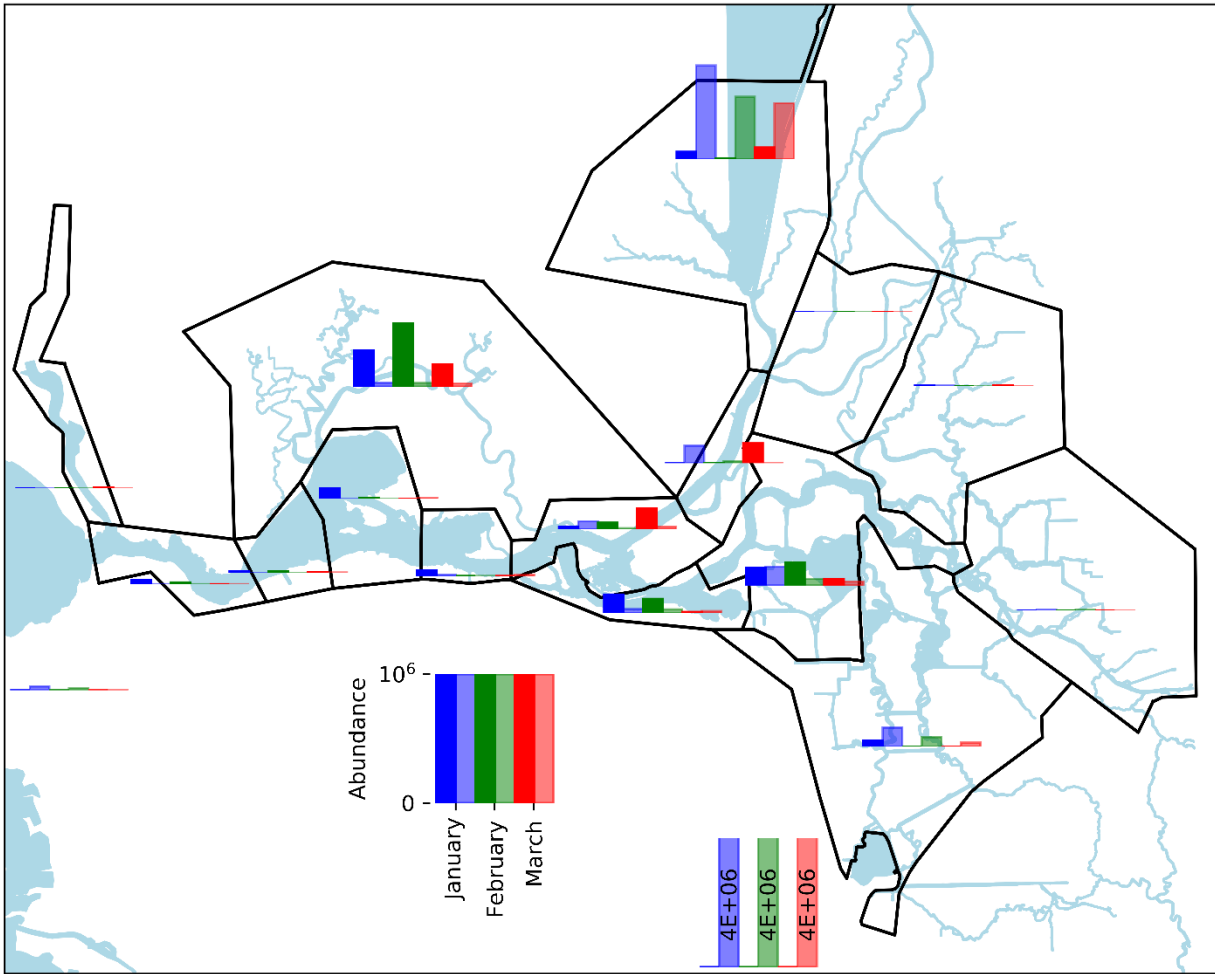


Figure 20. Comparison of predicted regional abundance for the turbidity seeking in turbid water behavior set, three-dimensional model results, water year 2002 to regional abundance estimated from the Spring Kodiak Trawl surveys. See caption for Figure 12.

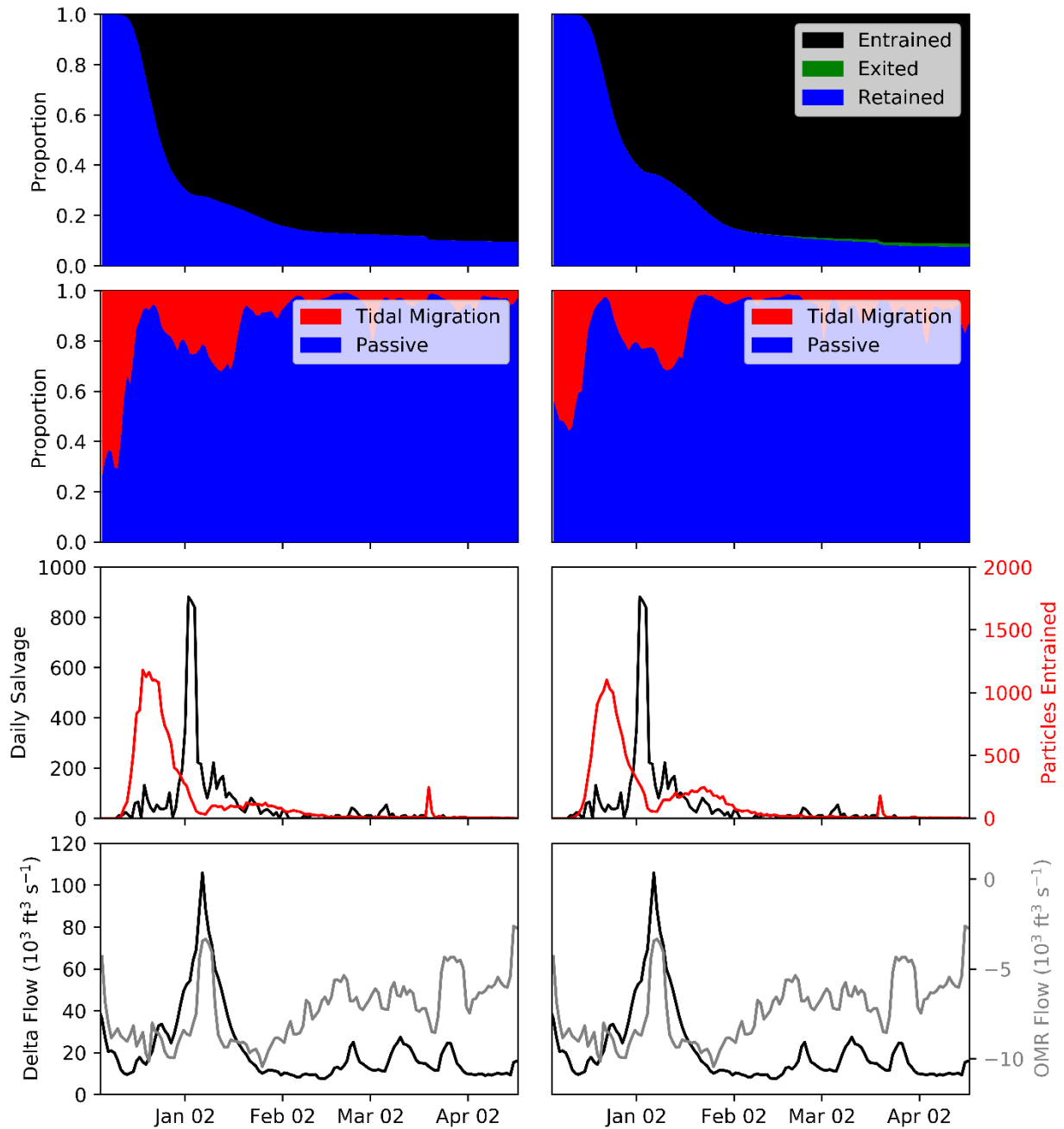


Figure 21. Results of tidal migration in turbid water behavior set (left panel) and tidal migration in highly turbid water behavior set (right panel) for three-dimensional model, water year 2002. See caption for Figure 11.

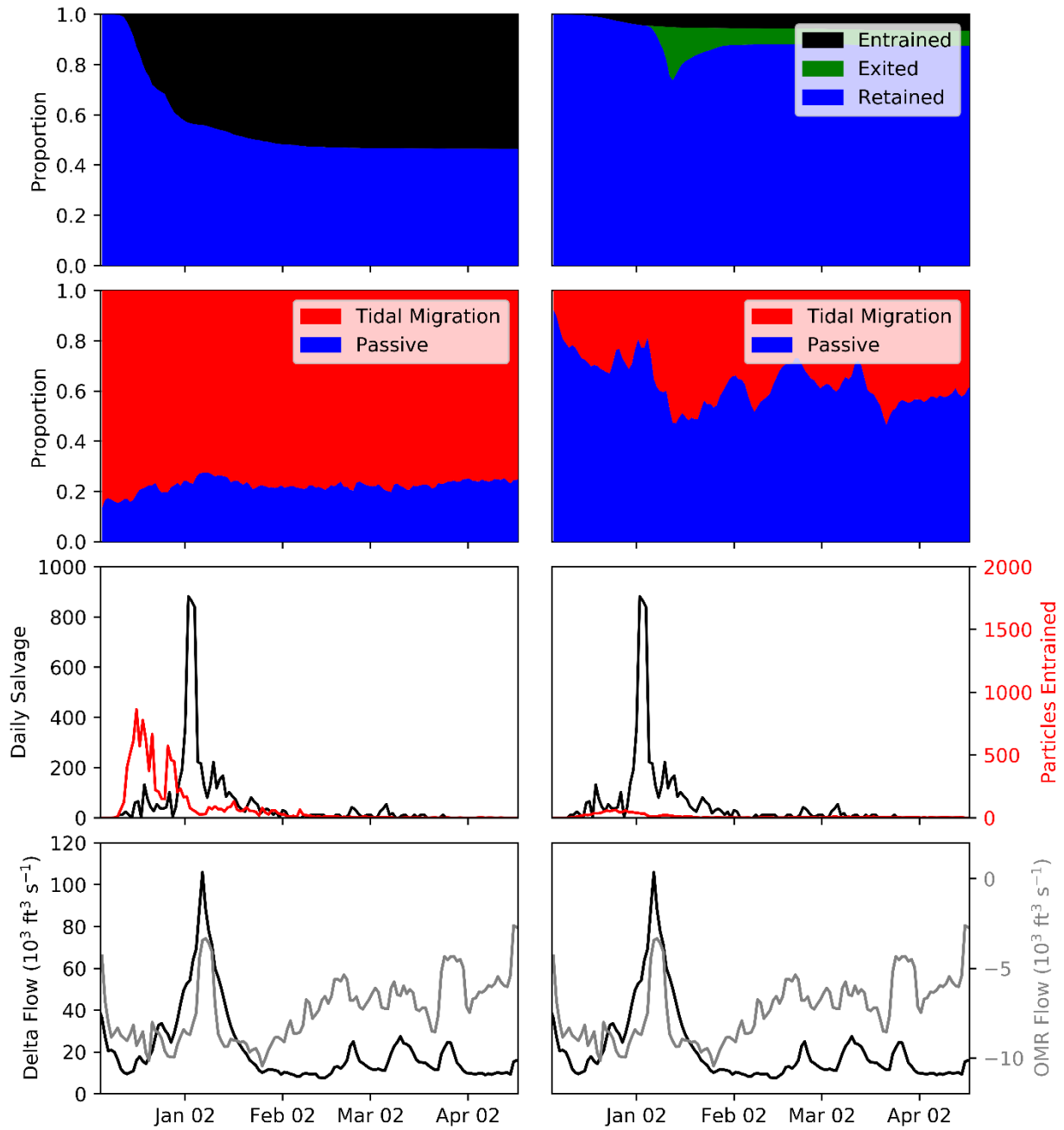


Figure 22. Results of tidal migration behavior set (left panel) and tidal migration in brackish water behavior set (right panel) for three-dimensional model, water year 2002. See caption for Figure 11.

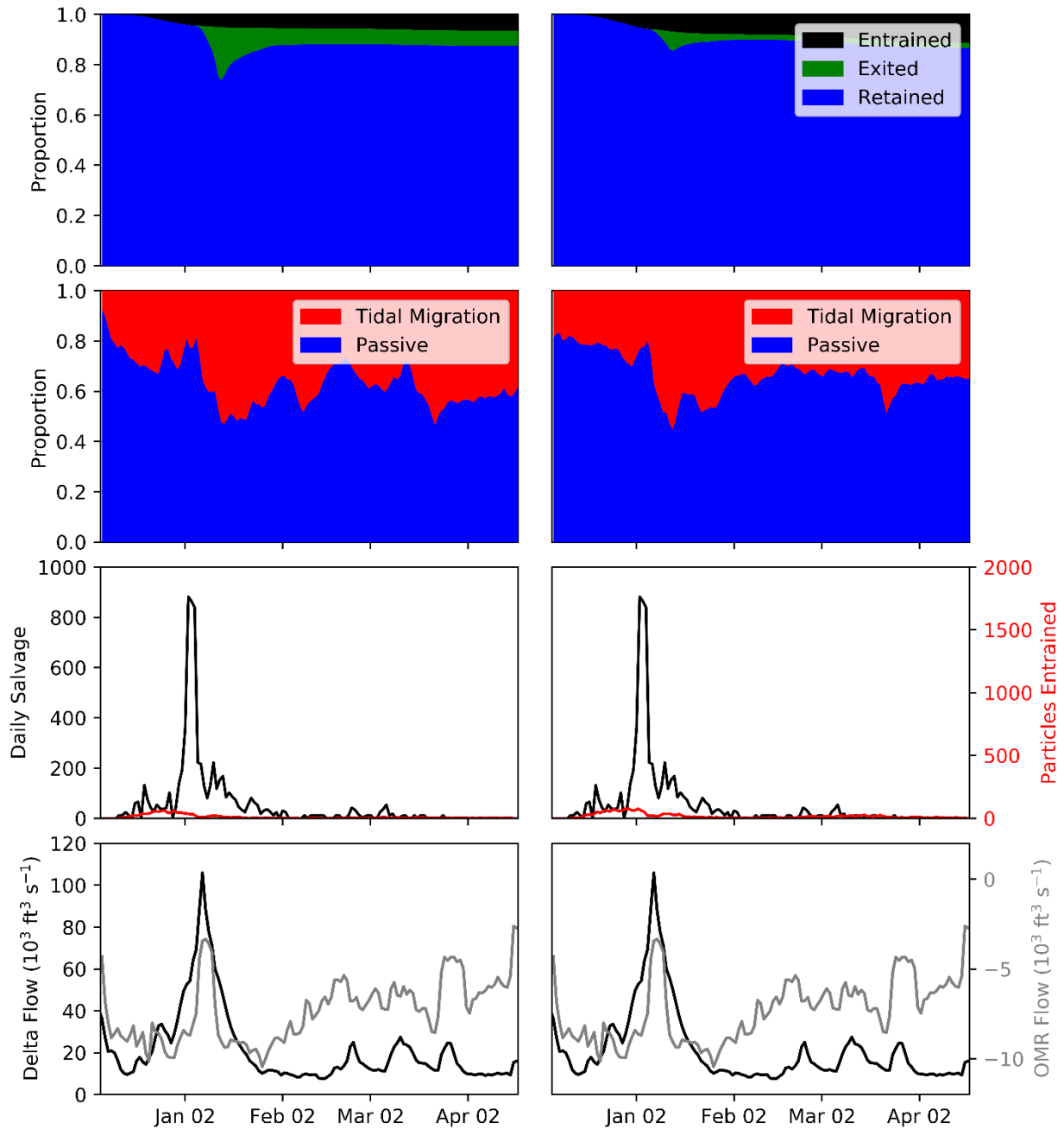


Figure 23. Results of tidal migration in brackish water behavior set (left panel) and persistent tidal migration in brackish water behavior set (right panel) for three-dimensional model, water year 2002. See caption for Figure 11.

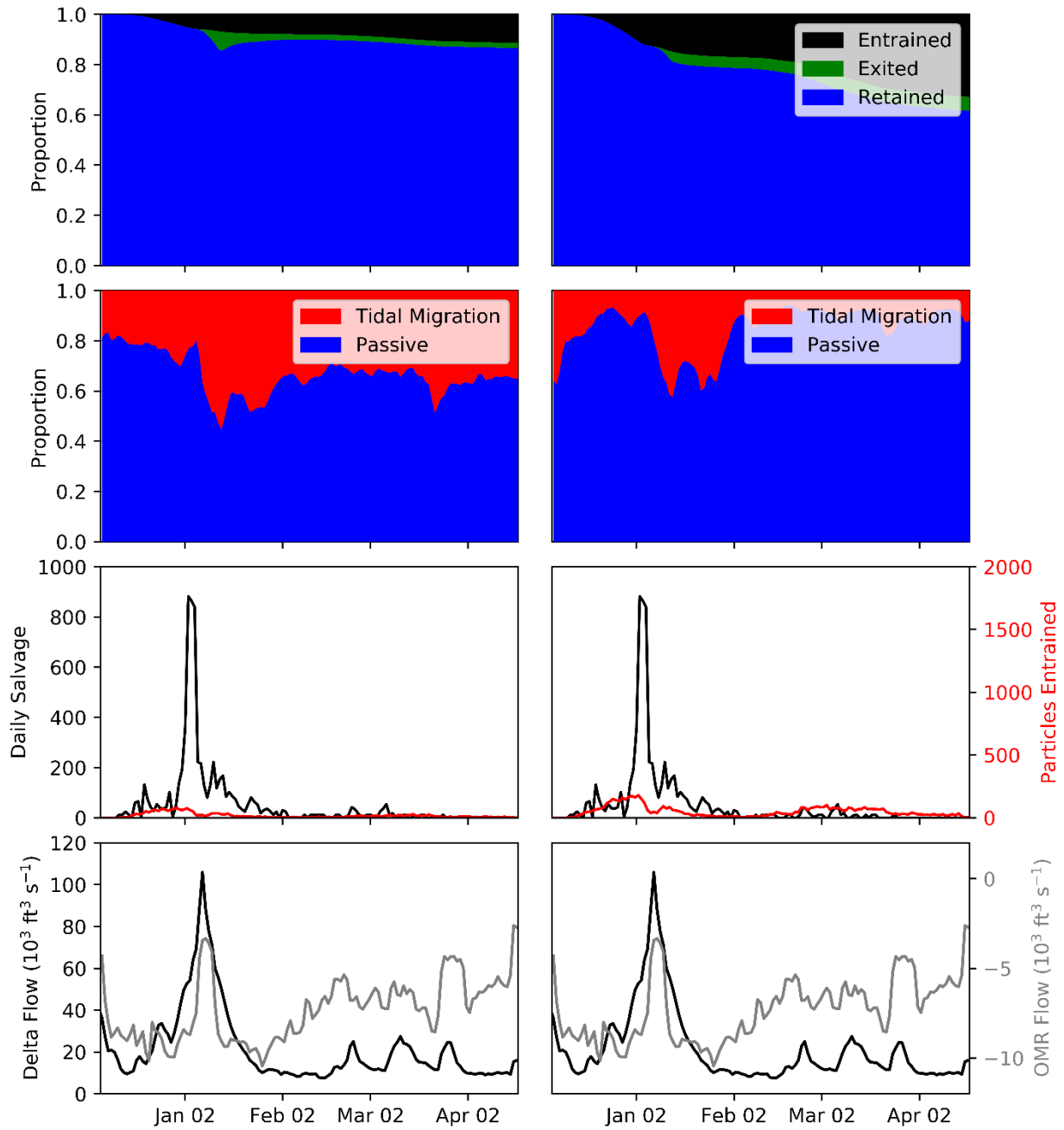


Figure 24. Results of persistent tidal migration in brackish water behavior set (left panel) and persistent tidal migration in increasing salinity behavior set (right panel) for three-dimensional model, water year 2002. See caption for Figure 11.

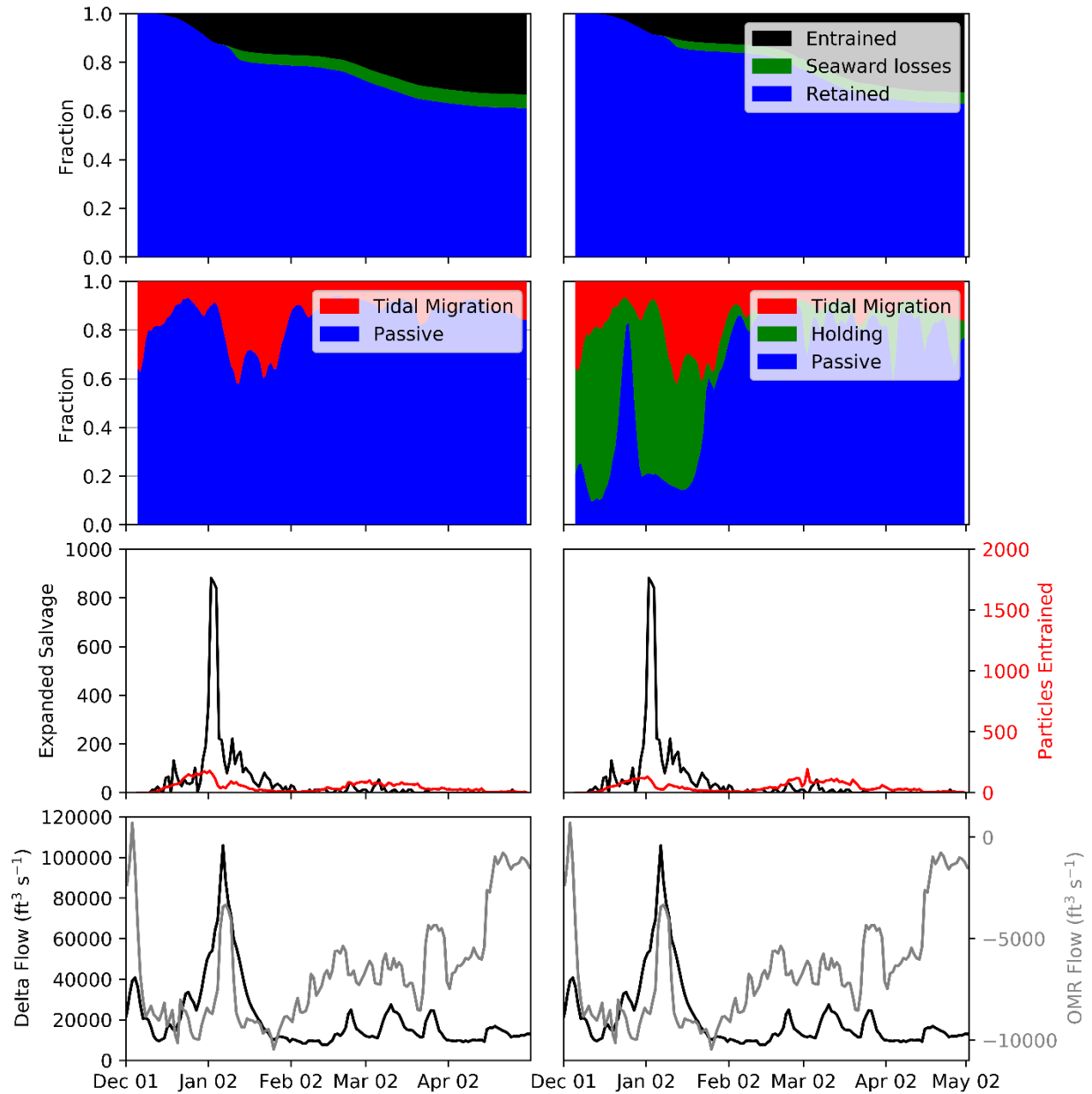


Figure 25. Results of and persistent tidal migration in increasing salinity behavior set (left panel) and persistent tidal migration in increasing salinity, otherwise move to shallow water on ebb in turbid water behavior set (right panel) for three-dimensional model, water year 2002. See caption for Figure 11.

Behavior Ranking

The consistency of predicted distribution with observed catch and salvage is represented by the negative log likelihood as described previously. For each behavior the statistical fitting estimated initial abundance, constant and uniform daily survival (representing natural mortality), and constant salvage efficiency at the SWP and CVP as free parameters. The predicted movement and proportional distribution is completely determined by the particle-tracking results. The initial abundance was

constrained to a maximum of 5 million and the daily survival was constrained to a minimum of 0.99. Salvage efficiency was not constrained.

The negative log likelihood for each behavior set for the Dec 5, 2001 release time is shown in Figure 26. All behaviors that did not use some form of tidal migration exhibited high domain losses. Tidal migration alone also performed poorly, as could be expected from the high entrainment shown in Figure 13.

The negative log likelihood for each behavior set for the Dec 5, 2001 release time for both 3D and 2D model results is shown in Figure 27. For the majority of the behaviors the negative log likelihood for the 2D model results is similar to the negative log likelihood for the 3D model results. Notable exceptions include behaviors involving freshwater seeking.

Two-dimensional model results for each behavior set were generated for water year 2004. The negative log likelihood for each behavior set for the Dec 5, 2001 release time and Dec 12, 2003 release time for 2D model results is shown in Figure 28. There are large differences in negative log likelihood for several behaviors, with generally higher (worse) negative log likelihood for water year 2004 results. This is partially due to the unusual flow pattern in 2004, with peak flow in March which caused late season salvage (Figure 6). Despite differences in the performance of several behaviors, the best performing behaviors were fairly consistent between the two water years. For example, `ptmd_sal_gt_1_h8_ebb_shallow_t_gt_18_acclim` was among the lowest log likelihoods in the two different water years.

Because there is some uncertainty in the timing of the spawning migration, the sensitivity of model results to particle release time was also explored. The negative log likelihood for each behavior set for the Dec 5, 2001 release time and Dec 20, 2001 release time for 3D model results is shown in Figure 29. The negative log likelihood for each behavior set for the Dec 5, 2001 release time and Dec 20, 2001 release time for 2D model results is shown in Figure 30. The Dec 20, 2001 release time generally resulting in larger negative log likelihood for most behavior sets indicating poorer comparison to observations. However, the ranking of behavior sets by negative log likelihood was similar between the two release times. Due to the larger negative log likelihood of the Dec 20, 2001 release time, indicating poorer match to observed distribution, we have focused on the Dec 5, 2001 release time results.

The overall ranking in order of increasing negative log likelihood for each behavior set is shown in Table 1. The distribution of particles at the end of the analysis period for the 3D water year 2002 hydrodynamic scenario, is shown in order of increasing negative log likelihood in Figure 31. In this ordering the top ranked behavior is shown as the top row. The two-dimensional model results for water year 2002 and 2004 are shown in Figure 32 and Figure 33. All behaviors with poor retention are ranked near the bottom. All top ranked behavior sets show good retention but several have entrainment losses higher than suggested by previous studies (e.g. Kimmerer 2008). There are several possible reasons for that discrepancy which will be explored in Korman et al. (2018). The estimated initial abundance of delta smelt is provided in Table 2. The initial abundance is constrained to 5 million. The estimated initial abundance varies substantially among hydrodynamic scenarios and behavior sets and for several behavior sets reaches the maximum of 5 million delta smelt. The initial abundance and other fitting parameters will be explored and discussed in more detail in Korman et al. (2018). It should be noted that the proportion of particles in each region is determined entirely by the particle-tracking for each behavior set and therefore the predicted distribution is the focus of this report. The coefficient of determination in predicting regional abundance estimate from expansion of Spring Kodiak Trawl catch is

provided for each behavior and hydrodynamic scenario in Table 3. The particle-tracking for each behavior set also determines the timing of predicted entrainment though the survival parameter can alter the magnitude of late season predicted entrainment relative to earlier season entrainment to a limited extent.

Several behaviors are ranked high for all three hydrodynamic scenarios. Specifically, the behavior sets ptmd_sal_gt_1_h8_ebb_shallow_t_gt_18_acclim, tmd_sal_gt_1_ebb_shallow_t_gt_18, and tmd_sal_gt_1_ptmd_ptmd_sd_pt_1_switch are each top ranked in one hydrodynamic scenario and within the top 6 ranked behavior sets for all 3 hydrodynamic scenarios. Therefore, these behaviors have all been selected for further analysis which will include fitting an initial distribution and further exploration of salvage efficiency. Because all three of those top ranked behaviors had relatively high entrainment, two moderate entrainment scenarios, ptmd_si_pt_5_h8_t_gt_18_acclim and ptmd_sal_gt_1_si_pt_5, were also chosen more subjectively based on middle to high ranking, simplicity and moderate entrainment. The simplest scenarios including passive, turbidity seeking and tidal migration were also included for further analysis as those behavior types have been discussed in the literature. Lastly, since the top ranked behaviors all involve some form of salinity triggered tidal migration, both ptmd_sal_gt_1 and ptmd_si_pt_5 were also selected.

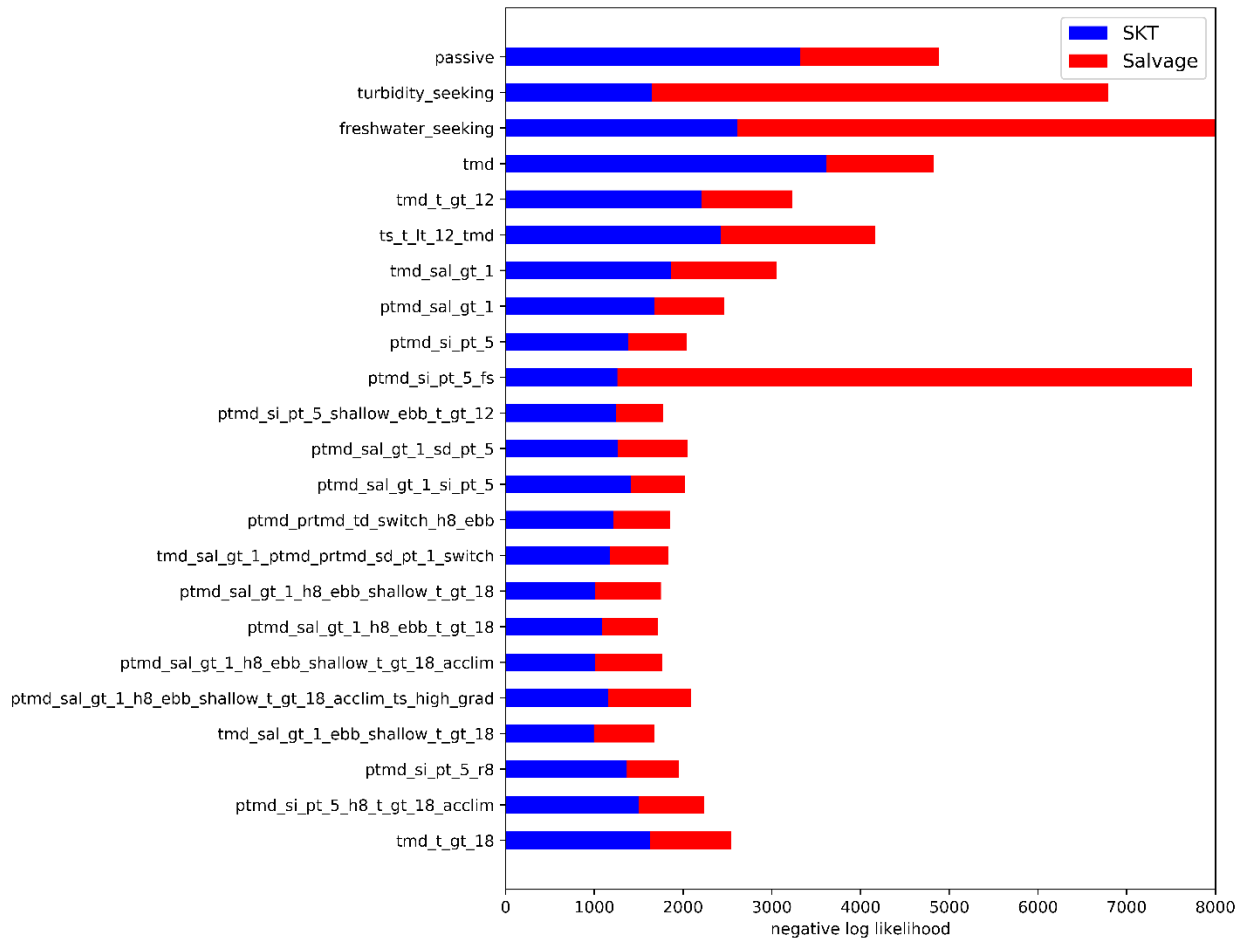


Figure 26. Three-dimensional model results for the Dec 5, 2001 release time. Blue bars indicate the portion of negative log likelihood associated with the comparison of predicted regional abundance with Spring Kodiak Trawl catch while the red bars indicate the portion of negative log likelihood associated the comparison of predicted entrainment with entrained based on observed daily salvage and salvage efficiency parameters. Results plotted as negative log likelihood so that shorter bars indicate more consistency between model results and observations. A description of the behavior set associated with each bar is given in Appendix A.

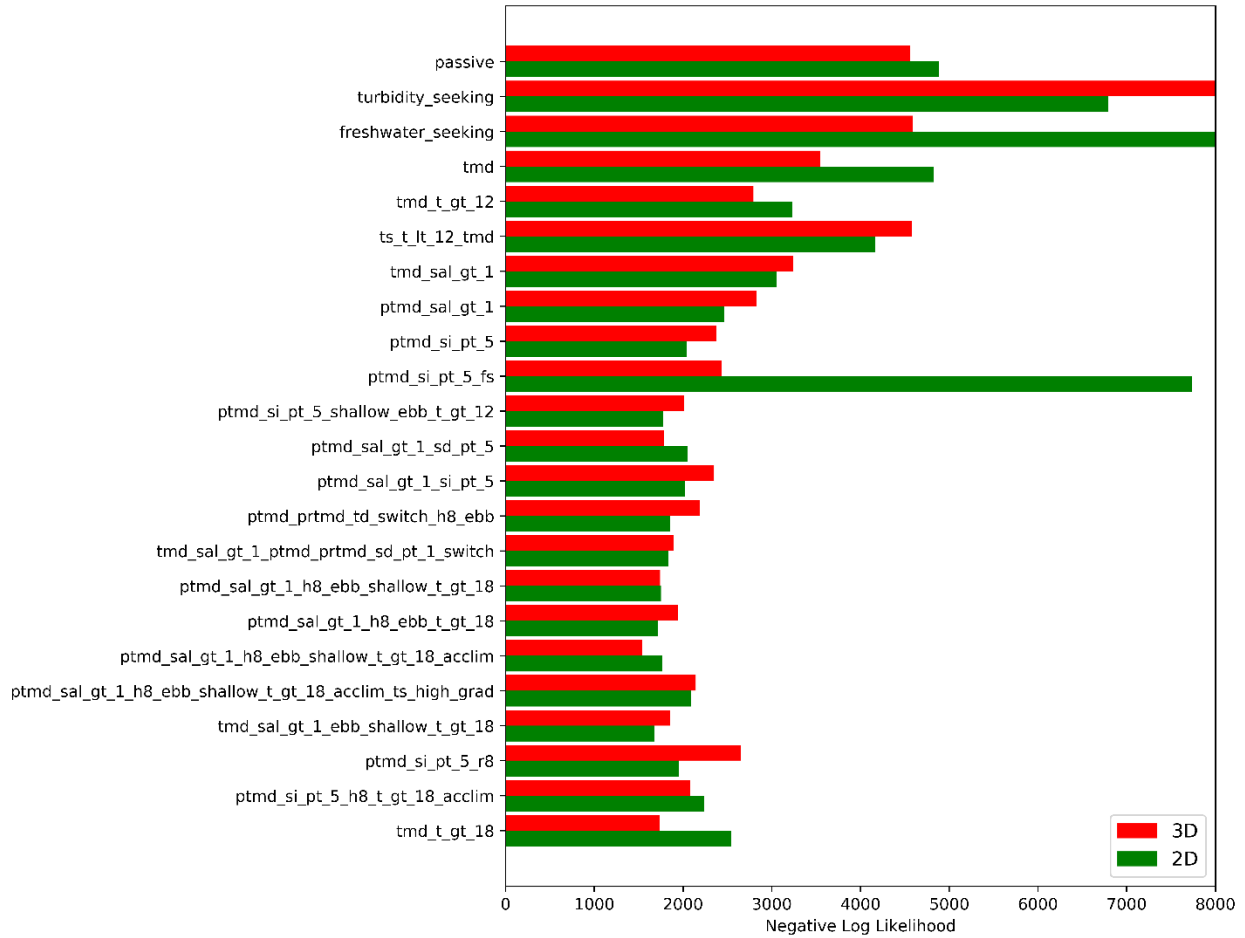


Figure 27. Negative log likelihood associated with three-dimensional and two-dimensional model results for Dec 5, 2001 release time. Each bar shows negative the log likelihood based on comparison with Spring Kodiak Trawl catch and observed daily salvage. Shorter bars indicate better results. A description of the behavior set associated with each bar is given in Appendix A.

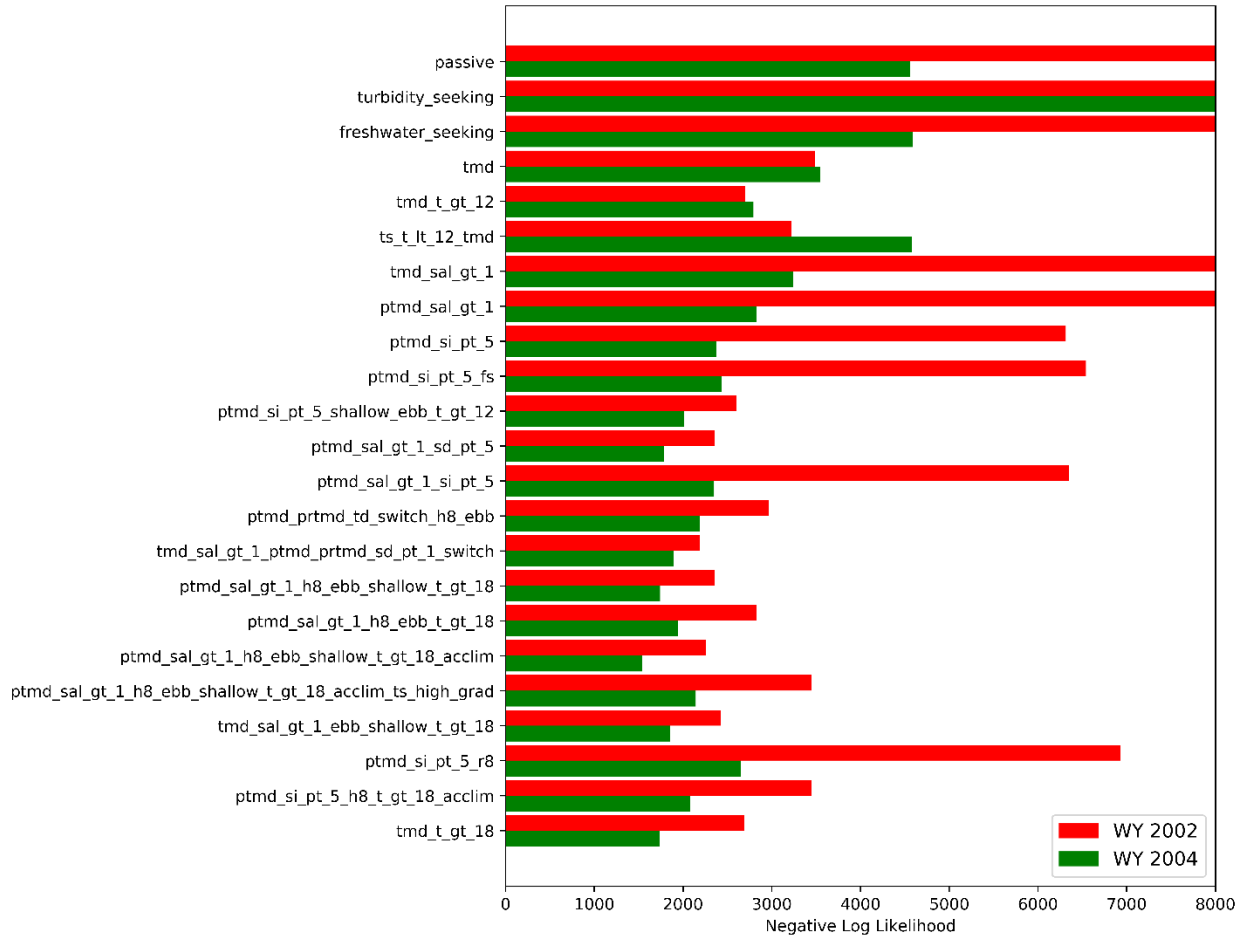


Figure 28. Negative log likelihood associated with two-dimensional model results for Dec 5, 2001 release time and Dec 12, 2003 release time. See caption for Figure 27.

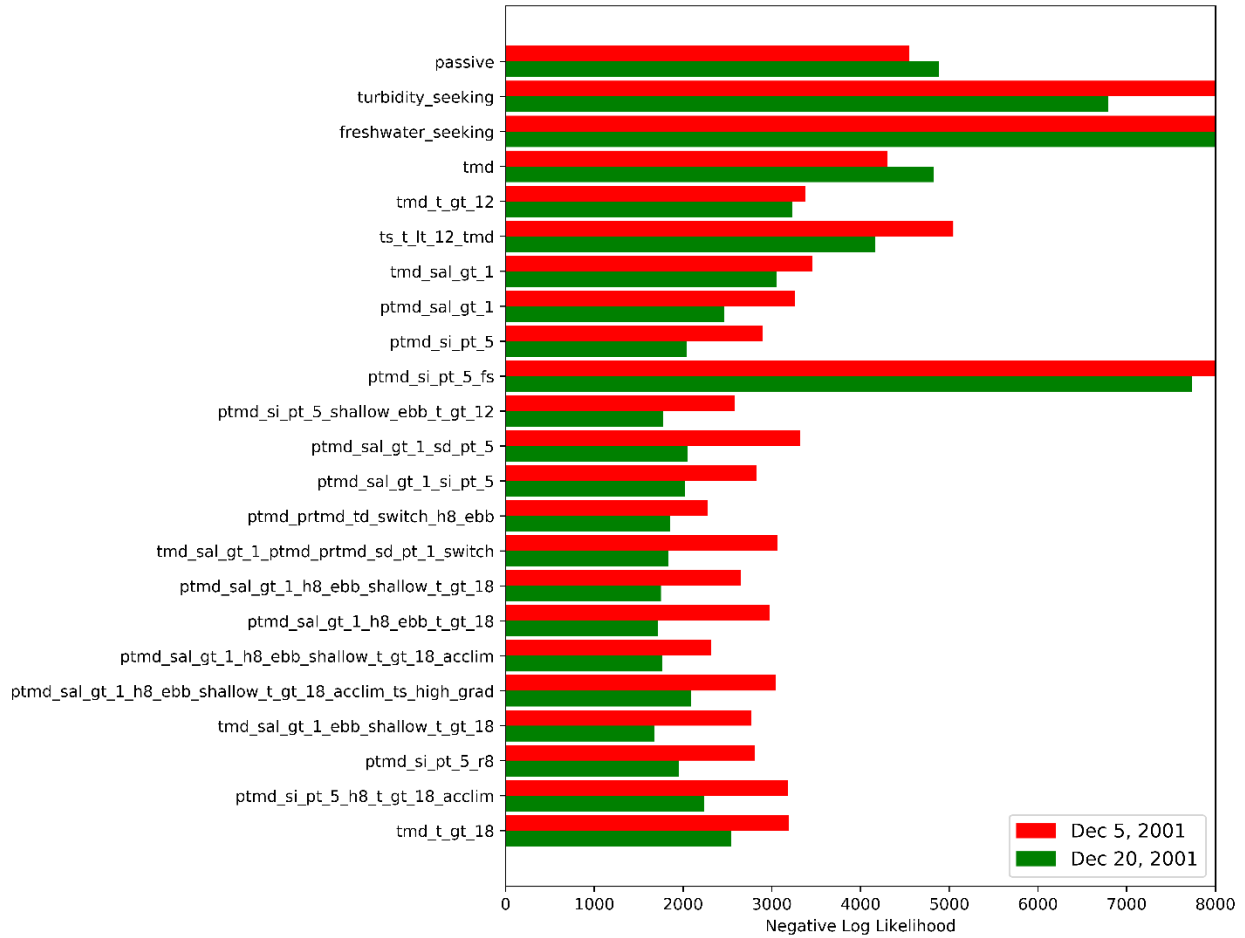


Figure 29. Negative log likelihood associated with three-dimensional model results for Dec 5, 2001 release time and Dec 20, 2001 release time. See caption for Figure 27.

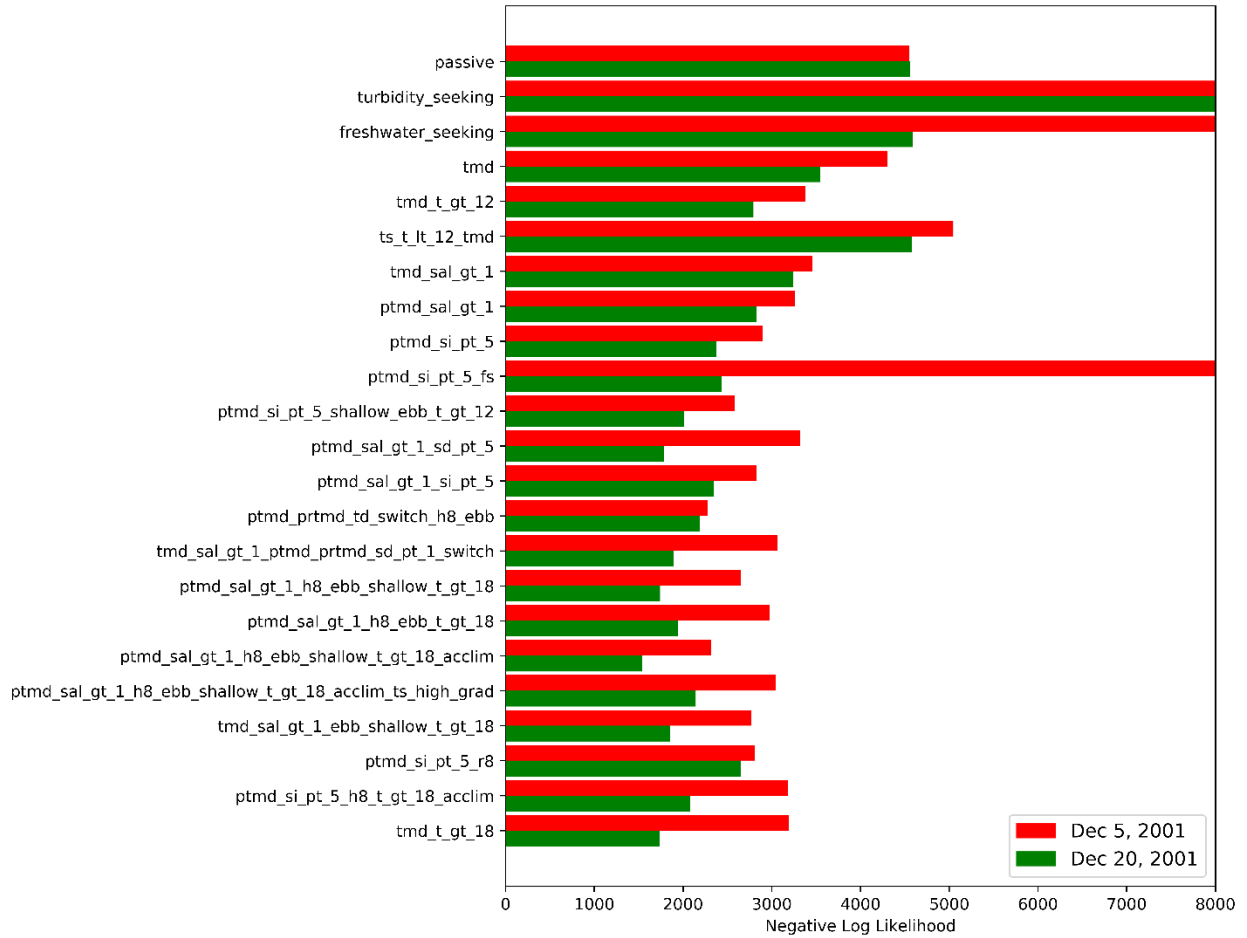


Figure 30. Negative log likelihood associated with two-dimensional model results for Dec 5, 2001 release time and Dec 20, 2001 release time. See caption for Figure 27.

Table 1. Ranking of behavior sets by increasing negative log likelihood for individual hydrodynamic scenarios.

Behavior	Rank			
	3D 2002	2D 2002	2D 2004	Average
ptmd_sal_gt_1_h8_ebb_shallow_t_gt_18_acclim	4	1	2	2.33
ptmd_sal_gt_1_h8_ebb_shallow_t_gt_18	3	3	4	3.33
tmd_sal_gt_1_ebb_shallow_t_gt_18	1	5	5	3.67
tmd_sal_gt_1_ptmd_prtmd_sd_pt_1_switch	6	6	1	4.33
ptmd_sal_gt_1_sd_pt_5	11	4	3	6.00
ptmd_sal_gt_1_h8_ebb_t_gt_18	2	7	9	6.00
ptmd_si_pt_5_shallow_ebb_t_gt_12	5	8	6	6.33
tmd_t_gt_18	15	2	7	8.00
ptmd_prtmd_td_switch_h8_ebb	7	11	10	9.33
ptmd_sal_gt_1_h8_ebb_shallow_t_gt_18_acclim_ts_high_grad	12	10	12	11.33
ptmd_si_pt_5_h8_t_gt_18_acclim	13	9	13	11.67
ptmd_sal_gt_1_si_pt_5	9	12	16	12.33
ptmd_si_pt_5	10	13	15	12.67
tmd_t_gt_12	17	16	8	13.67
ptmd_si_pt_5_r8	8	15	18	13.67
ptmd_sal_gt_1	14	17	19	16.67
ts_t_lt_12_tmd	18	21	11	16.67
Tmd	19	19	14	17.33
ptmd_si_pt_5_fs	22	14	17	17.67
tmd_sal_gt_1	16	18	21	18.33
Passive	20	20	20	20.00
turbidity_seeking	21	23	23	22.33
freshwater_seeking	23	22	22	22.33

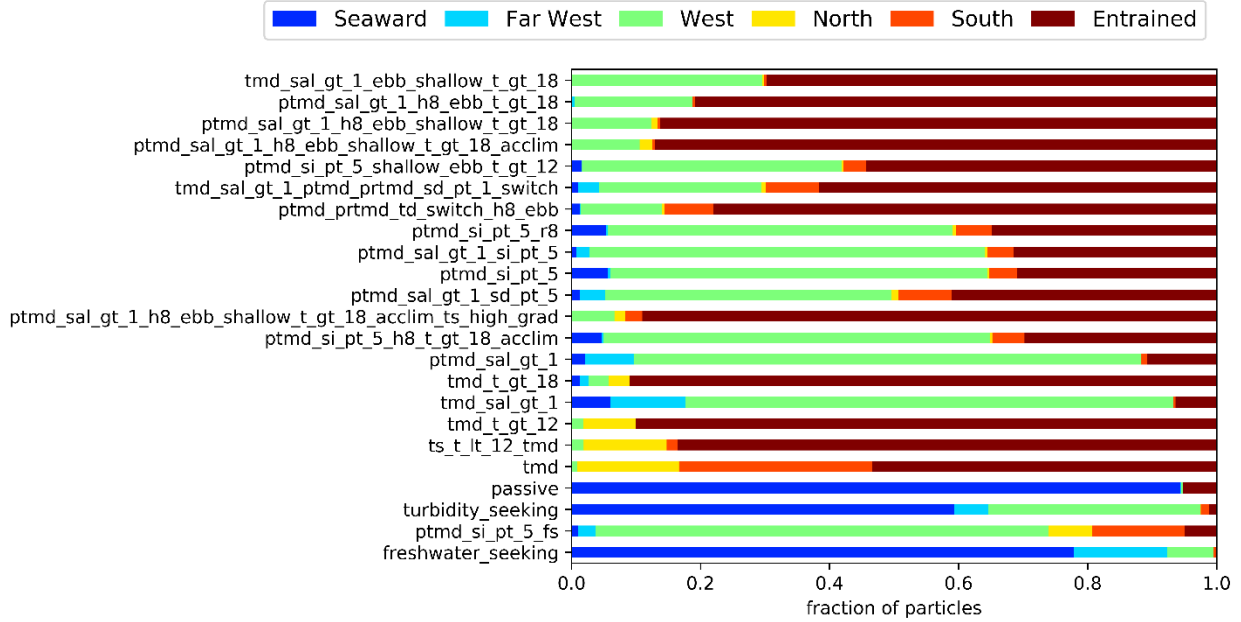


Figure 31. Particle distribution at the end of the simulation period in order of increasing negative log likelihood for the three-dimensional model results for water year 2002. In this ordering the best performing behavior set is the top row.

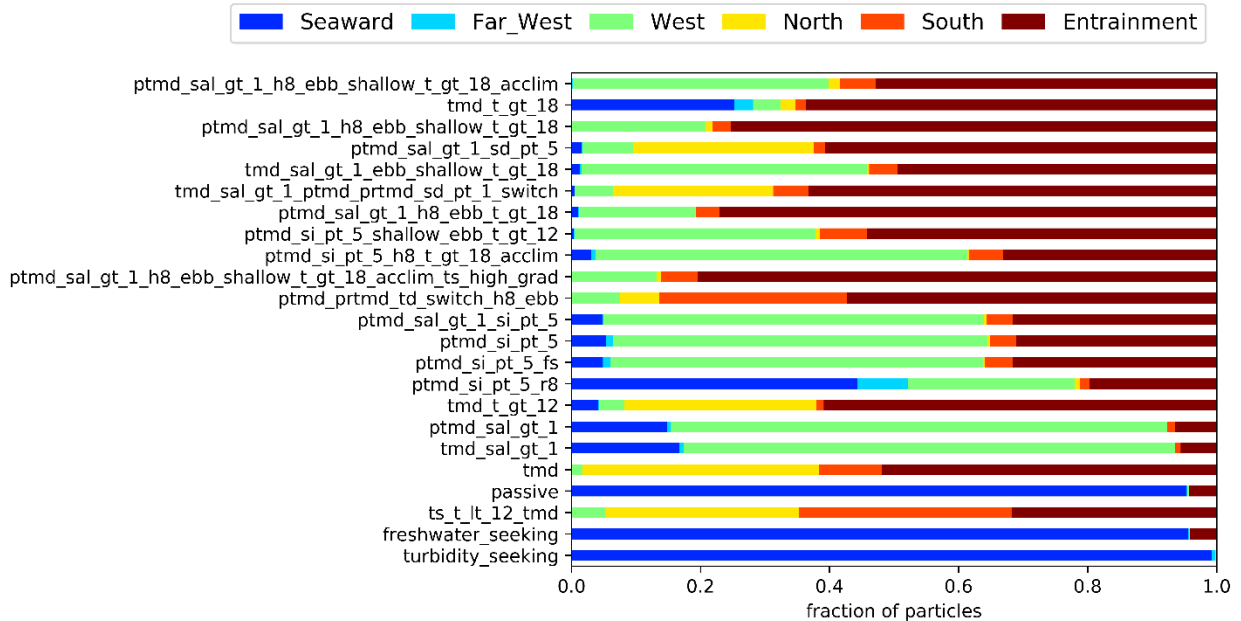


Figure 32. Particle distribution at the end of the simulation period in order of increasing negative log likelihood for the two-dimensional model results for water year 2002. In this ordering the best performing behavior set is the top row.

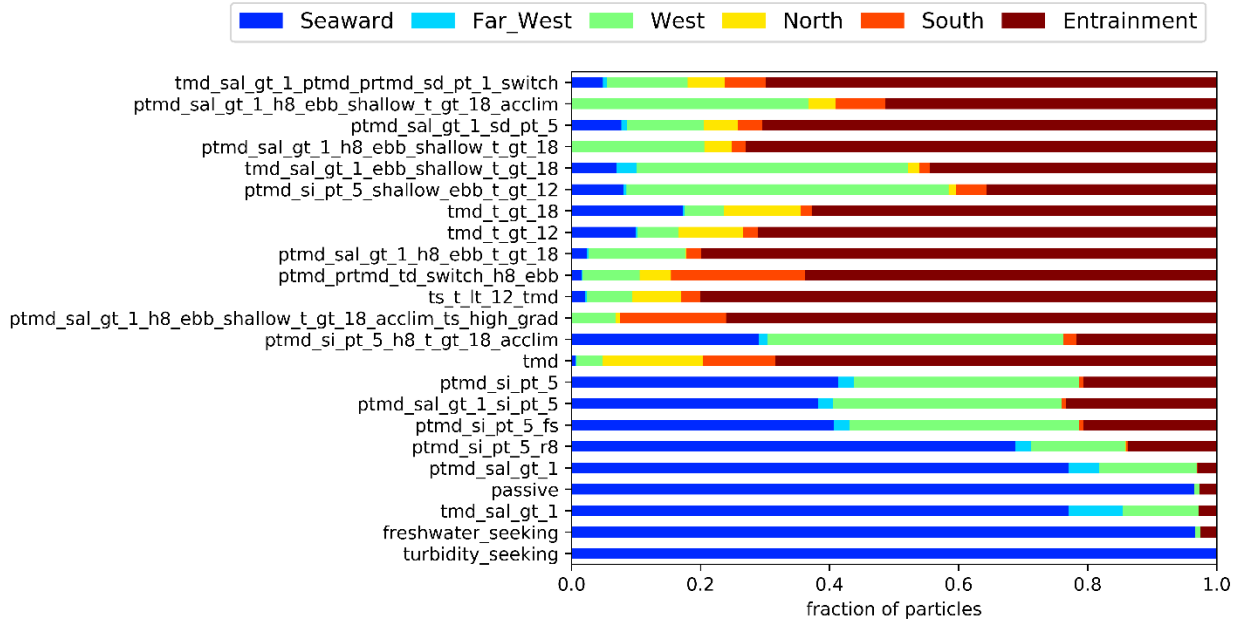


Figure 33. Particle distribution at the end of the simulation period in order of increasing negative log likelihood for the two-dimensional model results for water year 2004. In this ordering the best performing behavior set is the top row.

Table 2. Initial abundance of delta smelt estimated by statistical fitting approach for each hydrodynamic scenario and behavior set.

Behavior	Initial Abundance			
	3D 2002	2D 2002	2D 2004	Average
ptmd_sal_gt_1_h8_ebb_shallow_t_gt_18_acclim	4108430	2201310	1265230	2524990
ptmd_sal_gt_1_h8_ebb_shallow_t_gt_18	3835260	2459460	1630940	2641887
tmd_sal_gt_1_ebb_shallow_t_gt_18	2016970	2998520	1105280	2040257
tmd_sal_gt_1_ptmd_prtmd_sd_pt_1_switch	3372280	3156160	1752580	2760340
ptmd_sal_gt_1_sd_pt_5	2728070	3908340	1781980	2806130
ptmd_sal_gt_1_h8_ebb_t_gt_18	3275870	2987820	2126940	2796877
ptmd_si_pt_5_shallow_ebb_t_gt_12	3212940	3605730	1427520	2748730
tmd_t_gt_18	5000000	4669210	2733340	4134183
ptmd_prtmd_td_switch_h8_ebb	2785920	2349390	1854510	2329940
ptmd_sal_gt_1_h8_ebb_shallow_t_gt_18_acclim_ts_high_grad	5000000	2422490	2707370	3376620
ptmd_si_pt_5_h8_t_gt_18_acclim	2677140	2384630	1230730	2097500
ptmd_sal_gt_1_si_pt_5	2306470	2462100	1243280	2003950
ptmd_si_pt_5	2611660	2511790	1277700	2133717
tmd_t_gt_12	5000000	2940870	2776600	3572490
ptmd_si_pt_5_r8	2649580	3954610	2475620	3026603
ptmd_sal_gt_1	2240750	3444070	1918560	2534460
ts_t_lt_12_tmd	5000000	2474470	2766020	3413497
Tmd	2258580	2226860	2065920	2183787
ptmd_si_pt_5_fs	1005830	2590630	1221750	1606070
tmd_sal_gt_1	2661320	3545950	1927260	2711510
Passive	5000000	5000000	5000000	5000000
turbidity_seeking	2118090	5000000	2463190	3193760
freshwater_seeking	1839780	5000000	5000000	3946593

Table 3. Coefficient of determination in predicting regional abundance estimated from Spring Kodiak Trawl expansion for each behavior and hydrodynamic scenario.

Behavior	Coefficient of Determination		
	3D 2002	2D 2002	2D 2004
passive	0.031909	0.024486	0.237229
turbidity_seeking	0.57465	0.002381	0.005482
freshwater_seeking	0.123905	0.01833	0.221913
Tmd	0.016814	3.92E-05	5.09E-07
tmd_t_gt_12	0.001676	0.002002	0.018665
ts_t_lt_12_tmd	0.000721	0.001335	0.002388
tmd_sal_gt_1	0.013339	0.00023	0.003026
ptmd_sal_gt_1	0.095532	0.000667	0.002901
ptmd_si_pt_5	0.129063	0.064214	0.16394
ptmd_si_pt_5_fs	0.293752	0.064442	0.17096
ptmd_si_pt_5_shallow_ebb_t_gt_12	0.266572	0.041185	0.111315
ptmd_sal_gt_1_sd_pt_5	0.16249	0.061786	0.094033
ptmd_sal_gt_1_si_pt_5	0.212715	0.069109	0.198578
ptmd_ptmd_td_switch_h8_ebb	0.416543	0.032855	0.002429
tmd_sal_gt_1_ptmd_ptmd_sd_pt_1_switch	0.274307	0.066921	0.20091
ptmd_sal_gt_1_h8_ebb_shallow_t_gt_18	0.478761	0.425944	0.297024
ptmd_sal_gt_1_h8_ebb_t_gt_18	0.487087	0.240771	0.396036
ptmd_sal_gt_1_h8_ebb_shallow_t_gt_18_acclim	0.457475	0.504375	0.333959
ptmd_sal_gt_1_h8_ebb_shallow_t_gt_18_acclim_ts_high_grad	0.169067	0.178971	0.003889
tmd_sal_gt_1_ebb_shallow_t_gt_18	0.639325	0.249303	0.45373
ptmd_si_pt_5_r8	0.153901	0.004818	0.025226
ptmd_si_pt_5_h8_t_gt_18_acclim	0.079391	0.143412	0.098852
tmd_t_gt_18	0.021786	0.09594	0.015121

Discussion

We compared the relative performance of several alternative sets of delta smelt swimming behavior rules. A tidal migration behavior has been discussed in past publications (e.g. Sommer et al. 2011) as a likely spawning migration behavior leading to rapid landward movement of delta smelt. The simulations here are consistent with those expectations in that it does lead to rapid landward migration. However, a less well-established aspect of the tidal migration is the cue (or cues) to trigger initiation or cessation of tidal migration. If the simulated tidal migration behavior continues without regard to turbidity or other environmental cues it leads to high entrainment losses.

Bennett and Bureau (2014) also report evidence of tidal migration behavior but further hypothesize that this tidal migration may be driven by the combination of smelt seeking higher turbidity and the tidal phasing of turbidity gradients. A simple behavior driven by turbidity cues is swimming in the direction of

higher turbidity. This representation of behavior leads to poor predicted retention. Salinity has also been used as an environmental cue in delta smelt simulations (Rose et al. 2013). A simple salinity driven swimming response is swimming in the horizontal direction of decreasing salinity. Similar to the turbidity seeking behavior and passive behavior, this lead to poor retention in the estuary. However, a salinity triggered tidal migration behavior led to good retention.

Of the scenarios explored, the behavior rules which do not allow behavior to vary in time lead to unrealistic predictions of delta smelt distribution and fate. Tidal migration is too extreme in terms of shifting particles in the landward direction and the other simple behaviors retain particles poorly. The observed distributions of delta smelt suggest that a more realistic behavior should have an outcome intermediate to these extremes. As suggested by Bennett and Burau (2014) and other authors, it is likely that actual delta smelt swimming behavior can vary through time. For example, it may involve tidal migration but only during certain environmental conditions and may involve additional elements such as avoidance of deep channel (Bennett and Burau 2014), holding behavior in favorable habitat or prior to spawning (Sommer et al. 2011), or day-night variability (Bennet 2005). Triggers may also be more complex, for example relating to the perceived change in environmental properties that a particle experiences moving through the estuary (Goodwin et al. 2014). Several sets of behavior rules explored represent more complex behaviors which involve tidal migration under selective conditions such as high turbidity or a perceived increase in salinity.

The predicted particle fate for the simpler behaviors are broadly consistent with respect to particle release time and modeling tools applied. For example, turbidity seeking leads to poor retention for both the 2D and 3D tools. The predicted distributions associated with behaviors triggered by environmental stimuli, such as tidal migration when turbidity is perceived by a particle to be increasing, lead to larger differences in predicted fate between the 2D and 3D model. This is likely in part due to the substantial differences in predicted turbidity fields between the 2D and 3D models.

Avoidance of high salinity is one behavior that has somewhat consistent and predictable outcomes among scenarios. This behavior leads to good retention of particles and low entrainment. To a large extent persistent tidal migration when salinity is perceived to be increasing mimics this behavior because tidal migration is generally triggered when particles enter higher salinity, leading to retention in low salinity regions.

While there was variation in negative log likelihood between 2D and 3D and with particle release time, some were more robust than others. There was particular support for the conclusion that high or increasing salinity may trigger tidal migration. That response was also represented in previous modeling studies (RMA 2009). There was less success of behaviors with only turbidity-based triggers in reproducing observed distributions but that may be partially due to the higher uncertainty of turbidity predictions.

Two closely related questions motivating this work are 1) which environmental conditions trigger initiation of the spawning migration of delta smelt? and 2) which environmental conditions lead to adults entering the south Delta. After consultation with the CAMT DSST, we chose to start the simulations at a time thought to correspond roughly to the beginning of the spawning migration based on the arrival at Rio Vista of turbid water associated with a “first flush” event of each year. For each behavior evaluated, this allowed the assumption of a single set of behavior rules during the whole simulation period as opposed to a discrete switch from behavior rules prior to the spawning migration to spawning migration behavior

rules. Releasing particles at a time significantly prior to the spawning migration would introduce ambiguity, in attributing differences between observed and predicted distributions to: 1) uncertainties in representation of pre-spawning migration; 2) uncertainties in the trigger for initiation of spawning migration; or 3) uncertainties in representation of spawning migration behavior. However, behaviors that are relatively high ranked in both the Dec 5, 2001 release results and the Dec 20, 2001 release results generally involve salinity triggered tidal migration, suggesting that is a likely behavior both prior to and during the spawning migration. Several of the consistently high ranked behaviors also involve variations of holding in turbid water which generally lead to less seaward movement. Therefore, there is some support for a turbidity trigger resulting in a landward shift in distribution associated with the spawning migration. Table 1 indicates that the turbidity level which triggered holding behaviors was 18 NTU for the three highest ranked behaviors.

While some behavior sets yielded predicted distributions much more consistent with observed delta smelt distributions than other behavior sets, there were some biases common among most of the highest ranked behaviors. First, the predicted proportion of particles entrained was higher than estimated in Kimmerer et al. (2008) and may be unrealistic. Further support of overestimate of entrainment can be seen in the figures in Appendix B which indicate that best performing behaviors typically overestimate south Delta abundance. Two non-exclusive explanations seem most likely. One is that the behavior sets are missing a component of the actual delta smelt behavior that results in avoidance of the south Delta. The other is that the overestimate of entrainment and south Delta abundance may both be related in part to the use of spatially uniform natural mortality in this study. If south Delta natural mortality was higher than natural mortality in other regions, the use of uniform natural mortality would lead to overestimate both of south Delta abundance and entrainment. Variation in catchability of delta smelt with respect to turbidity in the Spring Kodiak Trawl surveys may also contribute to the discrepancy between predicted and observed south Delta abundance. While that one region contributes little to the overall log likelihood estimates it is particularly important for predicted entrainment.

All the behaviors explored so far share several simplifying assumptions. One is lack of stochasticity in swimming response. All responses occur at threshold levels each particle responds at the same threshold as other particles. Similarly, swimming speed is uniform among particles and direction is also fully deterministic (e.g. in the direction of shallower water) for most behaviors. Variability in behavior with life stage or and diel (day-night) variability are not considered. However, each behavior involves free parameters, such as the turbidity or salinity required to trigger tidal migration. In additional simulations not reported here we explored sensitivity to most of these parameters. However, due to the substantial computational expense of each behavior scenario simulated we have not done an automated fitting of behavior parameters so may not have found near optimal parameter values for the candidate behaviors.

While it is certain that none of the behaviors is a full description of actual delta smelt swimming behavior, several other uncertainties not related to the sets of behavior rules may limit accuracy of these distribution and entrainment predictions. A primary uncertainty is the accuracy and resolution required of the hydrodynamic model predictions. A limitation in both models is representation of nearshore velocity. Actual delta smelt are likely to be able to find small scale quiescent regions in shallow water, or small-scale eddies that are not resolved by the hydrodynamic models. In addition, the accuracy of turbidity predictions may not be adequate for the purposes of evaluating turbidity driven

behaviors. Comparisons to Secchi depth data suggested that turbidity in the central and south Delta is underestimated by both the 2D and 3D modeling tools in water year 2002 (Pete Smith, personal communication). This calls into question whether behaviors with turbidity cues have realistic responses. Behaviors that depend on turbidity gradients, such as turbidity seeking, or are triggered by perceived change in turbidity may be sensitive to the degree of patchiness of predicted turbidity fields. The turbidity fields predicted by RMA2 tools tend to be smoother than those predicted by UnTRIM and SediMorph. The ability to predict small scale turbidity gradients has not been explicitly evaluated so it is not clear if either set of tools is adequately predicting turbidity gradients for purposes of delta smelt behavior modeling. Salinity fields are more similar between the two models and calibrated at far more observation stations so is believed to be predicted more reliably.

The differences between observed catch and predicted distribution may also involve factors in addition to inaccuracy in the turbidity field or representation of swimming behavior of delta smelt. Uncertainty associated with initial distribution and release time of particles may be substantial. Latour (2016) reported significant variation in catch per unit effort (CPUE) with Secchi depth. Therefore, the actual distribution of delta smelt may vary from the distribution implied by CPUE effort in the FMWT surveys due to spatial variability in turbidity. The potential sensitivity to timing of the release was explored by simulating both a December 5, 2001 and December 20, 2001 release time and found to be significant though most of the best performing models for the earlier release also performed relatively well for the later release. Additional factors that will be explored to some extent in Korman et al. (2018) include temporal variability in salvage efficiency driven by mortality or other factors, temporal variability in natural mortality, and initial distribution of delta smelt.

Conclusions

The predicted distribution and fate of particles varied greatly with specified swimming behavior. Some but not all behaviors evaluated were adequate to offset seaward transport by net flows experienced by passive particles. Among the behaviors that resulted in retention of particles, predicted entrainment ranged from near zero to the dominant fate of particles.

The simplest representations of delta smelt swimming behavior did not produce realistic distributions. The observed distribution based on estimates of abundance in Spring Kodiak Trawl surveys appears to find a fine balance between enough tidal migration to be retained in the northern estuary and not so much tidal migration to result in excessive entrainment in water export facilities. The modeling results here suggest that somewhat realistic outcomes can be achieved by some form of selective tidal migration. It particularly shows support for tidal migration triggered by high salinity or perceived increases in salinity. There is much less certainty about what additional environmental stimuli may trigger tidal migration behavior and the cessation of tidal migration behavior or which additional behaviors (e.g. holding) may be exhibited by delta smelt.

The sets of behavior rules selected here will be explored further in additional simulations which do not assume a given initial distribution (Korman 2018). These simulations will allow fitting of initial regional abundance and will incorporate Fall Midwater Trawl Survey observations in addition to Spring Kodiak Trawl observations to fit initial regional abundance and additional parameters. Korman et al. (2018) will also discuss additional factors that may contribute to observed catch and salvage patterns, including spatial variability in natural mortality, and variation in salvage efficiency with turbidity.

References

- Anchor QEA, 2017. Collaborative Adaptive Management Team Investigations on Understanding Factors that Affect Entrainment of Delta Smelt, Hydrodynamic and Sediment Transport Modeling Study, December 2017.
- Ahrestani FS, Hebblewhite M, Post E. 2013. The importance of observation versus process error in analyses of global ungulate populations. *Scientific Reports* 3:3125. DOI: 10.1038/srep03125.
- BAW, 2005. Mathematical Module SediMorph, Validation Document, Version 1.1, The Federal Waterways Engineering and Research Institute.
- Bennett, WA. 2005. Critical assessment of the delta smelt population in the San Francisco Estuary, California. *San Francisco Estuary and Watershed Science*. Available from <http://www.escscholarship.org/uc/item/0725n5vk>
- Bennett WA, Burau JR. 2015. Riders on the storm: Selective tidal movements facilitate the spawning migration of threatened delta smelt in the San Francisco Estuary. *Estuaries and Coasts* 38: 826–835.
- Bever AJ and MacWilliams ML. 2013. Simulating sediment transport processes in San Pablo Bay using coupled hydrodynamic, wave, and sediment transport models. *Marine Geology*. 345, 235-253. <http://dx.doi.org/10.1016/j.margeo.2013.06.012>
- Brown LR, Kimmerer WJ, and Brown R. 2009. Managing water to protect fish: A review of California's environmental water account, 2001–2005. *Environmental Management* 43:357–368.
- Casulli V, Walters RA. 2000. An unstructured, three-dimensional model based on the shallow water equations, *International Journal for Numerical Methods in Fluids*, 32: 331 - 348.
- [CDWR] California Department of Water Resources, 2016a. Chronological Reconstructed Sacramento and San Joaquin Valley Water Year Hydrological Classification Indices. (<http://cdec.water.ca.gov/cgi-progs/iodir/wsihist>). (Accessed 5 July 2016).
- [CDWR] California Department of Water Resources, 2016b. Dayflow, An Estimate of Daily Average Delta Outflow. (<http://www.water.ca.gov/dayflow>). (Accessed 5 July 2016).
- Feyrer F, Nobriga ML, Sommer TR. 2007. Multidecadal trends for three declining fish species: habitat patterns and mechanisms in the San Francisco Estuary, California, USA. *Can J Fish Aquat Sci* 64:723–734. doi: <http://dx.doi.org/10.1139/f07-048>
- Fournier DA, Skaug HJ, Ancheta J, Ianelli J, Magnusson A, Maunder MN, Nielsen A, Sibert J. 2011. AD Model Builder: using automatic differentiation for statistical inference of highly parameterized complex nonlinear models. *Optimization Methods & Software*. Available from <http://admb-project.org/> [accessed 17 February 2012].
- Goodwin RA, Politano M, Garvin JW, Nestler JM, Hay D, Anderson JJ, Weber LJ, Dimperio E, Smith DL, Timko MA. 2014. Fish navigation of large dams emerges from their modulation of flow field experience. *Proceedings of the National Academy of Sciences*, 111, 5277-5282.

- Grimaldo LF, Sommer T, Van Ark N, Holland E, Jones G, Herbold B, Smith P, Moyle P. 2009. Factors affecting fish entrainment into massive water diversions in a freshwater tidal estuary: Can fish losses be managed?" *North American Journal of Fisheries Management* 29:1253–1270.
- Hammock BG, Hobbs JA, Slater SB, Acuña S, Teh SJ. 2015. Contaminant and food limitation stress in an endangered estuarine fish. *Sci Total Environ* 532:316–326. doi: <http://dx.doi.org/10.1016/j.scitotenv.2015.06.018>
- Ketefian GS, Gross ES, Stelling GS. 2016. Accurate and consistent particle tracking on unstructured grids, *International Journal for Numerical Methods in Fluids*, 80(11): 648–665, doi:10.1002/flid.4168.
- Kimmerer WJ. 2008. Losses of Sacramento River Chinook Salmon and Delta Smelt to Entrainment in Water Diversions in the Sacramento-San Joaquin Delta. *San Francisco Estuary and Watershed Science*, 6(2), Retrieved from: <http://escholarship.org/uc/item/7v92h6fs>
- King IP. 1986. "Finite Element Model for Two-Dimensional Depth Averaged Flow, RMA2V, Version 3.3", Resource Management Associates.
- Korman J, Gross ES, Smith PE, Saenz B, Grimaldo LF. 2018. Statistical Evaluation of Particle-Tracking Models Predicting Proportional Entrainment Loss for Adult Delta Smelt in the Sacramento-San Joaquin Delta. Report to the CAMT DSST.
- Lai YG, Goodwin A, Smith DL, Reeves RL. 2017. Complex Unsteady Flow Patterns at a River Junction and Their Relation with Fish Movement Behavior. *World Environmental and Water Resources Congress 2017*: 8-14.
- Moyle PB, Brown LR, Durand JR, and Hobbs JA. 2016. Delta smelt: Life history and decline of a once-abundant species in the San Francisco Estuary. *San Francisco Estuary and Watershed Science* 14: 1–30.
- Murphy DD, Hamilton, SA. 2013. Eastward Migration or Marshward Dispersal: Exercising Survey Data to Elicit an Understanding of Seasonal Movement of Delta Smelt. *San Francisco Estuary and Watershed Science*, 11(3). Jmie_sfews_15805.
- Newman K, Polansky L, and Mitchell L. 2015. Adult Delta Smelt entrainment estimation and monitoring plan (draft May 24, 2015).
- Polansky L, Newman KB, Nobriga ML, Mitchell L. 2017. Spatiotemporal Models of an Estuarine Fish Species to Identify Patterns and Factors Impacting Their Distribution and Abundance. *Estuaries and Coasts*. DOI 10.1007/s12237-017-0277-3.
- Resource Management Associates. 2009. Particle Tracking and Analysis of Adult and Larval/Juvenile Delta Smelt for 2-Gates Demonstration Project, Draft report prepared for Metropolitan Water District of Southern California, 2009, http://www.baydeltalive.com/-/catalog/download.php?f=/assets/05058ccde7595f531c3f6b5eda7faa2f/application/pdf/Appendix_B_Particle_Tracking_and_Analysis_of_Adult_and_Larval_Juvenile_Delta_Smelt.pdf
- Resource Management Associates. 2017. Calibration of the Hydrodynamic, Salinity and Turbidity Models for the Adult Delta Smelt Behavior Study. Report for the Collaborative Adaptive Management Team.

Rose KA, Kimmerer WJ, Edwards KP, Bennett WA. 2013. Individual-based modeling of delta smelt population dynamics in the upper San Francisco Estuary: I. Model description and baseline results. *Transactions of the American Fisheries Society* 142: 1238–1259.

Schoellhamer DH. 2011. Sudden clearing of estuarine waters upon crossing the threshold from transport to supply regulation of sediment transport as an erodible sediment pool is depleted: San Francisco Bay, 1999. *Est Coasts* 34(5):885-899

Sommer T, Mejia F, Nobriga M, Feyrer F, Grimaldo L. 2011. The Spawning Migration of Delta Smelt in the Upper San Francisco Estuary. *San Francisco Estuary and Watershed Science* 9(2), 16 pages.

Sommer, T. and F. Mejia, 2013, A Place to Call Home: A Synthesis of Delta Smelt Habitat in the Upper San Francisco Estuary, *San Francisco Estuary and Watershed Science* 11(2).

SWAN Team. 2009. SWAN Scientific and Technical Documentation 40.72. Delft University of Technology.

Swanson C, Young PS, Cech JJ Jr (1998) Swimming performance of delta smelt: maximum performance, and behavioral and kinematic limitations on swimming at submaximal velocities. *J Exp Biol* 201:333–345

Statistical Evaluation of Particle-Tracking Models Predicting Proportional Entrainment Loss for Adult Delta Smelt in the Sacramento-San Joaquin Delta

Josh Korman, Ecometric Research, 3560 W 22nd Ave., Vancouver, BC, V6S 1J3

Edward S. Gross, Resource Management Associates, 1840 San Miguel Dr., Suite 102, Walnut Creek, CA 94596, and Center for Watershed Sciences, University of California Davis
One Shields Avenue, Davis, CA 95616

Peter E. Smith (retired), US Geological Survey, California Water Science Center, California State University, 6000 J Street, Placer Hall, Sacramento, CA 95819

Benjamin Saenz, Resource Management Associates, 1840 San Miguel Dr., Suite 102, Walnut Creek, CA 94596

Lenny F. Grimaldo, ICF, 650 Folsom St., Suite 200, San Francisco, CA. 94107

April-11-2018

Abstract

Entrainment of fish at dam and water intake structures results in directly-observed mortality that can trigger protective management actions. The impact of entrainment on the viability of fish populations has been challenging to determine and has led to considerable debate and litigation about the efficacy of protection actions. There has been particularly intense debate regarding the population-level effects of the entrainment of endangered fish at water export facilities located in the Sacramento-San Joaquin River Delta. Water from the Sacramento and San Joaquin Rivers flows into the Delta and is diverted through large export pumping facilities to supply water to millions of Californians and a very large agricultural industry. These water export facilities can entrain substantial numbers of fish, including Delta Smelt (*Hypomesus transpacificus*), a small pelagic fish endemic to the San Francisco Estuary that is listed as endangered and threatened under California and federal Endangered Species Acts, respectively. In some years, some Delta Smelt disperse into the less saline water in the eastern Delta in winter prior to spawning in spring, and this movement brings a proportion of the adult population in closer proximity to pumping facilities which puts them at greater risk to entrainment. In this paper we use a particle-tracking model (PTM) in conjunction with a population dynamics model to estimate the proportion of the adult population that is lost to entrainment (proportional entrainment loss, PEL). We use a two-stage modelling procedure. In the first stage, a computationally-intensive PTM simulates a variety of potential behaviors of Delta Smelt to predict movement of particles among regions in the Delta as well as the proportion of particles from each region that are entrained. These predictions are based on behavioral rules that represent different hypotheses about how Delta Smelt movement is related to hydrodynamics (depth, velocity, and flow direction), salinity, and turbidity. In the second stage, we use a population dynamics model, driven by unscaled movement and entrainment rates from the PTM, to predict abundance over time in each region as well as the number of fish from each region that are entrained, which are in turn used to compute proportional entrainment loss. Parameters of the population model are estimated by non-linear search by statistically comparing predictions to data from Fall Midwater Trawl and Spring Kodiak Trawl surveys as well as observed daily salvage records. Our objectives are to evaluate the reliability of different movement hypotheses to rank estimates of PEL based on how well each combined PTM and population dynamic model

fits the data, and to sharpen our understanding of the data for making future research and monitoring decisions.

We found that PTMs that simulated more complex fish movement behaviors that included lagged responses to multiple cues fit the data much better than simpler models based solely on behavioural rules like tidal surfing, or movement towards more turbid or saline water. Estimates of proportional entrainment loss varied considerably among PTMs and among water years, but were similar across alternate population model structures. Estimates of PEL of adult Delta Smelt from PTMs that were most consistent with the data were approximately 35% in water year 2002, 50% in 2004, 15% in 2005, and 3% in 2011. The 2002, 2004, and 2005 estimates were more than double those from Kimmerer (2008) which were 15%, 19% and 7%, respectively. Our estimates of PEL were higher because movement predictions from the PTM resulted in greater entrainment.

Fits of our model to data from 2002 and 2004 were greatly improved by allowing salvage efficiency (proportion of entrained fish that are observed as salvage) to vary with turbidity. The improved fit could indicate that peak salvage events during periods of high turbidity are caused by reduced predation loss rather than the prevailing hypothesis that movement towards the pumps increase with turbidity. Alternatively, turbidity-related changes in activity or micro-habitat could affect the vulnerability of Delta Smelt to entrainment. Lack of support for a turbidity-salvage efficiency relationship in 2005, and inconsistencies in the relationship between 2002 and 2004, suggest it may be spurious and is instead compensating for temporal or spatial error in predictions of entrainment from the PTMs. This in turn could lead to overestimates of PEL. Best fits in each water year were often obtained by either different PTMs or different assumptions about population and observation dynamics. This suggests our PEL estimates may be unreliable, and makes it challenging to determine which PTM to apply in more recent and future years where SKT catch and salvage is too low to evaluate model fit. Further refinement and evaluation of the combined PTM and population dynamics models is required before they can be used to guide flow management decisions.

Mark-recapture experiments to estimate salvage expansion directly from field data are critical to resolve uncertainties in predictions of movement towards export facilities and estimates of PEL. Ideally, these experiments would be conducted over a number of years and

across varying turbidity levels to provide adequate replication and contrasting conditions which would affect mortality between release and salvage locations. Improved estimates of salvage expansion factors from these experiments could be used to evaluate PTMs in earlier years (e.g., 2002, 2004, 2005) when there was better information on abundance and entrainment. This in turn would identify the PTMs that are most consistent with historical data, and determine the set of PTMs which could be used to guide future decisions on export regimes. It seems likely that many years of field effort would be required to provide sufficient information on expansion factors to better resolve which PTMs are more reliable.

Introduction

Worldwide over 58,000 dams and diversion structures (>15 m height) have been constructed to provide water supply, flood control, and hydroelectric power generation (ICOLD 2015). The presence and operations of these facilities can create a number of challenges for fish populations, including habitat fragmentation, reductions in habitat quantity and quality, promotion of non-native species, and direct mortality resulting from entrainment (Rytwinski et al. 2017). The latter effect is one of the most obvious impacts because it is often easily observed through tagging or collection of dead fish on screens and louvers. Directly-observed mortality can trigger protective management actions intended to eliminate or minimize destruction of fish or ‘take’ as specified in the Canadian Fisheries Act and the US Endangered Species Act (ESA), respectively. Significant efforts to quantify and reduce mortality associated with entrainment have been undertaken in a number of large river systems in the US including the Hudson River, Columbia River, and the Sacramento-San Joaquin River Delta. The net effect of entrainment on the viability of fish populations in these systems has been challenging to determine, often because the proportion of the population that is lost to entrainment is not known. Uncertainty in the proportion of the population lost to entrainment hampers effective decision-making about the cost effectiveness of entrainment reduction measures versus other protective actions.

Entrainment of Delta Smelt (*Hypomesus transpacificus*) and other fish at water export facilities located in the Sacramento-San Joaquin River Delta, and associated export constraining regulatory measures have led to intensive study and debate regarding entrainment effects on fish population viability. Delta Smelt is a small pelagic fish endemic to the San Francisco Estuary. Abundance of this species declined in the 1980s, and it was listed as a threatened under both California and federal ESA in 1993 (Feyrer et al. 2007). A rapid and sustained drop in Delta Smelt abundance beginning in ca. 2002, coincident with the decline of other pelagic species (the Pelagic Organism Decline, Sommer et al. 2007, Mac Nally et al. 2010) resulted in a revision of the listing to endangered under the California ESA in 2009. Over their annual life cycle, juvenile Delta Smelt typically spend the summer and fall in brackish (1-6 practical salinity units) regions of Suisun Bay and the western and northern portions of the Sacramento-San Joaquin Delta (hereafter referred to as the “Delta”). In anticipation of spring spawning, there is commonly a landward migration into less saline water (Grimaldo et al. 2009, Sommer et al. 2011, Fig. 1). This spawning migration is believed to be triggered by higher inflows and turbidity caused by

the first large precipitation event in winter, which is referred to as the “first flush” (Grimaldo et al. 2009).

The Delta is a key part of the water supply for California. Water from the Sacramento and San Joaquin river drainages flow into the Delta, and approximately 30-60% of this inflow is diverted through massive state (State Water Project; SWP) and federal (Central Valley Project; CVP) export pumping facilities to supply water for about 25 million Californians and a multi-billion dollar agricultural industry (Kimmerer 2004, Thomson et al. 2010). These pumping facilities, located in the south-eastern portion of the Delta (Fig. 1), substantially alter seasonal patterns in flow and can entrain large numbers of Delta Smelt and other fish species under certain hydrodynamic, physical, and biological conditions (Kimmerer 2008, Grimaldo et al. 2009). The landward spawning migration of Delta Smelt results in some of the population moving closer to pumping facilities which makes them more vulnerable to entrainment. Fish screening facilities located upstream of the pumping plants collect some of the fish that would otherwise be entrained into the pumps. These collections, known as “salvage”, provide an imperfect index of seasonal and annual variation in entrainment.

Entrainment of Delta Smelt has been suggested as one of the potential causes for its decline (Sommer et al. 2007; Brown et al. 2009). Concern over effects of entrainment losses prompted the USFWS to issue a Biological Opinion on the SWP and CVP with targeted Reasonable and Prudent Alternative (RPA) actions designed to minimize Delta Smelt entrainment (USFWS 2008). These include including prescriptive and conditions-based constraints on the magnitude of reverse flows towards the pumps in Old and Middle rivers (OMR flows). OMR reverse flow restrictions can require reductions in water export rates, which have been the subject of considerable litigation (Wanger 2007 and 2010). A better understanding of the migratory dynamics of Delta Smelt is warranted to evaluate the effectiveness of current and future flow and export management options. Moreover, improved estimates of Delta Smelt entrainment losses are also needed to understand how water exports may impact population viability and recovery (Maunder and Deriso 2011; Rose et al 2013). Kimmerer (2008) provided the first estimates of the proportion of the population lost to entrainment, most commonly referred to as Proportional Entrainment Loss (PEL). His estimates, which were as high as 40%, indicate that entrainment could be having substantive population-level effects in some years. These initial estimates have been the subject of debate (Miller 2011, Kimmerer 2011), and there is continued interest in

reducing scientific uncertainty associated with Delta Smelt entrainment dynamics and improving PEL estimates.

Proportional entrainment loss for adult Delta Smelt has been calculated based on the ratio of entrainment to population size (Kimmerer 2008 and 2011, Miller 2011). In these studies, entrainment was calculated by expanding the observed salvage, and population size was calculated by expanding catches from a Delta-wide scientific survey used to index abundance. There are two limitations to this ‘ratio approach’ for estimating PEL. First, it relies very heavily on uncertain expansion assumptions used to calculate entrainment and population size. Second, the method cannot be used to predict how future operations will affect PEL, since historical estimates depend on the magnitude and timing of inflow and export rates in each year. Particle-tracking models (PTMs) provide an alternative way of predicting entrainment losses that can be used to evaluate future operations. These models simulate movement of particles as determined by hydrodynamic predictions and other factors thought to control the distribution of fish such as salinity, water temperature, and turbidity. PTMs have been used to predict entrainment in the Delta, especially for zooplankton and eggs and larval stages of Delta Smelt and other fishes that are assumed to behave as passively drifting particles (Culberson et al. 2004, RMA 2014). The advantage of using PTMs to predict proportional entrainment loss is that they can be used to evaluate population-level effects of different operating strategies. However, it is uncertain whether this approach can be used to model movement and entrainment vulnerability for older life stages of fish which exhibit a variety of complex behaviors in response to changes in abiotic and biotic conditions.

The central objective of the work presented here is to evaluate whether particle-tracking models can be used to simulate movement and estimate proportional entrainment loss for adult Delta Smelt. Our approach differs from past efforts (e.g. Rose et al. 2013) because we test predictions by comparing them directly to data. We use a two-stage modelling procedure. A computationally-intensive PTM simulates a variety of potential behaviors of Delta Smelt to predict movement of particles among regions in the Delta as well as the proportion of particles from each region that are entrained. These predictions are based on behavioral rules that represent different hypotheses about how Delta Smelt respond to hydrodynamics (depth, velocity, and flow direction), salinity, and turbidity. A key advantage of this approach is that it allowed us to test hypotheses about factors that affect Delta Smelt migration which are not well-

understood and represent a key management issue for this species (Sommer et al. 2011, Bennet and Bureau 2014). Proportional entrainment predictions from the PTM are unscaled or naïve in the sense that they do not account for variation in abundance among regions at the start of the simulation, or losses due to natural mortality prior to and during entrainment. The initial distribution of the population would have an important effect on proportional entrainment loss owing to differences in vulnerability to entrainment among regions, and proportional entrainment loss will be underestimated if natural mortality is not accounted for (Kimmerer 2008). In the second stage of our modelling procedure, we use a population dynamics model, driven by unscaled movement and entrainment rates from the PTM, to estimate initial regional abundance, natural mortality rate, and salvage expansion factors. The population model predicts abundance over time in each region as well as the number of fish from each region that are entrained, which are in turn used to compute proportional entrainment loss. Parameters of the population model are estimated by non-linear search by statistically comparing predictions of initial distribution, abundance, and entrainment to field observations.

There are three main objectives of our modelling effort:

1. To evaluate behavioral rules predicting movement and entrainment vulnerability of adult Delta Smelt. We do this by comparing the fit of predictions from the population dynamics model to observed spatial and temporal changes in catch from historical fish field surveys (Fall Midwater Trawl and Spring Kodiak Trawl), and daily salvage estimates at the state and federal fish collection facilities.
2. To translate unscaled estimates of proportional entrainment loss generated from the PTMs into a metric that quantifies the proportion of the population lost due to entrainment via the population model. PEL estimates from models that fit the data better would be considered more reliable than PEL estimates from models that don't fit the data as well. Model evaluation can be used to determine if best-fit models are good enough to be used for quantifying impacts of future export regimes.
3. To better understand the strengths and limitations of available information for estimating PEL. The process of formulating hypotheses as mathematical models and fitting them to observations leads to a sharper understanding of the data which can be invaluable for making future research and monitoring decisions.

The long-term goal of the work presented here is to support a more confident assessment of Delta Smelt entrainment and, stemming from that greater understanding, to assess the efficacy of management actions used to operate the water projects in a manner consistent with the ESA.

Methods

Model Description

Our population dynamic model predicts the abundance, distribution, survival, and entrainment of adult Delta Smelt on a daily time step over an approximate period of 4 months between early- to mid-December to mid- to late-April (Table 1). This simulation window was selected to begin just prior to the first flush and extend through most of the spawning period and include all Spring Kodiak Trawl surveys through April. The model was applied separately in water years 2002, 2004, 2005, and 2011. These years were selected to provide a contrast in flow conditions and seasonal salvage patterns. Two-dimensional (2D) PTMs were applied in each of these water years, and 3D PTMs were applied in 2002 only. A comparison of 2D- and 3D-based results in 2002 allows us to partially evaluate whether the higher resolution and more accurate hydrodynamics and turbidity fields produced by the 3D model effects predictions of movement and proportional entrainment loss.

The population dynamics model consists of process, observation, and likelihood (fitting) components (Fig. 2). The process component predicts the abundance of the population in each of 15 regions for each day of the simulation (Fig. 1). The model uses estimates of abundance in each region and the proportion of particles in that region that are entrained, as determined by a PTM, to predict the number entrained each day (Fig. 2). The observation component of the model translates predictions into catches from Fall Midwater Trawl (FMWT) and Spring Kodiak Trawl surveys (SKT), and daily salvage at each fish collection facility. The likelihood component compares predictions and observations to estimate process and observation parameters by maximizing the likelihood using a gradient search method. The model was fit to each water year using all combinations of ten alternate behaviours (PTMs) and 10 alternate versions of the population dynamic model. Thus a total of 100 different models were fit to each water year (and for both 2D and 3D PTMs for water year 2002).

Predictions of movement and entrainment from the PTM have a strong effect on the population dynamics model. Details of the PTM are provided in RMA (2018) and only a very brief summary is provided here. The PTM is initialized by placing a large number of uniformly distributed particles in each of the 15 regions. Each PTM run (a single behavior) requires 3-7 hours to simulate the movement of approximately 200,000 particles over 120-140 days even with threading the application over 24 XEON cores (2.5-3.0 GHz). Rules that specify the movement behaviour of each particle in response to hydrodynamic, salinity, and turbidity fields influence the location of each particle through the simulation. There is no stochastic variation in behavioural rules for individual particles; each particle will have the same response when exposed to the same stimuli. As noted previously, Delta Smelt behavior during migration is poorly understood (Sommer et al. 2011; Bennett and Burau 2014), so it was important to test several potential behaviors in the modeling process. Only ten of the many PTM behaviors developed by RMA (2018) are analyzed here. They were selected to represent a range of behaviours and fit, and include simple behaviours such as passive drift or movement towards more turbid or less saline water, to more complex behaviours based on multiple physical cues with different thresholds or acclimatization periods (Table 2). Simulation results from the PTM are summarized in an exchange or movement matrix $\mathbf{m}_{j,i,d}$, which is the cumulative proportion of the original particles released in region j that are present in region i on day d , or are entrained at each pumping facility ($i=k$). This exchange matrix is treated as a large set of fixed parameters by the population dynamics model (Fig. 2). Predictions of abundance and entrainment from the population model are translated into relative differences in FMWT catch at the start of the simulation, trends in SKT catch over space and time, and trends in salvage at each facility. These predictions are compared to data, and parameters are estimated by nonlinear search using a maximum likelihood approach. In the description of the population dynamics model which follows, Greek letters denote parameters that are estimated, upper case letters denote predicted state variables, and lower case letters denote indices (not bold), or data (bold) or fixed parameters (bold).

Process Model

The process component of the population dynamics model predicts the abundance of Delta Smelt adults by model day and region. Initial abundance is calculated from,

$$1) \quad N_{i,d=0} = e^{\gamma} \cdot \theta_i$$

where $N_{i,d=0}$ is initial abundance in each region i prior to the first day of the simulation ($d=0$), γ is the estimated initial total abundance across all 15 regions in log-space, and θ_i is the proportion of the total population in each region at the start of the simulation. Regional abundance on subsequent days depends on cumulative survival and movement, and is calculated from,

$$2) \quad N_{i,d} = \left[\sum_j N_{j,d=0} \right] \cdot \prod_d \phi_d \cdot \mathbf{m}_{j,i,d}$$

where ϕ is the estimated survival rate on day d , with the product of those rates up to day d (denoted by the \prod symbol) being the cumulative survival from the start of the simulation to the end of day d , and $\mathbf{m}_{j,i,d}$ is the cumulative proportion of fish that move from one region to another or are entrained (the exchange matrix from the PTM). Note that abundance in region i is the sum of surviving fish from source regions j that move to region i as well as surviving fish that remain in that region between time steps. We do not allow survival rate to vary across regions owing to the way PTM particle tracks were summarized in $\mathbf{m}_{j,i,d}$ (see RMA 2018). This matrix does not track the history of locations for each particle or group of particles, and therefore does not allow us to apply spatially varying survival rates. However, as discussed below, additional mortality for particles that are entrained is captured in the estimate of the salvage expansion factor.

The natural survival rate of Delta Smelt is modeled in one of four ways to account for potential temporal variation:

2a) $\phi_d = \text{logit}(\alpha_o)$ constant survival over time (hereafter referred to as survival model S_c). $\text{logit}()$ denotes that the value inside the parentheses is logit-transformed so $0 \leq \phi \leq 1$.

2b) $\phi_d = \text{logit}(\alpha_{1:N_{skt}})$ Survival rate is constant over days between each SKT survey, but can vary among each of the N_{SKT} intervals, but with the same survival rate for the interval before and after last survey (survival model S_{skt}).

- 2c) $\phi_d = \text{logit}(\alpha_o + \alpha_1 \cdot d)$ variable survival over time modelled as a logit-linear function of model day (survival model S_d). A negative value of α_1 will lead to declining survival rate over time.
- 2d) $\phi_d = \text{logit}(\alpha_o + \alpha_1 \cdot W_d)$ variable survival over time modelled as a logit-linear function of water temperature (W_d, survival model S_w).

Model 2a assumes that survival is constant over time, while 2b allows it to vary among SKT surveys but makes no assumptions about the timing or factors causing variable survival rates. Model 2c allows survival to potentially decline over time which may occur due to spawning-related mortality. Model 2d allows survival rate to vary with water temperature which may affect spawn-timing and therefore spawning-related mortality.

The cumulative number of fish entrained is calculated from,

$$3) \quad N_Ent_{k,d} = \sum_i N_{i,d=0} \cdot \prod_d \phi_d \cdot \mathbf{m}_{i,k,d}$$

where N_Ent is the number entrained from the start of the simulation through day d at pumping location k , and $\mathbf{m}_{i,k,d}$ is the cumulative proportion of fish from source region i that are entrained at pumping location k , as determined by the PTM. Equation 3 scales the proportional entrainment rates from the PTM ($\mathbf{m}_{i,k,d}$) by accounting for differences in initial abundance among regions and losses due to natural mortality. The proportion of the initial population that is entrained at each pumping location up to and including day d is calculated from,

$$4) \quad p_Ent_{k,d} = 1 - \prod_d \left(1 - \frac{N_Ent_{k,d} - N_Ent_{k,d-1}}{\sum_i N_{i,d-1}} \right)$$

Equation 4 follows the same logic as Kimmerer (2008) and assumes natural and entrainment mortality are continuous processes over the duration of the model simulation. As a result, proportional entrainment on each day depends on the abundance at the end of the previous day, where that abundance in turn depends on the initial abundances, and cumulative natural and entrainment losses. The ratio in eqn. 4 is the proportion of fish entrained on day d from all regions relative to the total abundance (across all regions) at the end of the previous day. The

term inside the product symbol (\prod) is therefore the proportion of the population surviving entrainment on day d , and that product over days is the cumulative proportion surviving from the start of the simulation through day d . Thus $1 -$ this product is the proportion of the population that is lost due to entrainment. Entrainment losses include both pre-screen losses and direct losses to the pumps.

We provide three proportional entrainment metrics in this analysis. We refer to the output from eqn. 4 as proportional entrainment loss (PEL). We also compute the ratio of total entrainment over the simulation ($N_Ent_{k,d=D}$, where D is the last day of the simulation) to the initial abundance ($\sum_i N_{i,d=0}$) and refer to this as the ‘discrete proportional entrainment rate’. This value will be lower than PEL (eqn. 4) because it does not account for fish that would have died of natural causes prior to entrainment (hence the denominator is too large), but it is simpler to understand and closely tracks PEL (because both the numerator and denominator decline with decreases in the natural survival rate). We also refer to an ‘unscaled proportional entrainment rate’, which is just the output from the PTM for any region for the last simulation day D ($\mathbf{m}_{i,k,D}$). This value is the proportion of the initial particles from each region that are entrained by the end of the simulation. They describe relative differences in vulnerability to entrainment among our 15 regions. The contribution of each region to the total entrainment depends on these values but also on the initial abundance estimated for each region at the start of the simulation, and on the natural survival rate. Unscaled proportional entrainment provides a simple summary statistic to compare PTMs.

Observation Model

The observation model predicts SKT catch for each station and survey period from,

$$5a) \quad \hat{C}_{SKT_{s,d}} = N_{i(s),d} \cdot \theta_{SKT_{s,d}}$$

where, $\hat{C}_{SKT_{s,d}}$ is the predicted SKT catch at station s on day d , $N_{i(s),d}$ is the abundance in region i where station s is located ($i(s)$), and $\theta_{SKT_{s,d}}$ is the proportion of the population in region i sampled at station s on day d . This SKT sampling efficiency term is calculated from,

$$5b) \quad \theta_{SKT_{s,d}} = \theta_{c_{s,d}} \frac{\mathbf{vtow}_{s,d}}{\mathbf{vreg}_i}$$

where $\theta_{c_{s,d}}$ is an estimate of the proportion of smelt within the volume towed at a station that are captured (sampling efficiency), \mathbf{vreg} is the volume of region i that Delta Smelt are distributed in, and \mathbf{vtow} is the volume for the tow at station s sampled on day d . We assumed that Delta Smelt were evenly distributed to a maximum depth of 4 m (as in Kimmerer 2008) but alternate distributions (upper 2 m, entire water column) are easily explored. Assumptions about the depth distribution of Delta Smelt have no effect on our estimates of PEL because they are accounted for in the estimates of salvage expansion factors. For example, if the maximum depth is set to 2 m, the abundance of the population will be lower than the estimated based on a maximum depth of 4 m. However to match the observed salvage data, the salvage expansion under the 2 m depth distribution will be higher than at 4 m. This dynamic is reviewed in more detail in the discussion section. The proportion of smelt within the volume towed that are captured can either be set to 1 or calculated from,

$$5c) \quad \theta_{c_{s,d}} = \text{logit}(\beta_0 + \beta_1 \cdot \text{secchi}_{s,d})$$

where β_0 and β_1 are parameters predicting SKT sampling efficiency as function of Secchi disc depth recorded at each station on each SKT survey. The logit() term indicates that the prediction is logit-transformed so the efficiency estimates is limited to values ranging from 0 to 1. Delta Smelt may be able to avoid capture to a greater extent when the water is clear which would result in a negative estimate for β_1 (Latour 2015). Increased water clarity may also result in a change in the vertical or lateral distribution of Delta Smelt which could also impact sampling efficiency. Other factors that could affect sampling efficiency could also be modelled using the format in eqn. 5c, but were not explored in this paper for brevity. Catchability, the proportion of the population in a region captured at a station, is the product of θ_c and $\mathbf{vtow}/\mathbf{vreg}$ (eqn. 5b). Station-specific effects on catchability (θ_c) are easily excluded by not estimating parameters defining $\theta_{c_{s,d}}$ and instead fixing this value at 1. In this case, catchability for any region is simply the ratio of the volume sampled in that region across stations on a particular survey to the volume over which smelt are assumed to be distributed over. Owing to the very large volumes of each region, the proportion of the population sampled is very small (Table 3).

Salvage in the population dynamics model is calculated from,

$$7) \quad \hat{C}_{SAL_{k,d}} = (N - Ent_{k,d} - N - Ent_{k,d-1}) \cdot \theta_{S_{k,d}} \cdot \mathbf{p}_{s_k}$$

where $\hat{C}_{SAL_{k,d}}$ is the predicted salvage on model day d at salvage location k , $\theta_{S_{k,d}}$ is the proportion of entrained fish that enter the salvage facility, and \mathbf{p}_{s_k} is the proportion of the flow in the salvage facility that is sampled per day. For consistency with past efforts, we often refer to the inverse of salvage efficiency (θ_s^{-1}) as the salvage expansion factor. Time-specific values for \mathbf{p}_s for each facility were not available for all relevant time periods (Table 1). The ‘observed’ daily salvage data available to us was already expanded to account for the proportion of volume sampled each day. By using expanded salvage observations one is assuming that $\mathbf{p}_s=1$. However, when fitting the model, using expanded salvage data would overweight the importance of the salvage data relative to other data sources (FMWT, SKT). To correct for this, \mathbf{p}_s was set to values that reflects the typical proportion of fish at each salvage facility that are sampled. We set \mathbf{p}_s to 0.08 (sampling 10 minutes out of every two hours) for the federal facility (CVP) and 0.18 (sampling 21.6 minutes every two hours) at the state facility (SWP). These values were very close to the average sampling proportions across all days during the modelled periods in water years 2002 (CVP=0.084, SWP=0.188) and 2004 (CVP=0.083 SWP=0.175). We do not add the predicted number of Delta Smelt that are salvaged at the facilities to the populations in the region where the salvage is released. The contribution of these releases is negligible because the number of fish released is small relative to the population size in release regions, and because the survival rate of these fish is assumed to be very low (Bennett 2005, Miller 2011, Newman et al. 2014).

The simplest model of salvage efficiency ($\theta_{S_{k,d}}$) assumes it can vary across facilities but does not vary over time,

$$8a) \quad \theta_{S_{k,s}} = \text{logit}(\lambda_{0k})$$

where λ_0 is the proportion of entrained fish that enter the salvage facility k on day d and are counted, in logit space. Alternate models allow salvage efficiency to vary over time as a function of covariates using,

$$8b) \quad \theta_{S_{k,d}} = \text{logit}(\lambda_{0_k} + \lambda_{1_k} \cdot \mathbf{X}_{k,d})$$

where λ_0 is the proportion of entrained fish entering the facility when the covariate \mathbf{X} is 0, and λ_1 is a linear effect of the covariate $\mathbf{X}_{k,d}$, which varies over time and can vary across facilities. We explored effects of export rates from each salvage facility (as calculated by the DAYFLOW model) water clarity, as indexed by turbidity measured at Clifton Court Forebay (CCF), and water temperature as measured at Mallard. Salvage efficiency could change with export rate due to changes in the efficiency of the louvers to screen fish and changes in the time fish are exposed to predators during the entrainment process (pre-screen losses). Turbidity could also affect the efficiency of the louvers to screen fish and the ability of visual sight predators like striped bass or largemouth bass to detect and capture Delta Smelt. If higher turbidity reduces predation and hence pre-screen losses, salvage efficiency should increase (thus λ_1 should be positive). Water temperature could affect pre-screen loss through changes in predator behavior, their energetic requirements, or the behaviour of Delta Smelt. For brevity, we only show results based on turbidity, which led to the greatest improvements in fit to the salvage data.

Model Fit (Likelihood)

The model is fit to the data by minimizing a negative log likelihood (NLL_{TOT}) that quantifies the combined fit of the model to FMWT catch (NLL_{FMWT}), SKT catch (NLL_{SKT}), and salvage data (NLL_{SAL}). The total negative log likelihood (NLL_{TOT}) is computed from,

$$9) \quad NLL_{TOT} = NLL_{FMWT} + NLL_{SKT} + NLL_{SAL}$$

Each likelihood component is described below. Note that the total negative log likelihood only quantifies the discrepancy between predictions and observations (observation error). There is no component that penalizes process variation in population dynamics because that variation is not modelled. For example, we could have allowed daily survival rates to be drawn from a distribution where we estimated both the mean and the extent of variation across days. In data-limited situations it is not possible to separate process error from observation error. Including both would increase computational time considerably and would require informative priors on the extent of process or observation error, with total variance estimates conditional on those priors. We therefore use an ‘observation error only’ model (see Ahrestani et al. 2013).

It is widely acknowledged that the FMWT program does not provide a sensitive index of Delta Smelt abundance, and that the survey has an unknown capture probability (Newman et al. 2015). In this modelling effort, we assume only that the FMWT catch provides a reliable index of relative differences in abundance across the 15 regions at the start of the simulation in early winter. Correcting for differences in sampling effort in each region in terms of the proportion of the volume that is sampled relative to the volume over which Delta Smelt are distributed, the total FMWT catch of Delta Smelt in each region summed across the four surveys between September and December can be thought of as a random variable drawn from a multinomial distribution,

$$10) \quad NLL_{FMWT} = -\sum_i \log(\text{multinom}(\mathbf{c}_{FMWT_i}, \theta_i))$$

where NLL_{FMWT} is the sum of negative log likelihood values from a multinomial distribution¹ across the 15 regions, with observed catches \mathbf{c}_{FMWT} , and initial regional proportions defined by model-estimated θ_i values in eqn. 1 (the proportion of the initial population in each CAMT region at the start of the simulation). In the absence of any other information, this error structure will result in a set of estimated initial proportions equivalent to the ratio of each regions catch relative to the total catch. The certainty in those proportion estimates will increase with the total catch. Values of \mathbf{c}_{FMWT} used in the computation were adjusted to reflect differences in relative sampling effort while conserving the total catch across regions².

We assume that the SKT surveys provide a reliable index of abundance over both space (across regions) and time (over SKT survey periods in a year). Unlike the FMWT likelihood, we

¹ A multinomial distribution is used to model the probabilities associated with more than two outcomes. As an example, a multinomial distribution can be used to model the probability of obtaining values of 1 through 6 on a six-sided dice based on a total of N rolls. If the dice is balanced, the probability for each of the six possible outcomes is 1/6. This probability can be precisely estimated if many trials are conducted (say 1000 dice rolls). However, uncertainty in estimates of the probability of obtaining any outcome (say rolling a one) will be much greater when fewer trials are conducted. In the application of the multinomial distribution in this model, the total FMWT catch across all regions on the December survey represents the number of trials, the catch in each region represents the number of dice rolls for each outcome, and θ_i represents the estimated probability of each outcome.

² Adjusted \mathbf{c}_{FMWT} values were computed by expanding the sum of catches across all stations in a region by the proportion of the useable volume of the region sampled by the sum of tow volumes. These sample volume-adjusted catch values for each region were then standardized by dividing them by their sum across regions. The sum of the standardized values across regions is identical to the sum of original catches across regions, preserving the total sample size.

assume that the capture probability of the SKT survey is known and is accurately determined by the scaling factors in eqn. 5a. SKT catch at each station and SKT survey period is assumed to be a random variable drawn from a negative binomial distribution (negbin),

$$11) \quad NLL_{SKT} = -\sum_{s,d} \log(\text{negbin}(\mathbf{c}_{SKT_{s,d}}, \hat{C}_{SKT_{s,d}}, \tau))$$

where, NLL_{SKT} is the sum of negative log likelihoods across all sampling days (d) and stations (s), $\mathbf{c}_{SKT_{s,d}}$ is the observed SKT catch by station and day, $\hat{C}_{SKT_{s,d}}$ is the predicted catch from eqn. 5, and τ represents the extent of overdispersion in the data. In the form of the negative binomial we use, this latter parameter is the variance-to-mean ratio and reflects the average extent of variation in catches across stations averaged over all regions and surveys. We estimated its value for each modelled water year by fixing the density on each SKT survey and region at its conditional maximum likelihood value (sum of catches across stations divided by sum of tow volumes). For each region and SKT survey, we multiplied this density by the tow volume at each station to compute $\hat{C}_{SKT_{s,d}}$. We then used non-linear search to find the value of τ that returned the lowest value of the NLL from the negative binomial distribution. τ therefore represents the average extent of overdispersion in the SKT catch data across stations and surveys if the mean density could be perfectly predicted. τ estimates were 11 (water year 2002), 16 (2004), 8 (2005), and 30 (2011), which are very high levels of overdispersion. We selected a value of $\tau=10$ to use for all years as higher values result in very poor fits to the SKT data because they imply that there is little information about mean density (by region and SKT survey). To simulate greater belief in the SKT data, we also examined fits of the population dynamic model where τ was set to 1. In this case the negative binomial distribution is equivalent to the Poisson, where the variance is equal to the mean³. Our approach to modelling error in the SKT data is rather ad-hoc, but as we discuss in the conclusions section, there is insufficient information to accurately model the error.

³ The poisson distribution can be used to predict the probability of obtaining X events based on sampling for a fixed period of time or over a fixed area or volume. In this example, X would be the catch of Delta Smelt at a station based on sampling the typical volume of water swept by an SKT tow. The poisson distribution has only one parameter which is the mean rate (e.g. typical catch per volume) across stations within a region. The variance of a poisson distribution is assumed equal to the mean rate. Due to random processes there will be some variation in catches across stations even if the densities (mean rate) are the same across stations, and the extent of this variation in a relative sense depends on the sample size (catch in each tow). The poisson variance assumption (variance=mean rate) may not be sufficient to explain the variation in catches across stations in a region. A negative binomial

The observed salvage at each salvage location is assumed to be poisson-distributed (pois) random variable⁴,

$$12) \quad NLL_{SAL} = -\sum_{k,d} \log(pois(\mathbf{c}_{SAL_{k,d}} \cdot \mathbf{p}_{s_k}, \hat{C}_{SAL_{k,d}}))$$

where, NLL_{SAL} is the sum of the negative log likelihoods across all days, $\mathbf{c}_{SAL_{k,d}}$ is the reported expanded daily salvage at facility k on day d , \mathbf{p}_{s_k} is the average proportion of water that is sampled for fish at the salvage facility, and $\hat{C}_{SAL_{k,d}}$ is the predicted salvage computed from eqn. 7. By including the proportion of water sampled for fish at the salvage facility for both observations (eqn. 12) and predictions (eqn. 7), approximately correct samples sizes are used in the likelihood.

Parameters of the model were estimated by maximum likelihood using nonlinear search in AD model-builder (ADMB, Fournier et al. 2011). We ensure convergence had occurred based on the gradients of change in parameter values relative to changes in the log likelihood and the condition of the Hessian matrix returned by ADMB. Asymptotic estimates of the standard error of parameter estimates at their maximum likelihood values were computed from the Hessian matrix within ADMB.

Model Comparison

We used the Akaike Information Criteria (AIC) to compare PTMs and alternate versions of the population model. AIC measures the trade-off between model complexity and fit and is calculated from,

distribution can be used to model the probability distribution for the rate parameter across stations in a region, with the overdispersion term describing how much variance there is in this mean rate across stations. Under the formulation used here, the negative binomial distribution is equivalent to the poisson distribution when $\tau=1$. During estimation, τ increases to reflect the degree of extra-poisson variation in the catches across stations.

⁴ Theoretically, the number of Delta Smelt that are salvaged should be a binomially distributed random variable that depends on the total number entrained (the number of trials) and the probability of salvaging a fish (proportion of entrained water sampled * proportion of fish salvaged from sampled water). However, the binomial probability distribution cannot be calculated when the observed number of salvaged fish exceeds the predict number that are entrained. This situation can occur in the model during the non-linear search since (depending on estimates of initial abundance, survival, etc.). Unlike the binomial distribution, the probability from a poisson distribution is calculable in such circumstances. For a given dataset, the expected values and variance returned a poisson distribution will be indistinguishable from a binomial distribution except when the sample size is very small or probability of success is very large (with the latter being quite unlikely).

$$13) \quad AIC = 2 \cdot K - 2 \cdot LL$$

where K is the number of estimated parameters and LL is the log likelihood calculated as $-NLL_{Tot}$ in eqn. 9. More complex models with more parameters (higher K) may fit the data better (higher LL) than simpler models, but parameter estimates will be less precise. Models with lower AIC (i.e., higher LL and lower K) are considered to have better predictive performance when applied to replicate data sets. Models within 0-2 AIC units of the most parsimonious model (the one with the lowest AIC) are considered to have strong support and cannot be distinguished; models within 2-7 units are considered to have moderate support, and models that had AIC values > 7 units relative to the best model are considered to have weak support (Burnham and Anderson 2002).

Our main analysis consists of comparing 10 different versions of the population dynamics model for each of the 10 PTM behaviours. The different population dynamics models are intended to span the range of potential process and observation dynamics. The simplest population model we examined estimates 19 parameters which include the total initial abundance, 15 initial abundance proportions, 2 constant salvage efficiencies (one for each facility), and one constant survival rate. The most complex model we examined estimates 26 parameters, which includes two additional parameters to model salvage efficiency as a function of turbidity, 3 extra parameters to allow survival to vary between SKT surveys, and two extra parameters to model the effect of Secchi depth on SKT sampling efficiency.

The ten population models we fit include all four methods for estimating the daily survival rate (eqn.'s 2a-2d) and two methods for estimating salvage efficiency (eqn.'s 8a and 8b (X =turbidity) for a total of 8 different versions of the population dynamics model with constant SKT sampling efficiency ($\theta_c=1$ in eqn. 5b). We also fit the Secchi-SKT efficiency model (eqn. 5c) with the time-based survival model (eqn. 2c) under constant and turbidity-based salvage efficiency. Thus we estimated 10 alternate population dynamics models for each of the 10 PTM behaviours ($10 \times 10 = 100$). These models were fit using both high overdispersion in SKT catch data (variance-to-mean ratio $\tau=10$, see eqn. 11), and assuming error in SKT catch data was poisson-distributed (variance-to-mean ratio $\tau=1$). Thus we fit 200 models for each of the five scenarios (3D for water year 2002, 2D for water years 2002, 2004, 2005, and 2011) for a total of

1000 models. Best models identified by AIC may still fit the data poorly or exhibit obvious biases. In addition, because we could not model all variance components (e.g. process error in survival, uncertainty in movement), we definitely underestimate the extent of variance in predictions. As a result, AIC differences overestimate differences in information loss among models. We therefore use the AIC analysis as a screening tool to identify a manageable number of models whose fit we then examine in detail, but do not adhere strictly to the Burnham and Anderson (2002) AIC difference criteria in identifying the best models.

Results and Discussion

Owing to the large number of models that were evaluated, we begin by ranking the models for each water year based on the AIC analysis, and then examine the predictions and fit for some of the better models. Four general patterns are evident in the AIC analysis.

1. More complex PTMs result in much better fits compared to simpler PTMs. This is seen by lower Δ AIC values and higher rank order for more complex PTMs under the same population model structure (moving down rows within columns in Table 4). As more complex PTM behaviours do not increase the number of parameters estimated in the population model (recall the PTM movement matrix are treated as fixed parameters in the population model), the improved fits result in higher log likelihoods with no parameter penalty, and hence lower AIC values and higher model ranks. This pattern occurred in all water years except 2011 which was challenging year to fit owing to a very limited number of salvage observations. The AIC model selection approach correctly identifies simpler models as better in this more data-limited situation.
2. The ranking of PTMs was generally very consistent across alternate population model structures (no or small change in rank moving across columns within rows in Table 4). Within PTMs, increasing the complexity of the population model (moving from left to right in Table 4) resulted in substantially lower AIC values. The addition of only one extra parameter to predict daily salvage efficiency as a function of turbidity (λ_1 in eqn. 8b, population models 5-8 and 10) reduced AIC values by hundreds of points in water years 2002 and 2004 due to the improved fit to the salvage data. This indicates very strong statistical support for turbidity-based variation in salvage efficiency in these years. Allowing

daily variation in natural survival rates also lowered AIC values relative to the constant survival model (e.g. population model 1 vs. 3-4 in Table 4), but the improvement was much less than the AIC reduction associated with using turbidity to predict salvage efficiency. Allowing SKT sampling efficiency to vary with Secchi disc depth generally resulted in smaller or no reductions in AIC compared to models that assumed SKT sampling efficiency was constant (thus only varying with the ratio of tow and regional 4 m volumes).

3. There was substantial variation in proportional entrainment loss estimates across PTMs and negligible variation across population models for a given PTM (Table 4). This indicates that movement predictions from the PTM (the \mathbf{m} exchange matrix in eqn. 3) dominate PEL estimates in the population model. Variation in the magnitude of initial abundances across regions has the potential to influence PEL estimates, but the extent of this variation was limited through fitting to FMWT and SKT data.
4. AIC differences between models (both across and within population model structures) were large and indicated very strong statistical support for more complex PTM behavioural rules and more complex population model structures. However, these differences likely overestimate the extent of model separation because we do not model important sources of variation, such as uncertainty in movement dynamics. As expected, AIC differences were generally smaller when we assumed greater error in the SKT data ($\tau=10$ vs $\tau=1$).

Water Year 2002 (3D)

Particle-tracking model 6 and population model 10 applied in water year 2002 had the lowest AIC value of all 100 models that were fit (Table 4a). It provided a good fit to the adjusted FMWT catch data ($r^2=0.98$, see Table A1a) and predicted an initial abundance of about 2.4 million fish (Fig. 3a top panels). This combination of models (hereafter referred to as ‘the model’) predicted a substantial decrease in daily survival rates starting in March, consistent with the hypothesis that mortality rates are higher during and following spawning (lower-left panel). The predicted total abundance of the population across regions was reasonably close to values calculated from expanding the SKT catch data (by the ratio of regional 4 m volume/tow volume) on the last two surveys, but the model substantially overpredicted abundance on the January survey (lower-right panel). The model predicted peak entrainment in mid-December through early January and more entrainment at the state facility (Fig. 3b, left panels). These patterns were

largely driven by the PTM-based unscaled entrainment rates (top-right panel in Fig. 3b). Proportional entrainment loss predicted from the population model was about 35% when summed across facilities, and was higher at the state facility. Discrete proportional entrainment values (entrainment/initial abundance) were lower owing to the fact that this metric does not account for losses from natural mortality that occurs over the simulation period (thus denominator in eqn. 4 is too large and hence entrainment proportion too low), but differences were relatively modest. The model predicted some highly variable and perhaps unlikely patterns in abundance over time in some regions (Fig. 3c). Of particular concern are large abundance estimates in some of the southern and eastern regions (sjr_ant, cdelta, sdelta) early in the simulation. As these regions have relatively high values of unscaled proportional entrainment (as determined by m from the PTM, Fig. 3b), these potential overestimates of abundance would lead to overestimates of entrainment. The population model provided a reasonable fit to most of the SKT catch data as predictions of mean catch rate by region and trip (red dots, Fig. 3d) were generally within the range of observed values and close to the observed means (large open dots, Fig. 3d). The model explained 80% of the variation in SKT catch across survey trips and regions when the data were averaged across stations (Table A1a). The model predicted that SKT catch efficiency declined with increases in water clarity (Fig. 3e), a similar finding to Latour (2015) based on his analysis of FMWT data for Delta Smelt and other species. This relationship lowered AIC by 28 units compared to assuming capture efficiency was constant under poisson error (Table 4a, models 7 vs. 10), but there was no AIC difference between these models under negative binomial error which assumes there is less information in the SKT data (Table 4b). The population model provided a very good fit to temporal patterns in salvage at both facilities and explained 63% and 91% of the variation in observed daily salvage at federal and state facilities, respectively. (Fig. 3e, Table A1a). It predicted that salvage expansion factors were very sensitive to turbidity changes, with much higher expansions at lower turbidity (Fig.'s 3f and g). Expansion factor at SWP were higher and more sensitive to turbidity compared to those at CVP. This could be driven by higher pre-screen loss at SWP as fish move through the Clifton Court Forebay (CCF), or because the model overpredicts the relative amount of entrainment at SWP (requiring a greater expansion factor to compensate for that overprediction).

In our model, salvage efficiency (inverse of the expansion factor) is estimated to maximize the fit to the salvage data. As the salvage observations are fixed (data), the salvage expansion

factor will increase with the predicted level of entrainment. Estimates of the salvage expansion, whether constant or varying with turbidity (Table 4), are larger than previously published values derived from the ratio of predicted entrainment to salvage, but are within ranges from mark-recapture based estimates (Table 5). Kimmerer (2008) calculated an expansion factor for both facilities of 29, where entrainment was calculated as the product of abundance in the south Delta (determined from SKT surveys) and the proportion of passively drifting particles in that area that were entrained as determined by a hydrodynamic model. Kimmerer (2011) later revised his expansion factor to 22 (95% confidence interval of 13-33). More recently Smith et al. (in prep.) calculated PEL from the ratio of calculated entrainment to observed salvage using improved hydrodynamic predictions and passive particle movement from the same 3D model used here. Their expansion factors ranged from 35 (CVP) to 50 (SWP). In comparison, our estimates of the salvage expansion at the state facility for the top-ranked PTMs for some of the better population models (PTM models 6, 7 and 10 for population model 3 in Table 4a) ranged from about 45-115. Castillo et al. (2012) estimated salvage expansion at the state facility empirically by releasing known numbers of marked cultured adult Delta Smelt immediately in front of the louvers as well as at the CCF gates. They estimated salvage expansions of 32 and 250 from two separate release experiments conducted in February and March, 2009 (Table 5). These values span the range of time-averaged salvage expansion (blue line in Fig. 3f), however predicted expansion factors on some dates exceeded Castillo et al.'s maximum value (dashed line in Fig. 3e).

In water years 2002, population models that did not allow salvage expansion to vary over time (models 1-4 and 9 in Table 4), overpredicted salvage early in the simulation at the state facility prior to the first flush when the water was clear, and underpredicted peak salvage, especially at the state facility when the water was more turbid (Fig. 4). These models explained much less of the variation in observed salvage relative to models where salvage efficiency could vary over time (Table 1Aa). The salvage efficiency-turbidity function predicts low salvage efficiency in clear water (Fig. 3g) and hence leads to lower salvage predictions early in the simulation (Fig. 4 blue line) which are more consistent with the data (leading to better fit to the salvage data and lower AIC values). In this example, the turbidity-salvage efficiency relationship improved the fit to the salvage data by hundreds of AIC units compared to the model which assumed salvage efficiency was constant over time. The turbidity-based model implies that peak salvages are the result of reduced pre-screen loss due to high turbidity, rather than the prevailing

interpretation that greater entrainment rates occur when there is a turbidity bridge between the south Delta and the pumps. Higher levels of turbidity have the potential to lower predation rates and hence reduce pre-screen loss and the magnitude of the salvage expansion factor. However, we suspect the magnitude of the turbidity effect estimated by the model (in this and other water years) may be too high. Turbidity, as measured at CCF, ranged from about 15-35 NTUs during the period when salvage was observed in water year 2002. This resulted in salvage expansion factors ranging from about 200 (at 15 NTUs) to 75 (at 35 NTUs) at CVP, and 350-25 at SWP. Castillo et al. (2012) estimated salvage expansions of 32 at an average turbidity of 11.5 NTUs (February 2009), and 250 at an average turbidity of 13.5 NTUs (March 2009, Table 5). While the range in salvage expansion factors estimated by the turbidity model were typically within the range estimated by Castillo et al., their study does not provide any empirical support for a negative relationship between the salvage expansion factor and turbidity. However, Castillo et al. estimated pre-screen loss from the CCF gates, while the expansion factor used in our model applies to all fish that are entrained. As the majority of fish entering the south Delta and other southern-eastern regions will be entrained (Fig. 3b), our salvage expansion therefore applies to an area well upstream of CCF where turbidity effects would have more time to effect survival and hence salvage expansion factors. To some extent our model accounts for reduced survival in southern-eastern regions that are more vulnerable to entrainment by increasing the salvage expansion factor.

To examine this issue in more detail, we estimated the potential additional mortality in southern-eastern regions and CCF by combining our estimate of salvage efficiencies with field-based estimates of total facility efficiency at SWP. All fish that are entrained must pass through our south Delta region. The proportion of Delta Smelt surviving from their location of entrainment (say the center of the sdelta region) to salvage at the state facility is the product of survival from the entrainment point to the CCF gates and the total facility efficiency (louver efficiency and pre-screen loss in CCF). Thus, given a total salvage efficiency estimated by the model and the total facility efficiency estimated by Castillo et al. (2012) for SWP in 2009 (which we assume here applies in 2002), the proportion lost between the entrainment point and the CCF gates can be back-calculated (Table 5). For example, given a relatively low salvage efficiency of 0.0025 predicted by the model (expansion of $1/0.0025 = 400$, Fig. 3e), about 90% and 40% of Delta Smelt must be lost to predation between the entrainment point and the CCF gates. Such

high loss rates in southern-eastern Delta regions may not be that unrealistic (e.g. Fig. 3b top-right panel).

Water Year 2002 (2D)

Particle-tracking model 8 fit the data best in water year 2002 using the 2D simulation framework (Table 4c, Fig. 5). This model produced similar estimates of PEL of ~35% (Fig. 5b) to the best 3D model (PTM 6). It also overpredicted abundance on the January SKT survey (Fig. 5a), largely due to overestimating abundance in cache_dwsc and sac_sherm regions (Fig. 5c and d). The model estimated a steep negative relationship between Secchi depth and SKT sampling efficiency (Fig. 5e) as it did for the 3D simulation in 2002. The model fit the salvage data very well (Fig. 5f), and like the 3D model in 2002, also predicted a very steep positive relationship between turbidity and salvage efficiency (Fig. 5g). The 2D model explained a similar amount of variation in FMWT, SKT, and salvage data (Tables A1c and d) as the 3D model (Tables A1a and b).

Water Year 2004

Particle-tracking model 10 fit the data best in water year 2004 (Table 4e and f). As in 2002 (both 2D and 3D models), there was strong support for models that used turbidity to predict salvage efficiency (e.g. population model 1 vs 5). There was less support for population models that allowed survival to vary as a smooth function of model day compared to 2002. For example the AIC for population model 3 was only one unit lower than model 1 (Table 4e). However, models that allowed survival to vary freely among SKT surveys or as a function of water temperature provided better fits and predicted a large decrease in survival beginning in early March. The best-fit model in water year 2004 explained less variation in FMWT data ($r^2=0.69$) and especially salvage data ($r^2=0.20$ and 0.17 for CVP and SWP respectively. Tables A1e and f) compared to 2002 (Tables A1 a-d). Using Secchi depth to predict salvage efficiency led to large reductions in AIC, but the slope of the relationship was positive which makes the unlikely prediction that sampling efficiency increases with water clarity (results not shown for brevity). This is a good example where the lowest AIC model may be misleading relative to a model with a higher AIC value. We therefore examined the fit of population model 8, which allows survival to vary as a function of water temperature and salvage efficiency to vary as a function of

turbidity, but without a Secchi depth effect on SKT sampling efficiency (Fig. 6). This model produced a reasonable estimate of the initial abundance and feasible pattern in daily survival rate (Fig. 6a). To provide better fits to the SKT and salvage data, the model estimated a higher proportion of the initial population in the smmarsh region and a lower proportion in cache_dwsc relative to what the FMWT data indicate. The model estimates that PEL was 49% with considerable entrainment over an extended period between late December and early March (Fig. 6d). However, PEL may have been overestimated as the model substantially overpredicted abundance in sjr_stk and sdelta regions (Fig. 6c) where unscaled proportional entrainment values were large (Fig. 6b). The fit to the SKT catch data in 2004 was poor in some regions but explained a similar amount of variation ($r^2=0.8$) compared to 2002 (Fig. 6d, Tables A1e and f). The model did not fit the salvage data as well compared to other years ($r^2=0.20$ and 0.17 for CVP and SWP, respectively), perhaps because the two separate salvage peaks in 2004 provide a more rigorous test for the model. The model predicted that the first peak salvage event occurred too early in the year, but predicted the timing and magnitude of the second peak salvage event relatively well (Fig. 6e), The turbidity-salvage efficiency relationship at SWP was similar to the one estimated in 2002 (Fig. 6f). The CVP relationship in 2004 was steeper compare to one in 2002. This could indicate that the PTM is underpredicting the amount of entrainment at CVP relative to SWP.

Water Year 2005

Particle-tracking model 8 fit the data best in water year 2005 assuming poisson error in SKT data (Table 4g) and PTM 8 or 9 fit the data best assuming negative binomial error (Table 4h). There was some evidence for daily variation in survival rate, but unlike water years 2002 and 2004, there was no evidence for a turbidity effect on salvage efficiency. The lowest AIC model included a negative effect of Secchi depth on SKT efficiency. However, it predicted that SKT efficiency was very low even when Secchi depth was low, leading to very large estimates of abundance which in turn led to unrealistically high salvage expansion factors (plots not shown for brevity but see Table 4g). This is another example where the lowest AIC model is likely misleading. The next lowest AIC models which allowed survival rate to vary between SKT surveys had unrealistic survival patterns (near 1 except between the 3rd and 4th survey). We therefore examined the fit of population model 4, which was the lowest AIC model that did not

exhibit unrealistic abundance or survival patterns. This model allows for time-varying survival rate as a function of water temperature but no effects of turbidity on salvage efficiency or Secchi depth on SKT efficiency. This model provided good fits to the FMWT catch data ($r^2=0.93$, Table A1g) and expanded SKT population estimates ($r^2=0.73$, Table A1g), and predicted a reasonable initial abundance and declining survival rate over time (Fig. 7a). Proportional entrainment estimates were relatively low (~15%) even though the unscaled rates in southern and eastern regions were large (Fig. 7b). This occurred because the model estimated that the majority of the population at the start of the simulation was located in regions with relatively low vulnerability to entrainment. Lower levels of entrainment resulted in lower estimates of salvage expansion factors (Table 4g and h) compared to other years. As in other water years, the model appears to overpredict abundance in some regions (sjr_ant, sdelta) with high unscaled entrainment rates (Fig. 7c and d). The model did not fit the daily salvage very well ($r^2=0.17$ and 0.37 for CVP and SWP, respectively, Table A1g), which is perhaps not surprising since salvage expansion factors for population model 4 did not vary over time (Fig. 7e).

Observed salvage of adult Delta Smelt in winter peaked during the “first flush” when turbidity was higher in all our study years except 2011 (Fig. 8). Recall there was strong support for a turbidity-salvage efficiency relationship in 2002 and 2004, but not in 2005. PTM 8 in 2005 correctly predicted the timing of the initial increase in salvage in mid-January at both facilities when turbidity reached maximum values (Fig.’s 7e, 8). However, the observed peak in salvage occurred after the peak in turbidity. Thus a positive turbidity-salvage efficiency relationship would have led to a poorer fit to the salvage data since it would have overestimated salvage in mid-January and underestimated it during peak salvage in late-January. Peak salvage also lagged behind peak turbidity during the first peak salvage event in 2004, and this led to an overprediction of salvage in early January (Fig. 6e). These patterns suggest that the turbidity-salvage efficiency relationship may be an artefact that is compensating for slightly mistimed entrainment predictions from the PTM. Similarly, inconsistencies in how these relationships differ between CVP and SWP among years may be an artefact that is compensating for error in the relative difference in entrainment between these locations.

Water Year 2011

Water year 2011 was challenging to fit as few Delta Smelt were salvaged and SKT catch was low. 2011 was selected because outflows during the winter were high, providing a unique condition to evaluate PTM predictions. Water year 2011 is also representative of challenges in fitting the model to the current situation of very low Delta Smelt abundance which leads to virtually no salvage observations and highly uncertain and low abundance estimates. PTM model 6 fit the data best assuming poisson error in SKT catch data (Table 4i), while PTM 10 was best assuming negative binomial error (Table 4j). Model selection was more sensitive to assumptions about SKT error in 2011 because there was very little information about the initial distribution from FMWT data or the timing of entrainment from the salvage data due to low sample size. Concerning aspects of fitting to 2011 data include ranking the PTM 1 as the 2nd-best model (Table 4i) and estimation of very large salvage expansion factors. The latter result is not surprising as there was such limited observed salvage that salvage expansion factors were essentially not estimable. Given limitations in the 2011 data, we examined the fit of the simplest population model (1) which estimated a low initial abundance and fit the expanded SKT catch data (across regions) relatively well (Fig. 9a). It estimated a lower survival rate compared to other years and did not fit the FMWT data very well ($r^2=0.63$, Table A1i) compared to water years 2002 and 2005 ($r^2=0.93-0.98$). This occurred because the total FMWT catch in 2011 (summed across Sep, Oct, Nov, and Dec surveys) was only 49 fish, so there was little penalty in predicting initial across-region population proportions that did not match these limited data. Unscaled proportional entrainment rates were essentially zero for most regions which is a sensible prediction from the PTM due to the very large outflows (Fig. 9b). The model estimated that the majority of the population was located in the cache_dwsc region which had a near-zero unscaled entrainment rate in 2011 owing to the high flows. As a result, the PEL estimated by the model was very low (3%). Fits to the expanded abundance (Fig. 9c) estimates and SKT catches (Fig. 9d) were poor ($r^2=0.33$, Table A1i) compared to other years (Fig. 9a).

Comparison of Models Across Water Years

The PTM which fit the data best varied across water years and even across 2D and 3D versions in water year 2002 (Table 6). However, PTMs 8 and 9 were ranked as either the 1st- or 2nd-best model in 2002, 2004, and 2005 (2D, 2011 excluded due to limitations in data). The differences in AIC among the top-ranked models in any year were large relative to the 0-10 unit

scale typically used to differentiate among competing models, suggesting strong support for the PELs associated with the best model. However these differences should be interpreted cautiously owing to our inability to model important components of the variance. Fortunately, from a policy perspective, distinguishing among alternate PTMs does not always matter. For example, the 1st and 2nd ranked models in water years 2002 (2D), 2005, and 2011 produce very similar estimates of proportional entrainment loss. However the 1st- and 2nd-ranked models for the 3D PTMs in water year 2002, and the 2D PTMs in water year 2004, have substantively different PEL estimates. We therefore compare the graphical fit of these PTMs in each of these water years to provide a clearer sense of whether these models are as distinguishable as the AIC analysis suggests. In water year 2002, the fits of the 3D 1st- (PTM 6) and 2nd- (PTM 10) ranked PTMs to the salvage and FMWT data were almost indistinguishable (Fig. 10a). The pattern between predicted and observed SKT catches from PTM 6 and 10 were also similar (Fig. 9b). The log likelihood values indicate that PTM 10 actually fit the FMWT and SKT data slightly better than PTM 6 (higher log likelihood) but provided a worse fit to the salvage data (lower log likelihood), which led to a lower value for the total log likelihood (Table 7). This results in an AIC difference between models of 91 units. It is hard to rationalize such strong statistical support for PTM 6 compared to PTM 10 given the very modest differences seen in the graphical comparison. In our view, the data do not allow us to differentiate among these two alternate PTMs which is disappointing as they have such different PELs (0.35 vs 0.46, respectively). In water year 2004, the AIC difference between the 1st- (PTM 10) and 2nd (PTM 9) -ranked models was 306 units. In this case the better fit to the second observed salvage peak of the top-ranked model is apparent in the graphical comparison, as is the better fit to the FMWT data (Fig. 11a). As for 2002, the difference in fit to the SKT data between models is not distinguishable from the plots (Fig. 11b). The log likelihoods for PTM 10 from all three data sources were higher than for PTM 9. Relative to the 3D 2002 example, it is perhaps easier to rationalize the strong statistical support for the top-ranked model in water year 2004, which has a considerably higher PEL estimate (0.50) compared to the 2nd-ranked model (0.37).

Conclusions

The objectives of our analysis were to: 1) evaluate particle-tracking models predicting the movement of adult Delta Smelt and their vulnerability to entrainment by comparing predictions

to data; 2) provide proportional entrainment loss estimates from the more reliable models; and to 3) better understand the strengths and weaknesses of available information with respect to quantifying PEL to inform future research and monitoring decisions. We found that PTMs that simulated more complex behaviors fit the data much better than simpler models. Simple behavioural rules like tidal surfing (Sommer et al. 2011), movement towards more turbid water (Bennett and Burau 2015), or movement towards less saline water (Rose et al. 2013) did not on their own do well at explaining the seasonal and spatial variability in adult Delta Smelt catch rates and salvage. More complex models that combined some of these behaviours and included lagged responses fit the data much better. Estimates of proportional entrainment loss could vary considerably among PTMs and among water years, but were similar across alternate population model structures. PEL estimates from the models that provided good fits to the data were much higher than previously reported values. Our statistical analysis suggests that PEL estimates are relatively well defined, but this result is an artefact of the strong assumptions made in our modelling approach which were required due to limitations in the data. Better definition of salvage expansion factors through field experiments would improve our ability to distinguish among PTMs based on comparisons of fit to historical data with sufficient information in fish surveys and salvage trends. This in turn would increase the reliability of PTMs to predict how future alternate export regimes affect PEL.

We estimated that proportional entrainment loss of adult Delta Smelt from PTMs that were most consistent with the data was approximately 35% in water year 2002, 50% in 2004, 15% in 2005, and 3% in 2011 (values varied slightly across alternate population models). These estimates are more than double those from Kimmerer (2008) which were 15% (5-24% confidence limit) in water year 2002, 19% (6-31%) in 2004, and 7% (2-12%) in 2005. Our estimates of PEL were higher because movement predictions from the PTM resulted in greater entrainment. In order to fit the scale of the observed salvage, our models needed to estimate much larger salvage expansion factors than those of Kimmerer (2008 and 2011) and Miller (2011). In our view, estimates of salvage expansion factors and PEL from earlier studies, which rely on estimates of abundance in the southern Delta regions, are highly uncertain owing to uncertainty in both the abundance and entrainment components of the calculation. The abundance estimates are based on expanding catches from a very limited number of samples. There are no data to support the assumption that Delta Smelt are distributed evenly to a depth of

4 m in both deep and shallower water habitats, or that this distribution does not vary with abundance or other conditions. To our knowledge there are no studies that indicate that individual fish within a population are uniformly distributed, justifying the use of a volumetric population expansion. These strong assumptions were unavoidable, and Kimmerer (2008, 2011) and Miller (2011) acknowledge the uncertainty in their PEL and salvage expansion factor estimates. Their work has been very helpful in advancing discussions on entrainment on Delta Smelt and other species. Our point here is only that their estimates do not provide a reliable baseline from which to judge PEL and salvage expansion factors estimated by our PTM-population modelling approach. Field-based estimates of salvage expansion factors, such as Castillo et al. (2012), are much more reliable because they avoid these highly uncertain assumptions. Unfortunately, only two estimates for Delta Smelt are available (and only for SWP) and they range by almost an order of magnitude (Table 5). The salvage expansions estimated in this modelling exercise for all years except 2011 fall within this range (2011 not reliably estimated due to very limited salvage). Thus, additional mark-recapture experiments upstream of both state and federal fish collection facilities to estimate salvage expansions (and relationships with covariates) are critical to resolve uncertainties about whether our estimates of high proportional entrainment loss are reasonable or are too high. Ideally, these experiments would be conducted over a number of years to provide adequate replication and contrasting conditions which would affect mortality between release salvage locations. In the long run, releasing fish at greater distances from screening facilities (e.g. compared to CCF gate release points of Castillo et al.) should be considered to estimate the total loss between fish collection facilities and locations where Delta Smelt are unlikely to escape entrainment (e.g. head of Old and Middle Rivers). These efforts should only be conducted if we can assume that pre-screen loss estimates, or relationships between pre-screen loss and covariates like turbidity, are exchangeable among years. In this case they could be used in modelling efforts like this one to better distinguish among PTMs that are applied to historical data where there is more information on abundance and entrainment to evaluate the models. We also recommend that additional PTM modelling and statistical evaluation be conducted with the objective of determining whether similar or better fits to the data could be achieved from behaviours that result in lower PEL estimates more in-line with previously published values. Much of the effort in the current project has gone to

development of simulation and statistical evaluation frameworks, and costs for conducting additional runs would be relatively low.

Fits of our model to data from 2002 and 2004 were greatly improved by allowing salvage efficiency to vary with turbidity. The improved fit could indicate that peak salvage events during periods of high turbidity are caused by reduced predation loss (turbidity-predation loss hypothesis) rather than the prevailing hypothesis that movement towards the pumps increase with turbidity (turbidity-movement hypothesis, Grimaldo et al. 2009). However, the lack of support for this relationship in 2005, and inconsistencies in relationships across years within locations, suggests it may be artefact that compensates for temporal or spatial error in predictions of entrainment from the PTM. It is important to distinguish among these competing interpretations. The remarkable fit to the salvage data based on models that include a turbidity-salvage efficiency suggest that PEL estimates may be reliable, however this conclusion is wrong if these relationships are spurious. There is certainly lots of evidence from other systems that support the turbidity-predation hypothesis (Ginetz and Larking 1976, Gregory and Levings 1998, Johnson and Hines 1999, Yard et al. 2011). But there are also many studies that document increased movement or vulnerability to sampling during periods of higher turbidity supporting the turbidity-movement hypothesis (Gradall and Swenson 1982, Guthrie and Muntz 1993, Miner and Stein 1996, Korman et al 2016, Korman and Yard 2017). Turbidity-predation and – movement hypotheses are almost certainly related because reduced predation risk associated with higher turbidity would reduce concealment behaviours and lead to increased movement (Yackulic et al. 2017), which in turn would increase vulnerability to entrainment. There is no empirical support of a turbidity-salvage efficiency relationship at the state facility where whole facility efficiency for Delta Smelt has been estimated, but only two estimates are available to date. Conducting mark recapture-based salvage efficiency estimates over contrasting turbidity conditions would help resolve this uncertainty.

Differences in AIC among PTMs were very large, which implies a high degree of certainty in identifying the best PTM of the ones that were examined, and hence the most reliable PEL estimate. This result is largely an artefact of our two-step modelling procedure where the PTM is used to calculate a movement exchange values, which are then treated as fixed parameters with no uncertainty in the population model. This strategy was necessary because the PTM simulation

is much too slow to run in an optimization environment where thousands if not millions of iterations would be needed to jointly fit movement and population parameters. If PTM parameters were estimated there would likely be many alternate combinations that fit the data well, some of which could have very different PELs. This approach would lead to much larger PEL variance estimates and much smaller differences in AIC among alternate PTM structures. Limitations in data did not allow us to include process error in population model predictions which would also lead to underestimates of variance and AIC differences among models. Owing to these issues, the AIC results presented here should not be used to quantify the degree of statistical support for various levels of proportional entrainment loss. Instead they should be used as a tool to order alternative PTMs and population model structures and to understand sensitivities (e.g., limited effects of population model structure). This is a disappointing result as there can be large differences in PEL among some PTMs. The more complex and integrated structure in the Delta Smelt life cycle modelling work (Newman et al. 2014) addresses many of these limitations, but fitting this life cycle model has been problematic. Future modelling work could explore options for directly estimating movement parameters in an optimization environment. This could be achieved by limiting the number of spatial regions (Newman et al 2014), use of cloud computing, and developing more efficient ways of drawing parameters during optimization (Noble et al. 2017).

Estimating proportional entrainment loss of Delta Smelt is extremely challenging, and shares many of the problems in commercial fisheries stock assessments. There has been considerable work identifying limitations in stock assessments which therefore apply to understanding limitations in estimating PEL. Stock assessments largely rely on catch data from fisheries and sometimes fishery-independent surveys. These measures are equivalent to the observed salvage at fish collection facilities and SKT survey data, respectively. A central objective of stock assessments is to estimate an exploitation rate in a single year or an exploitation rate history. This is equivalent to the Delta science objectives of estimating PEL in particular years as we do here, or a historical time series of PEL as in Kimmerer (2008) or Smith et al., in prep.). One of the equations central to almost all stock assessments is:

$$C=q \cdot N$$

where C is the catch from a survey or fishery, N is the abundance, and q is the catchability. Rearranging this equation to solve for q it is easy to see that catchability represents the proportion of the population that is sampled. In other words, if q were known, then abundance can be estimated from catch. In the vast majority of stock assessment cases, q is not known, even for statistically designed fisheries-independent surveys (like the SKT survey). Thus catch data alone provides no information on abundance (Maunder and Piner 2014), though it may provide a useful index of relative changes in abundance over time and space if q doesn't vary too much. Historical PEL estimates (e.g., Kimmerer 2008) are based on a volumetric expansion of catch data from SKT surveys combined with a similar expansion of salvage,

$$PEL \approx \frac{salvage \cdot \theta_s^{-1}}{SKT_catch \cdot \theta_{SKT}^{-1}}$$

In other words, PEL estimates assume that q (θ^{-1}) for both salvage and SKT surveys is known. Such catchability assumptions are not used in stock assessments, a field which is at times infamous for making assumptions that have led to some unfortunate collapses of major fisheries (Hilborn and Walters 1982). In our model, we use the same volumetric assumption to convert abundance to catch densities for fitting to the SKT data, but we allow the salvage expansions to freely vary to accommodate this assumption (similar to estimating q in stock assessments). If we decrease the volumetric expansion (e.g. assume Delta Smelt are distributed to 2 m rather than 4 m depth), the abundance estimated by the model will decline which will in turn lead to lower estimates for salvage expansion factor so that the scale of observed salvage is correctly predicted. Our PEL estimates therefore do not depend and are not sensitive to population expansion assumption directly. However, predictions of SKT catch are sensitive to the differences in volumetric expansions across regions, and our approach requires a perhaps equally uncertain assumption that some PTMs provide reliable estimates of the vulnerability to entrainment over space and time. So both ratio- and PTM-based PEL methods have issues. The two main advantages of the PTM approach are that: 1) predictions of movement and entrainment vulnerability can be checked against observations so we do not have to blindly trust the behavioral rules and movement predictions; and 2) it can be used to evaluate alternate future export and flow release strategies and other flow-related management actions. PTMs 8 and 9 were ranked as either the 1st- or 2nd-best model in 2002, 2004, and 2005 (2D simulations, 2011

excluded due to limitations in data). At this point, these are the best models to use to evaluate the relative benefits of alternate export regimes for reducing PEL of Delta Smelt.

A concerning aspect of our results is that different PTMs and population dynamic model structures fit the data best in different water years. For example PTM 8 fit the data best in water years 2002 and 2005 but PTM 10 fit the data best in water years 2004. There was strong evidence for turbidity effects on salvage efficiency in water years 2002 and 2004, but not in water year 2005. These differences could be driven by a number of factors including error in hydrodynamic and turbidity predictions, and error in movement behaviours. They suggest that the ability of existing PTMs to estimate proportional entrainment should be considered relatively poor. In the absence of identifying a model structure that fits the data well in different data years, it is impossible to identify the correct model to apply in future years for evaluating pumping alternatives.

Additional field work on expansion factors used for salvage and SKT data would increase certainty in identifying the best PTM and predictions of PEL. In our view, estimation of salvage efficiency from mark-recapture using cultured Delta Smelt should be an annual activity once the genetic plan for Delta Smelt is approved. A multi-year effort is required to provide ‘pre-screen’ loss estimates under contrasting environmental conditions, and in some cases using release locations further upstream from salvage facilities relative to experiments conducted to date. Note estimates of salvage expansions from these experiments would contribute to the evaluation of models applied in earlier years when there are sufficient numbers of Delta Smelt to evaluate the fit the model (e.g. some salvage and sufficient catch in SKT surveys). Determining the SKT population expansion factor and how it varies across regions and over time will remain a challenge. The Enhanced Delta Smelt Survey (EDSM) will improve the precision of the abundance index relative to the SKT survey and provide some data to verify or refute some aspects of the volumetric expansion assumptions. Currently, abundance estimates from EDSM are very imprecise owing to low abundance and extensive variability in the catch densities among stations (USFWS 2017). Additional years of data collection will however provide insight on depth distributions and how they change with physical covariates (turbidity) or offshore-onshore position. In our model, such data would provide more reliable conversions of regional abundance to catch for fitting to the SKT data. Future investments in salvage efficiency estimates

would be very useful for sorting among alternate PTMs, and would therefore lead to more reliable predictions of the effects of export regimes on proportional entrainment loss. Improving understanding of salvage efficiency through mark-recapture experiments will take a number of years to achieve in order to capture the range in abiotic and biotic conditions that influence variability in pre-screen losses. Furthermore, even if this aspect of the model is improved, there will likely be continued uncertainty about the reliability of the SKT data to estimate population abundance. Thus managers should be aware that developing a reliable model for estimating proportional entrainment is a distant goal, and one that may be difficult to achieve.

Acknowledgements

Funding for this study was provided by the United States Bureau of Reclamation, State and Federal Contractors Water Agency, and the California Department of Water Resources through the Collaborative Science Adaptive Management Program. This study was done under the direction of CSAMP's Collaborative Adaptive Management Team (CAMT) and the Delta Smelt Scoping Team (DSST). We would like to thank Ken Newman, Leo Polansky, and William Smith for providing much of the data used in our analysis and for many insightful conversations over the course of this project. Our analysis relied heavily on long-term trawl and salvage datasets. We thank the many biologists and technicians working for California Department of Fish and Wildlife, the US Fish and Wildlife Service, and Bureau of Reclamation for the collection and maintenance of these data. We thank the DSST for providing comments on an earlier draft of this manuscript.

References

- Ahrestani, F.S., Hebblewhite, M., and Post, E. 2013. The importance of observation versus process error in analyses of global ungulate populations. *Scientific Reports* 3:3125. DOI: 10.1038/srep03125.
- Bennett W.A. 2005. Critical assessment of the Delta Smelt population in the San Francisco Estuary, California. *San Francisco Estuary and Watershed Science*. 3(2).
- Bennett W.A, and Burau J.R. 2015. Riders on the storm: Selective tidal movements facilitate the spawning migration of threatened Delta Smelt in the San Francisco Estuary. *Estuaries and Coasts* 38: 826–835.
- Brown, L.R., Kimmerer, W., and R. Brown. 2009. Managing water to protect fish: A review of California's environmental water account, 2001-2005. *Environmental Management* 43:357-368.
- Burnham, K. P., and Anderson, D. R. 2002. *Model selection and multimodel inference*, 2nd edition. Springer-Verlag, New York.
- Castillo, G., Morinaka, J., Lindberg, J., Fujimura, R., Baskerville-Bridges, B., Hobbs, J., ... & Ellison, L.(2012). Pre-screen loss and fish facility efficiency for Delta Smelt at the south Delta's State Water Project, California. *San Francisco Estuary and Watershed Science*, 10(4).
- Culberson, S.D., Harrison, C.B., Enright, C. and Nobriga, M.L. 2004. Sensitivity of larval fish transport to location, timing, and behavior using a particle tracking model in Suisun March, California.
- Feyrer F, Nobriga M, Sommer T. 2007. Multi-decadal trends for three declining fish species: habitat patterns and mechanisms in the San Francisco Estuary, California, U.S.A. *Canadian Journal of Fisheries and Aquatic Sciences* 64: 723–734.
- Fournier, D.A., H.J. Skaug, Ancheta, J., Ianelli, J., Magnusson, A., Maunder, M.N., Nielsen, A., and Sibert, J. 2011. AD Model Builder: using automatic differentiation for statistical inference of highly parameterized complex nonlinear models. *Optimization Methods & Software*. [Available from](http://admb-project.org/) <http://admb-project.org/> [accessed 17 February 2012].

- Ginetz, R. M., and Larkin, P.A. 1976. Factors affecting rainbow trout (*Salmo gairdneri*) predation on outmigrant fry of sockeye salmon (*Oncorhynchus nerka*). *Journal of the Fisheries Research Board of Canada* 33:19–24.
- Gradall, K. S., and Swenson, W.A. 1982. Response of brook trout and creek chubs to turbidity. *Transactions of the American Fisheries Society* 111:392–395.
- Gregory, R. S., and Levings, C.D. 1998. Turbidity reduces predation on migrating juvenile Pacific salmon. *Transactions of the American Fisheries Society* 127:275–285.
- Grimaldo, L., T. Sommer, N. Van Ark, G. Jones, E. Holland, P. Moyle, P. Smith, and Herbold, B. 2009. Factors affecting fish entrainment into massive water diversions in a freshwater tidal estuary: can fish losses be managed? *North American Journal of Fisheries Management* 29:1253-1270.
- Guthrie, D. M., and Muntz, W.R.A. 1993. Role of vision in fish behaviour. Pages 89–121 in T. J. Pitcher, editor. in. Chapman and Hall, New York.
- Hilborn, R., and Walters, C.J. 1992. *Quantitative fisheries stock assessment*. Chapman and Hall, New York, NY. 570 pp.
- International Commission on Large Dams (ICOLD). Register of Dams— general synthesis. (2015). http://www.icold-cigb.net/GB/World_register/general_synthesis.asp. Accessed 24 Nov 2016.
- Johnson, J. D., and Hines, R.T. 1999. Effect of suspended sediment on vulnerability of young razorback suckers to predation. *Transactions of the American Fisheries Society* 128:648–655.
- Kimmerer, W. J. 2004. Open water processes of the San Francisco Estuary: from physical forcing to biological responses. *San Francisco Estuary and Watershed Science* 2(1):1.
- Kimmerer, W.J. 2008. Losses of Sacramento River chinook salmon and Delta Smelt to entrainment in water diversions in the Sacramento-San Joaquin Delta. *San Francisco Estuary and Watershed Science* 6(2)
- Kimmerer, W.J. 2011. Modeling Delta Smelt losses at the South Delta export facilities. *San Francisco Estuary and Watershed Science* 9(1).
- Korman, J, Yard, M.D., and Yackulic, C.B. 2016. Factors controlling the abundance of rainbow trout in the Colorado River in Grand Canyon in a reach utilized by endangered humpback chub. *Canadian Journal of Fisheries and Aquatic Sciences*. Sci. 73:105-124.

- Korman, J., and Yard, M.D. 2017. Effects of environmental covariates and density on the catchability of fish populations and the interpretation of catch per unit effort trends. *Fish. Res.* 189:18-34.
- Latour, R.J. 2015. Explaining patterns of pelagic fish abundance in the Sacramento-San Joaquin Delta. *Estuaries and Coasts* 39:233-247.
- Mac Nally, R., J.R. Thomson, W.J. Kimmerer, F. Feyrer, K.B. Newman, A. Sih, W. A. Bennett, L. Brown, E. Fleishman, S. D. Culberson, and G. Castillo. 2010. Analysis of pelagic species decline in the upper San Francisco Estuary using multivariate autoregressive modeling (MAR). *Ecological Applications* 20:1417-1430.
- Maunder, M.N., and Deriso, R.B. 2011. A state-space multistage life cycle model to evaluate population impacts in the presence of density dependence: illustrated with application to Delta Smelt (*Hypomesus transpacificus*). *Canadian Journal of Fisheries and Aquatic Sciences* 68:1285-1306.
- Maunder, M.N. and Piner, K.R. 2014. Contemporary fisheries stock assessment: many issues still remain. *ICES Journal of Marine Science* 72:7-18.
- Miner, J. G., and Stein, R.A. 1996. Detection of predators and habitat choice by small bluegills: effects of turbidity and alternative prey. *Transactions of the American Fisheries Society* 125:97–103.
- Miller, W.J. 2011. Revisiting assumptions that underlie estimates of proportional entrainment of Delta Smelt by State and Federal water diversions from the Sacramento-San Joaquin Delta. *San Francisco Estuary and Watershed Science* 9(1).
- Newman, K.B., Polansky, L., Mitchell, L., Kimmerer, W., Smith, P., Baxter, R., Bennet, W., Mander, M., Nobriga, M., Meiring, W., Laca, E., and Feyrer, F. 2014. A Delta Smelt life cycle model. Draft reported prepared by USFWS Dec 17, 2014.
- Newman, K., Polansky, L., and L. Mitchell. 2015. Adult Delta Smelt entrainment estimation and monitoring plan (draft May 24, 2015).
- Noble, H., Jennings, E., Cirss, A., Danner, E., Sridharan, V., Greene, C.M., Imaki, H., and Lindley, S.T. 2017. Model description for the Sacramento River winter-run chinook salmon life cycle model.

- Resource Management Associates [RMA]. 2014. Estimates of Delta Smelt Hatching Distribution, Abundance and Entrainment using Three-Dimensional Hydrodynamic and Particle Tracking Model Results. Report submitted to IEP.
- Resource Management Associates [RMA]. 2018. Estimation of adult Delta Smelt distribution for hypothesized swimming behaviors using hydrodynamic, suspended sediment, and particle-tracking models. Report prepared by Resource Management Associates. 52 pp.
- Rose KA, Kimmerer WJ, Edwards KP, Bennett WA. 2013. Individual-based modeling of Delta Smelt population dynamics in the upper San Francisco Estuary: I. Model description and baseline results. *Transactions of the American Fisheries Society* 142: 1238–1259.
- Rytwinski, T, Algera, D.A., Taylor, J.J., Smokorowski, K.E., Bennett, J.R., Harrison, P.M., and Cooke, S.J. 2017. Water are the consequences of fish entrainment and impingement associated with hydroelectric dams on fish productivity? A systematic review protocol. *Environmental Evidence* 6:8
- Sommer T, Mejia F, Nobriga M, Feyrer F, Grimaldo L. 2011. The Spawning Migration of Delta Smelt in the Upper San Francisco Estuary. *San Francisco Estuary and Watershed Science* 9(2), 16 pages.
- Thomson, J.R., Kimmerer, W.J., Brown, L.R., Newman, K.B., Mac Nally, R., Bennett, W.A., Feyrer, F., and E. Fleishman. 2010. Bayesian change point analysis of abundance trends for pelagic fishes in the upper San Francisco Estuary. *Ecological Applications* 20 (5), 1431–1448.
- Wanger, O. W. 2007. Findings of fact and conclusions of law re interim remedies re: Delta Smelt ESA remand and reconsultation. Case 1: 05-cv-01207-OWW-GSA. Document 561. United States District Court, Eastern District of California, Fresno, California, USA.
- Wanger, O. W. 2010. Memorandum decision re. Cross motions for summary judgment. Case 1: 09-cv-00407-OWW-DLB. Document 561. United States District Court, Eastern District of California, Fresno, California, USA.
- Yackulic, C.B., Korman, J., Yard, M.D., and Dzul, M. 2017. Inferring species interactions through joint mark-recapture analysis. *Ecology (in press)*.
- Yard, M.D., Coggins, L.G. Jr., Baxter, C.V., G.E. Bennett, and Korman, J. 2011. Trout piscivory in the Colorado River, Grand Canyon: Effects of turbidity, temperature, and fish prey availability. *Transactions of the American Fisheries Society* 140:471-486.

US Fish and Wildlife Service (USFWS). 2008. 2008 Biological Opinion for Delta Smelt.

https://www.fws.gov/sfbaydelta/documents/SWP-CVP_OPs_BO_12-15_final_OCR.pdf

US Fish and Wildlife Service (USFWS). 2017. Enhanced Delta Smelt monitoring. Preliminary abundance analysis (draft), March 31, 2017. 22 pp.

Table 1. Start and end dates of particle tracking model (PTM) simulations in relation to the last dates associated with Spring Kodiak Trawl (SKT) surveys and salvage observations.

Water Year	PTM Runs			SKT Data (last survey date)			Salvage (last observation)	
	Start	End	Days	March	April	May	in a Sequence	Last in Spring
2002	Dec-05-01	Apr-17-02	134	Mar-07			Mar-24	Apr-25
2004	Dec-12-03	Apr-17-04	128	Mar-12	Apr-08	May-07	Mar-17	May-16
2005	Dec-14-04	Apr-29-05	137	Mar-25	Apr-21		Feb-16	Feb-16
2011	Dec-17-10	Apr-17-11	122	Mar-10	Apr-07	May-05	Apr-01	Apr-01

Table 2. Summary of particle tracking model behaviors. See RMA 2018 for additional details.

PTM #	Model Name	Behavior Summary
1	passive	Passive particles move with water parcels.
2	turbidity_seeking	Seek higher turbidity by orienting swimming direction to be along the turbidity gradient towards higher turbidity.
3	tmd	Uses water column depth gradients to choose direction of swimming. Nearshore swimming toward shallow water could lead to repeated swimming into the shoreline so passive behavior is specified nearshore.
4	ptmd_sal_gt_1	Tidal migration in brackish water. This behavior triggers tidal migration in brackish water. Once tidal migration behavior is triggered it will continue for 24 hours. At that time it may be triggered again depending on the salinity at the particle location.
5	ptmd_si_pt_5	Persistent tidal migration when the salinity the particle experiences as it moves through the estuary increases.
6	ptmd_si_pt_5_shallow_ebb_t_gt_12	Persistent tidal migration when the salinity the particle experiences as it moves through the estuary increases. Otherwise move to shallow water on ebb when in turbid water.
7	ptmd_sal_gt_1_si_pt_5	Persistent tidal migration in brackish water or if perceived salinity is increasing.
8	ptmd_sal_gt_1_h8_ebb_shallow_t_gt_18_acclim	Persistent tidal migration in brackish water. Moving to shallow water and holding on ebb if acclimated turbidity is higher than 18 NTU.
9	tmd_sal_gt_1_ebb_shallow_t_gt_18	Tidal migration in brackish water. Movement to shallow water during ebb in turbid water.
10	tmd_sal_gt_1_ptmd_prtmd_sd_pt_1_switch	Tidal migration in brackish water. Persistent tidal migration as long as the salinity experienced by a particle is decreasing. Change direction of tidal migration if the salinity experienced by a particle increases substantially.

Table 3. Ratio of Spring Kodiak Trawl (SKT) tow volume (vtow) in 2002 to the regional volume over which Delta Smelt are distributed over (assumed depth of 4 m, Vreg). The inverse of this ratio can be used to expand the total catch on a trip across stations in a region to calculate abundance (see Eqn. 5b). Tow volumes values used in the ratios below represents the average tow volume for reach region.

Region Name	Region Abbreviation	Efficiency (vtow/Vreg)	Expansion (vtow/Vreg)⁻¹
Napa River	napa	2.20E-04	4,570
Carquinez Strait	carq	7.20E-05	13,986
West Suisun Bay	wsuisb	1.50E-04	6,591
Mid Suisun Bay	msuisb	1.20E-04	8,429
Suisun Marsh	smarsh	6.20E-04	1,617
Chippis Island	chippis	2.00E-04	5,078
Sacramento River near Sherman Lake	sac_sherm	2.20E-04	4,452
Sacramento River near Rio Vista	sac_rio	2.50E-04	3,965
Cache slough and SDWSC	cache_dwsc	2.40E-04	4,188
Sacramento River and Steamboat Slough	sac_steam	5.50E-04	1,822
San Joaquin River near Antioch	sjr_ant	2.60E-04	3,874
Central Delta and Franks Tract	cdelta	1.80E-04	5,526
North and South Forks Mokelumne River	mok	6.60E-04	1,518
San Joaquin near Stockton	sjr_stk	2.70E-04	3,697
South Delta	sdelta	1.90E-04	5,283
Average		2.80E-04	4,973

Table 4. Comparison of models based on 10 different particle-tracking model (PTM) behaviours (rows, see Table 2) and structures in the population dynamic models (columns) by water year and PTM type (2D or 3D), assuming poisson error in SKT catch data (variance-to-mean ratio of $\tau=1$) or negative binomial error ($\tau=10$). The ΔAIC tables show the difference between each models AIC relative to the model with the lowest AIC among all PTMs and population model structures (thus model with $\Delta AIC=0$ has the lowest AIC and is considered the best model). Dark grey and grey shaded cells identify models within 2, or 2-7 units of the best model, respectively. The model rank table shows the rank of each PTM within each population model type (column, rank 1= best model). Dark grey, grey, and light grey shaded cells identify the 1st-, 2nd-, and 3rd-ranked PTMs, respectively. The proportional entrainment table shows the most likely estimate of the total proportional entrainment loss across facilities. The SWP salvage expansion table shows the average salvage expansion factor over the simulation at the state facility. Blank cells occur for models that do not meet non-linear convergence criteria.

Table 4. Con't.

a) 3D WY 2002 Poisson error in SKT data ($\tau=1$)

Population model number	1	2	3	4	5	6	7	8	9	10
Salvage efficiency structure	const	const	const	const	~turb	~turb	~turb	~turb	const	~turb
Natural survival structure	S _c	S _{SKT}	S _d	S _w	S _c	S _{SKT}	S _d	S _w	S _d	S _d
SKT efficiency structure (θ_{c-SKT})	=1	=1	=1	=1	=1	=1	=1	=1	~Secchi	~Secchi
ΔAIC										
1) passive	1,847	1,851	1,829	1,829	859	863	845	845	1,789	782
2) turbidity_seeking	6,430	6,370	6,367	6,416	4,752	4,738	4,739	4,749	6,106	4,497
3) tmd	4,787	4,778	4,778	4,778	2,339	2,334	2,339	2,339	4,778	2,030
4) ptmd_sal_gt_1	1,776	1,578	1,580	1,722	713	618	632	695	1,573	625
5) ptmd_si_pt_5	1,561	1,346	1,350	1,493	542	425	437	511	1,304	380
6) ptmd_si_pt_5_shallow_ebb_t_gt_12	1,089	975	971	1,046	83	24	28	63	943	0
7) ptmd_sal_gt_1_si_pt_5	1,314	1,108	1,110	1,249	290	180	189	260	1,101	176
8) ptmd_sal_gt_1_h8_ebb_shallow_t_gt_18_acclim	1,855	1,855	1,846	1,846	294	297	290	290	1,805	249
9) tmd_sal_gt_1_ebb_shallow_t_gt_18	1,531	1,512	1,534	1,534	147	142	145	149	1,525	134
10) tmd_sal_gt_1_ptmd_prtmd_sd_pt_1_switch	1,395	1,246	1,252	1,359	184	115	119	167	1,227	92
Model Rank										
1) passive	7	7	7	7	8	8	8	8	7	8
2) turbidity_seeking	10	10	10	10	10	10	10	10	10	10
3) tmd	9	9	9	9	9	9	9	9	9	9
4) ptmd_sal_gt_1	6	6	6	6	7	7	7	7	6	7
5) ptmd_si_pt_5	5	4	4	4	6	6	6	6	4	6
6) ptmd_si_pt_5_shallow_ebb_t_gt_12	1	1	1	1	1	1	1	1	1	1
7) ptmd_sal_gt_1_si_pt_5	2	2	2	2	4	4	4	4	2	4
8) ptmd_sal_gt_1_h8_ebb_shallow_t_gt_18_acclim	8	8	8	8	5	5	5	5	8	5
9) tmd_sal_gt_1_ebb_shallow_t_gt_18	4	5	5	5	2	3	3	2	5	3
10) tmd_sal_gt_1_ptmd_prtmd_sd_pt_1_switch	3	3	3	3	3	2	2	3	3	2
Proportional Entrainment Loss										
1) passive	0.02	0.02	0.02	0.02	0.02	0.02	0.03	0.03	0.02	0.03
2) turbidity_seeking	0.08	0.08	0.08	0.08	0.07	0.07	0.07	0.07	0.03	0.04
3) tmd	0.35	0.35	0.35	0.35	0.34	0.34	0.34	0.34	0.35	0.38
4) ptmd_sal_gt_1	0.06	0.06	0.06	0.06	0.08	0.08	0.08	0.08	0.06	0.08
5) ptmd_si_pt_5	0.20	0.20	0.20	0.20	0.22	0.22	0.22	0.22	0.20	0.22
6) ptmd_si_pt_5_shallow_ebb_t_gt_12	0.34	0.34	0.34	0.34	0.35	0.35	0.35	0.35	0.34	0.35
7) ptmd_sal_gt_1_si_pt_5	0.24	0.24	0.24	0.24	0.26	0.26	0.25	0.26	0.24	0.26
8) ptmd_sal_gt_1_h8_ebb_shallow_t_gt_18_acclim	0.60	0.60	0.60	0.60	0.60	0.60	0.60	0.60	0.61	0.61
9) tmd_sal_gt_1_ebb_shallow_t_gt_18	0.48	0.48	0.48	0.48	0.49	0.49	0.49	0.49	0.49	0.49
10) tmd_sal_gt_1_ptmd_prtmd_sd_pt_1_switch	0.46	0.46	0.46	0.46	0.47	0.47	0.46	0.47	0.46	0.47
SWP Salvage Expansion Factor										
1) passive	104	104	103	103	266	266	262	262	120	340
2) turbidity_seeking	26	24	24	25	69	66	65	67	51	140
3) tmd	63	68	61	61	226	240	219	219	61	419
4) ptmd_sal_gt_1	13	11	12	13	39	33	33	38	337	58
5) ptmd_si_pt_5	59	47	49	56	143	110	114	134	64	179
6) ptmd_si_pt_5_shallow_ebb_t_gt_12	55	44	45	52	130	100	103	122	48	114
7) ptmd_sal_gt_1_si_pt_5	103	92	91	100	222	190	194	215	101	219
8) ptmd_sal_gt_1_h8_ebb_shallow_t_gt_18_acclim	271	276	267	267	708	714	694	694	312	817
9) tmd_sal_gt_1_ebb_shallow_t_gt_18	140	148	137	137	351	364	359	351	144	380
10) tmd_sal_gt_1_ptmd_prtmd_sd_pt_1_switch	137	116	115	132	311	253	261	298	131	300

Table 4. Con't.

b) 3D WY 2002 negative binomial error in SKT data ($\tau=10$)

Population model number	1	2	3	4	5	6	7	8	9	10
Salvage efficiency structure	const	const	const	const	~turb	~turb	~turb	~turb	const	~turb
Natural survival structure	S_c	S_{SKT}	S_d	S_w	S_c	S_{SKT}	S_d	S_w	S_d	S_d
SKT efficiency structure ($\theta_{c,SKT}$)	=1	=1	=1	=1	=1	=1	=1	=1	~Secchi	~Secchi
ΔAIC										
1) passive	1,336	1,339	1,328	1,328	297	301	292	292	1,332	288
2) turbidity_seeking	5,961	5,758	5,938	5,907	4,432	4,428	4,495	4,432	5,876	4,361
3) tmd	3,463	3,467	3,448	3,448	974	978	970	970	3,399	973
4) ptmd_sal_gt_1	1,324	1,107	1,121	1,279	290	214	224	281	1,125	228
5) ptmd_si_pt_5	1,242	961	1,008	1,188	277	155	175	262	1,011	179
6) ptmd_si_pt_5_shallow_ebb_t_gt_12	1,011	834	887	981	41	0	1	35	885	1
7) ptmd_sal_gt_1_si_pt_5	1,235	953	1,000	1,183	270	143	165	255	1,003	169
8) ptmd_sal_gt_1_h8_ebb_shallow_t_gt_18_acclin	1,790	1,791	1,783	1,783	210	214	209	209	1,785	211
9) tmd_sal_gt_1_ebb_shallow_t_gt_18	1,569	1,496	1,546	1,570	177	177	175	176	1,548	179
10) tmd_sal_gt_1_ptmd_ptmd_sd_pt_1_switch	1,348	1,084	1,154	1,321	182	95	111	178	1,158	115
Model Rank										
1) passive	5	6	6	6	8	8	8	8	6	8
2) turbidity_seeking	10	10	10	10	10	10	10	10	10	10
3) tmd	9	9	9	9	9	9	9	9	9	9
4) ptmd_sal_gt_1	4	5	4	4	7	6	7	7	4	7
5) ptmd_si_pt_5	3	3	3	3	6	4	4	6	3	4
6) ptmd_si_pt_5_shallow_ebb_t_gt_12	1	1	1	1	1	1	1	1	1	1
7) ptmd_sal_gt_1_si_pt_5	2	2	2	2	5	3	3	5	2	3
8) ptmd_sal_gt_1_h8_ebb_shallow_t_gt_18_acclin	8	8	8	8	4	7	6	4	8	6
9) tmd_sal_gt_1_ebb_shallow_t_gt_18	7	7	7	7	2	5	5	2	7	5
10) tmd_sal_gt_1_ptmd_ptmd_sd_pt_1_switch	6	4	5	5	3	2	2	3	5	2
Proportional Entrainment Loss										
1) passive	0.02	0.02	0.02	0.02	0.03	0.03	0.03	0.03	0.02	0.03
2) turbidity_seeking	0.02	0.02	0.02	0.02	0.04	0.04	0.06	0.04	0.02	0.03
3) tmd	0.39	0.39	0.39	0.39	0.38	0.38	0.38	0.38	0.40	0.38
4) ptmd_sal_gt_1	0.06	0.06	0.06	0.06	0.08	0.07	0.07	0.08	0.06	0.07
5) ptmd_si_pt_5	0.19	0.19	0.18	0.19	0.21	0.21	0.21	0.21	0.18	0.21
6) ptmd_si_pt_5_shallow_ebb_t_gt_12	0.35	0.35	0.34	0.35	0.36	0.36	0.36	0.36	0.34	0.36
7) ptmd_sal_gt_1_si_pt_5	0.24	0.24	0.23	0.24	0.26	0.26	0.25	0.26	0.23	0.25
8) ptmd_sal_gt_1_h8_ebb_shallow_t_gt_18_acclin	0.60	0.59	0.60	0.60	0.59	0.59	0.59	0.59	0.60	0.59
9) tmd_sal_gt_1_ebb_shallow_t_gt_18	0.48	0.46	0.47	0.48	0.49	0.48	0.49	0.49	0.47	0.49
10) tmd_sal_gt_1_ptmd_ptmd_sd_pt_1_switch	0.49	0.48	0.47	0.48	0.49	0.49	0.48	0.49	0.47	0.48
SWP Salvage Expansion Factor										
1) passive	57	57	57	57	137	137	135	135	57	186
2) turbidity_seeking	8	5	7	7	53	45	61	51	49	135
3) tmd	50	50	48	48	188	188	184	184	97	185
4) ptmd_sal_gt_1	10	9	9	10	27	23	24	26	316	24
5) ptmd_si_pt_5	39	31	32	38	93	67	72	87	808	72
6) ptmd_si_pt_5_shallow_ebb_t_gt_12	46	36	37	44	106	74	80	98	959	81
7) ptmd_sal_gt_1_si_pt_5	91	87	82	88	195	162	166	186	94	177
8) ptmd_sal_gt_1_h8_ebb_shallow_t_gt_18_acclin	219	231	215	215	570	570	556	556	241	561
9) tmd_sal_gt_1_ebb_shallow_t_gt_18	118	141	131	120	297	306	296	310	156	324
10) tmd_sal_gt_1_ptmd_ptmd_sd_pt_1_switch	135	115	113	130	302	217	238	284	>1000	247

Table 4. Con't.

c) 2D WY 2002 Poisson error in SKT data ($\tau=1$)

Population model number	1	2	3	4	5	6	7	8	9	10
Salvage efficiency structure	const	const	const	const	~turb	~turb	~turb	~turb	const	~turb
Natural survival structure	S_c	S_{SKT}	S_d	S_w	S_c	S_{SKT}	S_d	S_w	S_d	S_d
SKT efficiency structure ($\theta_{c,SKT}$)	=1	=1	=1	=1	=1	=1	=1	=1	~Secchi	~Secchi
ΔAIC										
1) passive	1,509	1,513	1,498	1,498	652	656	642	642	1,471	609
2) turbidity_seeking	49,649	49,653	49,635	49,635	49,642	49,646	49,629	49,629	49,392	49,387
3) tmd	2,426	2,381	2,389	2,425	1,082	1,069	1,092	1,082	2,267	945
4) ptmd_sal_gt_1	2,383	2,109	2,107	2,296	1,364	1,217	1,230	1,325	1,863	989
5) ptmd_si_pt_5	2,643	2,341	2,374	2,590	1,000	843	877	976	2,199	711
6) ptmd_si_pt_5_shallow_ebb_t_gt_12	1,694	1,557	1,564	1,644	507	453	446	482	1,510	386
7) ptmd_sal_gt_1_si_pt_5	2,544	2,249	2,282	2,493	997	841	874	973	2,124	721
8) ptmd_sal_gt_1_h8_ebb_shallow_t_gt_18_acclim	958	922	933	934	45	27	38	37	895	0
9) tmd_sal_gt_1_ebb_shallow_t_gt_18	1,556	1,479	1,553	1,549	370	351	372	360	1,535	334
10) tmd_sal_gt_1_ptmd_prtmd_sd_pt_1_switch	1,387	1,346	1,381	1,386	508	495	509	507	1,197	321
Model Rank										
1) passive	3	4	3	3	5	5	5	5	3	5
2) turbidity_seeking	10	10	10	10	10	10	10	10	10	10
3) tmd	7	9	9	7	8	8	8	8	9	8
4) ptmd_sal_gt_1	6	6	6	6	9	9	9	9	6	9
5) ptmd_si_pt_5	9	8	8	9	7	7	7	7	8	6
6) ptmd_si_pt_5_shallow_ebb_t_gt_12	5	5	5	5	3	3	3	3	4	4
7) ptmd_sal_gt_1_si_pt_5	8	7	7	8	6	6	6	6	7	7
8) ptmd_sal_gt_1_h8_ebb_shallow_t_gt_18_acclim	1	1	1	1	1	1	1	1	1	1
9) tmd_sal_gt_1_ebb_shallow_t_gt_18	4	3	4	4	2	2	2	2	5	3
10) tmd_sal_gt_1_ptmd_prtmd_sd_pt_1_switch	2	2	2	2	4	4	4	4	2	2
Proportional Entrainment Loss										
1) passive	0.02	0.02	0.02	0.02	0.03	0.03	0.03	0.03	0.03	0.03
2) turbidity_seeking	0.00	0.00	0.00	0.00	0.00	0.00	0.00	0.00	0.00	0.00
3) tmd	0.37	0.36	0.36	0.37	0.36	0.36	0.36	0.36	0.38	0.38
4) ptmd_sal_gt_1	0.06	0.05	0.05	0.05	0.06	0.06	0.06	0.06	0.05	0.06
5) ptmd_si_pt_5	0.22	0.22	0.21	0.22	0.25	0.24	0.24	0.25	0.21	0.24
6) ptmd_si_pt_5_shallow_ebb_t_gt_12	0.35	0.35	0.35	0.35	0.36	0.36	0.35	0.35	0.35	0.36
7) ptmd_sal_gt_1_si_pt_5	0.23	0.22	0.22	0.22	0.25	0.24	0.24	0.24	0.22	0.24
8) ptmd_sal_gt_1_h8_ebb_shallow_t_gt_18_acclim	0.36	0.36	0.36	0.35	0.37	0.36	0.37	0.37	0.36	0.37
9) tmd_sal_gt_1_ebb_shallow_t_gt_18	0.35	0.35	0.35	0.35	0.37	0.36	0.36	0.36	0.35	0.36
10) tmd_sal_gt_1_ptmd_prtmd_sd_pt_1_switch	0.47	0.47	0.47	0.47	0.47	0.47	0.48	0.47	0.49	0.49
SWP Salvage Expansion Factor										
1) passive	101	102	100	100	218	218	214	214	114	254
2) turbidity_seeking	5	5	5	5	6	6	6	6	36	42
3) tmd	60	65	63	61	149	149	137	151	85	198
4) ptmd_sal_gt_1	24	19	19	22	59	45	45	54	291	756
5) ptmd_si_pt_5	70	64	66	71	215	183	189	212	>1000	>1000
6) ptmd_si_pt_5_shallow_ebb_t_gt_12	107	96	92	103	250	211	210	238	112	266
7) ptmd_sal_gt_1_si_pt_5	68	63	65	69	194	166	172	192	>1000	>1000
8) ptmd_sal_gt_1_h8_ebb_shallow_t_gt_18_acclim	87	86	81	85	178	207	167	175	89	185
9) tmd_sal_gt_1_ebb_shallow_t_gt_18	106	100	105	105	255	320	256	249	110	297
10) tmd_sal_gt_1_ptmd_prtmd_sd_pt_1_switch	130	129	128	129	243	288	234	242	171	396

Table 4. Con't.

d) 2D WY 2002 negative binomial error in SKT data ($\tau=10$)

Population model number	1	2	3	4	5	6	7	8	9	10
Salvage efficiency structure	const	const	const	const	~turb	~turb	~turb	~turb	const	~turb
Natural survival structure	S_c	S_{SKT}	S_d	S_w	S_c	S_{SKT}	S_d	S_w	S_d	S_d
SKT efficiency structure ($\theta_{e,SKT}$)	=1	=1	=1	=1	=1	=1	=1	=1	~Secchi	~Secchi
ΔAIC										
1) passive	1,102	1,106	1,095	1,095	232	236	226	226	1,094	224
2) turbidity_seeking	47,530	47,534	47,531	47,531	47,514	47,511	47,516	47,515	47,533	47,520
3) tmd	1,795	1,727	1,786	1,794	384	386	384	382	1,767	365
4) ptmd_sal_gt_1	1,315	1,075	1,075	1,251	294	215	216	279	1,073	220
5) ptmd_si_pt_5	2,062	1,788	1,819	2,026	430	322	340	393	1,819	344
6) ptmd_si_pt_5_shallow_ebb_t_gt_12	1,298	1,040	1,156	1,267	125	89	87	119	1,144	79
7) ptmd_sal_gt_1_si_pt_5	1,993	1,725	1,754	1,958	452	345	362	443	1,755	366
8) ptmd_sal_gt_1_h8_ebb_shallow_t_gt_18_acclim	882	681	864	869	16	0	15	17	867	14
9) tmd_sal_gt_1_ebb_shallow_t_gt_18	1,164	797	1,152	1,130	73	32	69	71	1,150	70
10) tmd_sal_gt_1_ptmd_ptmd_sd_pt_1_switch	893	712	880	831	70	57	70	61	869	57
Model Rank										
1) passive	3	6	4	3	5	6	6	5	4	6
2) turbidity_seeking	10	10	10	10	10	10	10	10	10	10
3) tmd	7	8	8	7	7	9	9	7	8	8
4) ptmd_sal_gt_1	6	5	3	5	6	5	5	6	3	5
5) ptmd_si_pt_5	9	9	9	9	8	7	7	8	9	7
6) ptmd_si_pt_5_shallow_ebb_t_gt_12	5	4	6	6	4	4	4	4	5	4
7) ptmd_sal_gt_1_si_pt_5	8	7	7	8	9	8	8	9	7	9
8) ptmd_sal_gt_1_h8_ebb_shallow_t_gt_18_acclim	1	1	1	2	1	1	1	1	1	1
9) tmd_sal_gt_1_ebb_shallow_t_gt_18	4	3	5	4	3	2	2	3	6	3
10) tmd_sal_gt_1_ptmd_ptmd_sd_pt_1_switch	2	2	2	1	2	3	3	2	2	2
Proportional Entrainment Loss										
1) passive	0.03	0.03	0.03	0.03	0.03	0.03	0.03	0.03	0.03	0.03
2) turbidity_seeking	0.00	0.00	0.00	0.00	0.00	0.00	0.00	0.00	0.00	0.00
3) tmd	0.41	0.40	0.41	0.41	0.40	0.40	0.40	0.40	0.41	0.40
4) ptmd_sal_gt_1	0.06	0.05	0.05	0.05	0.07	0.07	0.06	0.07	0.05	0.06
5) ptmd_si_pt_5	0.23	0.21	0.21	0.22	0.25	0.24	0.24	0.24	0.21	0.24
6) ptmd_si_pt_5_shallow_ebb_t_gt_12	0.39	0.38	0.38	0.38	0.39	0.39	0.39	0.39	0.37	0.39
7) ptmd_sal_gt_1_si_pt_5	0.23	0.22	0.21	0.22	0.25	0.24	0.24	0.24	0.21	0.24
8) ptmd_sal_gt_1_h8_ebb_shallow_t_gt_18_acclim	0.34	0.34	0.34	0.34	0.37	0.37	0.36	0.37	0.34	0.36
9) tmd_sal_gt_1_ebb_shallow_t_gt_18	0.33	0.33	0.33	0.34	0.36	0.36	0.36	0.36	0.33	0.36
10) tmd_sal_gt_1_ptmd_ptmd_sd_pt_1_switch	0.50	0.50	0.51	0.50	0.51	0.51	0.51	0.51	0.51	0.51
SWP Salvage Expansion Factor										
1) passive	78	78	76	76	163	163	160	160	96	206
2) turbidity_seeking	2	2	2	2	4	4	4	4	38	4
3) tmd	48	66	55	47	109	116	105	117	84	183
4) ptmd_sal_gt_1	12	10	10	11	26	23	23	25	270	23
5) ptmd_si_pt_5	40	41	42	42	111	105	107	131	>1000	107
6) ptmd_si_pt_5_shallow_ebb_t_gt_12	82	76	71	79	186	155	154	175	96	193
7) ptmd_sal_gt_1_si_pt_5	40	40	41	41	104	98	101	104	>1000	101
8) ptmd_sal_gt_1_h8_ebb_shallow_t_gt_18_acclim	75	71	74	74	154	139	162	151	76	181
9) tmd_sal_gt_1_ebb_shallow_t_gt_18	82	63	82	82	199	151	211	203	105	214
10) tmd_sal_gt_1_ptmd_ptmd_sd_pt_1_switch	118	122	117	124	214	197	222	219	151	301

Table 4. Con't.

e) 2D WY 2004 Poisson error in SKT data ($\tau=1$)

Population model number	1	2	3	4	5	6	7	8	9	10
Salvage efficiency structure	const	const	const	const	~turb	~turb	~turb	~turb	const	~turb
Natural survival structure	S_c	S_{SKT}	S_d	S_w	S_c	S_{SKT}	S_d	S_w	S_d	S_d
SKT efficiency structure ($\theta_{c,SKT}$)	=1	=1	=1	=1	=1	=1	=1	=1	~Secchi	~Secchi
ΔAIC										
1) passive	4,390	4,382	4,325	4,325	3,025	3,008	2,974	2,974	4,127	2,770
2) turbidity_seeking	53,542	53,548	53,517	53,517	52,894	52,900	52,881	52,881	53,341	52,684
3) tmd	1,812	1,698	1,811	1,806	1,088	997	1,013	1,043	1,528	830
4) ptmd_sal_gt_1	4,909	4,913	4,846	4,846	3,451	3,455	3,397	3,397	4,736	3,290
5) ptmd_si_pt_5	4,346	4,331	4,290	4,290	3,037	3,023	2,996	2,996	4,126	2,842
6) ptmd_si_pt_5_shallow_ebb_t_gt_12	1,392	1,301	1,384	1,384	722	649	717	717	1,205	539
7) ptmd_sal_gt_1_si_pt_5	4,430	4,418	4,373	4,373	3,146	3,135	3,104	3,104	4,214	2,955
8) ptmd_sal_gt_1_h8_ebb_shallow_t_gt_18_acclim	1,103	934	1,073	1,095	594	439	586	598	745	220
9) tmd_sal_gt_1_ebb_shallow_t_gt_18	1,414	1,351	1,411	1,411	538	485	533	533	1,086	211
10) tmd_sal_gt_1_ptmd_prtmd_sd_pt_1_switch	771	689	770	770	222	154	227	211	542	0
Model Rank										
1) passive	7	7	7	7	6	6	6	6	7	6
2) turbidity_seeking	10	10	10	10	10	10	10	10	10	10
3) tmd	5	5	5	5	5	5	5	5	5	5
4) ptmd_sal_gt_1	9	9	9	9	9	9	9	9	9	9
5) ptmd_si_pt_5	6	6	6	6	7	7	7	7	6	7
6) ptmd_si_pt_5_shallow_ebb_t_gt_12	3	3	3	3	4	4	4	4	4	4
7) ptmd_sal_gt_1_si_pt_5	8	8	8	8	8	8	8	8	8	8
8) ptmd_sal_gt_1_h8_ebb_shallow_t_gt_18_acclim	2	2	2	2	3	2	3	3	2	3
9) tmd_sal_gt_1_ebb_shallow_t_gt_18	4	4	4	4	2	3	2	2	3	2
10) tmd_sal_gt_1_ptmd_prtmd_sd_pt_1_switch	1	1	1	1	1	1	1	1	1	1
Proportional Entrainment Loss										
1) passive	0.03	0.03	0.03	0.03	0.06	0.06	0.06	0.06	0.03	0.06
2) turbidity_seeking	0.02	0.02	0.02	0.02	0.04	0.04	0.04	0.04	0.04	0.04
3) tmd	0.43	0.42	0.43	0.42	0.41	0.41	0.40	0.40	0.41	0.40
4) ptmd_sal_gt_1	0.05	0.05	0.05	0.05	0.10	0.10	0.10	0.10	0.05	0.10
5) ptmd_si_pt_5	0.18	0.18	0.18	0.18	0.30	0.30	0.30	0.30	0.18	0.30
6) ptmd_si_pt_5_shallow_ebb_t_gt_12	0.20	0.19	0.20	0.20	0.20	0.19	0.20	0.20	0.19	0.19
7) ptmd_sal_gt_1_si_pt_5	0.22	0.22	0.22	0.22	0.35	0.36	0.35	0.35	0.22	0.35
8) ptmd_sal_gt_1_h8_ebb_shallow_t_gt_18_acclim	0.29	0.28	0.27	0.30	0.27	0.26	0.28	0.25	0.26	0.24
9) tmd_sal_gt_1_ebb_shallow_t_gt_18	0.37	0.36	0.37	0.37	0.36	0.36	0.37	0.37	0.36	0.35
10) tmd_sal_gt_1_ptmd_prtmd_sd_pt_1_switch	0.50	0.49	0.51	0.51	0.50	0.49	0.50	0.49	0.49	0.49
SWP Salvage Expansion Factor										
1) passive	96	96	96	96	462	473	447	447	89	426
2) turbidity_seeking	2	2	2	2	>1000	>1000	>1000	>1000	6	>1000
3) tmd	52	57	51	55	87	89	94	93	57	90
4) ptmd_sal_gt_1	9	9	9	9	96	97	92	92	9	95
5) ptmd_si_pt_5	25	27	25	25	180	191	170	170	28	184
6) ptmd_si_pt_5_shallow_ebb_t_gt_12	33	35	33	32	50	54	50	50	34	52
7) ptmd_sal_gt_1_si_pt_5	30	32	29	29	201	213	190	190	33	204
8) ptmd_sal_gt_1_h8_ebb_shallow_t_gt_18_acclim	33	36	35	32	42	47	42	43	37	49
9) tmd_sal_gt_1_ebb_shallow_t_gt_18	54	59	54	54	88	94	87	87	68	109
10) tmd_sal_gt_1_ptmd_prtmd_sd_pt_1_switch	71	74	71	71	100	105	100	102	77	109

Table 4. Con't.

f) 2D WY 2004 negative binomial error in SKT data ($\tau=10$)

Population model number	1	2	3	4	5	6	7	8	9	10
Salvage efficiency structure	const	const	const	const	~turb	~turb	~turb	~turb	const	~turb
Natural survival structure	S _c	S _{SKT}	S _d	S _w	S _c	S _{SKT}	S _d	S _w	S _d	S _d
SKT efficiency structure ($\theta_{e,SKT}$)	=1	=1	=1	=1	=1	=1	=1	=1	~Secchi	~Secchi
ΔAIC										
1) passive	3,544	3,550	3,479	3,479	1,922	1,928	1,867	1,867	3,447	1,871
2) turbidity_seeking	48,211	48,217	48,197	48,197	47,538	47,535	47,538	47,538	48,196	47,538
3) tmd	1,320	1,273	1,302	1,302	319	320	312	312	1,271	316
4) ptmd_sal_gt_1	3,338	3,344	3,275	3,275	1,758	1,764	1,705	1,705	3,267	1,706
5) ptmd_si_pt_5	3,394	3,400	3,328	3,328	1,933	1,939	1,881	1,881	3,314	1,885
6) ptmd_si_pt_5_shallow_ebb_t_gt_12	1,290	1,275	1,271	1,271	389	394	368	368	1,250	370
7) ptmd_sal_gt_1_si_pt_5	3,559	3,565	3,493	3,493	2,124	2,130	2,071	2,071	3,479	2,074
8) ptmd_sal_gt_1_h8_ebb_shallow_t_gt_18_acclim	1,194	1,174	1,173	1,173	402	406	385	385	1,136	580
9) tmd_sal_gt_1_ebb_shallow_t_gt_18	1,065	1,069	1,053	1,053	19	25	1	1	1,010	0
10) tmd_sal_gt_1_ptmd_ptmd_sd_pt_1_switch	672	668	663	663	111	115	106	106	652	98
Model Rank										
1) passive	8	8	8	8	7	7	7	7	8	7
2) turbidity_seeking	10	10	10	10	10	10	10	10	10	10
3) tmd	5	4	5	5	3	3	3	3	5	3
4) ptmd_sal_gt_1	6	6	6	6	6	6	6	6	6	6
5) ptmd_si_pt_5	7	7	7	7	8	8	8	8	7	8
6) ptmd_si_pt_5_shallow_ebb_t_gt_12	4	5	4	4	4	4	4	4	4	4
7) ptmd_sal_gt_1_si_pt_5	9	9	9	9	9	9	9	9	9	9
8) ptmd_sal_gt_1_h8_ebb_shallow_t_gt_18_acclim	3	3	3	3	5	5	5	5	3	5
9) tmd_sal_gt_1_ebb_shallow_t_gt_18	2	2	2	2	1	1	1	1	2	1
10) tmd_sal_gt_1_ptmd_ptmd_sd_pt_1_switch	1	1	1	1	2	2	2	2	1	2
Proportional Entrainment Loss										
1) passive	0.03	0.03	0.03	0.03	0.10	0.10	0.10	0.10	0.03	0.10
2) turbidity_seeking	0.02	0.02	0.02	0.02	0.06	0.07	0.06	0.06	0.02	0.06
3) tmd	0.30	0.21	0.31	0.31	0.33	0.32	0.33	0.33	0.29	0.33
4) ptmd_sal_gt_1	0.04	0.04	0.04	0.04	0.10	0.10	0.10	0.10	0.04	0.10
5) ptmd_si_pt_5	0.18	0.18	0.18	0.18	0.31	0.31	0.31	0.31	0.18	0.31
6) ptmd_si_pt_5_shallow_ebb_t_gt_12	0.18	0.17	0.18	0.18	0.14	0.14	0.14	0.14	0.18	0.14
7) ptmd_sal_gt_1_si_pt_5	0.22	0.22	0.22	0.22	0.37	0.37	0.37	0.37	0.22	0.36
8) ptmd_sal_gt_1_h8_ebb_shallow_t_gt_18_acclim	0.22	0.22	0.23	0.23	0.14	0.14	0.14	0.14	0.22	0.20
9) tmd_sal_gt_1_ebb_shallow_t_gt_18	0.25	0.25	0.26	0.26	0.18	0.18	0.18	0.18	0.25	0.18
10) tmd_sal_gt_1_ptmd_ptmd_sd_pt_1_switch	0.52	0.52	0.52	0.52	0.52	0.52	0.52	0.52	0.52	0.52
SWP Salvage Expansion Factor										
1) passive	19	19	18	18	169	169	167	167	40	167
2) turbidity_seeking	1	1	1	1	>1000	>1000	>1000	>1000	19	>1000
3) tmd	12	8	12	12	>1000	>1000	>1000	>1000	22	>1000
4) ptmd_sal_gt_1	4	4	4	4	115	115	113	113	241	112
5) ptmd_si_pt_5	15	15	14	14	100	100	98	98	18	98
6) ptmd_si_pt_5_shallow_ebb_t_gt_12	12	13	12	12	146	147	152	152	31	151
7) ptmd_sal_gt_1_si_pt_5	17	17	16	16	100	100	97	97	20	97
8) ptmd_sal_gt_1_h8_ebb_shallow_t_gt_18_acclim	14	16	13	13	53	54	51	51	23	24
9) tmd_sal_gt_1_ebb_shallow_t_gt_18	17	18	17	17	22	22	23	23	31	23
10) tmd_sal_gt_1_ptmd_ptmd_sd_pt_1_switch	43	46	43	43	57	59	56	56	54	72

Table 4. Con't.

g) 2D WY 2005 Poisson error in SKT data ($\tau=1$)

Population model number	1	2	3	4	5	6	7	8	9	10
Salvage efficiency structure	const	const	const	const	~turb	~turb	~turb	~turb	const	~turb
Natural survival structure	S_c	S_{SKT}	S_d	S_w	S_c	S_{SKT}	S_d	S_w	S_d	S_d
SKT efficiency structure ($\theta_{c,SKT}$)	=1	=1	=1	=1	=1	=1	=1	=1	~Secchi	~Secchi
ΔAIC										
1) passive	1,164	947	1,192	1,056	1,131	920	1,164	1,023	1,134	932
2) turbidity_seeking	14,979	14,982	14,978	14,978	14,983	14,986	14,982	14,982	14,682	14,686
3) tmd	804	731	784	780	650	546	602	578	722	557
4) ptmd_sal_gt_1	1,071	886	938	968	1,047	867	918	945	898	877
5) ptmd_si_pt_5	919	714	792	810	899	699	776	791	793	777
6) ptmd_si_pt_5_shallow_ebb_t_gt_12	468	293	360	351	461	281	350	343	205	196
7) ptmd_sal_gt_1_si_pt_5	875	670	749	766	859	657	735	750	751	738
8) ptmd_sal_gt_1_h8_ebb_shallow_t_gt_18_acclim	153	11	71	51	153	14	73	53	0	2
9) tmd_sal_gt_1_ebb_shallow_t_gt_18	261	198	227	215	190	95	134	121	119	34
10) tmd_sal_gt_1_ptmd_prtmd_sd_pt_1_switch	318	220	271	252	271	146	205	183	175	122
Model Rank										
1) passive	9	9	9	9	9	9	9	9	9	9
2) turbidity_seeking	10	10	10	10	10	10	10	10	10	10
3) tmd	5	7	6	6	5	5	5	5	5	5
4) ptmd_sal_gt_1	8	8	8	8	8	8	8	8	8	8
5) ptmd_si_pt_5	7	6	7	7	7	7	7	7	7	7
6) ptmd_si_pt_5_shallow_ebb_t_gt_12	4	4	4	4	4	4	4	4	4	4
7) ptmd_sal_gt_1_si_pt_5	6	5	5	5	6	6	6	6	6	6
8) ptmd_sal_gt_1_h8_ebb_shallow_t_gt_18_acclim	1	1	1	1	1	1	1	1	1	1
9) tmd_sal_gt_1_ebb_shallow_t_gt_18	2	2	2	2	2	2	2	2	2	2
10) tmd_sal_gt_1_ptmd_prtmd_sd_pt_1_switch	3	3	3	3	3	3	3	3	3	3
Proportional Entrainment Loss										
1) passive	0.06	0.06	0.06	0.06	0.06	0.06	0.06	0.06	0.10	0.10
2) turbidity_seeking	0.00	0.00	0.00	0.00	0.00	0.00	0.00	0.00	0.01	0.01
3) tmd	0.16	0.15	0.16	0.16	0.17	0.16	0.16	0.16	0.19	0.18
4) ptmd_sal_gt_1	0.09	0.09	0.09	0.09	0.09	0.09	0.09	0.09	0.10	0.11
5) ptmd_si_pt_5	0.15	0.15	0.15	0.15	0.15	0.15	0.15	0.15	0.15	0.16
6) ptmd_si_pt_5_shallow_ebb_t_gt_12	0.09	0.10	0.10	0.10	0.10	0.10	0.10	0.10	0.12	0.12
7) ptmd_sal_gt_1_si_pt_5	0.16	0.16	0.16	0.16	0.16	0.16	0.16	0.16	0.16	0.16
8) ptmd_sal_gt_1_h8_ebb_shallow_t_gt_18_acclim	0.14	0.16	0.15	0.15	0.15	0.16	0.15	0.15	0.17	0.17
9) tmd_sal_gt_1_ebb_shallow_t_gt_18	0.15	0.15	0.15	0.15	0.15	0.15	0.15	0.15	0.15	0.16
10) tmd_sal_gt_1_ptmd_prtmd_sd_pt_1_switch	0.30	0.30	0.30	0.30	0.29	0.30	0.29	0.29	0.31	0.31
SWP Salvage Expansion Factor										
1) passive	116	133	81	145	134	144	89	162	>1000	>1000
2) turbidity_seeking	>1000	>1000	>1000	>1000	>1000	>1000	>1000	>1000	>1000	>1000
3) tmd	45	38	42	41	64	62	62	64	764	>1000
4) ptmd_sal_gt_1	41	47	46	52	50	53	52	61	>1000	>1000
5) ptmd_si_pt_5	57	65	62	72	62	67	64	76	>1000	>1000
6) ptmd_si_pt_5_shallow_ebb_t_gt_12	59	55	54	60	61	57	56	62	>1000	>1000
7) ptmd_sal_gt_1_si_pt_5	58	65	62	73	63	68	65	76	>1000	>1000
8) ptmd_sal_gt_1_h8_ebb_shallow_t_gt_18_acclim	83	75	76	80	87	75	77	81	>1000	>1000
9) tmd_sal_gt_1_ebb_shallow_t_gt_18	72	68	69	69	81	86	82	84	>1000	>1000
10) tmd_sal_gt_1_ptmd_prtmd_sd_pt_1_switch	116	105	108	107	125	123	121	123	>1000	>1000

Table 4. Con't.

h) 2D WY 2005 negative binomial error in SKT data ($\tau=10$)

Population model number	1	2	3	4	5	6	7	8	9	10
Salvage efficiency structure	const	const	const	const	~turb	~turb	~turb	~turb	const	~turb
Natural survival structure	S _c	S _{SKT}	S _a	S _w	S _c	S _{SKT}	S _a	S _w	S _a	S _a
SKT efficiency structure ($\theta_{e,SKT}$)	=1	=1	=1	=1	=1	=1	=1	=1	~Secchi	~Secchi
ΔAIC										
1) passive	764	765	758	758	734	736	729	729	755	726
2) turbidity_seeking	14,285	14,291	14,286	14,286	14,289	14,295	14,290	14,290	14,285	14,293
3) tmd	606	409	604	607	445	355	431	427	607	435
4) ptmd_sal_gt_1	747	744	742	742	727	724	722	722	746	726
5) ptmd_si_pt_5	727	717	723	723	711	701	707	707	720	704
6) ptmd_si_pt_5_shallow_ebb_t_gt_12	294	258	274	280	274	248	261	268	276	262
7) ptmd_sal_gt_1_si_pt_5	686	675	682	682	672	662	668	668	677	664
8) ptmd_sal_gt_1_h8_ebb_shallow_t_gt_18_acclim	64	37	47	48	66	39	75	50	51	49
9) tmd_sal_gt_1_ebb_shallow_t_gt_18	123	39	121	123	34	0	27	26	124	28
10) tmd_sal_gt_1_ptmd_ptmd_sd_pt_1_switch	195	112	183	182	143	91	126	122	183	126
Model Rank										
1) passive	9	9	9	9	9	9	9	9	9	8
2) turbidity_seeking	10	10	10	10	10	10	10	10	10	10
3) tmd	5	5	5	5	5	5	5	5	5	5
4) ptmd_sal_gt_1	8	8	8	8	8	8	8	8	8	9
5) ptmd_si_pt_5	7	7	7	7	7	7	7	7	7	7
6) ptmd_si_pt_5_shallow_ebb_t_gt_12	4	4	4	4	4	4	4	4	4	4
7) ptmd_sal_gt_1_si_pt_5	6	6	6	6	6	6	6	6	6	6
8) ptmd_sal_gt_1_h8_ebb_shallow_t_gt_18_acclim	1	1	1	1	2	2	2	2	1	2
9) tmd_sal_gt_1_ebb_shallow_t_gt_18	2	2	2	2	1	1	1	1	2	1
10) tmd_sal_gt_1_ptmd_ptmd_sd_pt_1_switch	3	3	3	3	3	3	3	3	3	3
Proportional Entrainment Loss										
1) passive	0.10	0.09	0.10	0.10	0.10	0.10	0.10	0.10	0.10	0.11
2) turbidity_seeking	0.01	0.01	0.01	0.01	0.01	0.01	0.01	0.01	0.01	0.01
3) tmd	0.12	0.12	0.12	0.12	0.11	0.12	0.11	0.10	0.12	0.11
4) ptmd_sal_gt_1	0.09	0.09	0.09	0.09	0.10	0.10	0.10	0.10	0.09	0.10
5) ptmd_si_pt_5	0.15	0.15	0.15	0.15	0.15	0.15	0.15	0.15	0.15	0.15
6) ptmd_si_pt_5_shallow_ebb_t_gt_12	0.14	0.14	0.14	0.14	0.14	0.14	0.14	0.14	0.14	0.14
7) ptmd_sal_gt_1_si_pt_5	0.16	0.16	0.16	0.16	0.16	0.16	0.16	0.16	0.16	0.16
8) ptmd_sal_gt_1_h8_ebb_shallow_t_gt_18_acclim	0.17	0.18	0.18	0.17	0.17	0.18	0.18	0.17	0.18	0.18
9) tmd_sal_gt_1_ebb_shallow_t_gt_18	0.16	0.16	0.16	0.16	0.16	0.16	0.16	0.16	0.16	0.16
10) tmd_sal_gt_1_ptmd_ptmd_sd_pt_1_switch	0.33	0.33	0.33	0.33	0.33	0.33	0.33	0.33	0.33	0.33
SWP Salvage Expansion Factor										
1) passive	105	133	100	100	116	145	110	110	111	122
2) turbidity_seeking	>1000	>1000	>1000	>1000	>1000	>1000	>1000	>1000	>1000	>1000
3) tmd	30	20	29	29	35	26	33	33	332	33
4) ptmd_sal_gt_1	25	35	24	24	29	41	28	28	24	56
5) ptmd_si_pt_5	32	50	30	30	33	52	31	31	687	431
6) ptmd_si_pt_5_shallow_ebb_t_gt_12	34	58	48	50	33	55	48	48	48	>1000
7) ptmd_sal_gt_1_si_pt_5	32	51	30	30	33	52	32	32	853	583
8) ptmd_sal_gt_1_h8_ebb_shallow_t_gt_18_acclim	48	69	59	65	49	71	34	66	59	61
9) tmd_sal_gt_1_ebb_shallow_t_gt_18	66	61	68	67	62	66	69	71	>1000	71
10) tmd_sal_gt_1_ptmd_ptmd_sd_pt_1_switch	126	126	127	127	124	130	131	134	>1000	134

Table 4. Con't.

i) 2D WY 2011 Poisson error in SKT data ($\tau=1$)

Population model number	1	2	3	4	5	6	7	8	9	10
Salvage efficiency structure	const	const	const	const	~turb	~turb	~turb	~turb	const	~turb
Natural survival structure	S _c	S _{SKT}	S _a	S _w	S _c	S _{SKT}	S _a	S _w	S _a	S _a
SKT efficiency structure (θ_{c-SKT})	=1	=1	=1	=1	=1	=1	=1	=1	~Secchi	~Secchi
ΔAIC										
1) passive	38	33	40	40	41	36	43	43	28	31
2) turbidity Seeking	2,104	2,110	2,103	2,103	2,108	2,114	2,107	2,107	2,073	2,076
3) tmd	91	84	92	91	94	88	96	95	80	84
4) ptmd_sal_gt_1	517	454	488	483	519	457	553	486	464	467
5) ptmd_si_pt_5	445	426	436	435	448	429	440	439	398	401
6) ptmd_si_pt_5_shallow_ebb_t_gt_12	13	0	14	12	17	4	17	16	1	4
7) ptmd_sal_gt_1_si_pt_5	504	485	494	494	507	488	497	497	456	459
8) ptmd_sal_gt_1_h8_ebb_shallow_t_gt_18_acclim	121	98	123	122	124	101	126	125	100	102
9) tmd_sal_gt_1_ebb_shallow_t_gt_18	552	513	554	553	555	517	557	556	555	559
10) tmd_sal_gt_1_ptmd_prtmd_sd_pt_1_switch	293	274	281	281	296	278	285	285	250	253
Model Rank										
1) passive	2	2	2	2	2	2	2	2	2	2
2) turbidity Seeking	10	10	10	10	10	10	10	10	10	10
3) tmd	3	3	3	3	3	3	3	3	3	3
4) ptmd_sal_gt_1	8	7	7	7	8	7	8	7	8	8
5) ptmd_si_pt_5	6	6	6	6	6	6	6	6	6	6
6) ptmd_si_pt_5_shallow_ebb_t_gt_12	1	1	1	1	1	1	1	1	1	1
7) ptmd_sal_gt_1_si_pt_5	7	8	8	8	7	8	7	8	7	7
8) ptmd_sal_gt_1_h8_ebb_shallow_t_gt_18_acclim	4	4	4	4	4	4	4	4	4	4
9) tmd_sal_gt_1_ebb_shallow_t_gt_18	9	9	9	9	9	9	9	9	9	9
10) tmd_sal_gt_1_ptmd_prtmd_sd_pt_1_switch	5	5	5	5	5	5	5	5	5	5
Proportional Entrainment Loss										
1) passive	0.01	0.01	0.01	0.01	0.01	0.01	0.01	0.01	0.01	0.01
2) turbidity Seeking	0.01	0.01	0.01	0.01	0.01	0.01	0.01	0.01	0.02	0.02
3) tmd	0.10	0.09	0.10	0.09	0.09	0.09	0.09	0.09	0.12	0.12
4) ptmd_sal_gt_1	0.02	0.02	0.02	0.02	0.02	0.02	0.00	0.02	0.02	0.02
5) ptmd_si_pt_5	0.03	0.03	0.03	0.03	0.03	0.03	0.03	0.03	0.02	0.02
6) ptmd_si_pt_5_shallow_ebb_t_gt_12	0.03	0.03	0.03	0.03	0.03	0.03	0.03	0.03	0.03	0.03
7) ptmd_sal_gt_1_si_pt_5	0.03	0.03	0.03	0.03	0.03	0.03	0.03	0.03	0.02	0.02
8) ptmd_sal_gt_1_h8_ebb_shallow_t_gt_18_acclim	0.03	0.03	0.03	0.03	0.03	0.03	0.03	0.03	0.04	0.04
9) tmd_sal_gt_1_ebb_shallow_t_gt_18	0.03	0.03	0.03	0.03	0.03	0.03	0.03	0.03	0.03	0.03
10) tmd_sal_gt_1_ptmd_prtmd_sd_pt_1_switch	0.12	0.12	0.12	0.12	0.12	0.12	0.12	0.12	0.12	0.12
SWP Salvage Expansion Factor										
1) passive	>1000	>1000	>1000	>1000	>1000	>1000	>1000	>1000	>1000	>1000
2) turbidity Seeking	>1000	>1000	>1000	>1000	>1000	>1000	>1000	>1000	>1000	>1000
3) tmd	>1000	>1000	>1000	>1000	>1000	>1000	>1000	>1000	>1000	>1000
4) ptmd_sal_gt_1	>1000	>1000	>1000	>1000	>1000	>1000	>1000	>1000	>1000	>1000
5) ptmd_si_pt_5	>1000	>1000	>1000	>1000	>1000	>1000	>1000	>1000	>1000	>1000
6) ptmd_si_pt_5_shallow_ebb_t_gt_12	>1000	>1000	>1000	>1000	>1000	>1000	>1000	>1000	>1000	>1000
7) ptmd_sal_gt_1_si_pt_5	>1000	>1000	>1000	>1000	>1000	>1000	>1000	>1000	>1000	>1000
8) ptmd_sal_gt_1_h8_ebb_shallow_t_gt_18_acclim	>1000	>1000	>1000	>1000	>1000	>1000	>1000	>1000	>1000	>1000
9) tmd_sal_gt_1_ebb_shallow_t_gt_18	>1000	>1000	>1000	>1000	>1000	>1000	>1000	>1000	>1000	>1000
10) tmd_sal_gt_1_ptmd_prtmd_sd_pt_1_switch	>1000	>1000	>1000	>1000	>1000	>1000	>1000	>1000	>1000	>1000

Table 4. Con't.

j) 2D WY 2011 negative binomial error in SKT data ($\tau=10$)

Population model number	1	2	3	4	5	6	7	8	9	10
Salvage efficiency structure	const	const	const	const	~turb	~turb	~turb	~turb	const	~turb
Natural survival structure	S_c	S_{SKT}	S_d	S_w	S_c	S_{SKT}	S_d	S_w	S_d	S_d
SKT efficiency structure (θ_{c-SKT})	=1	=1	=1	=1	=1	=1	=1	=1	-Secch	-Secch
ΔAIC										
1) passive	88	94	90	90	92	98	93	93	91	92
2) turbidity_seeking	319	325	320	320	323	329	324	324	319	321
3) tmd	7	13	2,017	9	11	17	14	13	11	15
4) ptmd_sal_gt_1	144	145	143	142	146	147	146	144	145	150
5) ptmd_si_pt_5	77	83	79	79	81	86	83	83	78	81
6) ptmd_si_pt_5_shallow_ebb_t_gt_12	14	19	15	15	17	23	1,332	19	20	24
7) ptmd_sal_gt_1_si_pt_5	130	135	132	132	133	138	135	135	139	136
8) ptmd_sal_gt_1_h8_ebb_shallow_t_gt_18_acclim	61	66	63	63	63	69	65	65	64	67
9) tmd_sal_gt_1_ebb_shallow_t_gt_18	127	133	129	129	131	136	133	133	132	158
10) tmd_sal_gt_1_ptmd_prtmd_sd_pt_1_switch	0	5	348	3	3	9	5	5	0	4
Model Rank										
1) passive	6	6	4	6	6	6	5	6	6	6
2) turbidity_seeking	10	10	8	10	10	10	9	10	10	10
3) tmd	2	2	10	2	2	2	2	2	2	2
4) ptmd_sal_gt_1	9	9	7	9	9	9	8	9	9	8
5) ptmd_si_pt_5	5	5	3	5	5	5	4	5	5	5
6) ptmd_si_pt_5_shallow_ebb_t_gt_12	3	3	1	3	3	3	10	3	3	3
7) ptmd_sal_gt_1_si_pt_5	8	8	6	8	8	8	7	8	8	7
8) ptmd_sal_gt_1_h8_ebb_shallow_t_gt_18_acclim	4	4	2	4	4	4	3	4	4	4
9) tmd_sal_gt_1_ebb_shallow_t_gt_18	7	7	5	7	7	7	6	7	7	9
10) tmd_sal_gt_1_ptmd_prtmd_sd_pt_1_switch	1	1	9	1	1	1	1	1	1	1
Proportional Entrainment Loss										
1) passive	0.03	0.03	0.03	0.03	0.03	0.03	0.03	0.03	0.03	0.04
2) turbidity_seeking	0.03	0.03	0.03	0.03	0.03	0.03	0.03	0.03	0.03	0.04
3) tmd	0.14	0.14	0.00	0.14	0.14	0.14	0.14	0.14	0.14	0.14
4) ptmd_sal_gt_1	0.06	0.06	0.06	0.06	0.06	0.06	0.06	0.06	0.06	0.06
5) ptmd_si_pt_5	0.07	0.07	0.07	0.07	0.07	0.07	0.07	0.07	0.06	0.06
6) ptmd_si_pt_5_shallow_ebb_t_gt_12	0.07	0.07	0.07	0.07	0.07	0.07	0.03	0.07	0.06	0.07
7) ptmd_sal_gt_1_si_pt_5	0.08	0.08	0.08	0.07	0.08	0.08	0.08	0.08	0.08	0.07
8) ptmd_sal_gt_1_h8_ebb_shallow_t_gt_18_acclim	0.06	0.07	0.07	0.07	0.07	0.07	0.07	0.07	0.06	0.06
9) tmd_sal_gt_1_ebb_shallow_t_gt_18	0.08	0.08	0.08	0.08	0.08	0.08	0.08	0.08	0.08	0.01
10) tmd_sal_gt_1_ptmd_prtmd_sd_pt_1_switch	0.14	0.14	0.11	0.14	0.14	0.14	0.14	0.14	0.14	0.14
SWP Salvage Expansion Factor										
1) passive	>1000	>1000	>1000	>1000	>1000	>1000	>1000	>1000	>1000	>1000
2) turbidity_seeking	>1000	>1000	>1000	>1000	>1000	>1000	>1000	>1000	>1000	>1000
3) tmd	>1000	>1000	1	>1000	>1000	>1000	>1000	>1000	>1000	>1000
4) ptmd_sal_gt_1	>1000	>1000	>1000	>1000	>1000	>1000	>1000	>1000	>1000	>1000
5) ptmd_si_pt_5	>1000	>1000	>1000	>1000	>1000	>1000	>1000	>1000	>1000	>1000
6) ptmd_si_pt_5_shallow_ebb_t_gt_12	>1000	>1000	>1000	>1000	>1000	>1000	>1000	>1000	>1000	>1000
7) ptmd_sal_gt_1_si_pt_5	>1000	>1000	>1000	>1000	>1000	>1000	>1000	>1000	>1000	>1000
8) ptmd_sal_gt_1_h8_ebb_shallow_t_gt_18_acclim	>1000	>1000	>1000	>1000	>1000	>1000	>1000	>1000	>1000	>1000
9) tmd_sal_gt_1_ebb_shallow_t_gt_18	>1000	>1000	>1000	>1000	>1000	>1000	>1000	>1000	>1000	>1000
10) tmd_sal_gt_1_ptmd_prtmd_sd_pt_1_switch	>1000	>1000	1	>1000	>1000	>1000	>1000	>1000	>1000	>1000

Table 5. Comparison of salvage expansion factors (θ_s^{-1}) from previous studies. Expansion factors from Castillo et al. (2012) were determined from mark-recapture based estimates of louver efficiency and pre-screen losses, while those from Kimmerer and Smith et al. were based on the ratio of estimated entrainment to observed salvage, where entrainment was calculated as the product of population size and a hydrodynamic-based entrainment rate. Rows a)-e) demonstrate how efficiency and pre-screen losses are combined to estimate the total efficiency (θ_s) and expansion factor (θ_s^{-1}). Rows f)-i) demonstrate how the Castillo et al. total efficiency estimates can be separated from the salvage efficiencies estimated from the population dynamics model in this study to determine the additional loss between the entrainment point and the Clifton Court Forebay (CCF) gates, which was the boundary of the Castillo et al. study.

		Castillo et al. (2009) - SWP		Kimmerer (CVP=SWP)		Smith et al. (2017)	
		February	March	2008	2011	CVP	SWP
a) Louver efficiency		0.53	0.44				
b) Pre-screen loss		0.942	0.991				
c) Pre-screen efficiency (1 -b)		0.058	0.009				
d) Total efficiency (a*b)		0.03074	0.00396				
e) Salvage expansion factor (1/d)		32.5	252.5	29 (9-49)	22 (13-33)	35	50
f) Example salvage efficiency (θ_s) from population model for SWP	0.0025						
g) Example salvage expansion (1/f)	400						
h) Proportion lost from entrainment point to CCF (1-f/d)		0.92	0.37				
i) Expansion factor upstream of CCF (1/h)		12.3	1.6				

Table 6. Comparison of 10 particle-tracking models (PTMs) for each water year and PTM type (2D or 3D) scenario based on differences in AIC (Δ AIC) within scenarios (columns). Results are based on the population model with survival varying with model day (S_d) and salvage efficiency varying with turbidity (θ_{turb} , model 7 in Table 4), assuming a) negative binomial and b) poisson error in SKT catch data. Also shown are the total proportional entrainment losses. Dark-, medium-, and light-grey shaded cells identify the 1st-, 2nd-, and 3rd-ranked models, respectively.

a) Poisson error in SKT data (variance to mean ratio, $\tau=1$)

PTM Type Water Year	3D	2D			
	2002	2002	2004	2005	2011
ΔAIC					
1) passive	817	604	2,747	1,091	25
2) turbidity_seeking	4,711	49,591	52,654	14,909	2,090
3) tmd	2,311	1,054	786	528	78
4) ptmd_sal_gt_1	604	1,192	3,170	845	536
5) ptmd_si_pt_5	409	839	2,769	703	423
6) ptmd_si_pt_5_shallow_ebb_t_gt_12	0	408	490	277	0
7) ptmd_sal_gt_1_si_pt_5	161	836	2,877	662	480
8) ptmd_sal_gt_1_h8_ebb_shallow_t_gt_18_acclim	263	0	359	0	108
9) tmd_sal_gt_1_ebb_shallow_t_gt_18	117	334	306	60	540
10) tmd_sal_gt_1_ptmd_prtmd_sd_pt_1_switch	91	471	0	132	268
Proportional Entrainment Loss					
1) passive	0.03	0.03	0.06	0.06	0.01
2) turbidity_seeking	0.07	0.00	0.04	0.00	0.01
3) tmd	0.34	0.36	0.40	0.16	0.09
4) ptmd_sal_gt_1	0.08	0.06	0.10	0.09	0.00
5) ptmd_si_pt_5	0.22	0.24	0.30	0.15	0.03
6) ptmd_si_pt_5_shallow_ebb_t_gt_12	0.35	0.35	0.20	0.10	0.03
7) ptmd_sal_gt_1_si_pt_5	0.25	0.24	0.35	0.16	0.03
8) ptmd_sal_gt_1_h8_ebb_shallow_t_gt_18_acclim	0.60	0.37	0.28	0.15	0.03
9) tmd_sal_gt_1_ebb_shallow_t_gt_18	0.49	0.36	0.37	0.15	0.03
10) tmd_sal_gt_1_ptmd_prtmd_sd_pt_1_switch	0.46	0.48	0.50	0.29	0.12

Table 6. Con't.

b) Negative binomial error in SKT data (variance to mean ratio, $\tau=10$)

PTM Type Water Year	3D	2D			
	2002	2002	2004	2005	2011
ΔAIC					
1) passive	291	211	1,866	701	88
2) turbidity_seeking	4,495	47,501	47,537	14,262	319
3) tmd	970	370	311	403	9
4) ptmd_sal_gt_1	223	201	1,704	694	140
5) ptmd_si_pt_5	174	325	1,880	679	78
6) ptmd_si_pt_5_shallow_ebb_t_gt_12	0	72	367	233	1,326
7) ptmd_sal_gt_1_si_pt_5	164	348	2,070	641	130
8) ptmd_sal_gt_1_h8_ebb_shallow_t_gt_18_acclim	208	0	384	48	60
9) tmd_sal_gt_1_ebb_shallow_t_gt_18	175	54	0	0	128
10) tmd_sal_gt_1_ptmd_ptmd_sd_pt_1_switch	111	56	105	99	0
Proportional Entrainment Loss					
1) passive	0.03	0.03	0.10	0.10	0.03
2) turbidity_seeking	0.06	0.00	0.06	0.01	0.03
3) tmd	0.38	0.40	0.33	0.11	0.14
4) ptmd_sal_gt_1	0.07	0.06	0.10	0.10	0.06
5) ptmd_si_pt_5	0.21	0.24	0.31	0.15	0.07
6) ptmd_si_pt_5_shallow_ebb_t_gt_12	0.36	0.39	0.14	0.14	0.03
7) ptmd_sal_gt_1_si_pt_5	0.25	0.24	0.37	0.16	0.08
8) ptmd_sal_gt_1_h8_ebb_shallow_t_gt_18_acclim	0.59	0.36	0.14	0.18	0.07
9) tmd_sal_gt_1_ebb_shallow_t_gt_18	0.49	0.36	0.18	0.16	0.08
10) tmd_sal_gt_1_ptmd_ptmd_sd_pt_1_switch	0.48	0.51	0.52	0.33	0.14

Table 7. Comparison of fit statistics (log likelihood) by data source for 1st- and 2nd-ranked PTMs in water year 2002 (3D PTM) and 2004 assuming poisson error ($\tau=1$) in SKT catch data. Results are based on population model 7 (Table 4) where daily survival rate is a smooth function of model day and salvage expansion factors depend on turbidity. A higher log likelihood (closer to 0) indicates better fit. As the number of estimated parameters are the same for both PTMs, twice the difference in the total log likelihood between models is equivalent to the difference in AIC (Table 6).

Likelihood Source	3D WY 2002		2D 2004	
	PTM 6	PTM 10	PTM 10	PTM 9
FMWT	-50	-40	-49	-78
SKT	-800	-786	-1,385	-1,504
Salvage	-450	-520	-949	-955
Total	-1,300	-1,346	-2,383	-2,537
Δ AIC		91		306

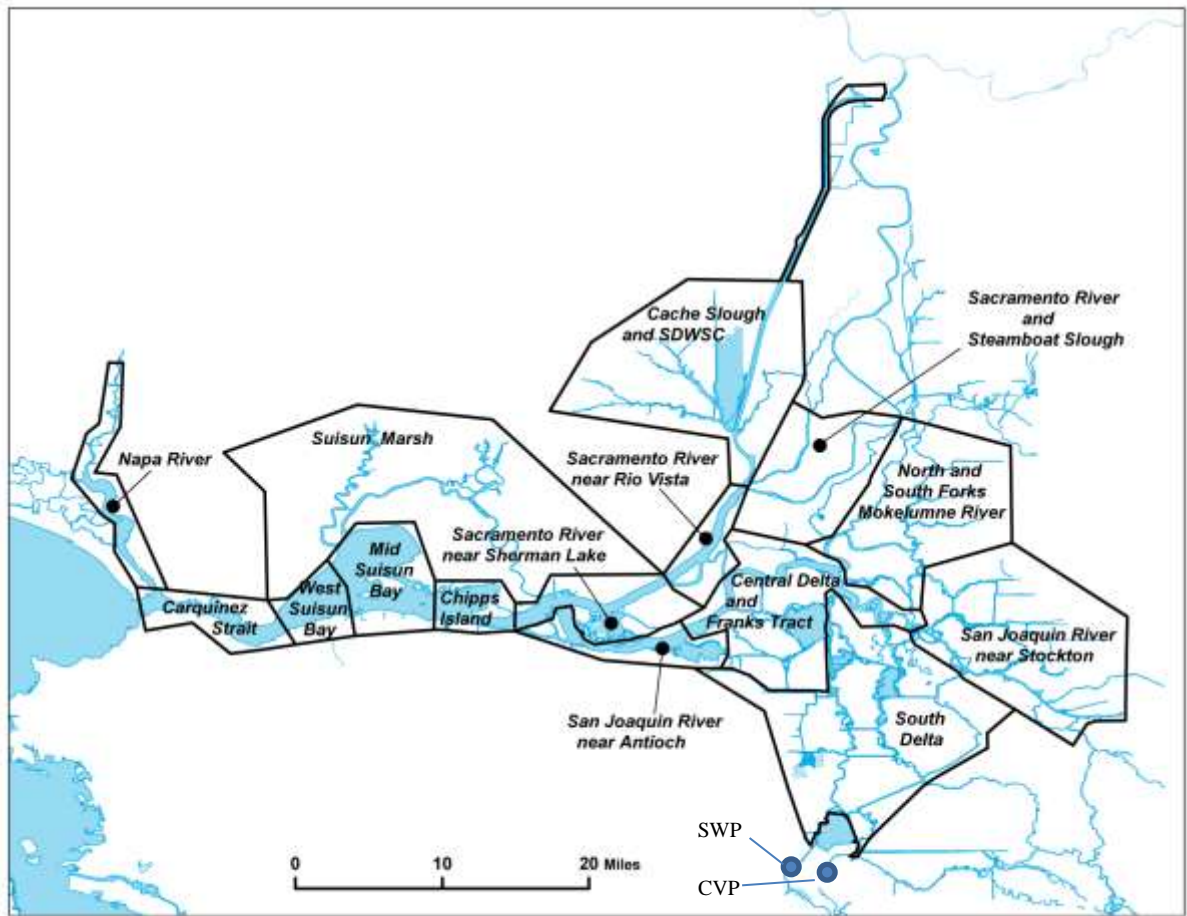


Figure 1. Boundaries of CAMT regions and the location of the State Water Project (SWP) and federal Central Valley Project (CVP) pumping plants.

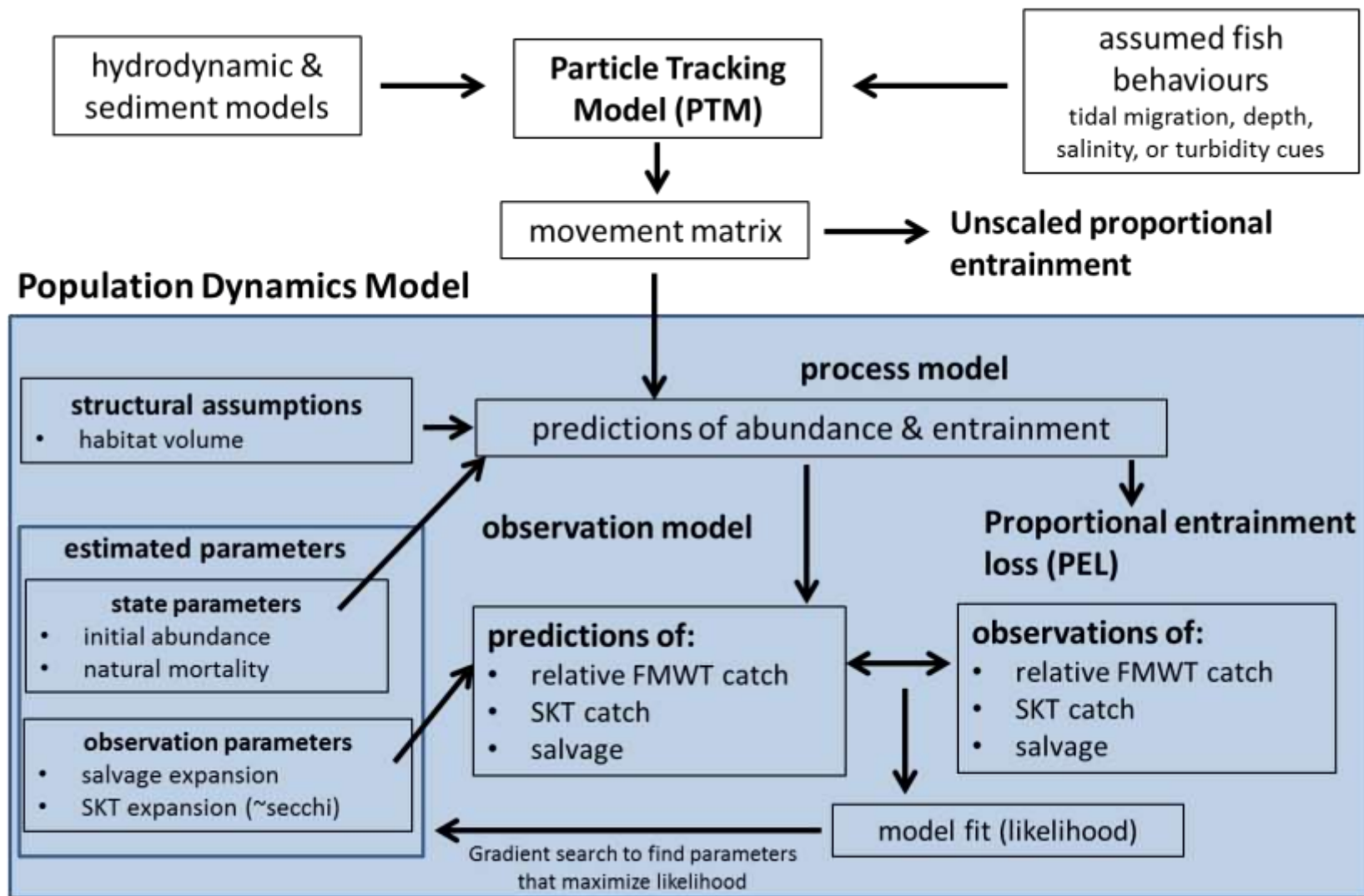


Figure 2. Overview of modelling approaches used to evaluate alternate Particle Tracking Models (PTMs) and predict proportional entrainment loss for adult Delta Smelt.

a)

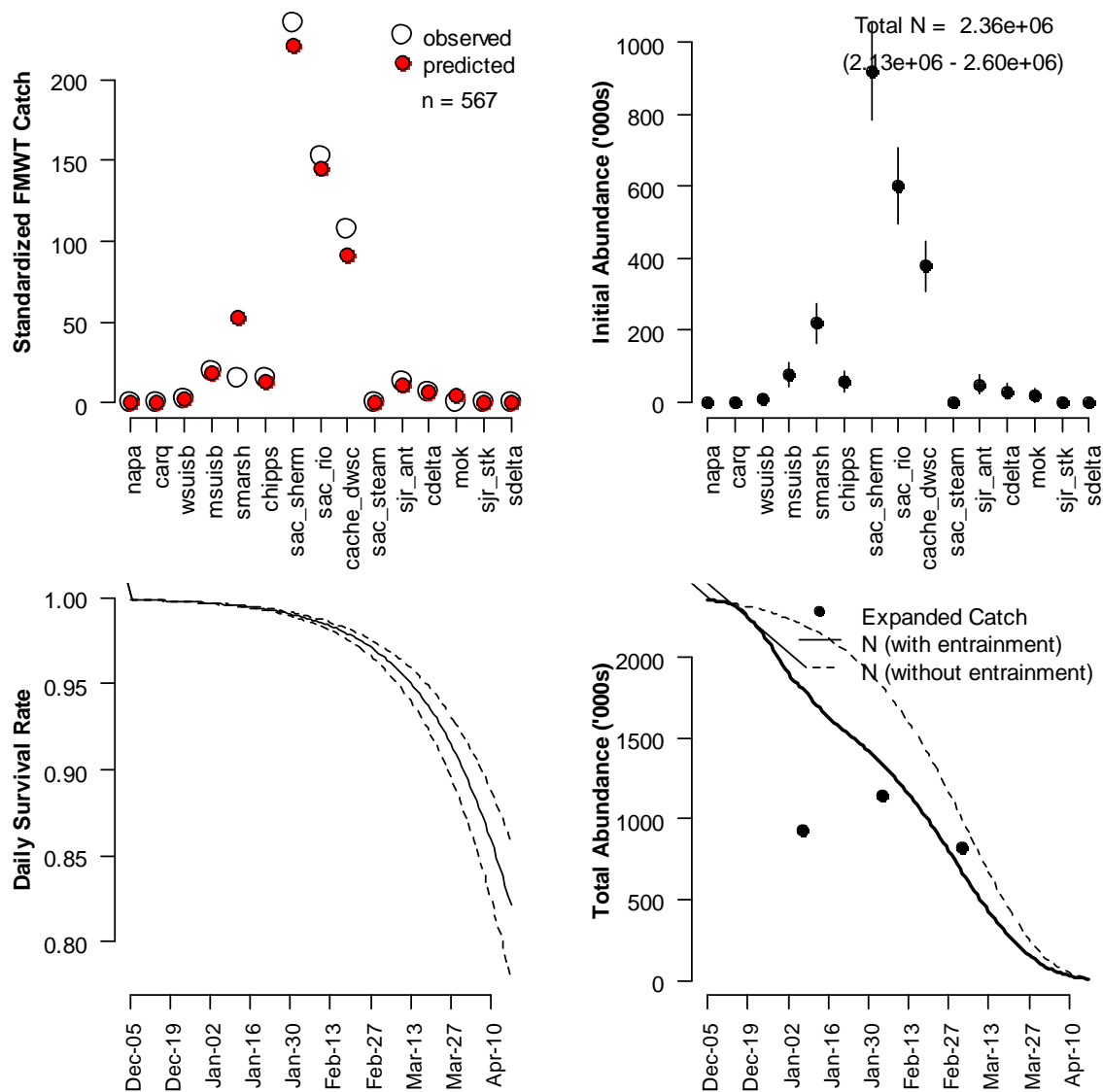


Figure 3. Model fit and predictions for the 3D-based PTM model 6 and population model 10 with poisson error in SKT catch data applied in water year 2002 (Table 4a). a) shows predicted and observed FMWT volume-corrected FMWT catch (top-left plot, observed catch summed across Sep, Oct, Nov, and Dec. surveys), regional population estimates with 95% credible intervals (top –right plot), predictions of the daily survival rate (solid line, bottom-left plot) with 95% credible intervals (dashed lines), and predicted total abundance across regions (bottom-right plot, solid and dashed lines) compared to estimates based on expanding the catch by the ratio of 4 m volume to the volume of tows and accounting for the estimated Secchi depth effect on SKT sampling efficiency.

b)

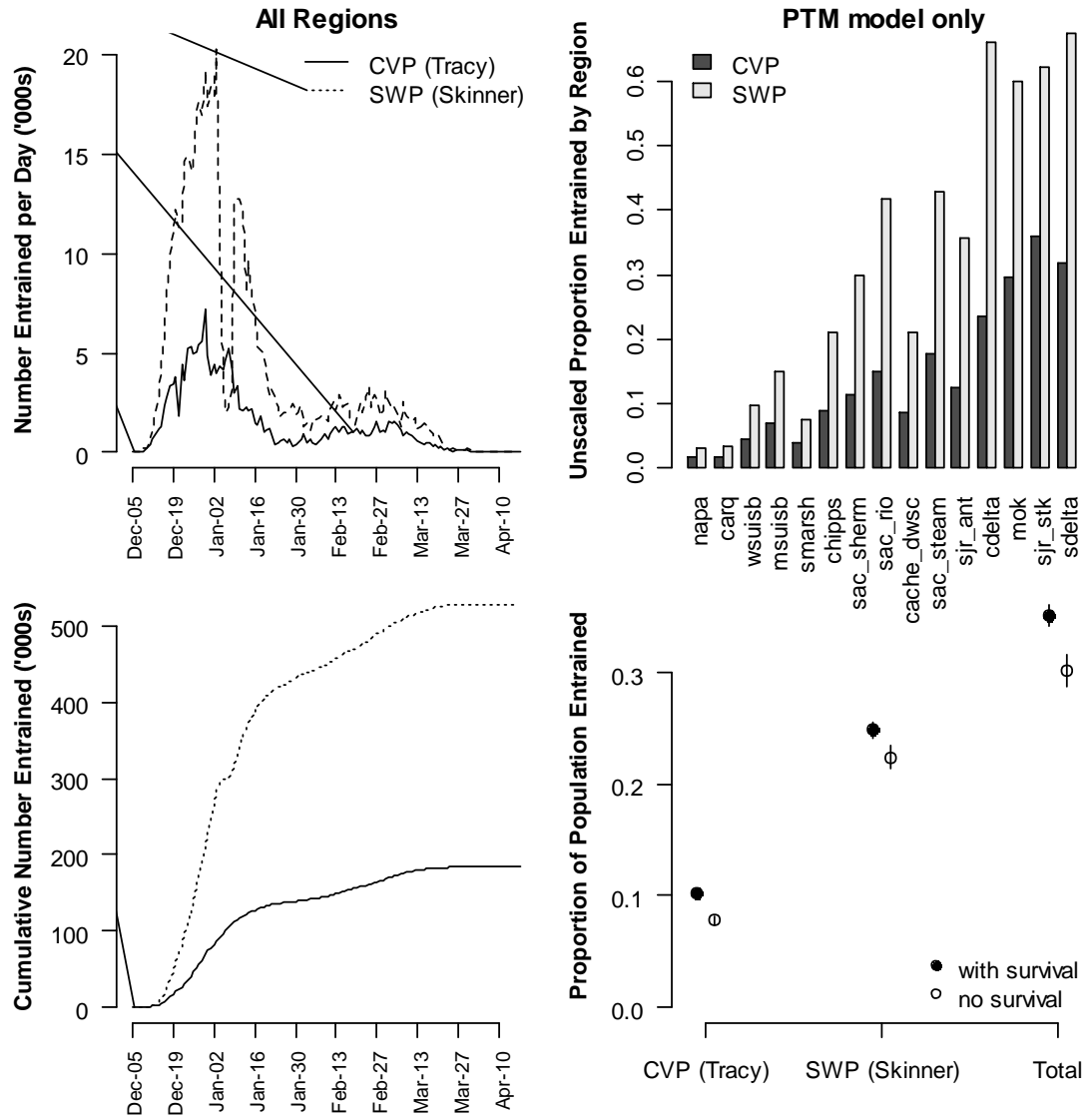


Figure 3. Con't. Predictions of daily salvage (left plots), the cumulative unscaled proportional entrainment for each region predicted by the PTM (top-right), and estimates of proportional entrainment (which include survival effects) and discrete proportional entrainment (which do not include survival effects as they are based on ratio of entrainment to initial abundance).

c)

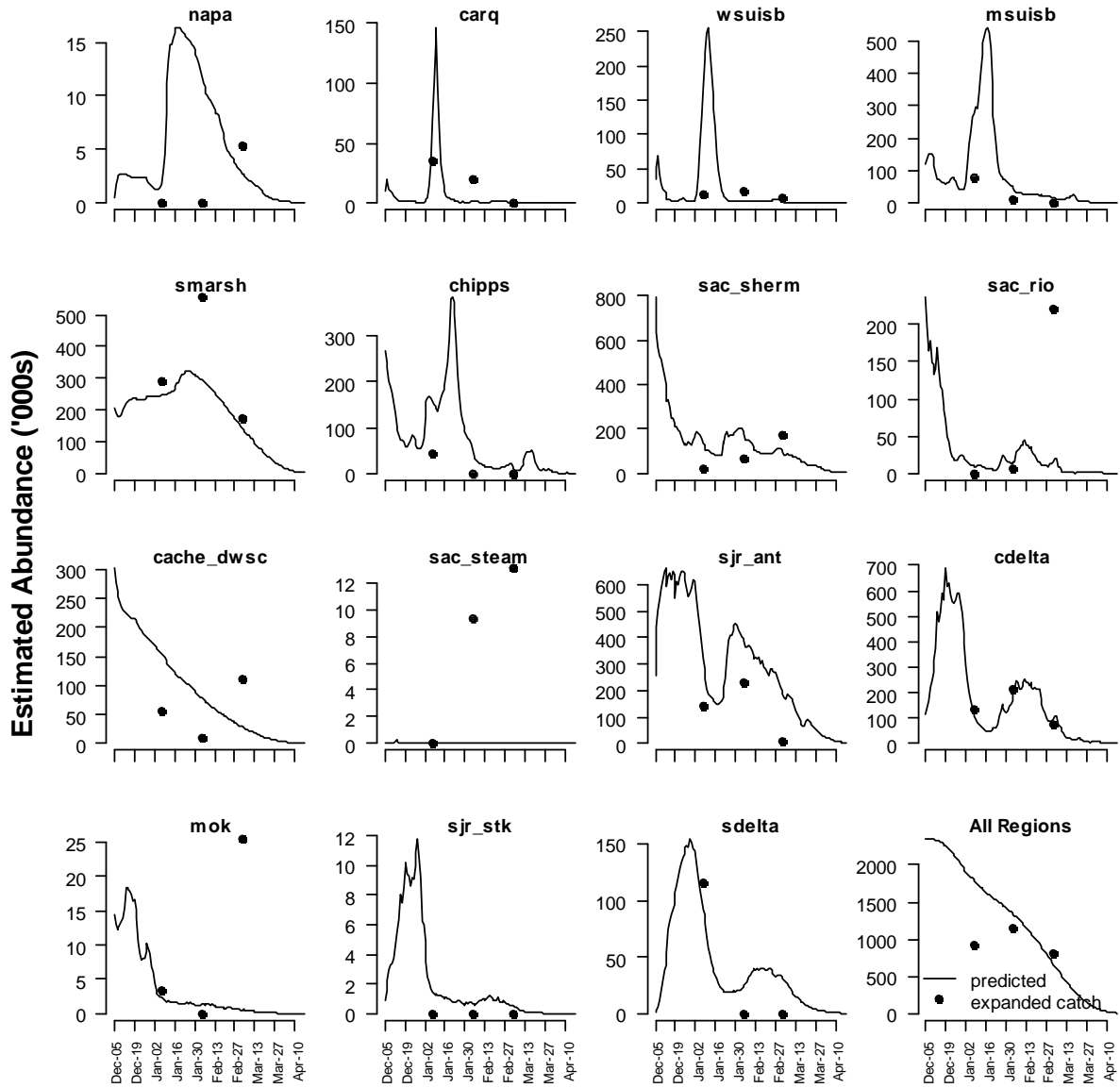


Figure 3. Con't. Abundance estimates by region and model day (lines) compared to estimates based on expanded catch (points). Note different y-axis scales among panels.

d)

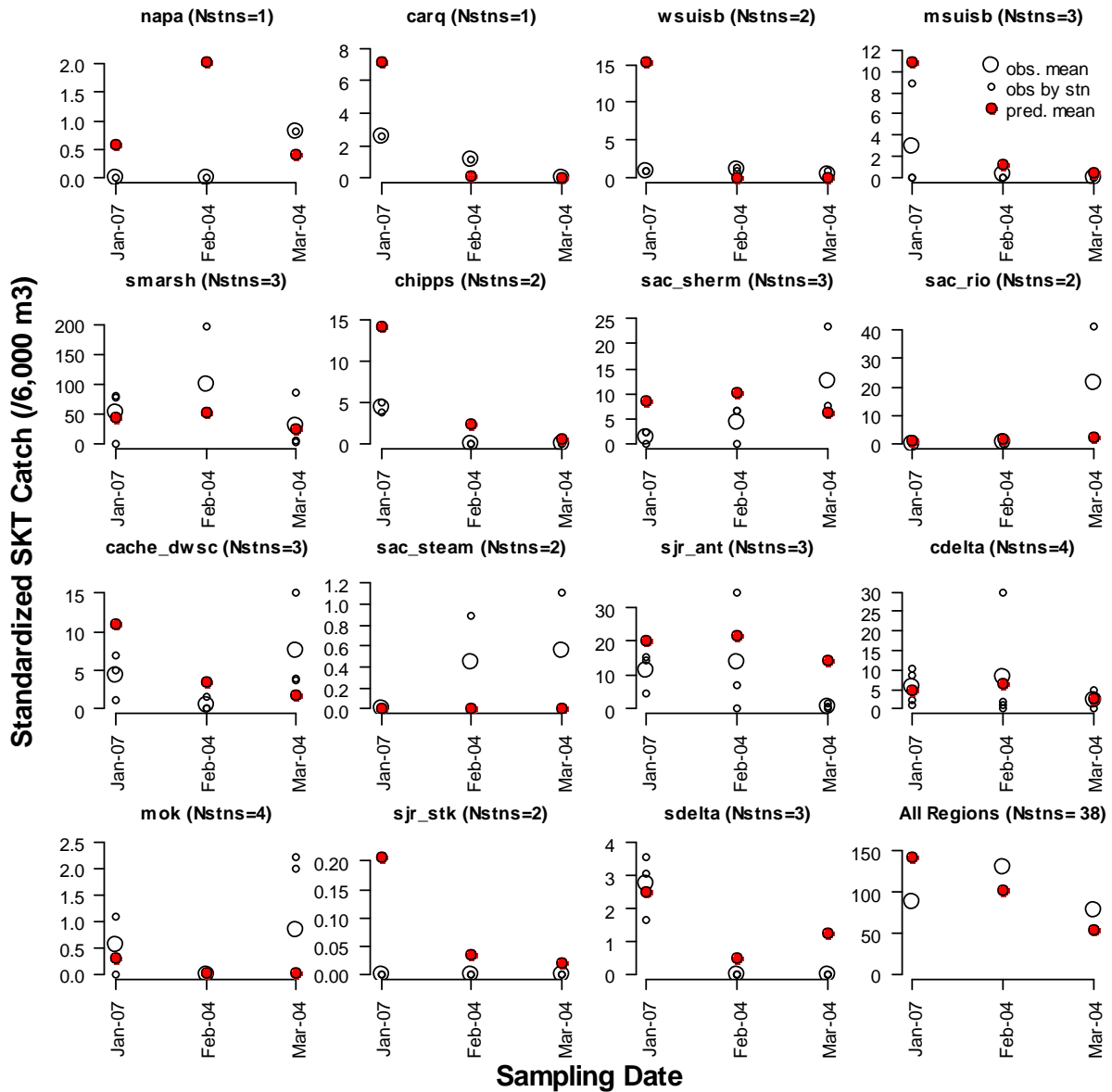


Figure 3. Con't. Comparison of predicted (red points) and mean observed (large open points) SKT catch by trip and region where catches are standardized by the approximate average tow volume. Also shown are the standardized station-specific standardized catches (small open points).

e)

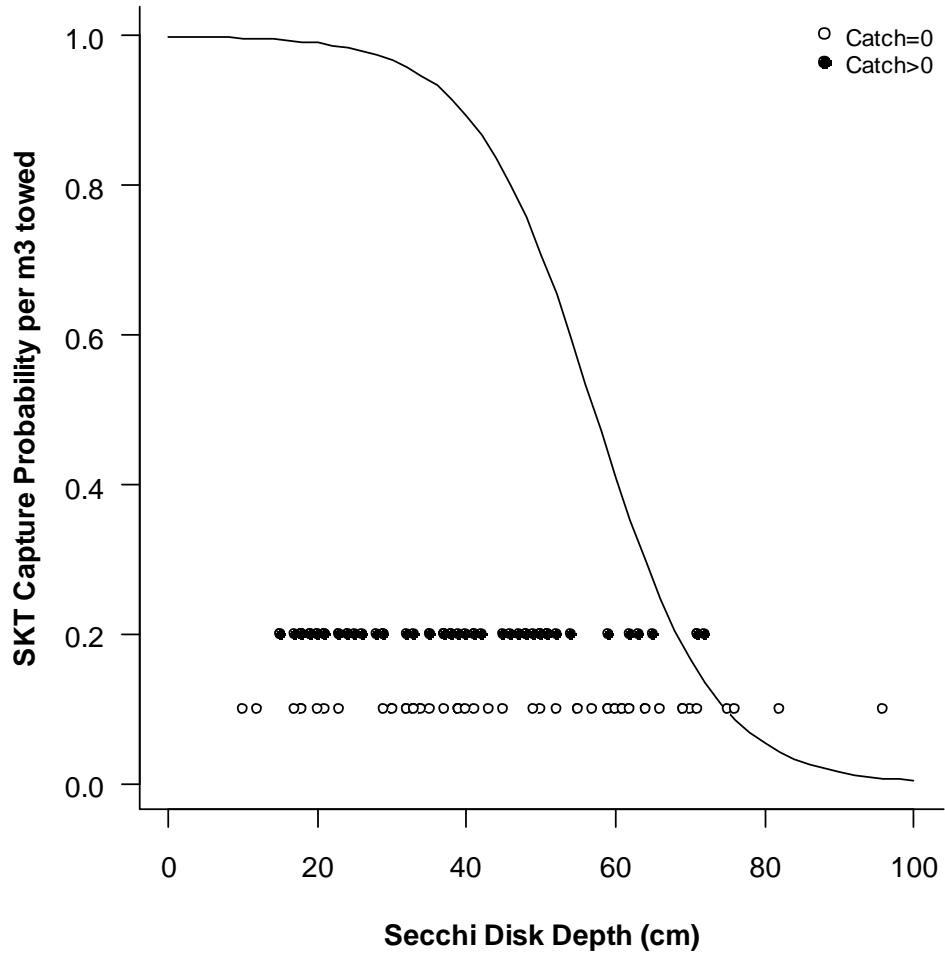


Figure 3. Con't. Estimated relationship between SKT efficiency and Secchi depth (eqn. 5c). Points show the measured Secchi depths across all surveys and stations where Delta Smelt were (closed) and were not (open) captured.

f)

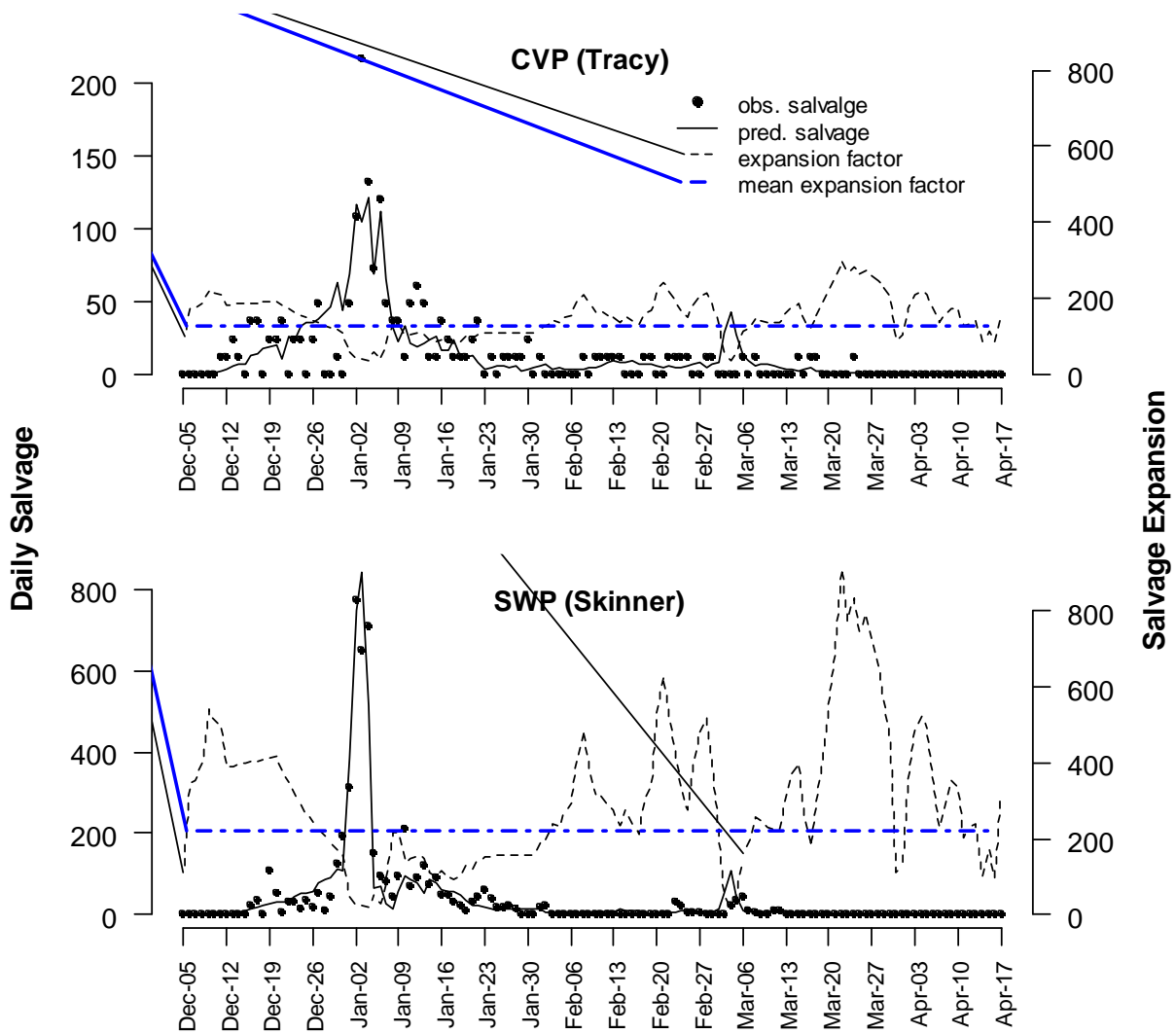


Figure 3. Con't. Predicted (solid line) and observed (points) daily salvage (left axis). Also shown are the daily salvage expansion factors ($1/\theta_s$, black dashed line right-hand axis) and the salvage-weighted average value across days (blue dashed line).

g)

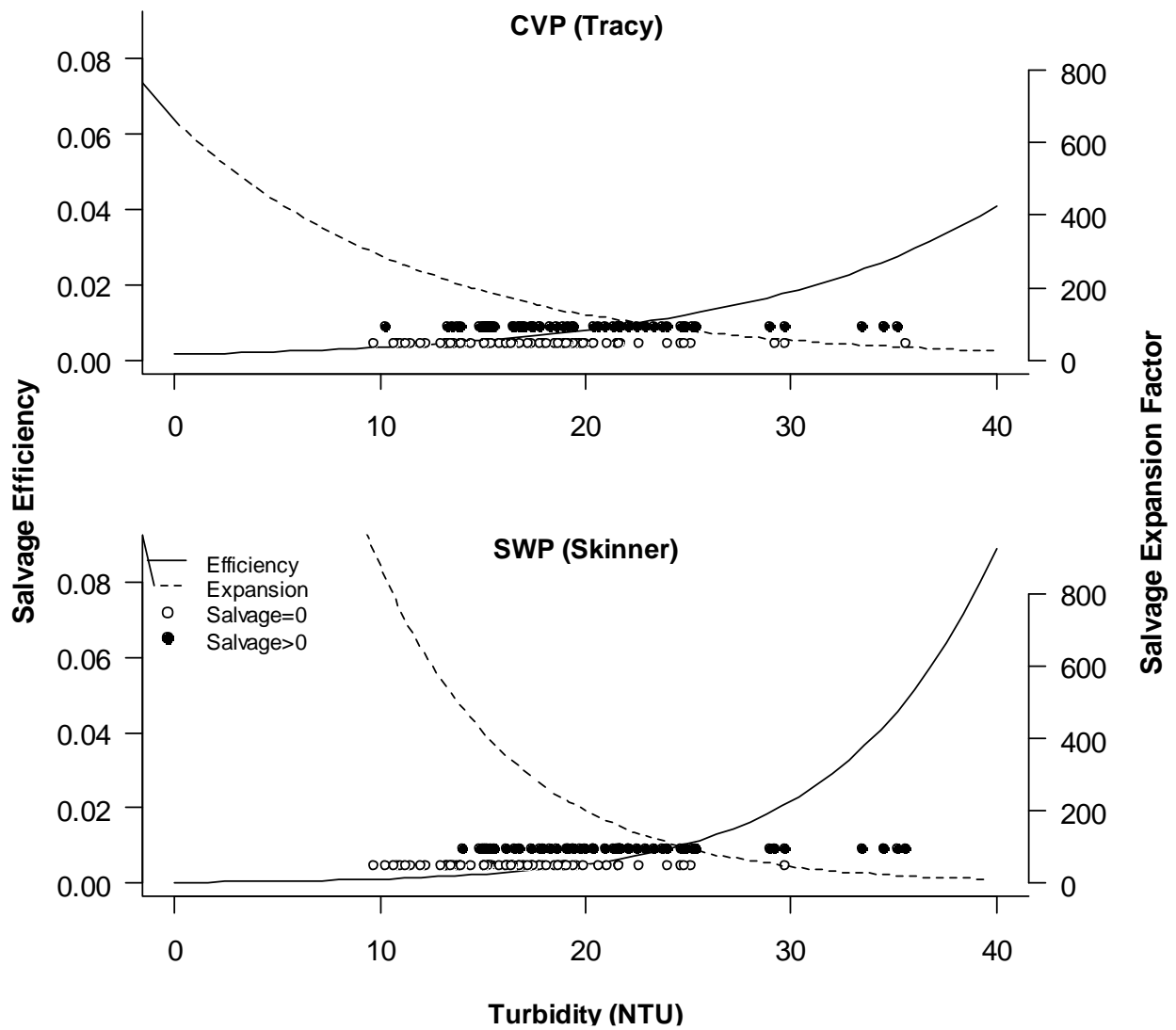


Figure 3. Con't. Estimated salvage efficiency-turbidity relationship (solid line, left-hand axis) and the inverse (expansion factor relationship, dashed line, right-hand axis). The solid and open points show the turbidity levels when salvage was and was not observed.

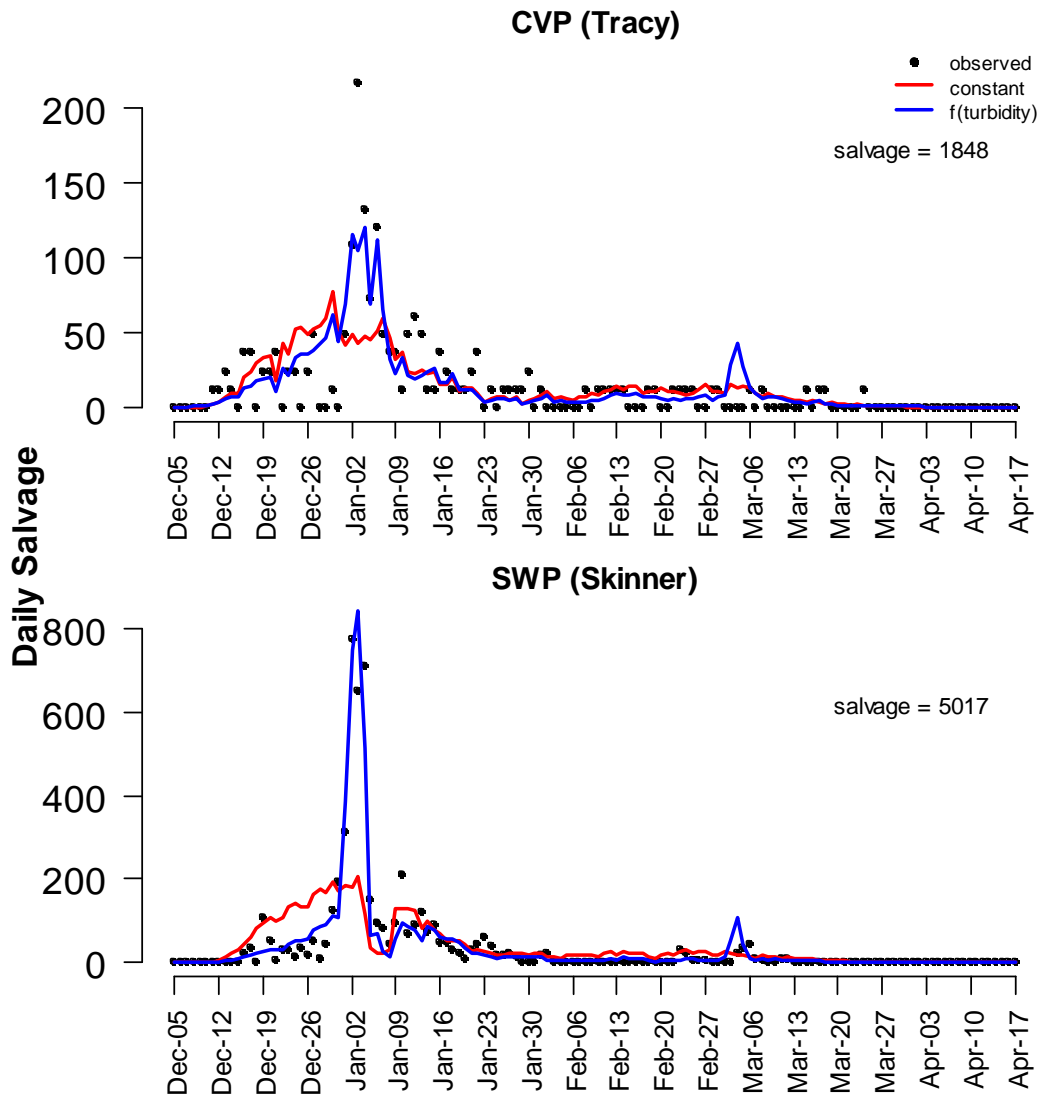


Figure 4. Comparison of fits to salvage in water year 2002 based on constant and turbidity-varying salvage efficiency models for 3D PTM 6 (population dynamic models 3 and 7, Table 4a).

a)

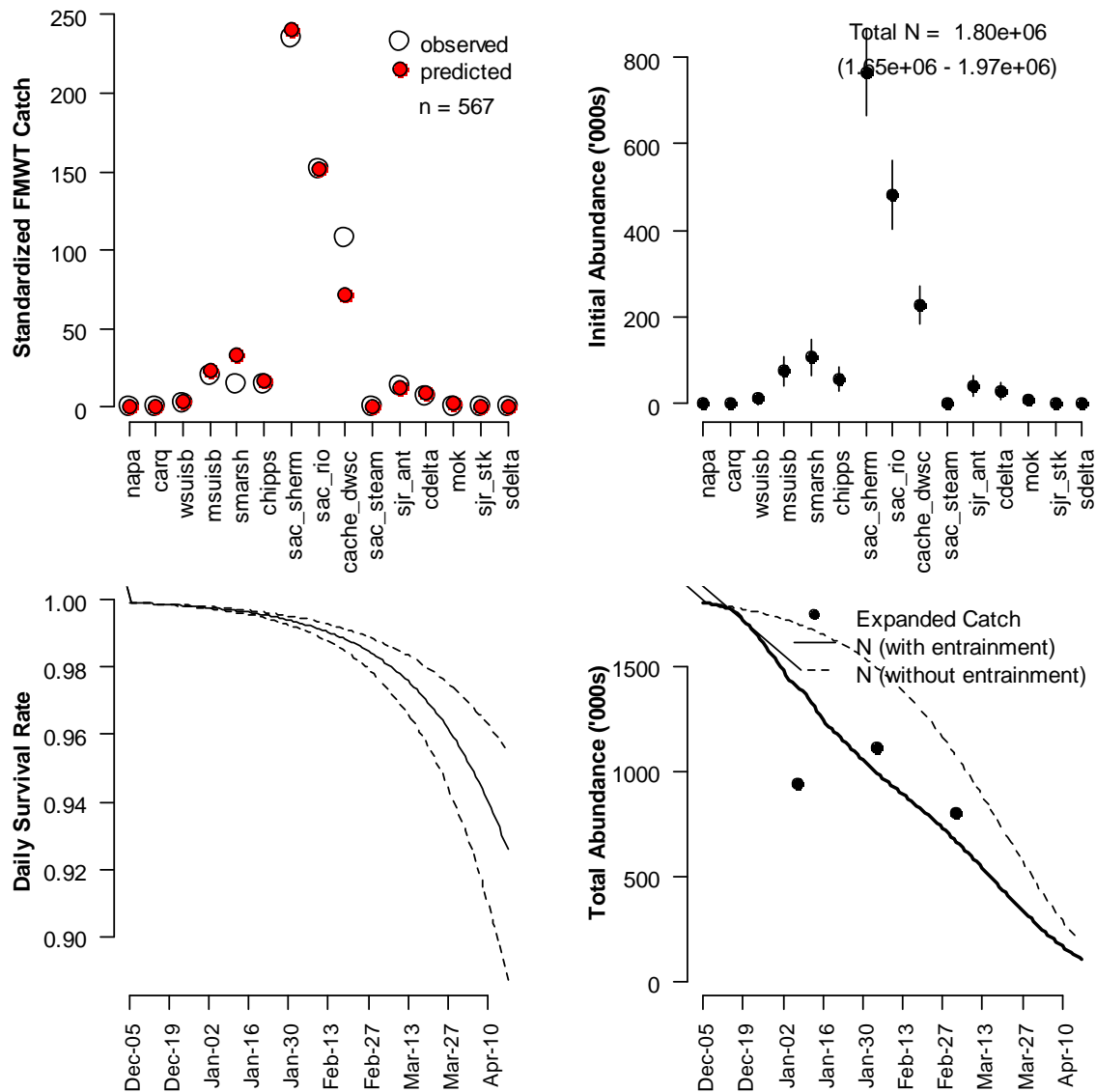


Figure 5. Model fit and predictions for the 2D-based PTM model 8 and population model 10 with poisson error in SKT catch data applied in water year 2002 (Table 4c). a) shows predicted and observed FMWT volume-corrected FMWT catch (top-left plot, observed catch summed across Sep, Oct, Nov, and Dec. surveys), regional population estimates with 95% credible intervals (top-right plot), predictions of the daily survival rate (solid line, bottom-left plot) with 95% credible intervals (dashed lines), and predicted total abundance across regions (bottom-right plot, solid and dashed lines) compared to estimates based on expanding the catch by the ratio of 4 m volume to the volume of tows and accounting for the estimated Secchi depth effect on SKT sampling efficiency.

b)

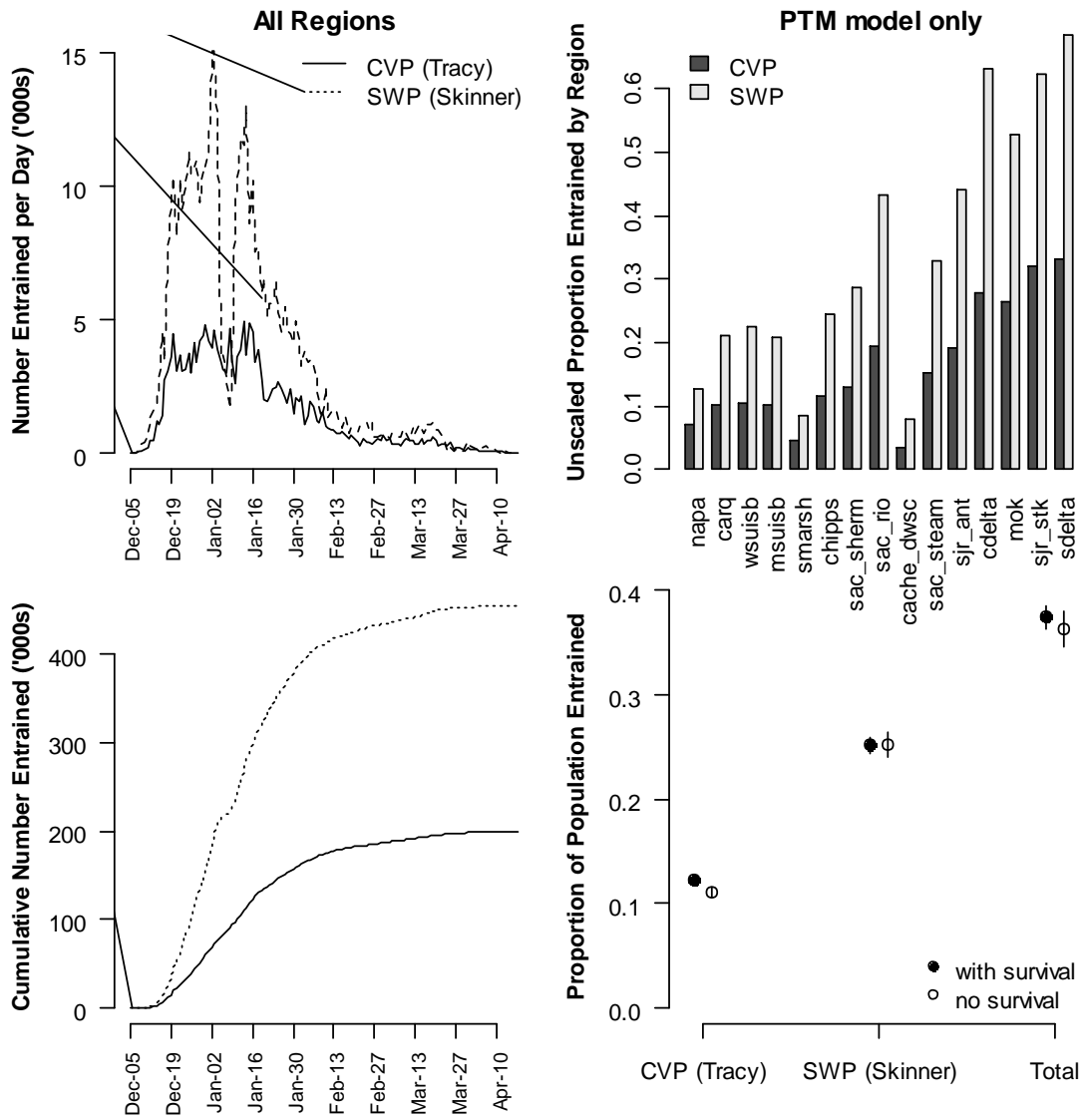


Figure 5. Con't. Predictions of daily salvage (left plots), the cumulative unscaled proportional entrainment for each region predicted by the PTM (top-right), and estimates of proportional entrainment (which include survival effects) and discrete proportional entrainment (which do not include survival effects as they are based on ratio of entrainment to initial abundance).

c)

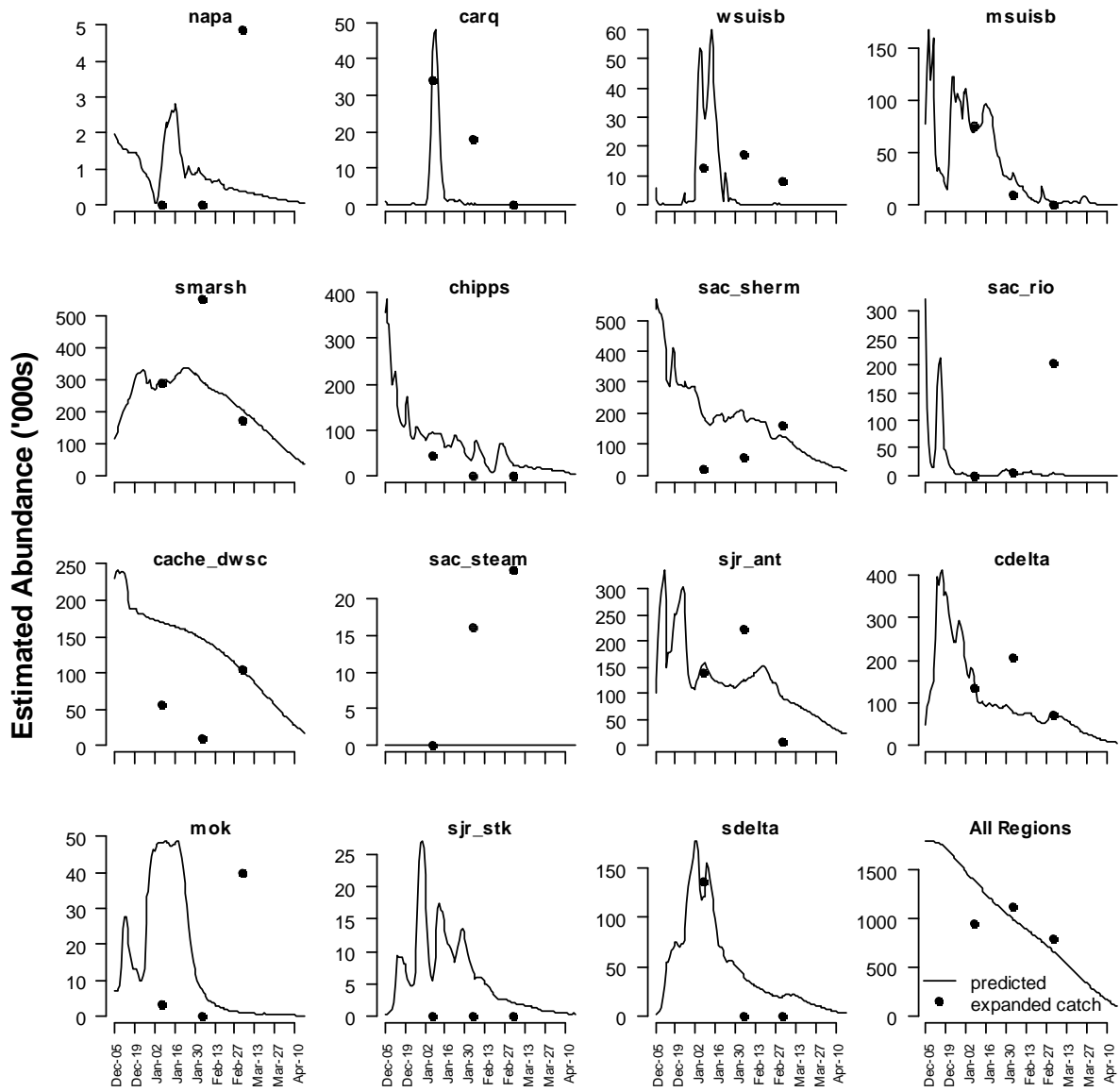


Figure 5. Con't. Abundance estimates by region and model day (lines) compared to estimates based on expanded catch (points).

d)

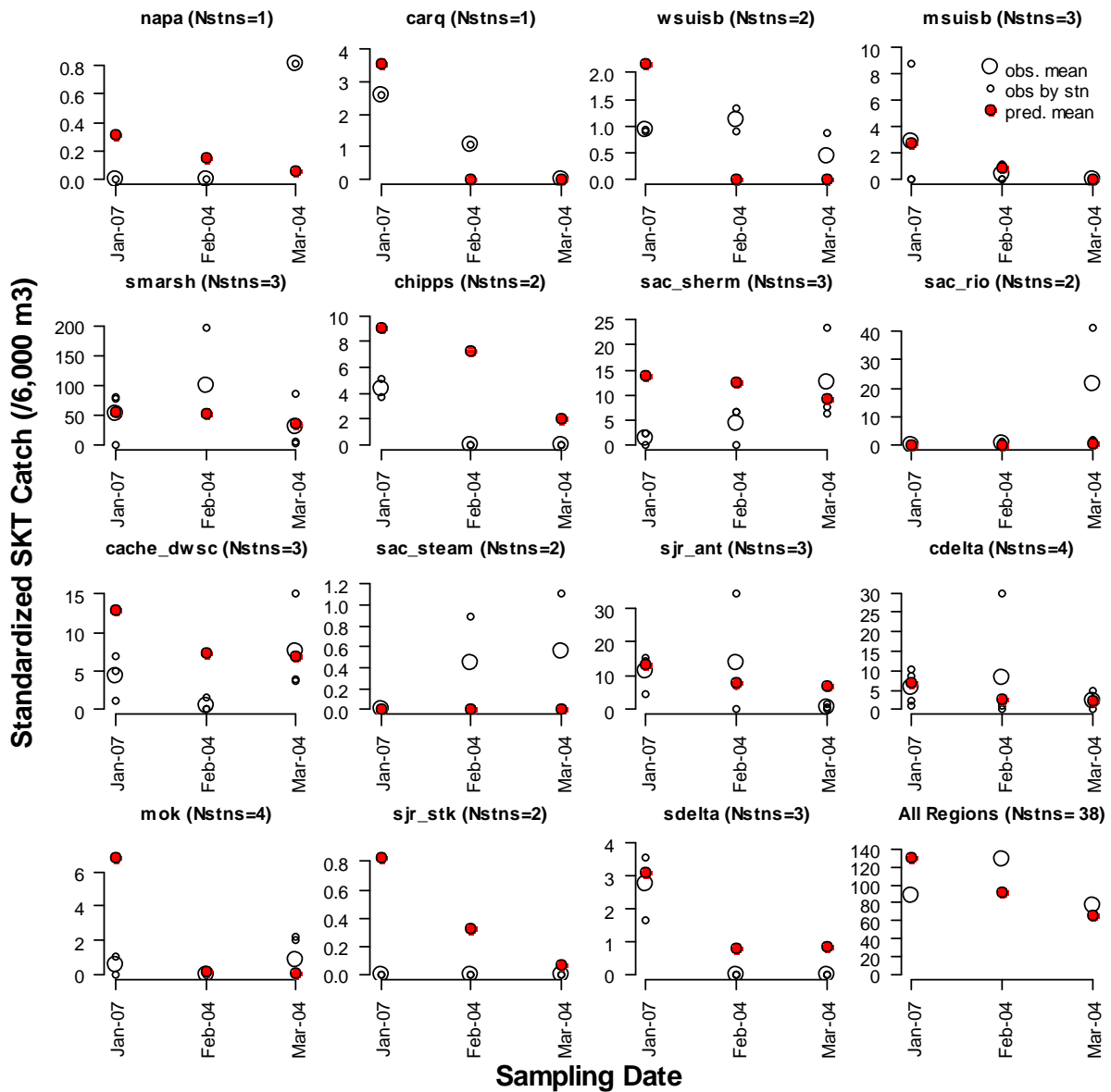


Figure 5. Con't. Comparison of predicted (red points) and mean observed (large open points) SKT catch by trip and region where catches are standardized by the approximate average tow volume. Also shown are the standardized station-specific standardized catches (small open points).

e)

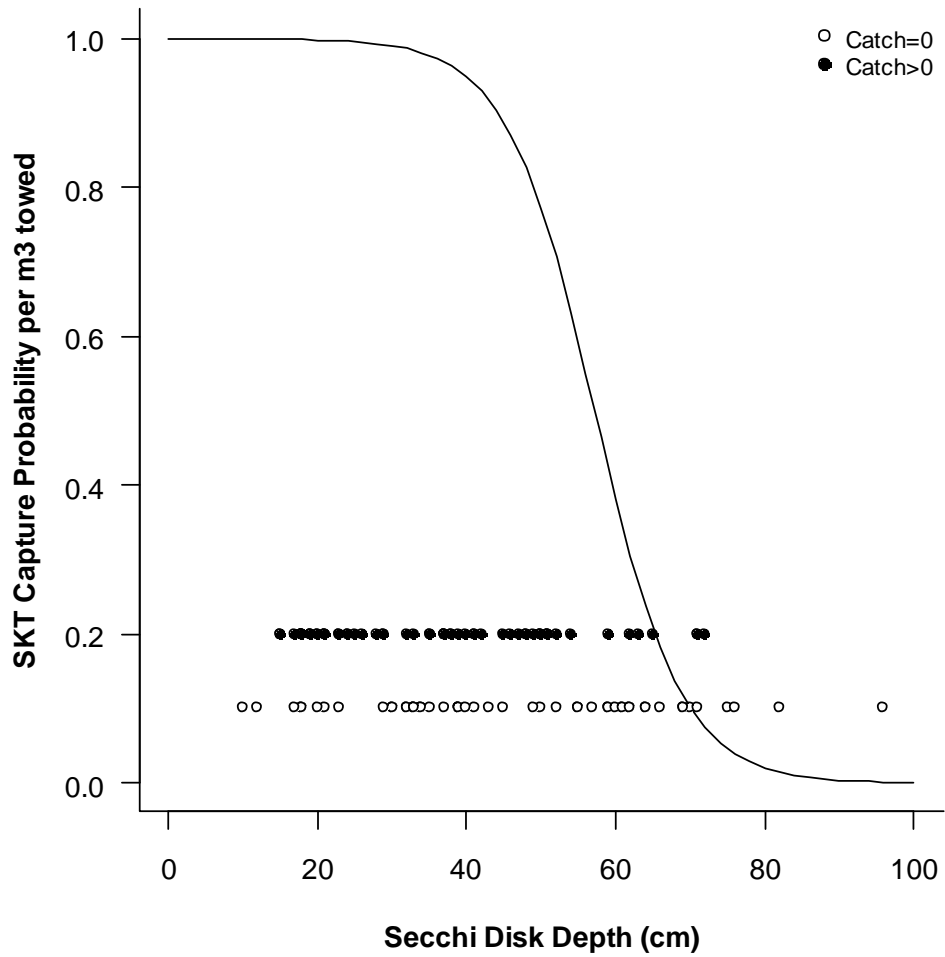


Figure 5. Con't. Estimated relationship between SKT efficiency and Secchi depth (eqn. 5c). Points show the measured Secchi depths across all surveys and stations where Delta Smelt were (closed) and were not (open) captured.

f)

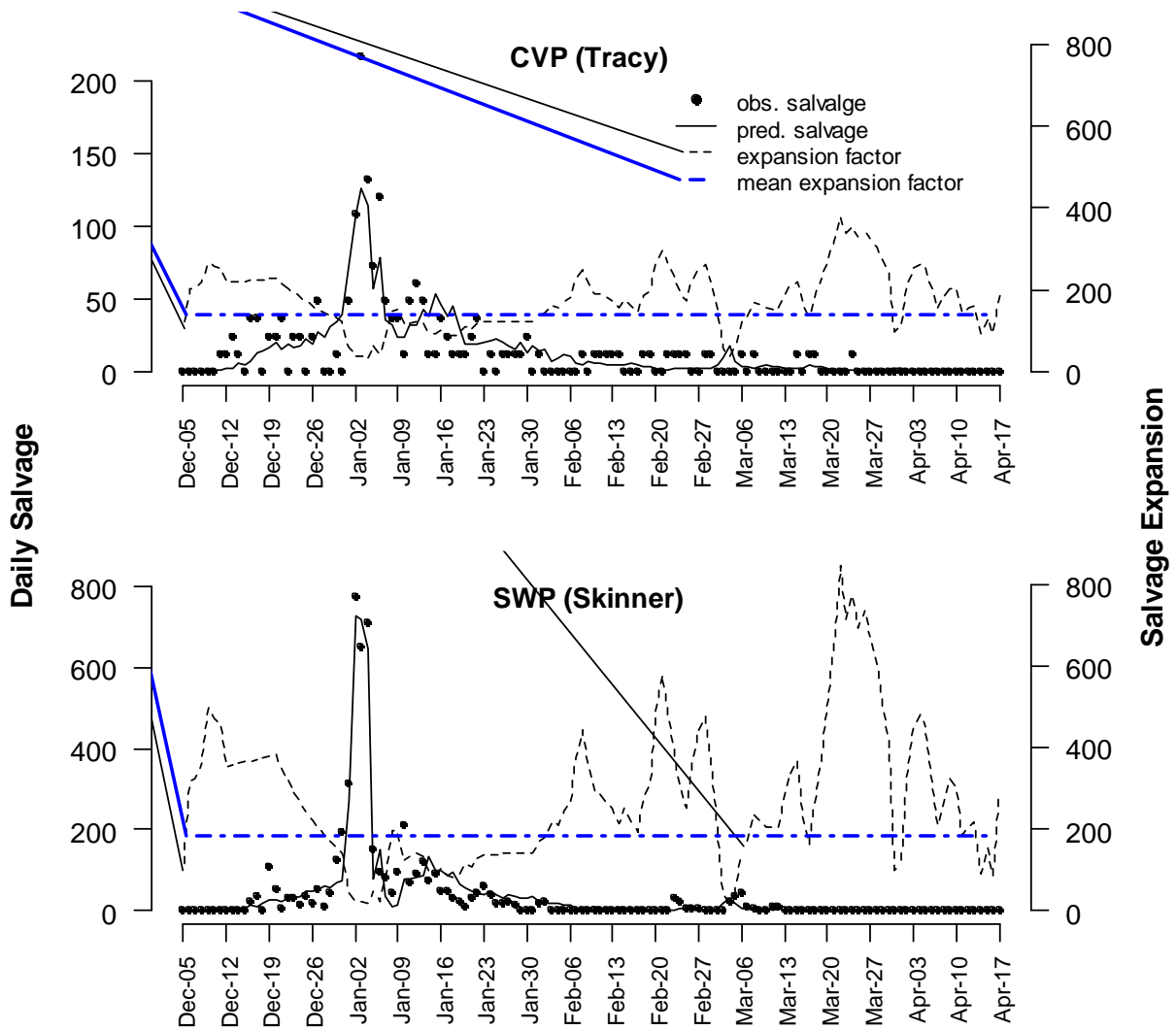


Figure 5. Con't. Predicted (solid line) and observed (points) daily salvage (left axis). Also shown are the daily salvage expansion factors ($1/\theta_s$, black dashed line right-hand axis) and the salvage-weighted average value across days (blue dashed line).

g)

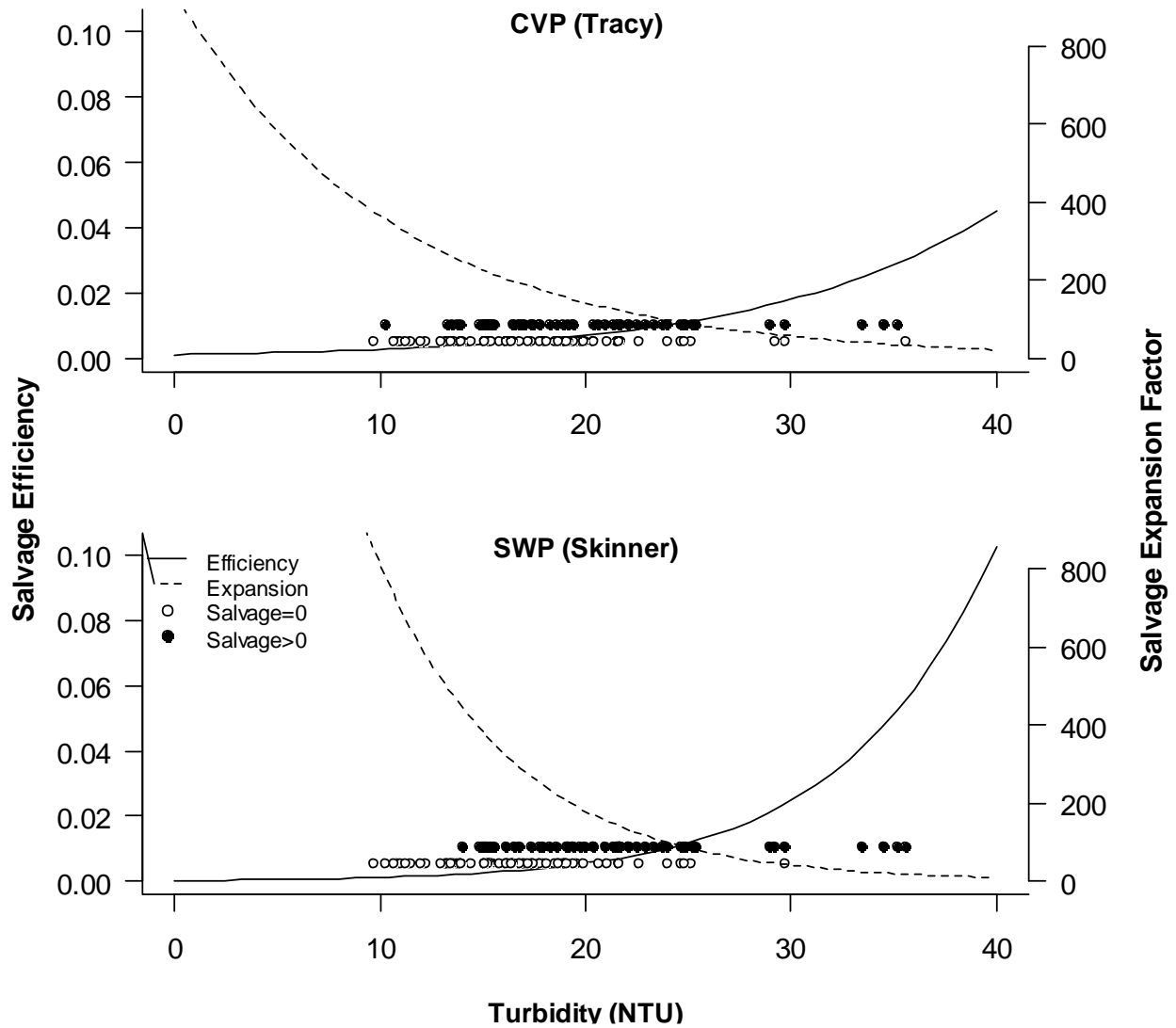


Figure 5. Con't. Estimated salvage efficiency-turbidity relationship (solid line, left-hand axis) and the inverse (expansion factor relationship, dashed line, right-hand axis). The solid and open points show the turbidity levels when salvage was and was not observed.

a)

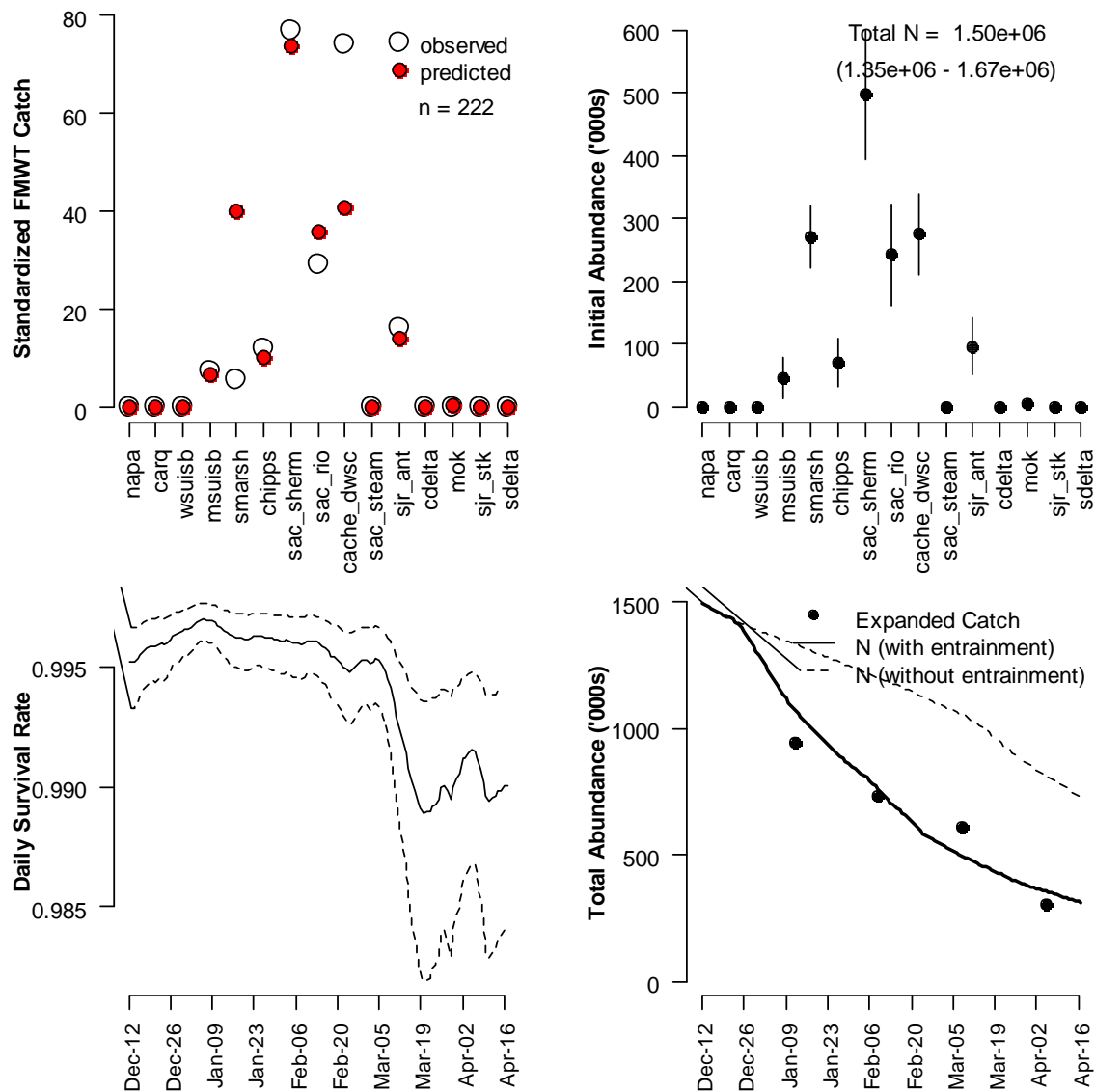


Figure 6. Model fit and predictions for the 2D-based PTM model 10 and population model 8 with poisson error in SKT catch data applied in water year 2004 (Table 4e). a) shows predicted and observed FMWT volume-corrected FMWT catch (top-left plot, observed catch summed across Sep, Oct, Nov, and Dec. surveys), regional population estimates with 95% credible intervals (top –right plot), predictions of the daily survival rate (solid line, bottom-left plot) with 95% credible intervals (dashed lines), and predicted total abundance across regions (bottom-right plot, solid and dashed lines) compared to estimates based on expanding the catch by the ratio of 4 m volume to the volume of tows.

b)

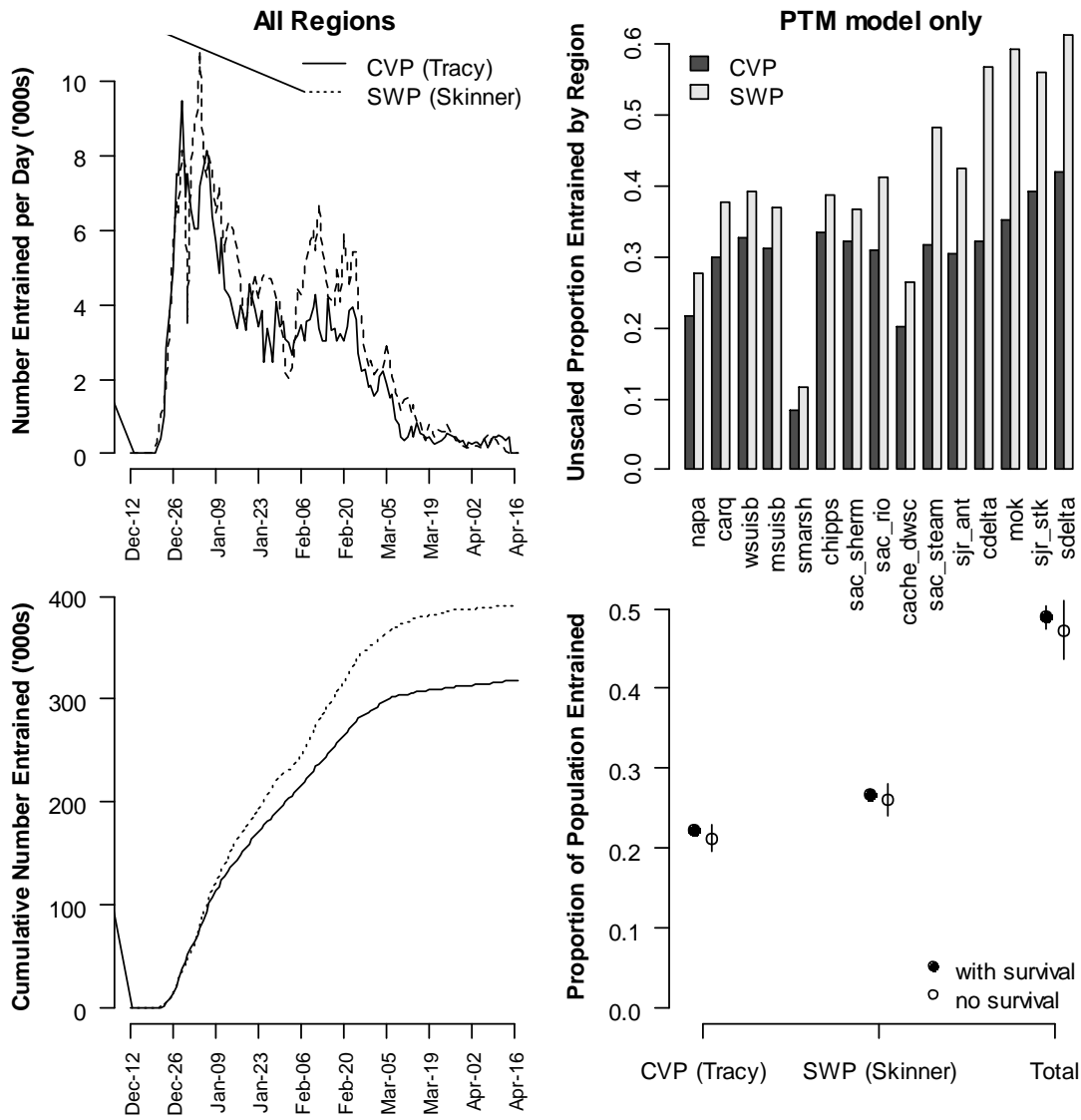


Figure 6. Con't. Predictions of daily salvage (left plots), the cumulative unscaled proportional entrainment for each region predicted by the PTM (top-right), and estimates of proportional entrainment (which include survival effects) and discrete proportional entrainment (which do not include survival effects as they are based on ratio of entrainment to initial abundance).

c)

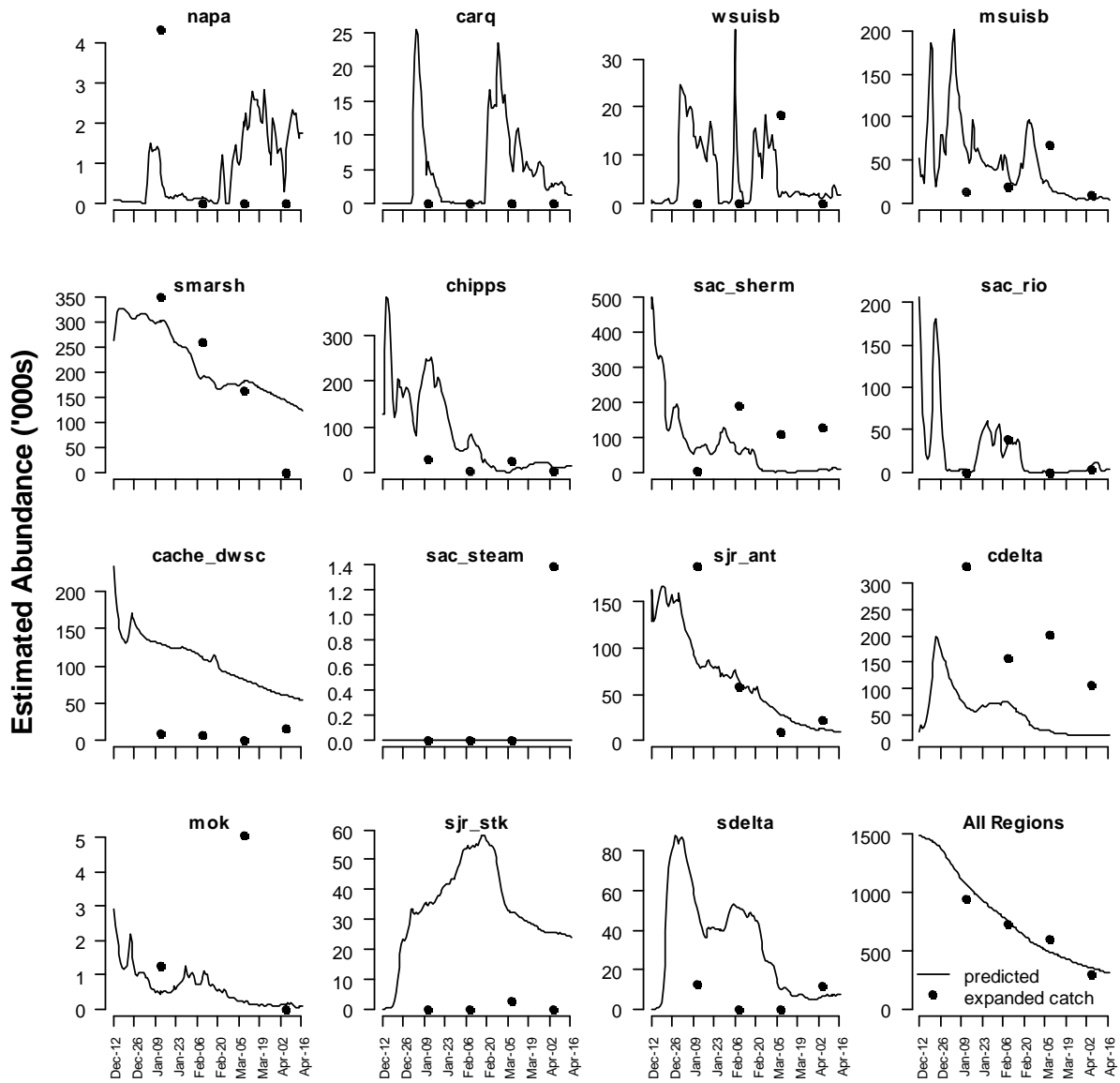


Figure 6. Con't. Abundance estimates by region and model day (lines) compared to estimates based on expanded catch (points).

d)

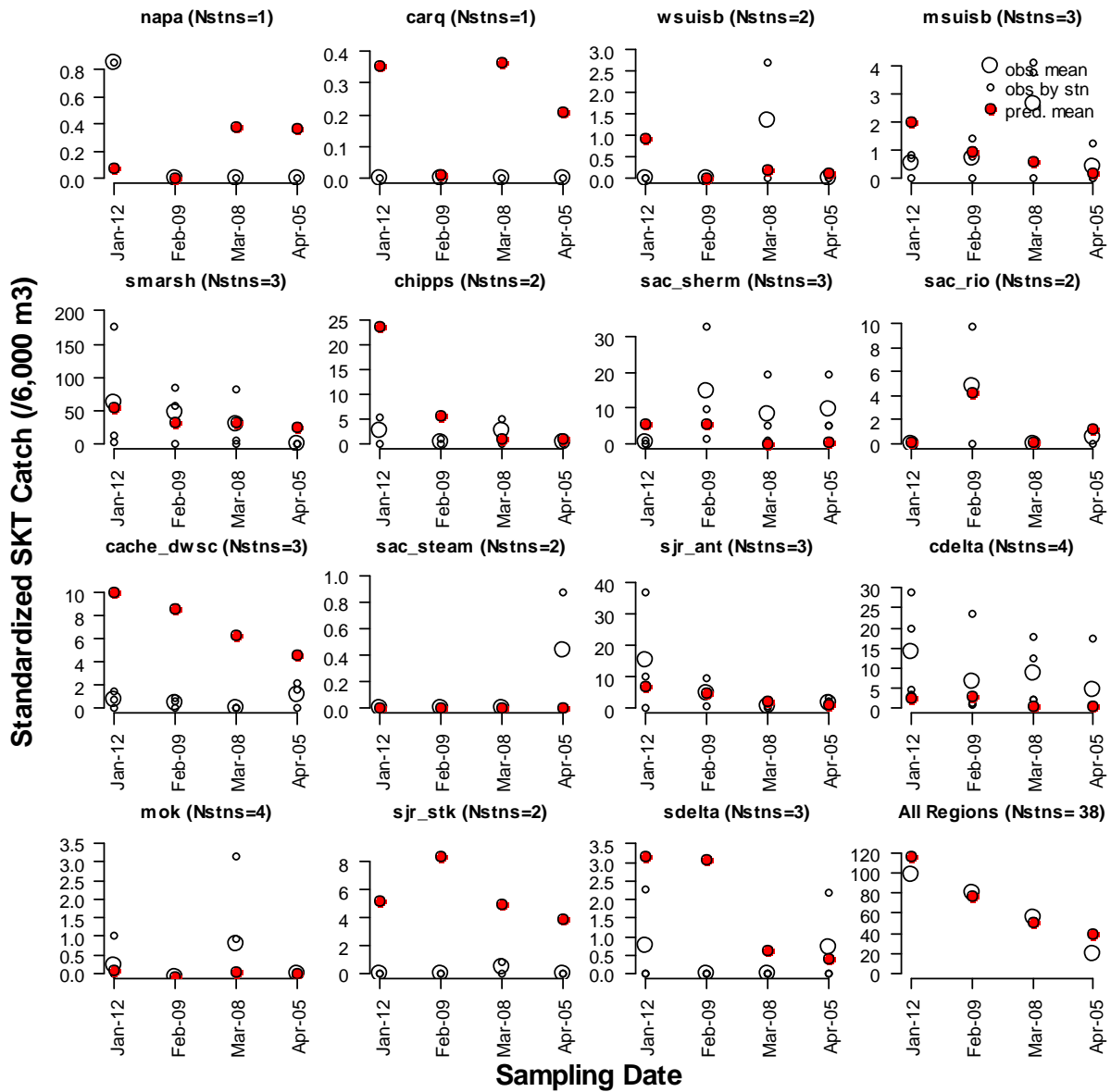


Figure 6. Con't. Comparison of predicted (red points) and mean observed (large open points) SKT catch by trip and region where catches are standardized by the approximate average tow volume. Also shown are the standardized station-specific standardized catches (small open points).

e)

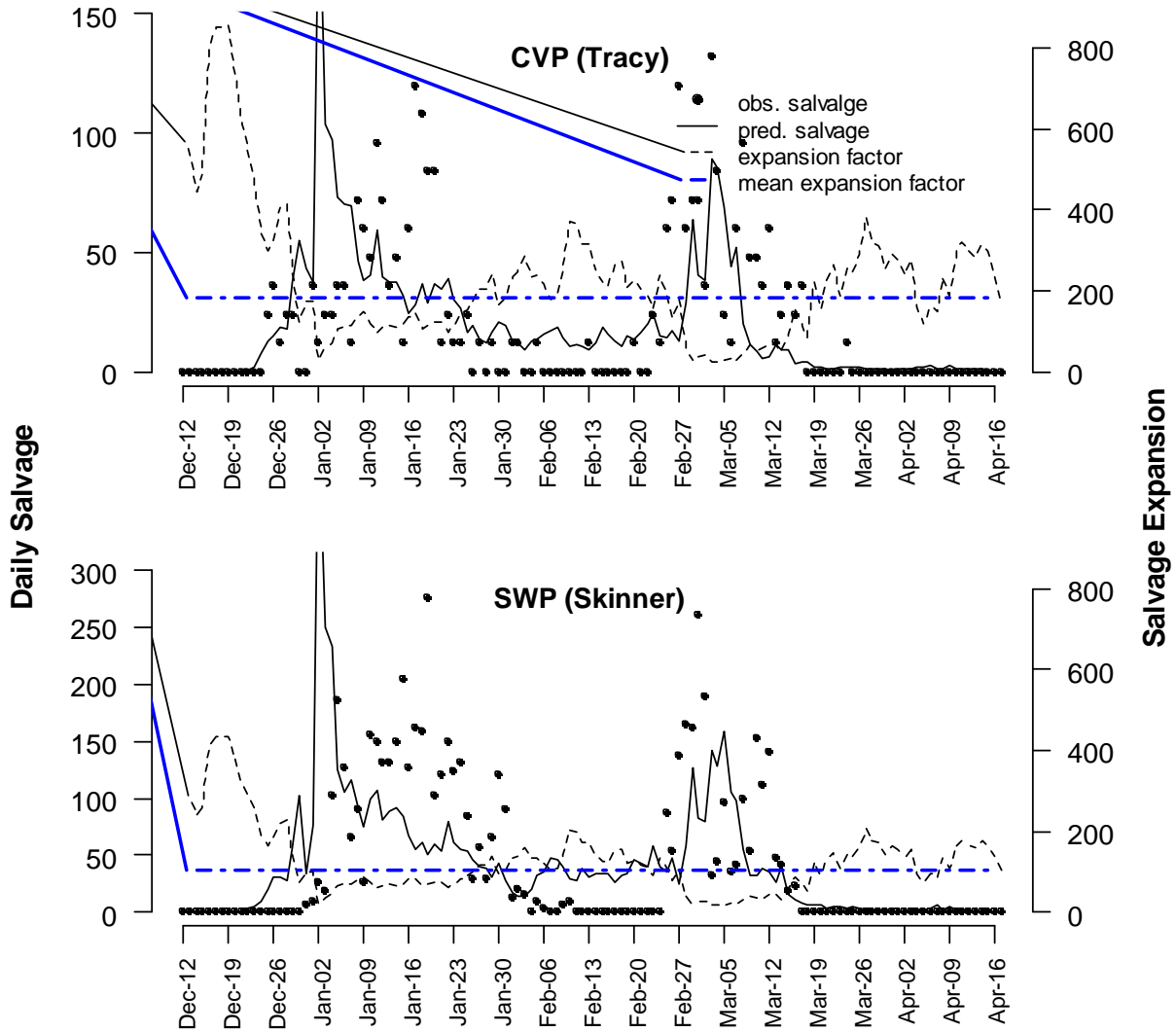


Figure 6. Con't. Predicted (solid line) and observed (points) daily salvage (left axis). Also shown are the daily salvage expansion factors ($1/\theta_s$, black dashed line right-hand axis) and the salvage-weighted average value across days (blue dashed line).

f)

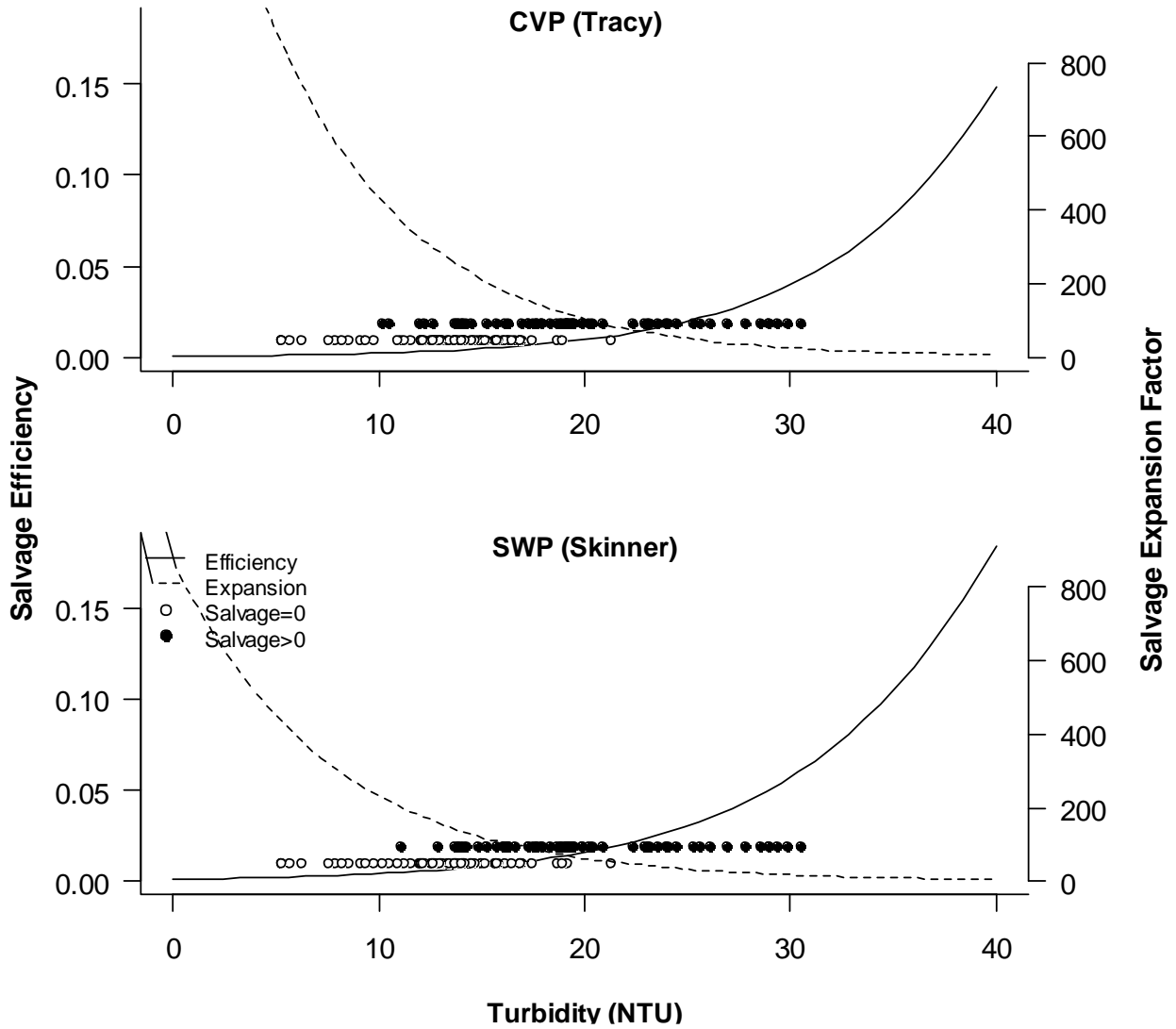


Figure 6. Con't. Estimated salvage efficiency-turbidity relationship (solid line, left-hand axis) and the inverse (expansion factor relationship, dashed line, right-hand axis). The solid and open points show the turbidity levels when salvage was and was not observed.

a)

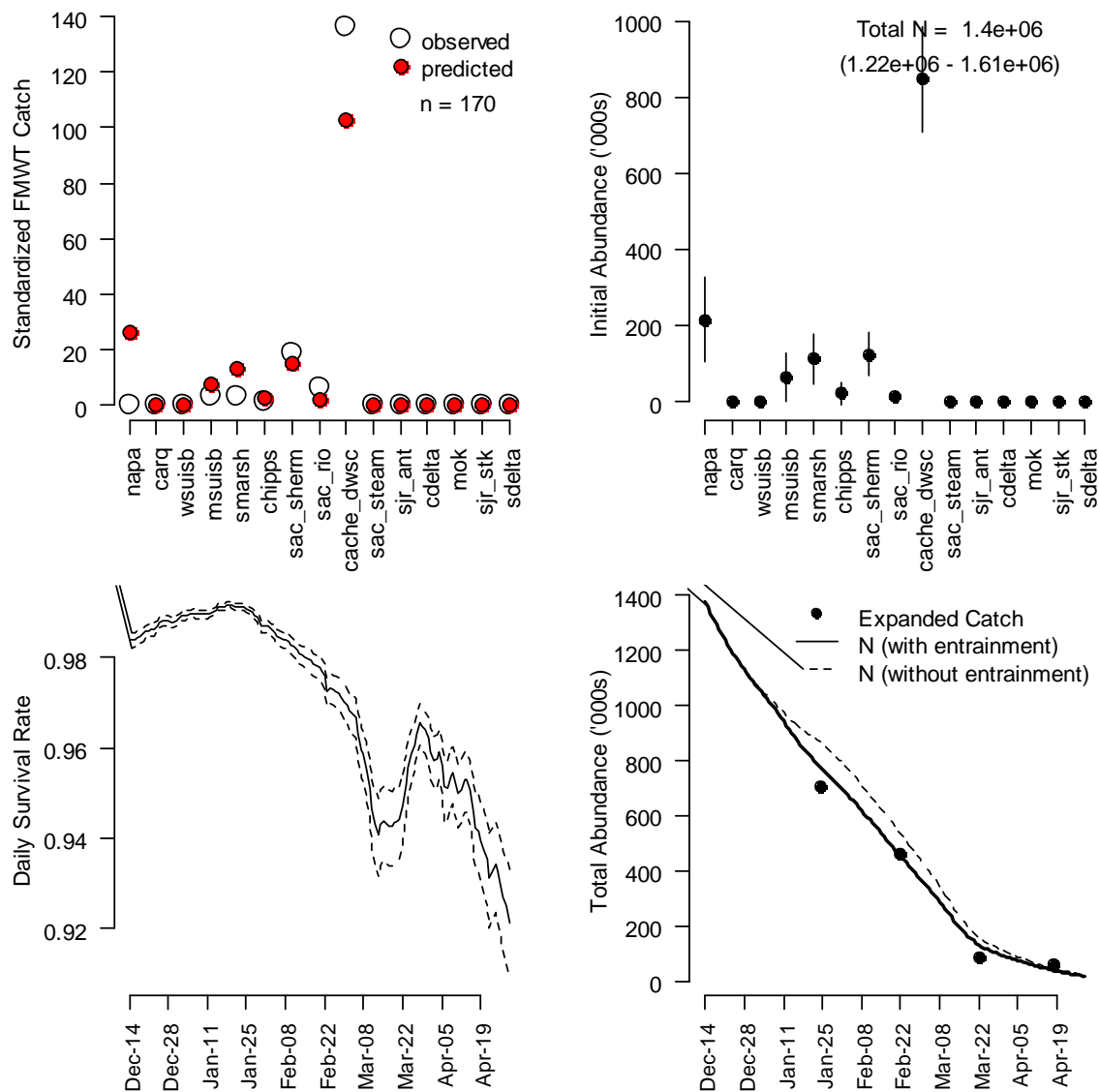


Figure 7. Model fit and predictions for the 2D-based PTM model 8 and population model 4 with poisson error in SKT catch data applied in water year 2005 (Table 4g). a) shows predicted and observed FMWT volume-corrected FMWT catch (top-left plot, observed catch summed across Sep, Oct, Nov, and Dec. surveys), regional population estimates with 95% credible intervals (top-right plot), predictions of the daily survival rate (solid line, bottom-left plot) with 95% credible intervals (dashed lines), and predicted total abundance across regions (bottom-right plot, solid and dashed lines) compared to estimates based on expanding the catch by the ratio of 4 m volume to the volume of tows.

b)

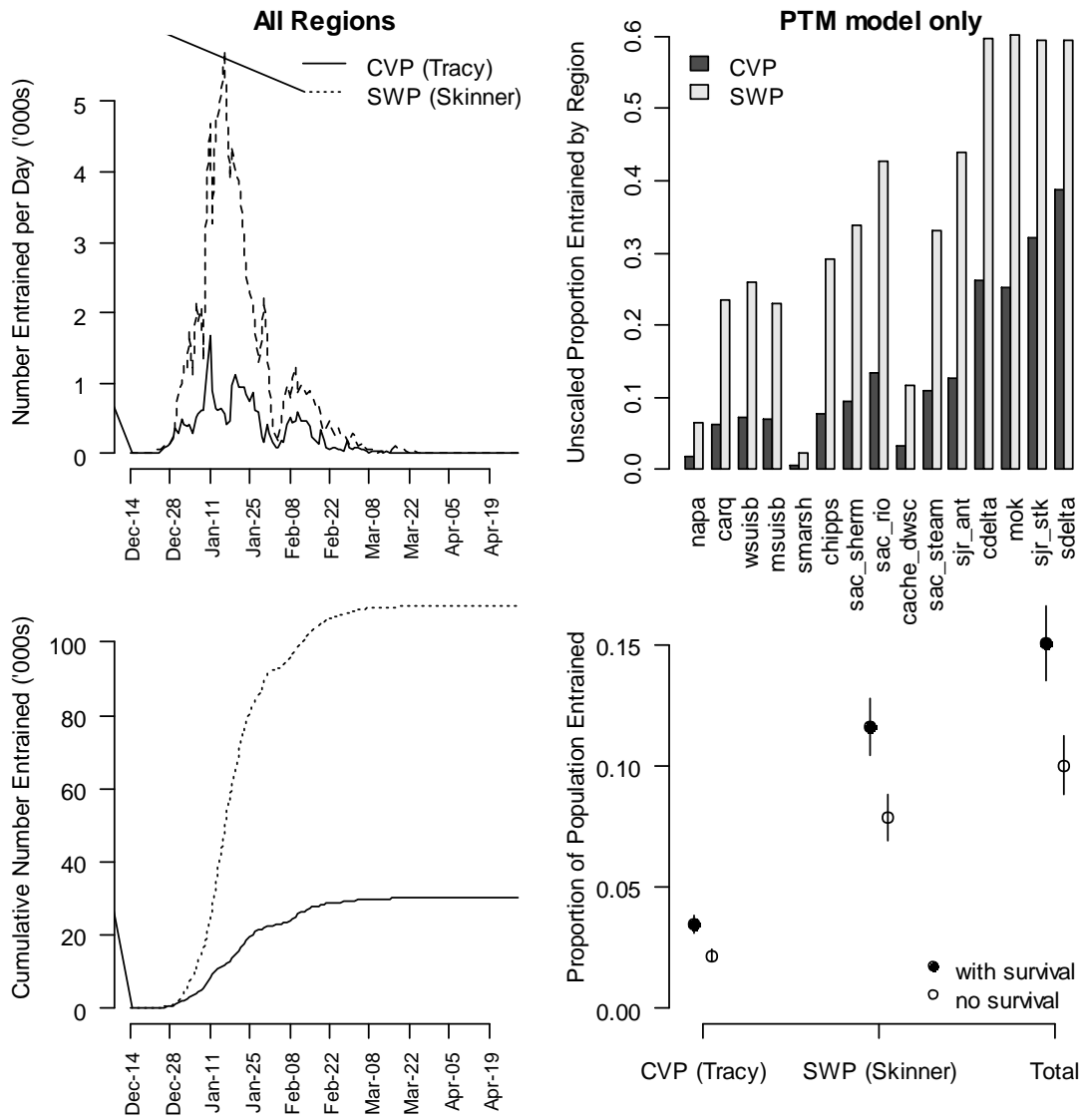


Figure 7. Con't. Predictions of daily salvage (left plots), the cumulative unscaled proportional entrainment for each region predicted by the PTM (top-right), and estimates of proportional entrainment (which include survival effects) and discrete proportional entrainment (which do not include survival effects as they are based on ratio of entrainment to initial abundance).

c)

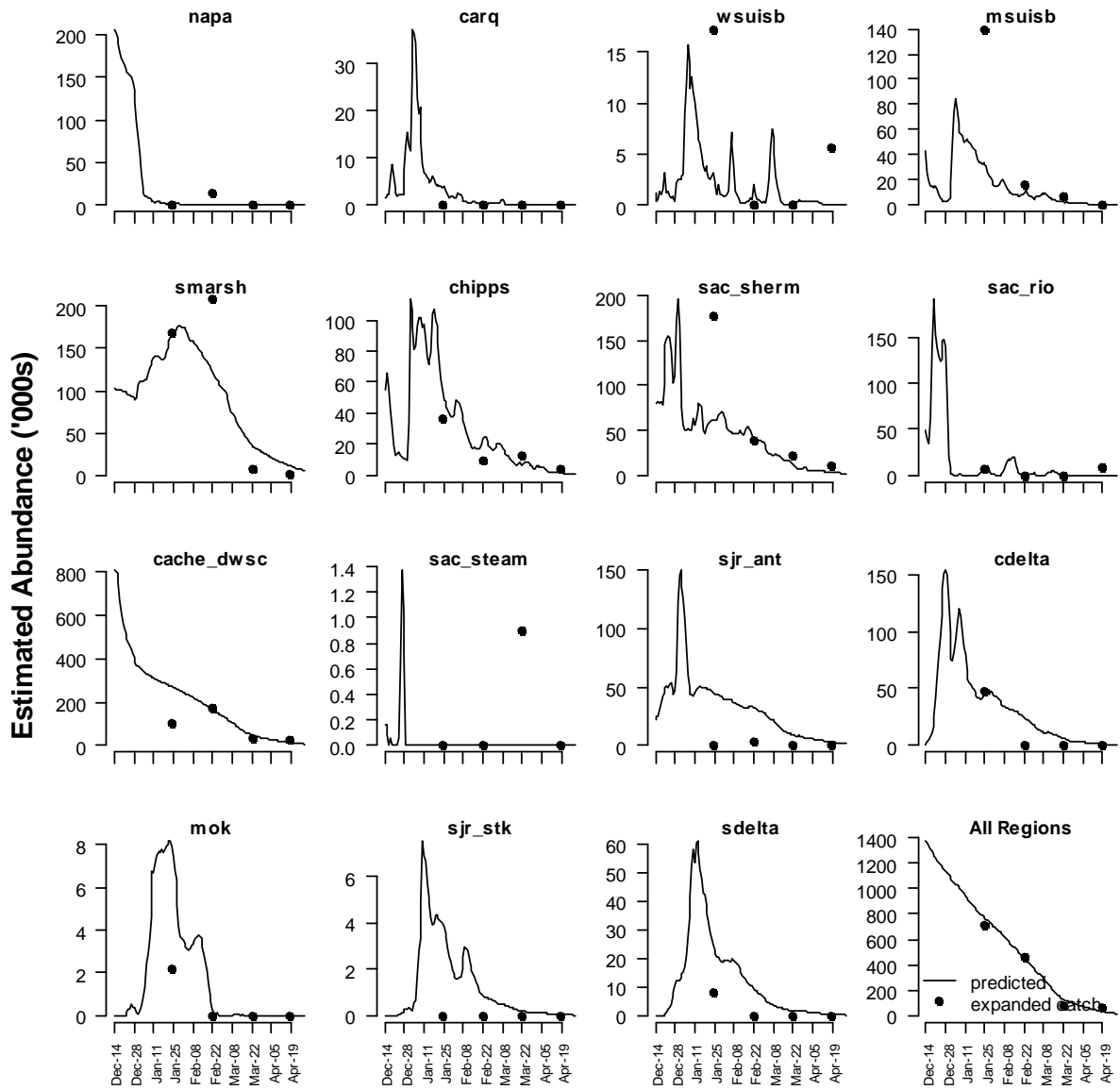


Figure 7. Con't. Abundance estimates by region and model day (lines) compared to estimates based on expanded catch (points).

d)

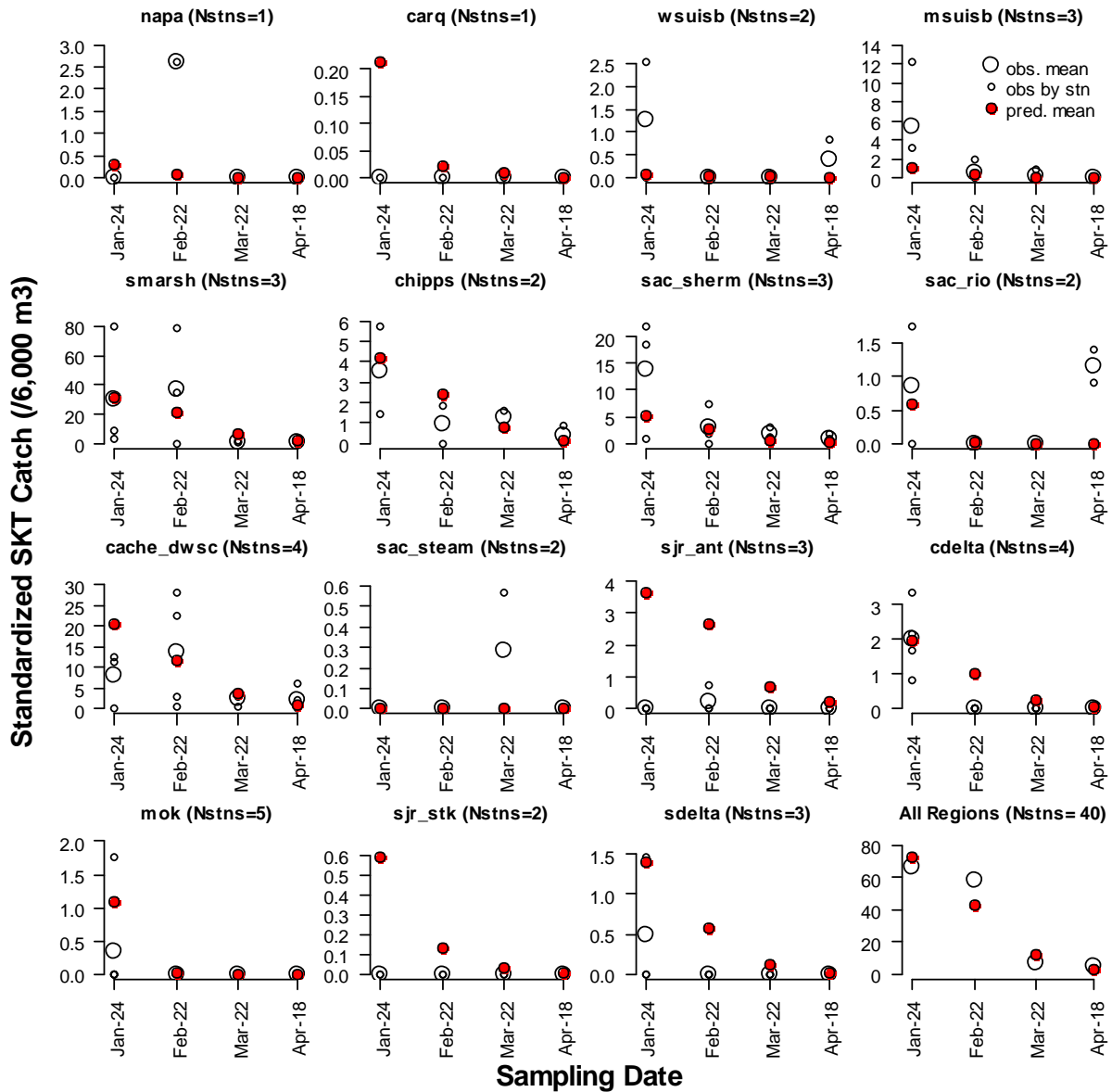


Figure 7. Con't. Comparison of predicted (red points) and mean observed (large open points) SKT catch by trip and region where catches are standardized by the approximate average tow volume. Also shown are the standardized station-specific standardized catches (small open points).

e)

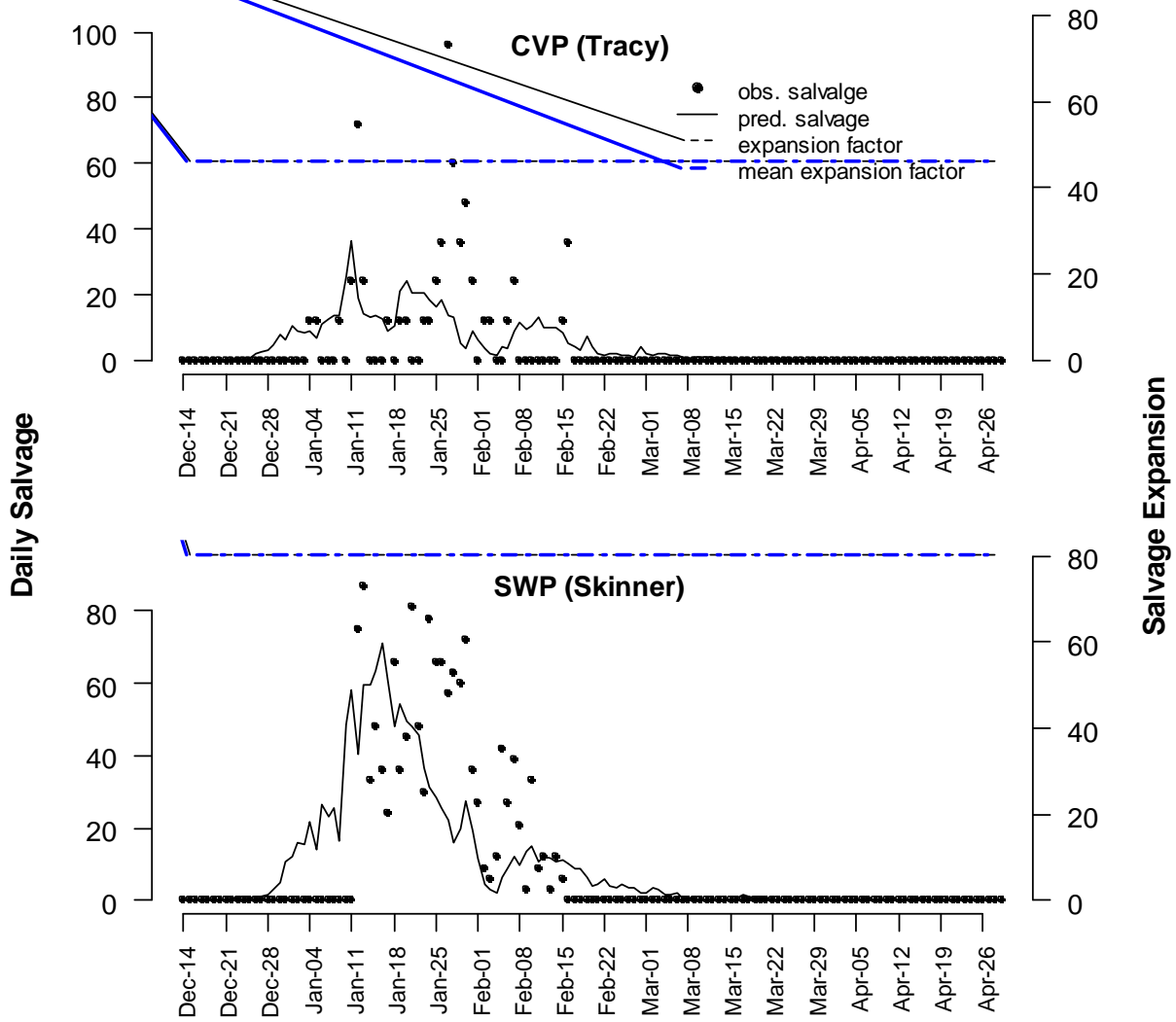


Figure 7. Con't. Predicted (solid line) and observed (points) daily salvage (left axis). Also shown are the daily salvage expansion factors ($1/\theta_s$, black dashed line right-hand axis) and the salvage-weighted average value across days (blue dashed line).

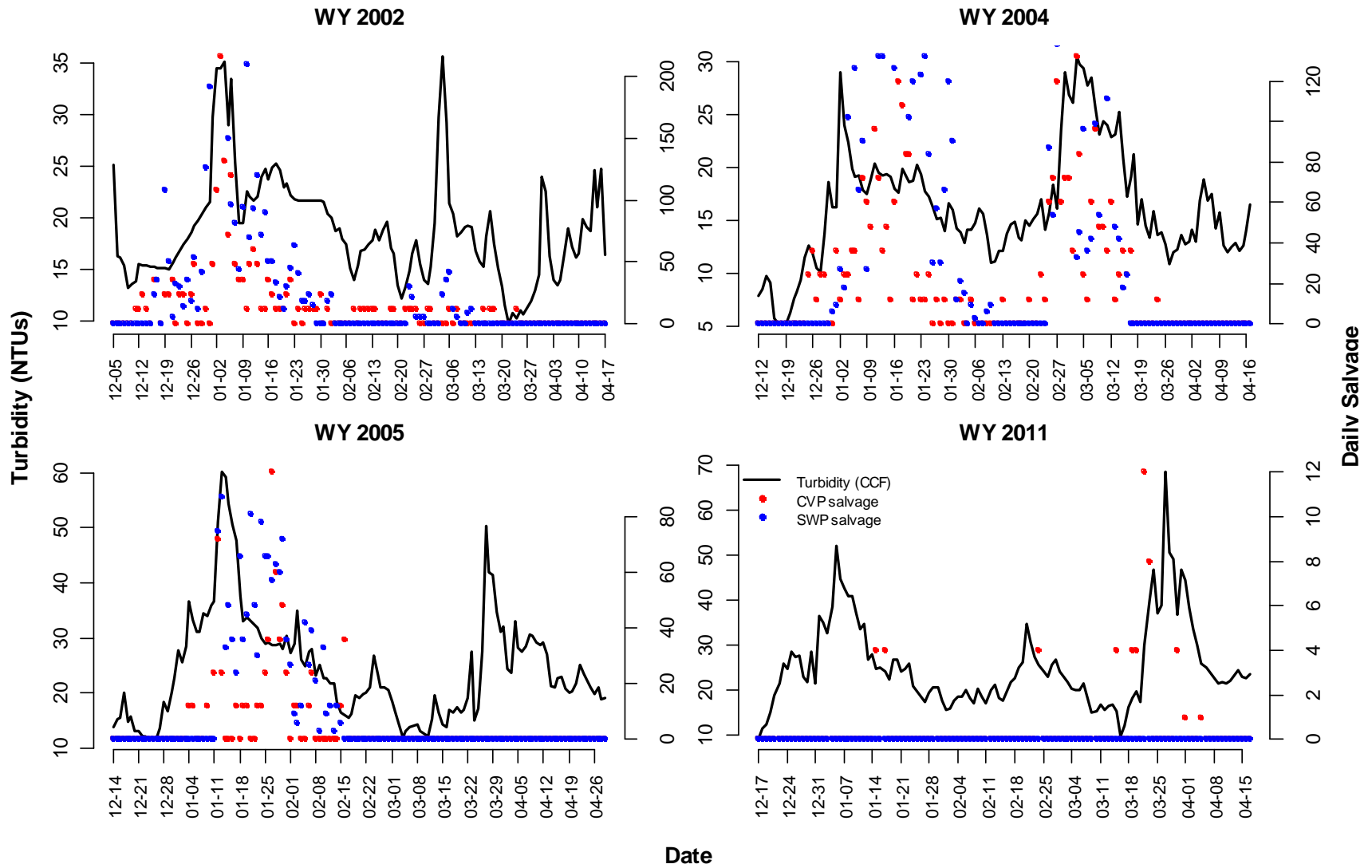


Figure 8. Relationship between turbidity measured at Clifton Court Forebay (CCF) and observed daily salvage at federal (CVP) and state (SWP) fish collection facilities.

a)

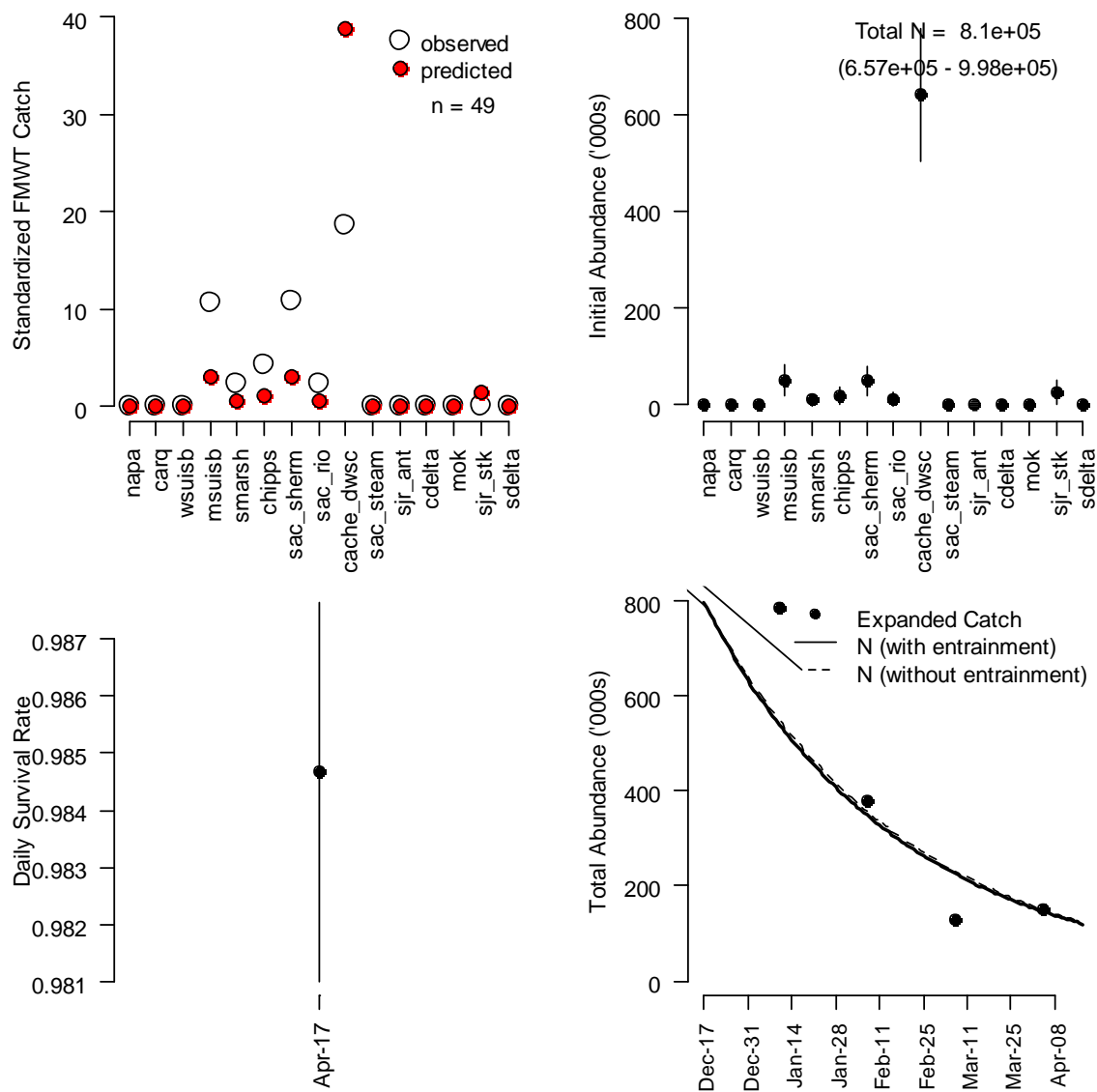


Figure 9. Model fit and predictions for the 2D-based PTM model 6 and population model 1 with poisson error in SKT catch data applied in water year 2011 (Table 4i). a) shows predicted and observed FMWT volume-corrected FMWT catch (top-left plot, observed catch summed across Sep, Oct, Nov, and Dec. surveys), regional population estimates with 95% credible intervals (top-right plot), predictions of the daily survival rate (solid line, bottom-left plot) with 95% credible intervals (dashed lines), and predicted total abundance across regions (bottom-right plot, solid and dashed lines) compared to estimates based on expanding the catch by the ratio of 4 m volume to the volume of tows.

b)

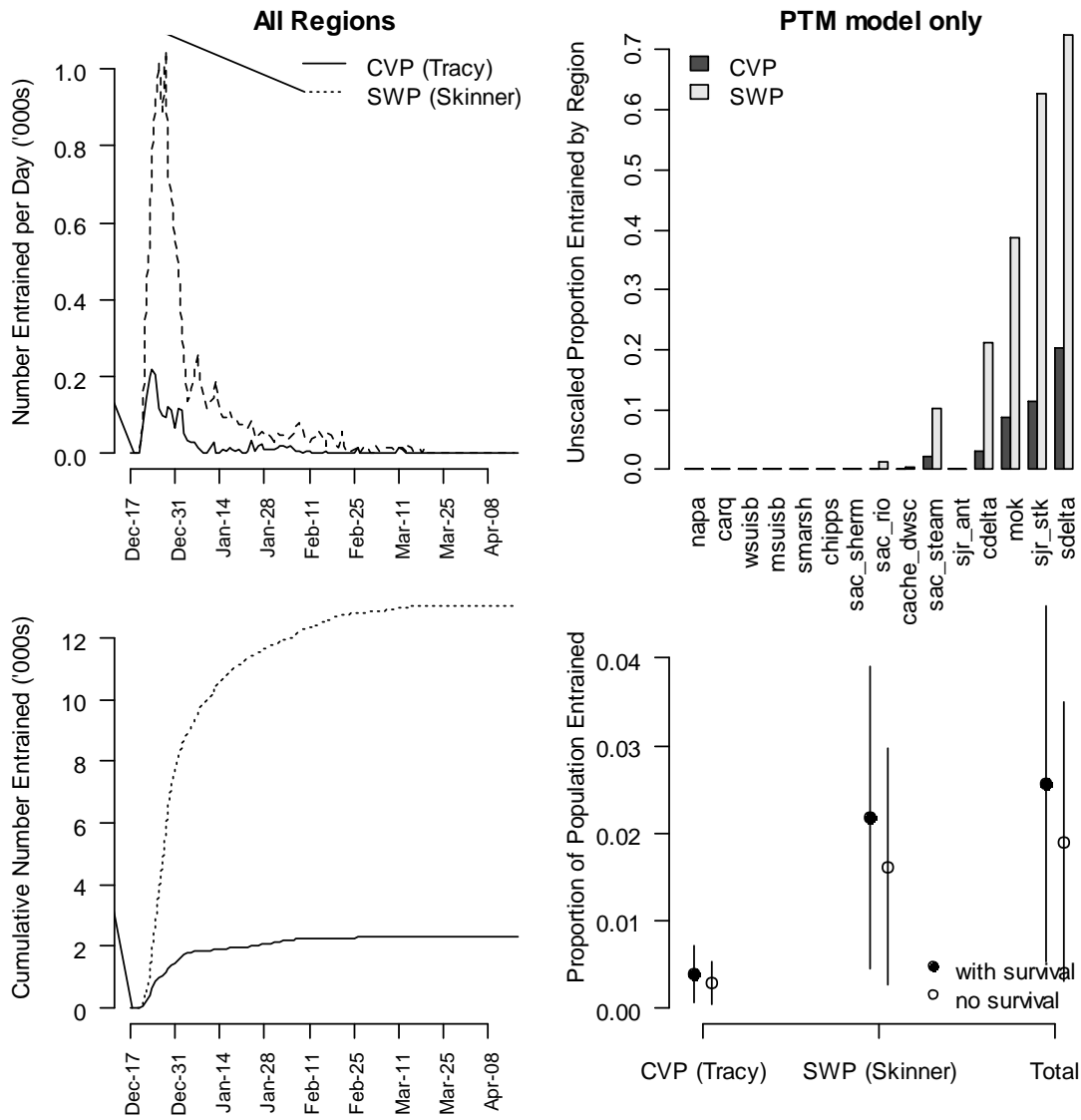


Figure 9. Con't. Predictions of daily salvage (left plots), the cumulative unscaled proportional entrainment for each region predicted by the PTM (top-right), and estimates of proportional entrainment (which include survival effects) and discrete proportional entrainment (which do not include survival effects as they are based on ratio of entrainment to initial abundance).

c)

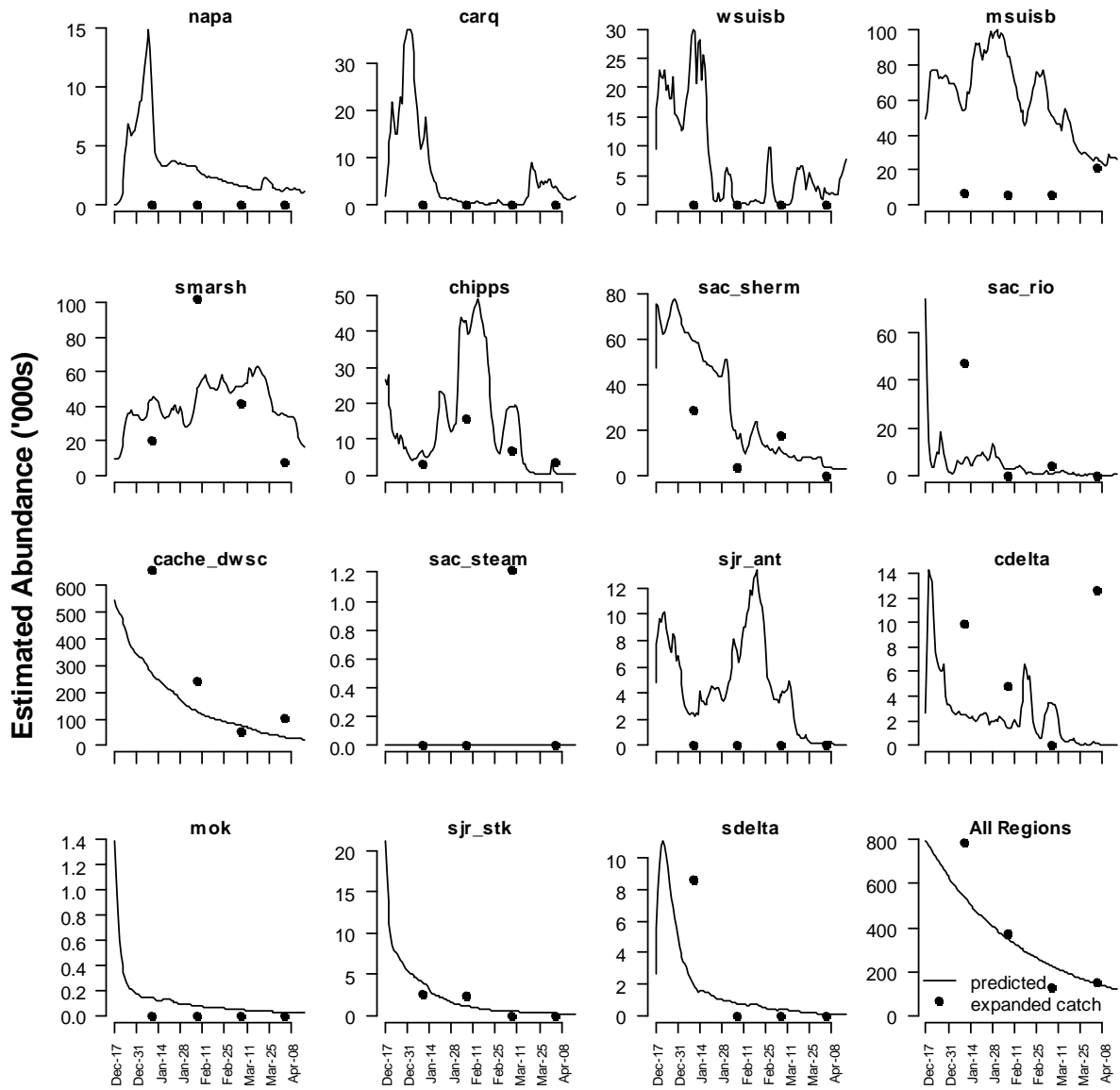


Figure 9. Con't. Abundance estimates by region and model day (lines) compared to estimates based on expanded catch (points).

d)

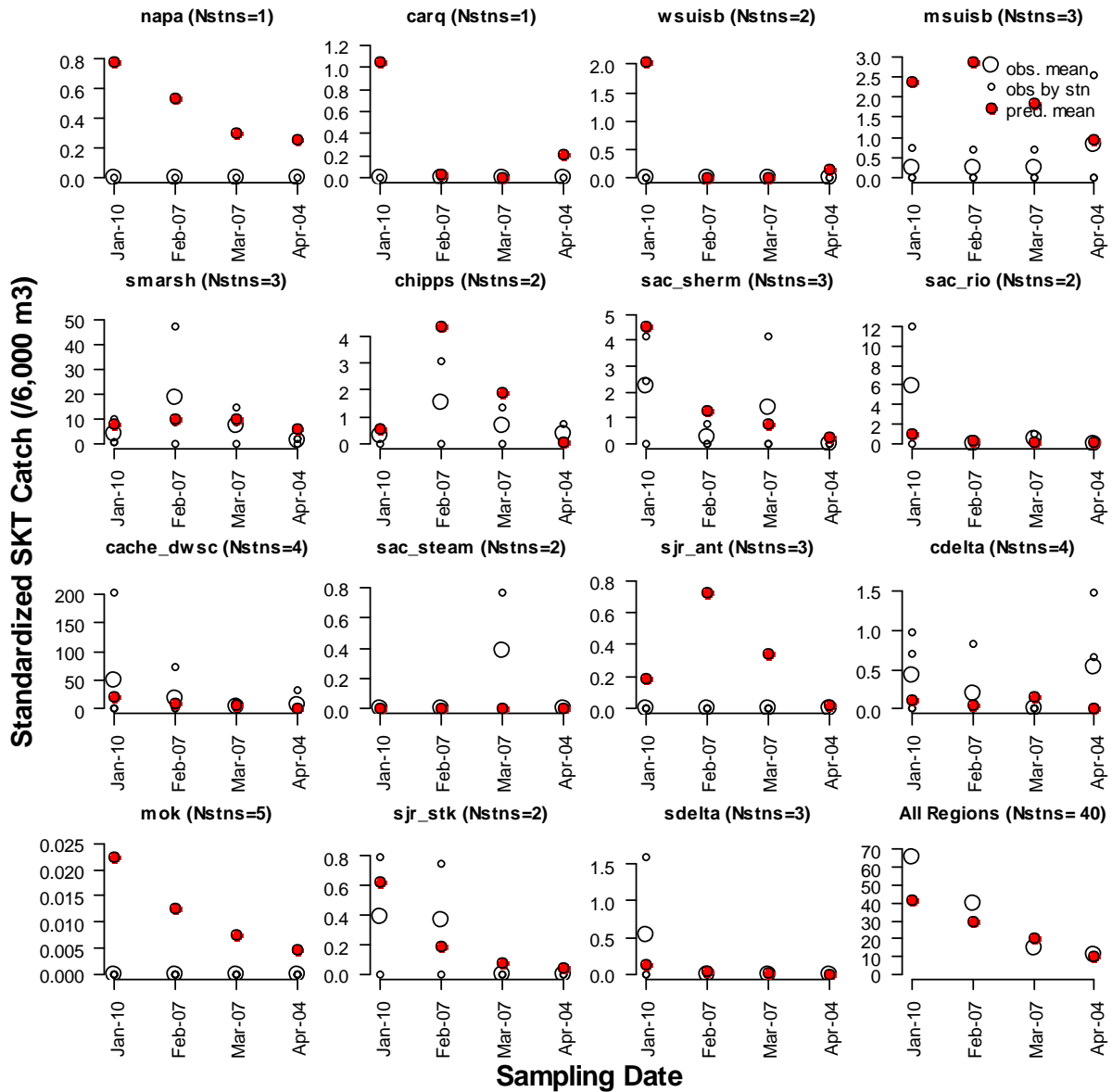


Figure 9. Con't. Comparison of predicted (red points) and mean observed (large open points) SKT catch by trip and region where catches are standardized by the approximate average tow volume. Also shown are the standardized station-specific standardized catches (small open points).

e)

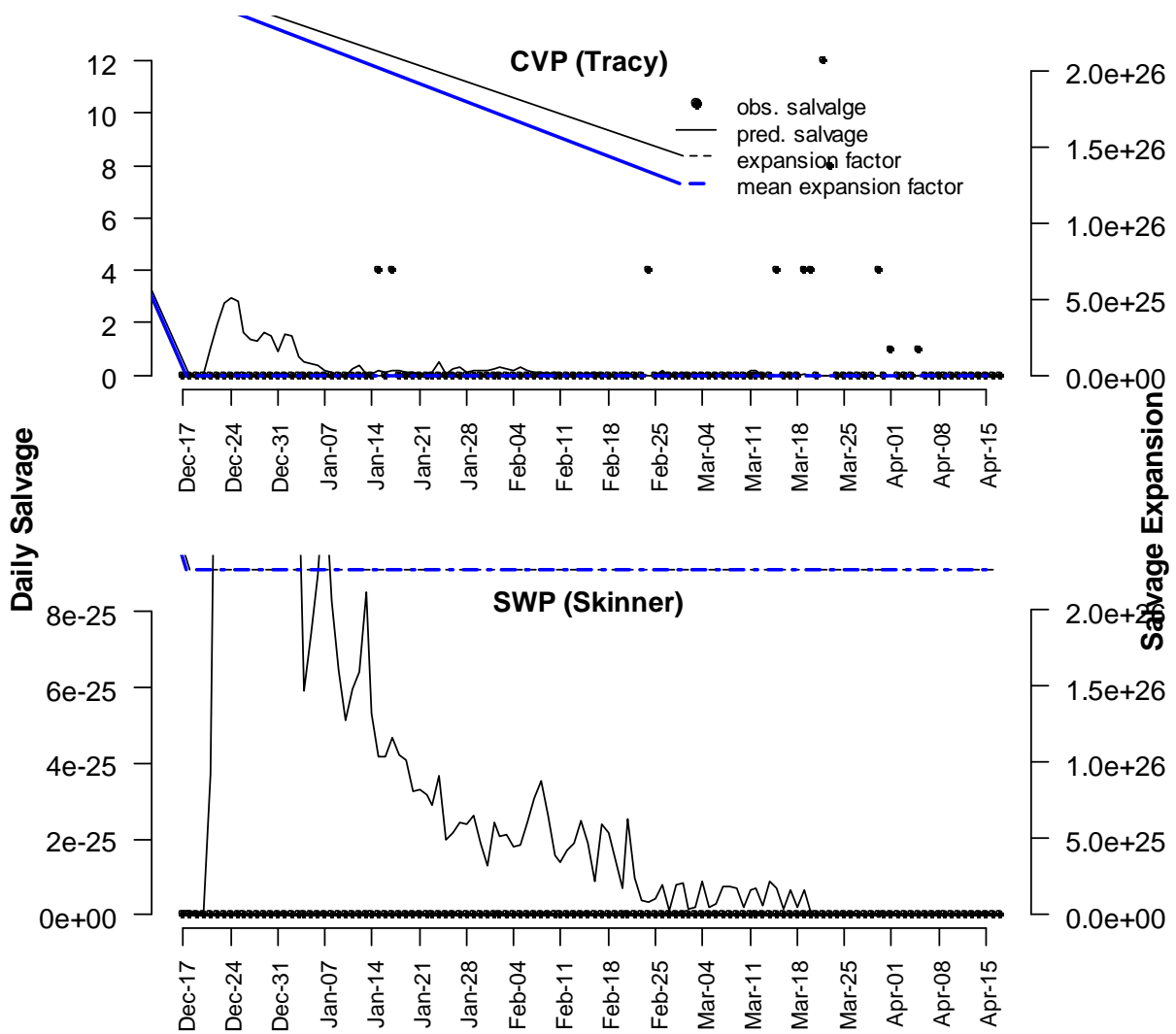


Figure 9. Con't. Predicted (solid line) and observed (points) daily salvage (left axis). Also shown are the daily salvage expansion factors ($1/\theta_s$, black dashed line right-hand axis) and the salvage-weighted average value across days (blue dashed line).

a)

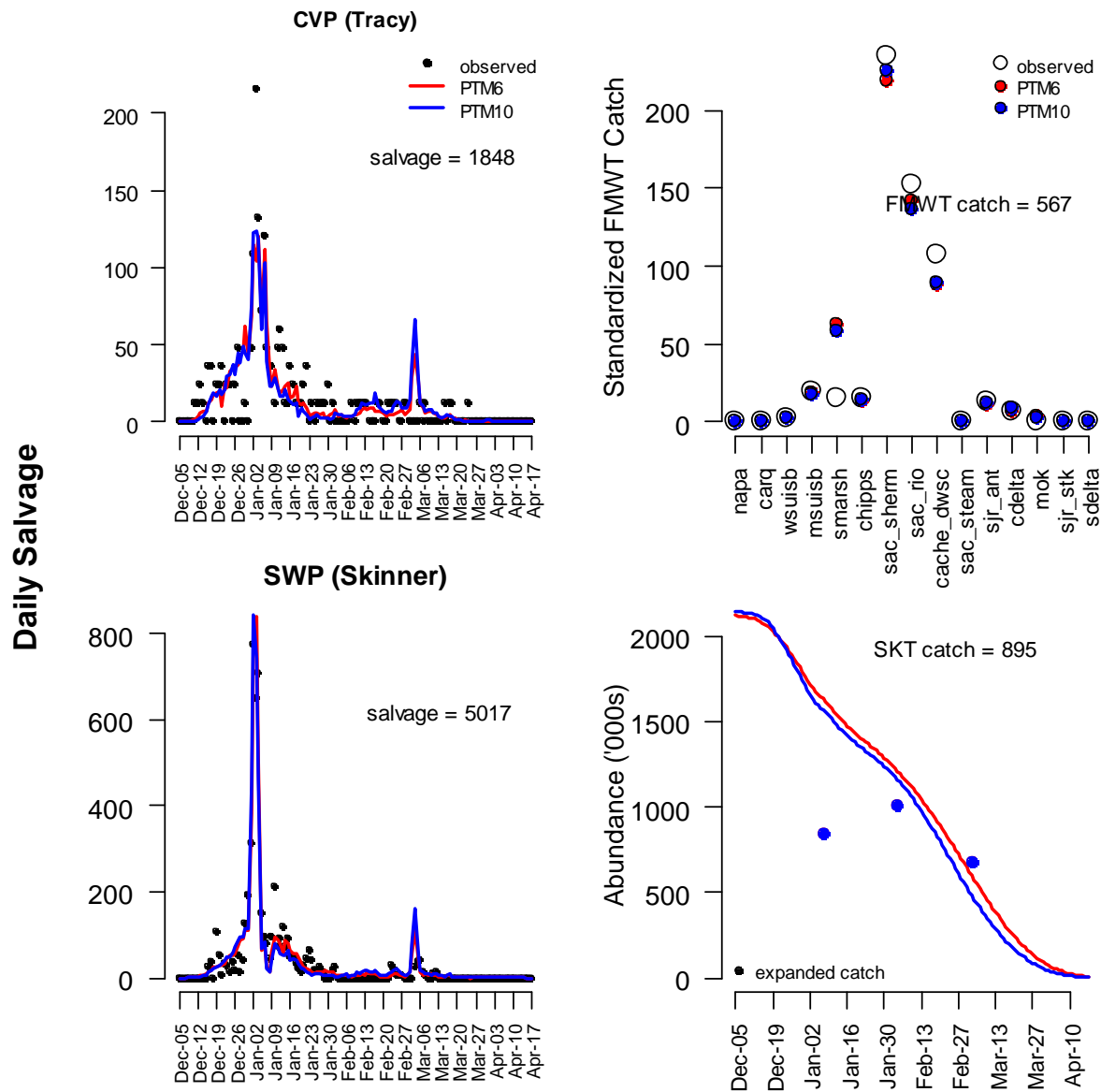


Figure 10. Comparison of fit 3D PTMs 6 (red, 1st ranked) and 10 (blue, 2nd-ranked) for water year 2002 assuming poisson ($\tau=1$) error in SKT catch data. Results are based on population model 7 (Table 4) where daily survival rate is a smooth function of model day and salvage expansion factors depend on turbidity. a) shows the fit to salvage and FMWT data and to expanded estimates of abundance from SKT data. b) compares predicted and observed SKT catches.

b)

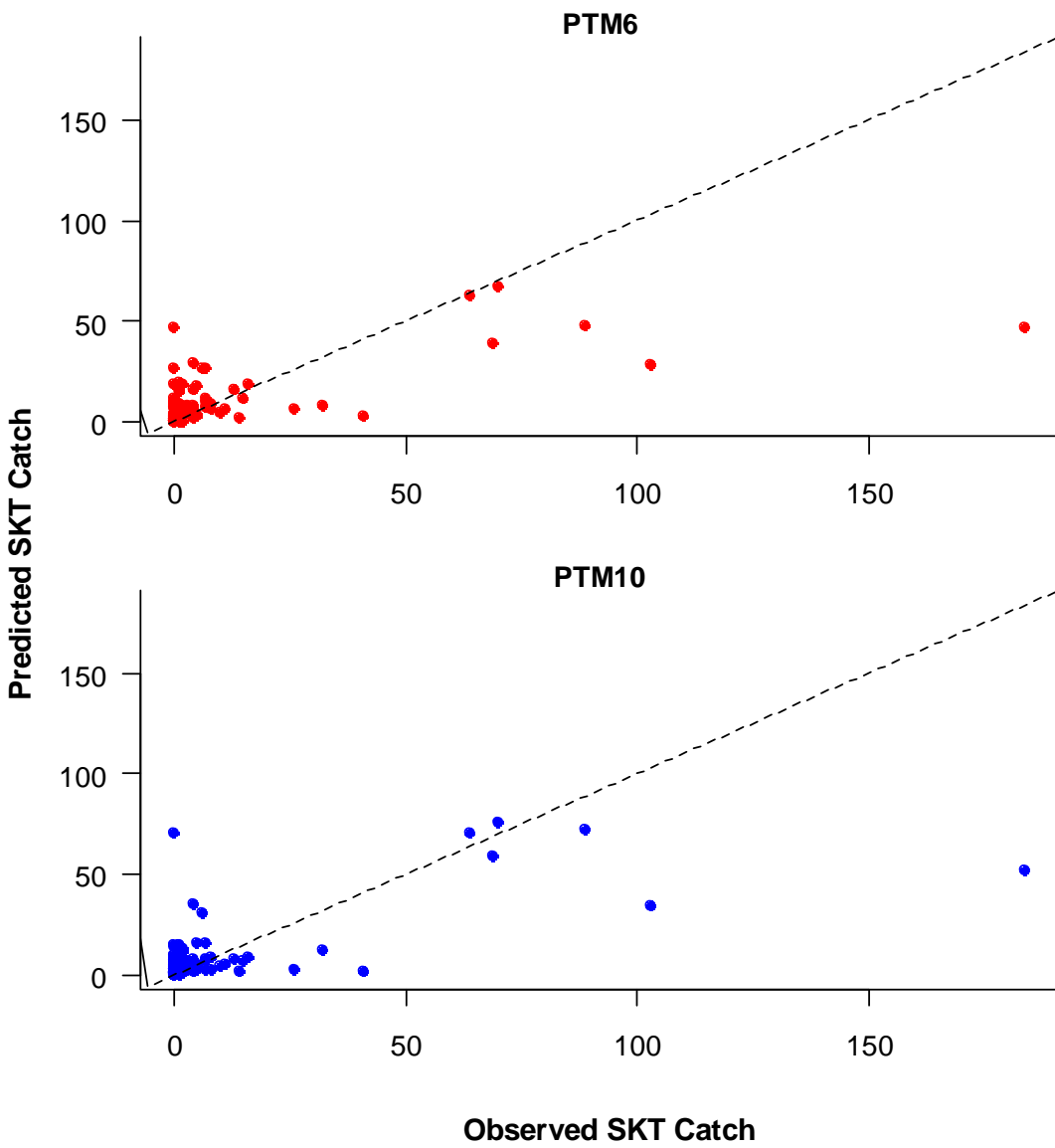


Figure 10. Con't.

a)

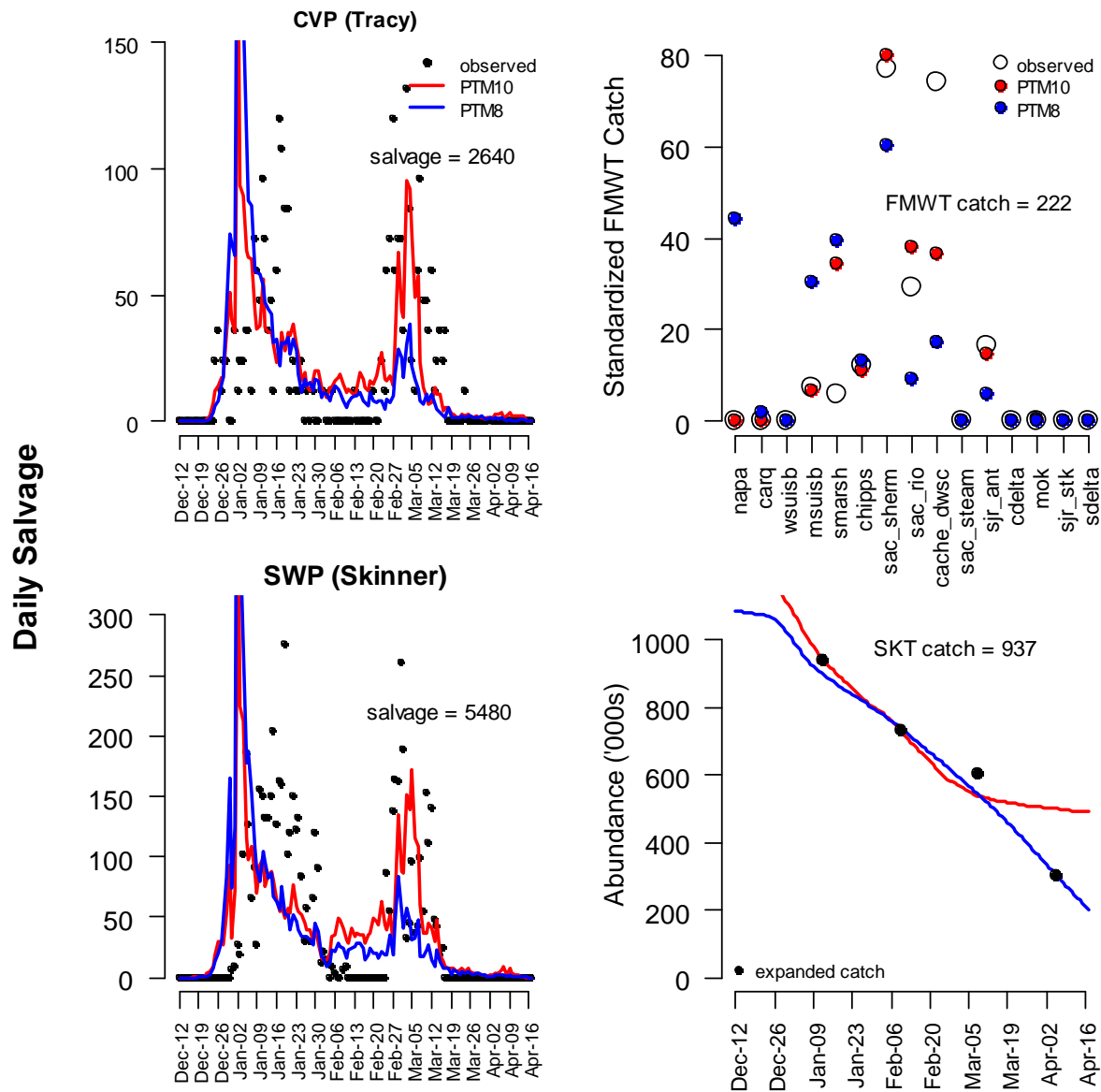


Figure 11. Comparison of fit 2D PTMs 10 (red, 1st ranked) and 8 (blue, 2nd-ranked) for water year 2004 assuming poisson ($\tau=1$) error in SKT catch data. Results are based on population model 7 (Table 4) where daily survival rate is a smooth function of model day and salvage expansion factors depend on turbidity. a) shows the fit to salvage and FMWT data and to expanded estimates of abundance from SKT data. b) compares predicted and observed SKT catches.

b)

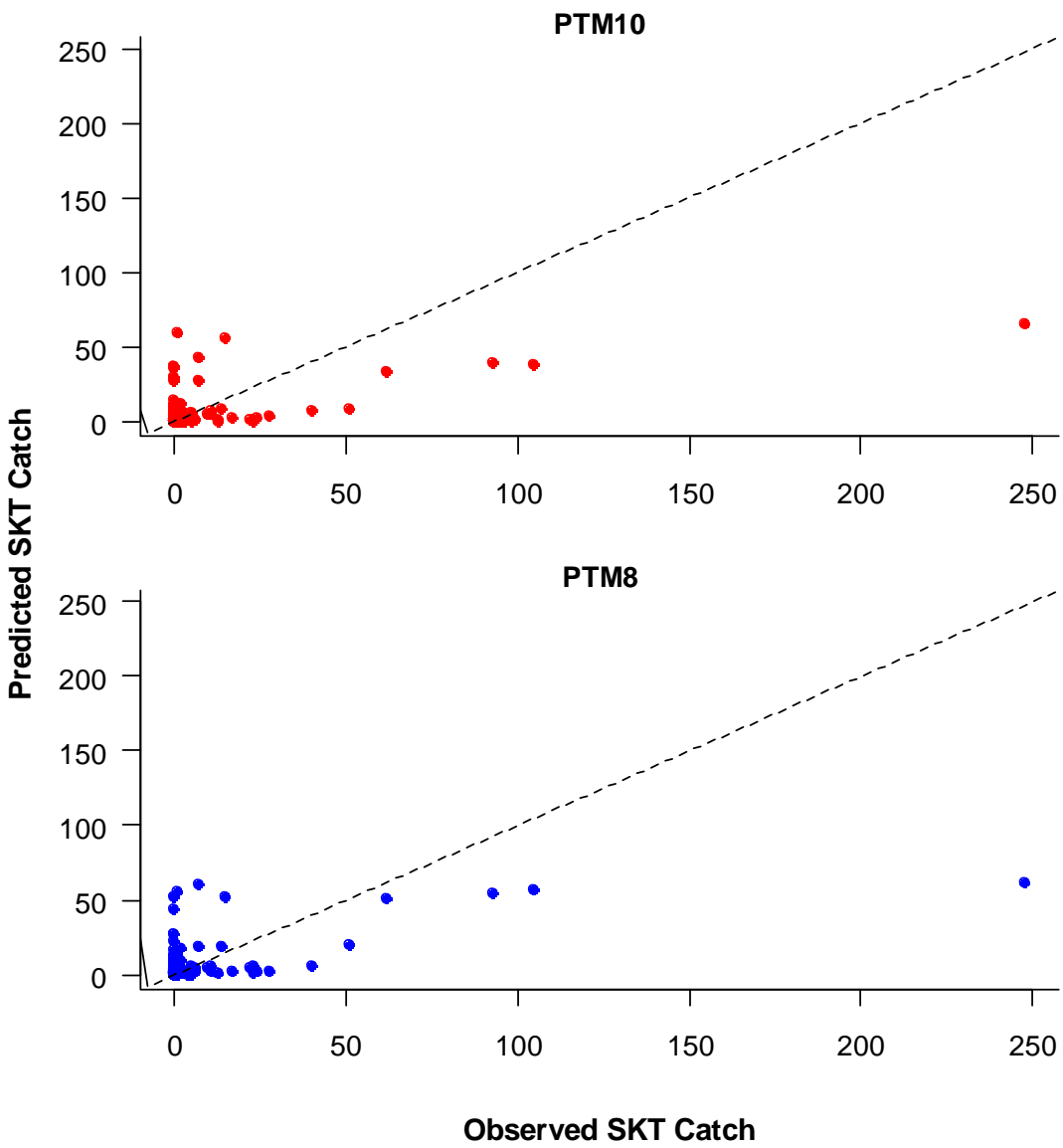


Figure 11. Con't.

Appendix A. Supplemental Tables

Table A1. Proportion of variability in observations explained by different combinations of particle tracking models (rows, see Table 2) and population dynamic models (columns) by water year and PTM type (2D or 3D), assuming poisson error in SKT catch data (variance-to-mean ratio of $\tau=1$) or negative binomial error ($\tau=10$). The table shows the square of the Pearson correlation coefficient quantifying the fit to the relative differences in Fall Midwater Trawl catch among regions (FMWT), the average Spring Kodiak Trawl catch by region and survey(SKT), and the daily expanded salvage at federal (CVP Salvage) and state (SWP salvage) fish collection facilities. #DIV/0! denote that r^2 values could not be computed because there were no salvage observations.

Table A1. Con't.

a) 3D WY 2002 Poisson error in SKT data ($\tau=1$)

Population model number	1	2	3	4	5	6	7	8	9	10
Salvage efficiency structure	const	const	const	const	~turb	~turb	~turb	~turb	const	~turb
Natural survival structure	S_c	S_{SKT}	S_d	S_w	S_c	S_{SKT}	S_d	S_w	S_d	S_d
SKT efficiency structure (θ_{c-SKT})	=1	=1	=1	=1	=1	=1	=1	=1	~Secchi	~Secchi
FMWT relative catch across regions										
1) passive	0.74	0.74	0.74	0.74	0.81	0.81	0.81	0.81	0.77	0.85
2) turbidity_seeking	0.88	0.88	0.86	0.89	0.89	0.89	0.89	0.89	0.98	0.98
3) tmd	0.62	0.62	0.62	0.62	0.69	0.69	0.69	0.69	0.63	0.85
4) ptmd_sal_gt_1	0.95	0.96	0.96	0.95	0.96	0.97	0.97	0.97	0.97	0.98
5) ptmd_si_pt_5	0.97	0.98	0.98	0.96	1.00	1.00	1.00	1.00	0.98	1.00
6) ptmd_si_pt_5_shallow_ebb_t_gt_12	0.93	0.94	0.94	0.93	0.96	0.96	0.96	0.96	0.96	0.98
7) ptmd_sal_gt_1_si_pt_5	0.96	0.98	0.98	0.96	0.99	0.99	0.99	0.99	0.98	0.99
8) ptmd_sal_gt_1_h8_ebb_shallow_t_gt_18_acclim	0.91	0.91	0.91	0.91	0.94	0.95	0.94	0.94	0.91	0.95
9) tmd_sal_gt_1_ebb_shallow_t_gt_18	0.97	0.97	0.97	0.97	0.99	0.99	0.98	0.99	0.98	0.99
10) tmd_sal_gt_1_ptmd_ptmd_sd_pt_1_switch	0.97	0.97	0.97	0.97	0.97	0.97	0.97	0.97	0.98	0.98
SKT catch by survey and region										
1) passive	0.59	0.59	0.59	0.59	0.58	0.58	0.59	0.59	0.59	0.59
2) turbidity_seeking	0.79	0.79	0.83	0.81	0.80	0.85	0.82	0.81	0.67	0.69
3) tmd	0.57	0.62	0.57	0.57	0.57	0.61	0.57	0.57	0.57	0.59
4) ptmd_sal_gt_1	0.60	0.67	0.64	0.62	0.63	0.69	0.66	0.64	0.68	0.69
5) ptmd_si_pt_5	0.37	0.48	0.45	0.41	0.40	0.51	0.47	0.44	0.51	0.54
6) ptmd_si_pt_5_shallow_ebb_t_gt_12	0.71	0.77	0.78	0.75	0.73	0.81	0.79	0.76	0.79	0.80
7) ptmd_sal_gt_1_si_pt_5	0.62	0.72	0.72	0.67	0.67	0.78	0.74	0.71	0.72	0.75
8) ptmd_sal_gt_1_h8_ebb_shallow_t_gt_18_acclim	0.75	0.77	0.75	0.75	0.75	0.76	0.74	0.74	0.75	0.75
9) tmd_sal_gt_1_ebb_shallow_t_gt_18	0.76	0.80	0.76	0.76	0.76	0.79	0.76	0.76	0.76	0.76
10) tmd_sal_gt_1_ptmd_ptmd_sd_pt_1_switch	0.71	0.76	0.78	0.75	0.75	0.84	0.80	0.78	0.78	0.80
CVP Salvage										
1) passive	0.22	0.22	0.22	0.22	0.63	0.63	0.63	0.63	0.21	0.62
2) turbidity_seeking	0.06	0.07	0.07	0.06	0.52	0.53	0.53	0.52	0.09	0.50
3) tmd	0.02	0.02	0.02	0.02	0.67	0.67	0.67	0.67	0.02	0.66
4) ptmd_sal_gt_1	0.13	0.17	0.17	0.14	0.64	0.66	0.65	0.64	0.17	0.65
5) ptmd_si_pt_5	0.16	0.22	0.21	0.17	0.55	0.58	0.57	0.55	0.20	0.57
6) ptmd_si_pt_5_shallow_ebb_t_gt_12	0.23	0.28	0.27	0.24	0.63	0.64	0.63	0.63	0.27	0.63
7) ptmd_sal_gt_1_si_pt_5	0.13	0.18	0.17	0.14	0.59	0.62	0.60	0.59	0.17	0.61
8) ptmd_sal_gt_1_h8_ebb_shallow_t_gt_18_acclim	0.09	0.09	0.09	0.09	0.65	0.65	0.66	0.66	0.09	0.66
9) tmd_sal_gt_1_ebb_shallow_t_gt_18	0.10	0.10	0.10	0.10	0.57	0.57	0.57	0.57	0.10	0.57
10) tmd_sal_gt_1_ptmd_ptmd_sd_pt_1_switch	0.14	0.19	0.18	0.15	0.63	0.66	0.64	0.63	0.18	0.64
SWP Salvage										
1) passive	0.26	0.26	0.27	0.26	0.90	0.90	0.90	0.90	0.26	0.90
2) turbidity_seeking	0.01	0.01	0.01	0.01	0.66	0.67	0.66	0.66	0.02	0.69
3) tmd	0.02	0.02	0.02	0.02	0.75	0.75	0.75	0.75	0.02	0.76
4) ptmd_sal_gt_1	0.28	0.32	0.32	0.29	0.89	0.90	0.90	0.89	0.32	0.90
5) ptmd_si_pt_5	0.30	0.36	0.35	0.31	0.88	0.89	0.89	0.88	0.35	0.89
6) ptmd_si_pt_5_shallow_ebb_t_gt_12	0.32	0.36	0.35	0.33	0.90	0.91	0.91	0.90	0.35	0.91
7) ptmd_sal_gt_1_si_pt_5	0.29	0.35	0.34	0.30	0.87	0.89	0.88	0.87	0.34	0.88
8) ptmd_sal_gt_1_h8_ebb_shallow_t_gt_18_acclim	0.09	0.09	0.09	0.09	0.88	0.88	0.88	0.88	0.09	0.88
9) tmd_sal_gt_1_ebb_shallow_t_gt_18	0.12	0.12	0.12	0.12	0.88	0.88	0.88	0.88	0.12	0.88
10) tmd_sal_gt_1_ptmd_ptmd_sd_pt_1_switch	0.22	0.27	0.26	0.22	0.88	0.89	0.89	0.88	0.26	0.88

Table A1. Con't.

b) 3D WY 2002 negative binomial error in SKT data ($\tau=10$)

Population model number	1	2	3	4	5	6	7	8	9	10
Salvage efficiency structure	const	const	const	const	~turb	~turb	~turb	~turb	const	~turb
Natural survival structure	S_c	S_{SKT}	S_d	S_w	S_c	S_{SKT}	S_d	S_w	S_d	S_d
SKT efficiency structure (θ_{c-SKT})	=1	=1	=1	=1	=1	=1	=1	=1	~Secchi	~Secchi
FMWT relative catch across regions										
1) passive	0.92	0.92	0.92	0.92	0.99	0.99	0.99	0.99	0.92	0.99
2) turbidity_seeking	0.99	0.99	0.99	0.99	0.99	0.99	0.98	0.99	0.99	1.00
3) tmd	0.96	0.96	0.96	0.96	0.99	0.99	0.99	0.99	0.96	0.99
4) ptmd_sal_gt_1	0.95	0.96	0.95	0.95	1.00	1.00	1.00	1.00	0.95	1.00
5) ptmd_si_pt_5	0.93	0.94	0.95	0.93	1.00	1.00	1.00	1.00	0.95	1.00
6) ptmd_si_pt_5_shallow_ebb_t_gt_12	0.94	0.95	0.96	0.95	1.00	1.00	1.00	1.00	0.96	1.00
7) ptmd_sal_gt_1_si_pt_5	0.93	0.95	0.96	0.94	1.00	1.00	1.00	1.00	0.95	1.00
8) ptmd_sal_gt_1_h8_ebb_shallow_t_gt_18_acclim	0.96	0.97	0.96	0.96	1.00	1.00	1.00	1.00	0.96	1.00
9) tmd_sal_gt_1_ebb_shallow_t_gt_18	0.99	0.98	0.99	0.99	1.00	1.00	1.00	1.00	0.99	1.00
10) tmd_sal_gt_1_ptmd_prtmd_sd_pt_1_switch	1.00	1.00	1.00	1.00	1.00	1.00	1.00	1.00	1.00	1.00
SKT catch by survey and region										
1) passive	0.06	0.05	0.06	0.06	0.04	0.04	0.04	0.04	0.06	0.06
2) turbidity_seeking	0.56	0.28	0.58	0.34	0.75	0.68	0.78	0.78	0.43	0.64
3) tmd	0.07	0.07	0.07	0.07	0.06	0.06	0.06	0.06	0.22	0.06
4) ptmd_sal_gt_1	0.47	0.54	0.50	0.50	0.49	0.56	0.53	0.51	0.49	0.53
5) ptmd_si_pt_5	0.30	0.36	0.38	0.36	0.35	0.48	0.43	0.40	0.36	0.43
6) ptmd_si_pt_5_shallow_ebb_t_gt_12	0.60	0.47	0.64	0.65	0.63	0.71	0.70	0.67	0.65	0.71
7) ptmd_sal_gt_1_si_pt_5	0.49	0.57	0.58	0.56	0.55	0.69	0.64	0.61	0.55	0.64
8) ptmd_sal_gt_1_h8_ebb_shallow_t_gt_18_acclim	0.62	0.59	0.62	0.62	0.58	0.58	0.58	0.58	0.65	0.58
9) tmd_sal_gt_1_ebb_shallow_t_gt_18	0.75	0.54	0.76	0.75	0.73	0.69	0.73	0.70	0.73	0.71
10) tmd_sal_gt_1_ptmd_prtmd_sd_pt_1_switch	0.55	0.46	0.58	0.61	0.59	0.70	0.66	0.65	0.57	0.66
CVP Salvage										
1) passive	0.21	0.21	0.21	0.21	0.63	0.63	0.63	0.63	0.21	0.63
2) turbidity_seeking	0.08	0.13	0.09	0.11	0.52	0.54	0.49	0.53	0.09	0.51
3) tmd	0.02	0.02	0.02	0.02	0.65	0.65	0.65	0.65	0.02	0.65
4) ptmd_sal_gt_1	0.14	0.18	0.18	0.14	0.63	0.66	0.64	0.63	0.18	0.64
5) ptmd_si_pt_5	0.18	0.25	0.24	0.18	0.56	0.60	0.59	0.56	0.24	0.59
6) ptmd_si_pt_5_shallow_ebb_t_gt_12	0.23	0.29	0.28	0.24	0.63	0.65	0.64	0.63	0.28	0.64
7) ptmd_sal_gt_1_si_pt_5	0.14	0.21	0.20	0.15	0.61	0.64	0.63	0.60	0.20	0.63
8) ptmd_sal_gt_1_h8_ebb_shallow_t_gt_18_acclim	0.09	0.09	0.09	0.09	0.66	0.66	0.66	0.66	0.09	0.66
9) tmd_sal_gt_1_ebb_shallow_t_gt_18	0.10	0.10	0.10	0.10	0.57	0.56	0.57	0.57	0.10	0.57
10) tmd_sal_gt_1_ptmd_prtmd_sd_pt_1_switch	0.15	0.22	0.20	0.15	0.66	0.69	0.68	0.66	0.20	0.68
SWP Salvage										
1) passive	0.25	0.25	0.26	0.26	0.91	0.91	0.91	0.91	0.26	0.91
2) turbidity_seeking	0.02	0.03	0.02	0.02	0.67	0.67	0.67	0.67	0.02	0.70
3) tmd	0.02	0.02	0.02	0.02	0.75	0.75	0.75	0.75	0.02	0.75
4) ptmd_sal_gt_1	0.28	0.34	0.33	0.29	0.89	0.90	0.90	0.89	0.33	0.90
5) ptmd_si_pt_5	0.30	0.38	0.37	0.31	0.88	0.90	0.90	0.88	0.37	0.90
6) ptmd_si_pt_5_shallow_ebb_t_gt_12	0.31	0.38	0.35	0.32	0.90	0.91	0.91	0.90	0.35	0.91
7) ptmd_sal_gt_1_si_pt_5	0.29	0.37	0.35	0.30	0.88	0.89	0.89	0.88	0.35	0.89
8) ptmd_sal_gt_1_h8_ebb_shallow_t_gt_18_acclim	0.08	0.08	0.08	0.08	0.88	0.88	0.88	0.88	0.08	0.88
9) tmd_sal_gt_1_ebb_shallow_t_gt_18	0.12	0.12	0.12	0.12	0.88	0.88	0.88	0.88	0.12	0.88
10) tmd_sal_gt_1_ptmd_prtmd_sd_pt_1_switch	0.20	0.28	0.26	0.21	0.88	0.90	0.89	0.88	0.26	0.89

Table A1. Con't.

c) 2D WY 2002 Poisson error in SKT data ($\tau=1$)

Population model number	1	2	3	4	5	6	7	8	9	10
Salvage efficiency structure	const	const	const	const	~turb	~turb	~turb	~turb	const	~turb
Natural survival structure	S_c	S_{SKT}	S_d	S_w	S_c	S_{SKT}	S_d	S_w	S_d	S_d
SKT efficiency structure (θ_{c-SKT})	=1	=1	=1	=1	=1	=1	=1	=1	~Secchi	~Secchi
FMWT relative catch across regions										
1) passive	0.85	0.85	0.85	0.85	0.89	0.89	0.89	0.89	0.86	0.90
2) turbidity_seeking	0.81	0.81	0.81	0.81	0.81	0.81	0.81	0.81	0.90	0.90
3) tmd	0.33	0.31	0.32	0.32	0.51	0.51	0.52	0.51	0.42	0.69
4) ptmd_sal_gt_1	0.88	0.88	0.88	0.88	0.89	0.89	0.89	0.89	0.95	0.97
5) ptmd_si_pt_5	0.86	0.85	0.84	0.84	0.99	0.99	0.99	0.99	0.82	0.99
6) ptmd_si_pt_5_shallow_ebb_t_gt_12	0.66	0.67	0.69	0.66	0.73	0.74	0.73	0.73	0.74	0.80
7) ptmd_sal_gt_1_si_pt_5	0.88	0.87	0.85	0.86	0.99	0.99	0.99	0.99	0.83	0.99
8) ptmd_sal_gt_1_h8_ebb_shallow_t_gt_18_acclim	0.93	0.93	0.94	0.93	0.97	0.96	0.97	0.97	0.95	0.98
9) tmd_sal_gt_1_ebb_shallow_t_gt_18	0.99	0.99	0.99	0.99	0.99	1.00	0.99	0.99	1.00	1.00
10) tmd_sal_gt_1_ptmd_prtmd_sd_pt_1_switch	0.88	0.87	0.88	0.88	0.85	0.85	0.86	0.85	0.96	0.96
SKT catch by survey and region										
1) passive	0.71	0.72	0.71	0.71	0.71	0.71	0.71	0.71	0.71	0.71
2) turbidity_seeking	0.01	0.01	0.01	0.01	0.01	0.01	0.01	0.01	0.09	0.09
3) tmd	0.66	0.66	0.69	0.67	0.64	0.68	0.62	0.64	0.72	0.67
4) ptmd_sal_gt_1	0.06	0.08	0.07	0.06	0.06	0.09	0.08	0.07	0.40	0.41
5) ptmd_si_pt_5	0.24	0.26	0.24	0.24	0.26	0.29	0.27	0.27	0.51	0.53
6) ptmd_si_pt_5_shallow_ebb_t_gt_12	0.52	0.52	0.57	0.55	0.53	0.60	0.58	0.56	0.57	0.58
7) ptmd_sal_gt_1_si_pt_5	0.26	0.28	0.26	0.26	0.28	0.31	0.29	0.28	0.51	0.53
8) ptmd_sal_gt_1_h8_ebb_shallow_t_gt_18_acclim	0.76	0.72	0.82	0.79	0.79	0.83	0.82	0.80	0.82	0.82
9) tmd_sal_gt_1_ebb_shallow_t_gt_18	0.62	0.52	0.64	0.65	0.65	0.71	0.65	0.69	0.65	0.61
10) tmd_sal_gt_1_ptmd_prtmd_sd_pt_1_switch	0.63	0.58	0.65	0.65	0.65	0.68	0.67	0.66	0.74	0.69
CVP Salvage										
1) passive	0.20	0.20	0.20	0.20	0.57	0.57	0.57	0.57	0.20	0.57
2) turbidity_seeking	0.00	0.00	0.00	0.00	0.00	0.00	0.00	0.00	0.00	0.01
3) tmd	0.16	0.17	0.17	0.16	0.68	0.68	0.68	0.68	0.17	0.68
4) ptmd_sal_gt_1	0.18	0.23	0.23	0.19	0.55	0.57	0.56	0.54	0.23	0.56
5) ptmd_si_pt_5	0.05	0.06	0.06	0.05	0.54	0.56	0.55	0.54	0.06	0.55
6) ptmd_si_pt_5_shallow_ebb_t_gt_12	0.20	0.25	0.24	0.21	0.67	0.68	0.68	0.67	0.24	0.68
7) ptmd_sal_gt_1_si_pt_5	0.05	0.07	0.07	0.05	0.59	0.61	0.60	0.59	0.07	0.60
8) ptmd_sal_gt_1_h8_ebb_shallow_t_gt_18_acclim	0.32	0.34	0.31	0.32	0.74	0.74	0.72	0.74	0.31	0.72
9) tmd_sal_gt_1_ebb_shallow_t_gt_18	0.21	0.27	0.21	0.21	0.68	0.67	0.68	0.68	0.21	0.68
10) tmd_sal_gt_1_ptmd_prtmd_sd_pt_1_switch	0.33	0.36	0.34	0.33	0.67	0.66	0.67	0.67	0.33	0.68
SWP Salvage										
1) passive	0.32	0.32	0.32	0.32	0.93	0.93	0.93	0.93	0.32	0.93
2) turbidity_seeking	0.01	0.01	0.01	0.01	0.00	0.00	0.00	0.00	0.01	0.00
3) tmd	0.19	0.21	0.20	0.19	0.93	0.93	0.92	0.93	0.19	0.92
4) ptmd_sal_gt_1	0.24	0.30	0.30	0.25	0.91	0.91	0.91	0.91	0.30	0.91
5) ptmd_si_pt_5	0.08	0.11	0.11	0.09	0.91	0.92	0.92	0.91	0.11	0.92
6) ptmd_si_pt_5_shallow_ebb_t_gt_12	0.27	0.34	0.31	0.28	0.92	0.92	0.92	0.92	0.31	0.92
7) ptmd_sal_gt_1_si_pt_5	0.10	0.12	0.12	0.10	0.89	0.90	0.90	0.89	0.12	0.89
8) ptmd_sal_gt_1_h8_ebb_shallow_t_gt_18_acclim	0.39	0.43	0.39	0.40	0.94	0.94	0.94	0.94	0.38	0.94
9) tmd_sal_gt_1_ebb_shallow_t_gt_18	0.26	0.33	0.26	0.26	0.92	0.92	0.92	0.92	0.26	0.92
10) tmd_sal_gt_1_ptmd_prtmd_sd_pt_1_switch	0.39	0.43	0.40	0.39	0.93	0.93	0.92	0.93	0.39	0.92

Table A1. Con't.

d) 2D WY 2002 negative binomial error in SKT data ($\tau=10$)

Population model number	1	2	3	4	5	6	7	8	9	10
Salvage efficiency structure	const	const	const	const	~turb	~turb	~turb	~turb	const	~turb
Natural survival structure	S_c	S_{SKT}	S_d	S_w	S_c	S_{SKT}	S_d	S_w	S_d	S_d
SKT efficiency structure (θ_{c-SKT})	=1	=1	=1	=1	=1	=1	=1	=1	~Secchi	~Secchi
FMWT relative catch across regions										
1) passive	0.94	0.94	0.94	0.94	0.98	0.98	0.98	0.98	0.94	0.98
2) turbidity_seeking	0.99	0.99	0.99	0.99	0.99	0.99	0.99	0.99	0.99	0.99
3) tmd	0.80	0.73	0.77	0.81	0.98	0.98	0.98	0.98	0.78	0.98
4) ptmd_sal_gt_1	0.96	0.95	0.95	0.95	1.00	1.00	1.00	1.00	0.95	1.00
5) ptmd_si_pt_5	0.86	0.84	0.83	0.84	0.99	0.99	0.99	0.99	0.83	0.99
6) ptmd_si_pt_5_shallow_ebb_t_gt_12	0.88	0.88	0.90	0.88	0.99	0.99	1.00	0.99	0.90	1.00
7) ptmd_sal_gt_1_si_pt_5	0.87	0.84	0.83	0.84	0.99	0.98	0.98	0.99	0.83	0.98
8) ptmd_sal_gt_1_h8_ebb_shallow_t_gt_18_acclim	0.94	0.94	0.95	0.95	1.00	1.00	1.00	1.00	0.96	1.00
9) tmd_sal_gt_1_ebb_shallow_t_gt_18	0.95	0.94	0.96	0.98	1.00	1.00	1.00	1.00	0.96	1.00
10) tmd_sal_gt_1_ptmd_prtmd_sd_pt_1_switch	1.00	1.00	1.00	1.00	1.00	1.00	1.00	1.00	1.00	1.00
SKT catch by survey and region										
1) passive	0.28	0.28	0.28	0.28	0.26	0.26	0.26	0.26	0.35	0.33
2) turbidity_seeking	0.00	0.00	0.00	0.00	0.00	0.00	0.00	0.00	0.01	0.00
3) tmd	0.12	0.14	0.16	0.12	0.07	0.08	0.07	0.08	0.28	0.18
4) ptmd_sal_gt_1	0.03	0.04	0.03	0.03	0.04	0.05	0.04	0.04	0.13	0.04
5) ptmd_si_pt_5	0.23	0.23	0.22	0.23	0.25	0.27	0.25	0.20	0.33	0.25
6) ptmd_si_pt_5_shallow_ebb_t_gt_12	0.18	0.07	0.17	0.20	0.18	0.16	0.19	0.20	0.26	0.27
7) ptmd_sal_gt_1_si_pt_5	0.25	0.25	0.24	0.25	0.27	0.29	0.27	0.27	0.34	0.27
8) ptmd_sal_gt_1_h8_ebb_shallow_t_gt_18_acclim	0.65	0.31	0.65	0.69	0.72	0.55	0.71	0.74	0.66	0.69
9) tmd_sal_gt_1_ebb_shallow_t_gt_18	0.47	0.17	0.46	0.25	0.58	0.34	0.57	0.52	0.39	0.57
10) tmd_sal_gt_1_ptmd_prtmd_sd_pt_1_switch	0.34	0.19	0.35	0.24	0.36	0.29	0.35	0.30	0.46	0.49
CVP Salvage										
1) passive	0.19	0.19	0.20	0.20	0.56	0.56	0.56	0.56	0.19	0.56
2) turbidity_seeking	0.00	0.00	0.00	0.00	0.00	0.00	0.00	0.00	0.00	0.00
3) tmd	0.15	0.17	0.15	0.15	0.67	0.67	0.68	0.67	0.15	0.68
4) ptmd_sal_gt_1	0.19	0.24	0.24	0.20	0.56	0.56	0.55	0.55	0.24	0.55
5) ptmd_si_pt_5	0.05	0.07	0.07	0.05	0.54	0.56	0.55	0.56	0.07	0.55
6) ptmd_si_pt_5_shallow_ebb_t_gt_12	0.18	0.25	0.23	0.19	0.67	0.68	0.68	0.67	0.23	0.68
7) ptmd_sal_gt_1_si_pt_5	0.05	0.08	0.07	0.05	0.60	0.61	0.60	0.60	0.07	0.60
8) ptmd_sal_gt_1_h8_ebb_shallow_t_gt_18_acclim	0.32	0.40	0.33	0.33	0.73	0.74	0.74	0.73	0.33	0.74
9) tmd_sal_gt_1_ebb_shallow_t_gt_18	0.22	0.33	0.23	0.25	0.68	0.68	0.68	0.68	0.23	0.68
10) tmd_sal_gt_1_ptmd_prtmd_sd_pt_1_switch	0.33	0.37	0.34	0.35	0.66	0.65	0.66	0.66	0.34	0.66
SWP Salvage										
1) passive	0.32	0.32	0.32	0.32	0.93	0.93	0.93	0.93	0.32	0.93
2) turbidity_seeking	0.01	0.01	0.01	0.01	0.00	0.00	0.00	0.00	0.01	0.00
3) tmd	0.16	0.19	0.17	0.16	0.93	0.93	0.92	0.93	0.17	0.92
4) ptmd_sal_gt_1	0.25	0.31	0.31	0.26	0.91	0.91	0.91	0.91	0.31	0.91
5) ptmd_si_pt_5	0.09	0.12	0.11	0.09	0.91	0.93	0.92	0.92	0.11	0.92
6) ptmd_si_pt_5_shallow_ebb_t_gt_12	0.24	0.34	0.30	0.26	0.92	0.92	0.92	0.92	0.30	0.92
7) ptmd_sal_gt_1_si_pt_5	0.10	0.13	0.12	0.10	0.89	0.90	0.90	0.89	0.12	0.90
8) ptmd_sal_gt_1_h8_ebb_shallow_t_gt_18_acclim	0.39	0.50	0.40	0.40	0.94	0.95	0.94	0.94	0.40	0.94
9) tmd_sal_gt_1_ebb_shallow_t_gt_18	0.27	0.43	0.28	0.28	0.93	0.93	0.93	0.93	0.28	0.93
10) tmd_sal_gt_1_ptmd_prtmd_sd_pt_1_switch	0.38	0.46	0.40	0.40	0.93	0.93	0.93	0.93	0.40	0.93

Table A1. Con't.

e) 2D WY 2004 Poisson error in SKT data ($\tau=1$)

Population model number	1	2	3	4	5	6	7	8	9	10
Salvage efficiency structure	const	const	const	const	~turb	~turb	~turb	~turb	const	~turb
Natural survival structure	S_c	S_{SKT}	S_d	S_w	S_c	S_{SKT}	S_d	S_w	S_d	S_d
SKT efficiency structure (θ_{c-SKT})	=1	=1	=1	=1	=1	=1	=1	=1	~Secchi	~Secchi
FMWT relative catch across regions										
1) passive	0.50	0.50	0.50	0.50	0.53	0.53	0.52	0.52	0.53	0.56
2) turbidity_seeking	0.69	0.69	0.69	0.69	0.68	0.68	0.68	0.68	0.70	0.62
3) tmd	0.07	0.07	0.08	0.05	0.09	0.13	0.09	0.08	0.08	0.14
4) ptmd_sal_gt_1	0.80	0.80	0.81	0.81	0.70	0.69	0.70	0.70	0.75	0.64
5) ptmd_si_pt_5	0.81	0.81	0.81	0.81	0.45	0.44	0.45	0.45	0.81	0.47
6) ptmd_si_pt_5_shallow_ebb_t_gt_12	0.29	0.30	0.29	0.29	0.29	0.30	0.29	0.29	0.25	0.24
7) ptmd_sal_gt_1_si_pt_5	0.73	0.73	0.73	0.73	0.30	0.30	0.31	0.31	0.73	0.33
8) ptmd_sal_gt_1_h8_ebb_shallow_t_gt_18_acclim	0.44	0.39	0.37	0.45	0.39	0.31	0.41	0.29	0.34	0.26
9) tmd_sal_gt_1_ebb_shallow_t_gt_18	0.61	0.62	0.60	0.60	0.61	0.61	0.60	0.60	0.62	0.62
10) tmd_sal_gt_1_ptmd_ptmd_sd_pt_1_switch	0.74	0.73	0.74	0.74	0.76	0.74	0.76	0.75	0.68	0.69
SKT catch by survey and region										
1) passive	0.69	0.73	0.69	0.69	0.66	0.72	0.65	0.65	0.78	0.76
2) turbidity_seeking	0.00	0.00	0.00	0.00	0.00	0.00	0.00	0.00	0.00	0.00
3) tmd	0.57	0.70	0.55	0.66	0.63	0.70	0.73	0.71	0.77	0.77
4) ptmd_sal_gt_1	0.39	0.39	0.38	0.38	0.44	0.45	0.44	0.44	0.42	0.47
5) ptmd_si_pt_5	0.63	0.65	0.62	0.62	0.62	0.63	0.61	0.61	0.64	0.62
6) ptmd_si_pt_5_shallow_ebb_t_gt_12	0.70	0.75	0.69	0.69	0.71	0.75	0.70	0.70	0.76	0.77
7) ptmd_sal_gt_1_si_pt_5	0.68	0.70	0.67	0.67	0.68	0.69	0.67	0.67	0.69	0.69
8) ptmd_sal_gt_1_h8_ebb_shallow_t_gt_18_acclim	0.56	0.74	0.73	0.54	0.54	0.72	0.53	0.64	0.87	0.87
9) tmd_sal_gt_1_ebb_shallow_t_gt_18	0.74	0.82	0.72	0.72	0.74	0.82	0.72	0.72	0.87	0.87
10) tmd_sal_gt_1_ptmd_ptmd_sd_pt_1_switch	0.65	0.76	0.63	0.63	0.65	0.75	0.63	0.72	0.80	0.80
CVP Salvage										
1) passive	0.00	0.00	0.00	0.00	0.01	0.01	0.01	0.01	0.00	0.01
2) turbidity_seeking	0.00	0.00	0.00	0.00	0.00	0.00	0.00	0.00	0.00	0.00
3) tmd	0.02	0.02	0.02	0.02	0.14	0.15	0.14	0.13	0.02	0.15
4) ptmd_sal_gt_1	0.00	0.00	0.00	0.00	0.02	0.02	0.02	0.02	0.00	0.02
5) ptmd_si_pt_5	0.00	0.00	0.00	0.00	0.01	0.01	0.01	0.01	0.00	0.01
6) ptmd_si_pt_5_shallow_ebb_t_gt_12	0.01	0.02	0.01	0.01	0.06	0.06	0.06	0.06	0.01	0.06
7) ptmd_sal_gt_1_si_pt_5	0.00	0.00	0.00	0.00	0.02	0.02	0.02	0.02	0.00	0.02
8) ptmd_sal_gt_1_h8_ebb_shallow_t_gt_18_acclim	0.04	0.04	0.04	0.04	0.03	0.04	0.03	0.03	0.04	0.04
9) tmd_sal_gt_1_ebb_shallow_t_gt_18	0.02	0.03	0.02	0.02	0.10	0.10	0.10	0.10	0.02	0.10
10) tmd_sal_gt_1_ptmd_ptmd_sd_pt_1_switch	0.06	0.07	0.06	0.06	0.18	0.19	0.19	0.16	0.06	0.20
SWP Salvage										
1) passive	0.00	0.00	0.00	0.00	0.03	0.03	0.03	0.03	0.00	0.03
2) turbidity_seeking	0.02	0.02	0.02	0.02	0.00	0.00	0.00	0.00	0.02	0.00
3) tmd	0.04	0.04	0.04	0.03	0.08	0.09	0.08	0.08	0.04	0.09
4) ptmd_sal_gt_1	0.01	0.01	0.01	0.01	0.04	0.04	0.04	0.04	0.01	0.04
5) ptmd_si_pt_5	0.00	0.00	0.00	0.00	0.03	0.03	0.03	0.03	0.00	0.03
6) ptmd_si_pt_5_shallow_ebb_t_gt_12	0.04	0.04	0.04	0.04	0.06	0.06	0.06	0.06	0.04	0.06
7) ptmd_sal_gt_1_si_pt_5	0.00	0.00	0.00	0.00	0.03	0.03	0.03	0.03	0.00	0.03
8) ptmd_sal_gt_1_h8_ebb_shallow_t_gt_18_acclim	0.06	0.07	0.06	0.06	0.05	0.06	0.05	0.05	0.06	0.06
9) tmd_sal_gt_1_ebb_shallow_t_gt_18	0.15	0.15	0.14	0.14	0.16	0.16	0.17	0.17	0.14	0.17
10) tmd_sal_gt_1_ptmd_ptmd_sd_pt_1_switch	0.10	0.10	0.10	0.10	0.16	0.17	0.17	0.15	0.10	0.17

Table A1. Con't.

f) 2D WY 2004 negative binomial error in SKT data ($\tau=10$)

Population model number	1	2	3	4	5	6	7	8	9	10
Salvage efficiency structure	const	const	const	const	~turb	~turb	~turb	~turb	const	~turb
Natural survival structure	S_c	S_{SKT}	S_d	S_w	S_c	S_{SKT}	S_d	S_w	S_d	S_d
SKT efficiency structure (θ_{c-SKT})	=1	=1	=1	=1	=1	=1	=1	=1	~Secchi	~Secchi
FMWT relative catch across regions										
1) passive	0.91	0.91	0.91	0.91	0.90	0.90	0.90	0.90	0.92	0.90
2) turbidity_seeking	0.96	0.96	0.96	0.96	0.94	0.93	0.95	0.95	0.98	0.94
3) tmd	0.57	0.49	0.59	0.59	0.40	0.40	0.42	0.42	0.57	0.42
4) ptmd_sal_gt_1	0.94	0.94	0.94	0.94	0.89	0.89	0.89	0.89	0.94	0.89
5) ptmd_si_pt_5	0.87	0.87	0.87	0.87	0.42	0.42	0.42	0.42	0.88	0.42
6) ptmd_si_pt_5_shallow_ebb_t_gt_12	0.83	0.80	0.85	0.85	0.65	0.64	0.67	0.67	0.84	0.67
7) ptmd_sal_gt_1_si_pt_5	0.76	0.76	0.77	0.77	0.25	0.25	0.26	0.26	0.77	0.26
8) ptmd_sal_gt_1_h8_ebb_shallow_t_gt_18_acclim	0.61	0.53	0.65	0.65	0.15	0.15	0.17	0.17	0.63	0.42
9) tmd_sal_gt_1_ebb_shallow_t_gt_18	0.95	0.95	0.95	0.95	0.82	0.82	0.85	0.85	0.95	0.84
10) tmd_sal_gt_1_ptmd_prtmd_sd_pt_1_switch	0.99	0.99	0.99	0.99	1.00	0.99	1.00	1.00	0.99	1.00
SKT catch by survey and region										
1) passive	0.15	0.15	0.14	0.14	0.13	0.13	0.12	0.12	0.27	0.12
2) turbidity_seeking	0.00	0.00	0.00	0.00	0.00	0.00	0.00	0.00	0.00	0.00
3) tmd	0.03	0.02	0.03	0.03	0.07	0.07	0.06	0.06	0.07	0.06
4) ptmd_sal_gt_1	0.17	0.17	0.17	0.17	0.18	0.18	0.18	0.18	0.14	0.18
5) ptmd_si_pt_5	0.62	0.62	0.61	0.61	0.61	0.61	0.60	0.60	0.62	0.60
6) ptmd_si_pt_5_shallow_ebb_t_gt_12	0.14	0.16	0.13	0.13	0.17	0.17	0.16	0.16	0.19	0.17
7) ptmd_sal_gt_1_si_pt_5	0.69	0.69	0.68	0.68	0.68	0.68	0.67	0.67	0.68	0.69
8) ptmd_sal_gt_1_h8_ebb_shallow_t_gt_18_acclim	0.29	0.39	0.27	0.27	0.19	0.23	0.18	0.18	0.52	0.50
9) tmd_sal_gt_1_ebb_shallow_t_gt_18	0.63	0.67	0.62	0.62	0.53	0.53	0.52	0.52	0.77	0.56
10) tmd_sal_gt_1_ptmd_prtmd_sd_pt_1_switch	0.39	0.43	0.38	0.38	0.36	0.38	0.35	0.35	0.45	0.42
CVP Salvage										
1) passive	0.00	0.00	0.00	0.00	0.03	0.03	0.03	0.03	0.00	0.03
2) turbidity_seeking	0.00	0.00	0.00	0.00	0.00	0.00	0.00	0.00	0.00	0.00
3) tmd	0.02	0.04	0.02	0.02	0.21	0.22	0.21	0.21	0.02	0.21
4) ptmd_sal_gt_1	0.00	0.00	0.00	0.00	0.03	0.03	0.03	0.03	0.00	0.03
5) ptmd_si_pt_5	0.00	0.00	0.00	0.00	0.02	0.02	0.03	0.03	0.00	0.03
6) ptmd_si_pt_5_shallow_ebb_t_gt_12	0.01	0.01	0.01	0.01	0.08	0.08	0.09	0.09	0.01	0.09
7) ptmd_sal_gt_1_si_pt_5	0.00	0.00	0.00	0.00	0.03	0.03	0.04	0.04	0.00	0.04
8) ptmd_sal_gt_1_h8_ebb_shallow_t_gt_18_acclim	0.03	0.04	0.03	0.03	0.10	0.10	0.10	0.10	0.03	0.04
9) tmd_sal_gt_1_ebb_shallow_t_gt_18	0.02	0.03	0.02	0.02	0.18	0.18	0.19	0.19	0.02	0.19
10) tmd_sal_gt_1_ptmd_prtmd_sd_pt_1_switch	0.06	0.07	0.06	0.06	0.19	0.19	0.19	0.19	0.06	0.20
SWP Salvage										
1) passive	0.00	0.00	0.00	0.00	0.07	0.07	0.07	0.07	0.00	0.07
2) turbidity_seeking	0.02	0.02	0.02	0.02	0.00	0.00	0.00	0.00	0.02	0.00
3) tmd	0.06	0.08	0.06	0.06	0.32	0.33	0.32	0.32	0.06	0.32
4) ptmd_sal_gt_1	0.01	0.01	0.01	0.01	0.07	0.07	0.08	0.08	0.01	0.08
5) ptmd_si_pt_5	0.00	0.00	0.00	0.00	0.07	0.07	0.07	0.07	0.00	0.07
6) ptmd_si_pt_5_shallow_ebb_t_gt_12	0.03	0.03	0.03	0.03	0.19	0.19	0.19	0.19	0.03	0.19
7) ptmd_sal_gt_1_si_pt_5	0.00	0.00	0.00	0.00	0.07	0.07	0.07	0.07	0.00	0.07
8) ptmd_sal_gt_1_h8_ebb_shallow_t_gt_18_acclim	0.06	0.07	0.06	0.06	0.27	0.28	0.27	0.27	0.06	0.07
9) tmd_sal_gt_1_ebb_shallow_t_gt_18	0.14	0.14	0.14	0.14	0.35	0.35	0.36	0.36	0.14	0.36
10) tmd_sal_gt_1_ptmd_prtmd_sd_pt_1_switch	0.10	0.10	0.10	0.10	0.17	0.17	0.17	0.17	0.10	0.17

Table A1. Con't.

g) 2D WY 2005 Poisson error in SKT data ($\tau=1$)

Population model number	1	2	3	4	5	6	7	8	9	10
Salvage efficiency structure	const	const	const	const	~turb	~turb	~turb	~turb	const	~turb
Natural survival structure	S_c	S_{SKT}	S_d	S_w	S_c	S_{SKT}	S_d	S_w	S_d	S_d
SKT efficiency structure (θ_{c-SKT})	=1	=1	=1	=1	=1	=1	=1	=1	~Secchi	~Secchi
FMWT relative catch across regions										
1) passive	0.85	0.85	0.85	0.84	0.85	0.85	0.85	0.84	0.89	0.89
2) turbidity_seeking	1.00	1.00	1.00	1.00	1.00	1.00	1.00	1.00	0.96	0.96
3) tmd	0.32	0.38	0.35	0.36	0.31	0.37	0.34	0.35	0.29	0.28
4) ptmd_sal_gt_1	0.99	0.99	0.99	0.99	0.99	0.99	0.99	0.99	0.99	0.99
5) ptmd_si_pt_5	1.00	1.00	1.00	1.00	1.00	1.00	1.00	1.00	1.00	1.00
6) ptmd_si_pt_5_shallow_ebb_t_gt_12	0.75	0.77	0.76	0.76	0.75	0.77	0.76	0.76	0.92	0.92
7) ptmd_sal_gt_1_si_pt_5	1.00	1.00	1.00	1.00	1.00	1.00	1.00	1.00	1.00	1.00
8) ptmd_sal_gt_1_h8_ebb_shallow_t_gt_18_acclim	0.91	0.95	0.93	0.93	0.92	0.95	0.94	0.93	0.94	0.94
9) tmd_sal_gt_1_ebb_shallow_t_gt_18	1.00	1.00	1.00	1.00	1.00	1.00	1.00	1.00	1.00	1.00
10) tmd_sal_gt_1_ptmd_prtmd_sd_pt_1_switch	0.86	0.87	0.86	0.86	0.85	0.86	0.85	0.85	0.95	0.94
SKT catch by survey and region										
1) passive	0.48	0.59	0.41	0.54	0.49	0.59	0.41	0.54	0.44	0.64
2) turbidity_seeking	0.22	0.22	0.22	0.22	0.22	0.22	0.22	0.22	0.32	0.32
3) tmd	0.51	0.51	0.55	0.57	0.54	0.63	0.60	0.62	0.60	0.65
4) ptmd_sal_gt_1	0.50	0.62	0.59	0.57	0.51	0.62	0.59	0.57	0.69	0.69
5) ptmd_si_pt_5	0.70	0.84	0.79	0.79	0.71	0.84	0.79	0.79	0.80	0.80
6) ptmd_si_pt_5_shallow_ebb_t_gt_12	0.58	0.67	0.64	0.62	0.59	0.68	0.65	0.63	0.77	0.77
7) ptmd_sal_gt_1_si_pt_5	0.71	0.84	0.79	0.80	0.71	0.84	0.79	0.80	0.80	0.80
8) ptmd_sal_gt_1_h8_ebb_shallow_t_gt_18_acclim	0.66	0.79	0.74	0.73	0.65	0.79	0.74	0.73	0.81	0.81
9) tmd_sal_gt_1_ebb_shallow_t_gt_18	0.60	0.63	0.64	0.66	0.62	0.73	0.68	0.67	0.76	0.80
10) tmd_sal_gt_1_ptmd_prtmd_sd_pt_1_switch	0.57	0.62	0.61	0.63	0.59	0.70	0.65	0.65	0.67	0.69
CVP Salvage										
1) passive	0.00	0.00	0.00	0.00	0.03	0.03	0.03	0.03	0.00	0.03
2) turbidity_seeking	0.01	0.00	0.00	0.01	0.01	0.00	0.01	0.00	0.01	0.01
3) tmd	0.05	0.05	0.04	0.03	0.17	0.15	0.16	0.16	0.05	0.17
4) ptmd_sal_gt_1	0.00	0.00	0.00	0.00	0.03	0.03	0.03	0.03	0.00	0.03
5) ptmd_si_pt_5	0.00	0.00	0.00	0.00	0.02	0.03	0.03	0.03	0.00	0.03
6) ptmd_si_pt_5_shallow_ebb_t_gt_12	0.03	0.05	0.05	0.04	0.06	0.09	0.08	0.07	0.04	0.08
7) ptmd_sal_gt_1_si_pt_5	0.00	0.00	0.00	0.00	0.01	0.01	0.01	0.01	0.00	0.01
8) ptmd_sal_gt_1_h8_ebb_shallow_t_gt_18_acclim	0.15	0.18	0.18	0.17	0.15	0.19	0.18	0.18	0.18	0.18
9) tmd_sal_gt_1_ebb_shallow_t_gt_18	0.14	0.16	0.16	0.15	0.26	0.28	0.29	0.29	0.16	0.29
10) tmd_sal_gt_1_ptmd_prtmd_sd_pt_1_switch	0.09	0.12	0.11	0.11	0.14	0.16	0.16	0.16	0.11	0.16
SWP Salvage										
1) passive	0.01	0.02	0.02	0.01	0.04	0.05	0.05	0.04	0.02	0.05
2) turbidity_seeking	0.01	0.01	0.01	0.01	0.01	0.01	0.01	0.01	0.01	0.01
3) tmd	0.14	0.17	0.13	0.12	0.28	0.30	0.29	0.29	0.15	0.30
4) ptmd_sal_gt_1	0.01	0.02	0.02	0.01	0.04	0.05	0.04	0.04	0.02	0.05
5) ptmd_si_pt_5	0.01	0.02	0.01	0.01	0.02	0.03	0.03	0.03	0.01	0.03
6) ptmd_si_pt_5_shallow_ebb_t_gt_12	0.08	0.14	0.12	0.11	0.11	0.17	0.16	0.14	0.12	0.15
7) ptmd_sal_gt_1_si_pt_5	0.01	0.02	0.02	0.02	0.03	0.04	0.04	0.04	0.02	0.04
8) ptmd_sal_gt_1_h8_ebb_shallow_t_gt_18_acclim	0.41	0.50	0.48	0.47	0.42	0.50	0.48	0.48	0.47	0.47
9) tmd_sal_gt_1_ebb_shallow_t_gt_18	0.33	0.40	0.37	0.37	0.44	0.50	0.49	0.49	0.37	0.49
10) tmd_sal_gt_1_ptmd_prtmd_sd_pt_1_switch	0.27	0.37	0.34	0.33	0.32	0.37	0.36	0.36	0.34	0.37

Table A1. Con't.

h) 2D WY 2005 negative binomial error in SKT data ($\tau=10$)

Population model number	1	2	3	4	5	6	7	8	9	10
Salvage efficiency structure	const	const	const	const	~turb	~turb	~turb	~turb	const	~turb
Natural survival structure	S_c	S_{SKT}	S_d	S_w	S_c	S_{SKT}	S_d	S_w	S_d	S_d
SKT efficiency structure (θ_{c-SKT})	=1	=1	=1	=1	=1	=1	=1	=1	~Secchi	~Secchi
FMWT relative catch across regions										
1) passive	0.98	0.98	0.98	0.98	0.98	0.98	0.98	0.98	0.97	0.97
2) turbidity_seeking	1.00	1.00	1.00	1.00	1.00	1.00	1.00	1.00	1.00	1.00
3) tmd	0.79	0.78	0.80	0.79	0.84	0.81	0.87	0.88	0.80	0.87
4) ptmd_sal_gt_1	0.99	0.99	0.99	0.99	0.99	0.99	0.99	0.99	0.99	0.99
5) ptmd_si_pt_5	1.00	1.00	1.00	1.00	1.00	1.00	1.00	1.00	1.00	1.00
6) ptmd_si_pt_5_shallow_ebb_t_gt_12	1.00	1.00	1.00	1.00	1.00	1.00	1.00	1.00	1.00	1.00
7) ptmd_sal_gt_1_si_pt_5	1.00	1.00	1.00	1.00	1.00	1.00	1.00	1.00	1.00	1.00
8) ptmd_sal_gt_1_h8_ebb_shallow_t_gt_18_acclim	1.00	1.00	1.00	1.00	1.00	1.00	1.00	1.00	1.00	1.00
9) tmd_sal_gt_1_ebb_shallow_t_gt_18	1.00	1.00	1.00	1.00	0.99	0.99	1.00	1.00	1.00	0.99
10) tmd_sal_gt_1_ptmd_prtmd_sd_pt_1_switch	1.00	1.00	1.00	1.00	1.00	1.00	1.00	1.00	1.00	1.00
SKT catch by survey and region										
1) passive	0.12	0.16	0.12	0.12	0.12	0.16	0.12	0.12	0.12	0.12
2) turbidity_seeking	0.22	0.22	0.22	0.22	0.22	0.22	0.22	0.22	0.22	0.25
3) tmd	0.12	0.06	0.13	0.13	0.14	0.07	0.16	0.17	0.15	0.16
4) ptmd_sal_gt_1	0.41	0.56	0.39	0.39	0.41	0.56	0.39	0.39	0.39	0.37
5) ptmd_si_pt_5	0.60	0.81	0.59	0.59	0.60	0.81	0.59	0.59	0.53	0.53
6) ptmd_si_pt_5_shallow_ebb_t_gt_12	0.20	0.28	0.27	0.27	0.19	0.31	0.27	0.26	0.27	0.32
7) ptmd_sal_gt_1_si_pt_5	0.60	0.81	0.58	0.58	0.60	0.81	0.58	0.58	0.53	0.53
8) ptmd_sal_gt_1_h8_ebb_shallow_t_gt_18_acclim	0.42	0.56	0.51	0.52	0.42	0.55	0.32	0.52	0.51	0.51
9) tmd_sal_gt_1_ebb_shallow_t_gt_18	0.60	0.37	0.61	0.61	0.63	0.47	0.67	0.68	0.65	0.68
10) tmd_sal_gt_1_ptmd_prtmd_sd_pt_1_switch	0.18	0.13	0.19	0.20	0.19	0.17	0.21	0.22	0.25	0.21
CVP Salvage										
1) passive	0.00	0.00	0.00	0.00	0.03	0.03	0.03	0.03	0.00	0.03
2) turbidity_seeking	0.01	0.01	0.01	0.01	0.01	0.01	0.00	0.01	0.01	0.01
3) tmd	0.06	0.22	0.06	0.06	0.17	0.26	0.17	0.17	0.06	0.17
4) ptmd_sal_gt_1	0.00	0.00	0.00	0.00	0.03	0.03	0.03	0.03	0.00	0.03
5) ptmd_si_pt_5	0.00	0.00	0.00	0.00	0.03	0.03	0.03	0.03	0.00	0.03
6) ptmd_si_pt_5_shallow_ebb_t_gt_12	0.04	0.05	0.05	0.04	0.09	0.09	0.08	0.08	0.05	0.08
7) ptmd_sal_gt_1_si_pt_5	0.00	0.00	0.00	0.00	0.02	0.01	0.02	0.02	0.00	0.02
8) ptmd_sal_gt_1_h8_ebb_shallow_t_gt_18_acclim	0.17	0.18	0.18	0.18	0.18	0.18	0.18	0.18	0.18	0.18
9) tmd_sal_gt_1_ebb_shallow_t_gt_18	0.15	0.26	0.16	0.16	0.28	0.33	0.29	0.29	0.16	0.29
10) tmd_sal_gt_1_ptmd_prtmd_sd_pt_1_switch	0.09	0.15	0.11	0.11	0.14	0.17	0.16	0.16	0.11	0.16
SWP Salvage										
1) passive	0.02	0.02	0.02	0.02	0.05	0.05	0.05	0.05	0.02	0.05
2) turbidity_seeking	0.01	0.01	0.01	0.01	0.01	0.00	0.01	0.01	0.01	0.01
3) tmd	0.16	0.44	0.17	0.16	0.27	0.38	0.28	0.28	0.17	0.28
4) ptmd_sal_gt_1	0.02	0.02	0.02	0.02	0.05	0.05	0.05	0.05	0.02	0.05
5) ptmd_si_pt_5	0.01	0.01	0.02	0.02	0.03	0.03	0.03	0.03	0.02	0.03
6) ptmd_si_pt_5_shallow_ebb_t_gt_12	0.12	0.13	0.13	0.12	0.17	0.17	0.16	0.15	0.13	0.16
7) ptmd_sal_gt_1_si_pt_5	0.02	0.02	0.02	0.02	0.04	0.04	0.05	0.05	0.02	0.05
8) ptmd_sal_gt_1_h8_ebb_shallow_t_gt_18_acclim	0.46	0.49	0.48	0.47	0.47	0.49	0.49	0.48	0.48	0.49
9) tmd_sal_gt_1_ebb_shallow_t_gt_18	0.34	0.50	0.36	0.36	0.48	0.54	0.49	0.49	0.36	0.49
10) tmd_sal_gt_1_ptmd_prtmd_sd_pt_1_switch	0.29	0.43	0.34	0.34	0.34	0.41	0.36	0.37	0.34	0.36

Table A1. Con't.

i) 2D WY 2011 Poisson error in SKT data ($\tau=1$)

Population model number	1	2	3	4	5	6	7	8	9	10
Salvage efficiency structure	const	const	const	const	~turb	~turb	~turb	~turb	const	~turb
Natural survival structure	S _c	S _{SKT}	S _a	S _w	S _c	S _{SKT}	S _a	S _w	S _a	S _a
SKT efficiency structure (θ_{c-SKT})	=1	=1	=1	=1	=1	=1	=1	=1	~Secchi	~Secchi
FMWT relative catch across regions										
1) passive	0.98	0.98	0.98	0.98	0.98	0.98	0.98	0.98	0.96	0.96
2) turbidity_seeking	0.73	0.73	0.73	0.73	0.73	0.73	0.73	0.73	0.72	0.72
3) tmd	0.82	0.82	0.83	0.83	0.82	0.82	0.83	0.83	0.80	0.80
4) ptmd_sal_gt_1	0.64	0.65	0.65	0.65	0.64	0.65	0.65	0.65	0.64	0.64
5) ptmd_si_pt_5	0.63	0.63	0.63	0.63	0.63	0.63	0.63	0.63	0.64	0.64
6) ptmd_si_pt_5_shallow_ebb_t_gt_12	0.66	0.66	0.66	0.66	0.66	0.66	0.66	0.66	0.64	0.64
7) ptmd_sal_gt_1_si_pt_5	0.62	0.62	0.62	0.62	0.62	0.62	0.62	0.62	0.63	0.63
8) ptmd_sal_gt_1_h8_ebb_shallow_t_gt_18_acclim	0.65	0.65	0.65	0.65	0.65	0.65	0.65	0.65	0.63	0.63
9) tmd_sal_gt_1_ebb_shallow_t_gt_18	0.63	0.63	0.63	0.63	0.63	0.63	0.63	0.63	0.63	0.63
10) tmd_sal_gt_1_ptmd_prtmd_sd_pt_1_switch	0.63	0.63	0.63	0.63	0.63	0.63	0.64	0.63	0.63	0.63
SKT catch by survey and region										
1) passive	0.70	0.73	0.71	0.70	0.70	0.73	0.71	0.70	0.66	0.66
2) turbidity_seeking	0.02	0.02	0.02	0.02	0.02	0.02	0.02	0.02	0.02	0.02
3) tmd	0.69	0.71	0.68	0.68	0.69	0.71	0.68	0.68	0.68	0.68
4) ptmd_sal_gt_1	0.18	0.20	0.19	0.19	0.18	0.20	0.19	0.19	0.18	0.18
5) ptmd_si_pt_5	0.34	0.33	0.31	0.31	0.34	0.33	0.31	0.31	0.38	0.38
6) ptmd_si_pt_5_shallow_ebb_t_gt_12	0.77	0.79	0.76	0.76	0.77	0.79	0.76	0.76	0.75	0.75
7) ptmd_sal_gt_1_si_pt_5	0.34	0.33	0.30	0.31	0.34	0.33	0.30	0.31	0.37	0.37
8) ptmd_sal_gt_1_h8_ebb_shallow_t_gt_18_acclim	0.67	0.71	0.67	0.67	0.67	0.71	0.67	0.67	0.64	0.64
9) tmd_sal_gt_1_ebb_shallow_t_gt_18	0.17	0.19	0.17	0.17	0.17	0.19	0.17	0.17	0.17	0.17
10) tmd_sal_gt_1_ptmd_prtmd_sd_pt_1_switch	0.33	0.32	0.31	0.31	0.33	0.32	0.31	0.31	0.34	0.34
CVP Salvage										
1) passive	0.01	0.01	0.01	0.01	0.01	0.01	0.01	0.01	0.01	0.01
2) turbidity_seeking	0.03	0.03	0.03	0.03	0.03	0.03	0.03	0.03	0.03	0.03
3) tmd	0.03	0.03	0.03	0.03	0.03	0.03	0.03	0.03	0.03	0.03
4) ptmd_sal_gt_1	0.01	0.01	0.01	0.01	0.01	0.01	0.01	0.00	0.01	0.00
5) ptmd_si_pt_5	0.01	0.01	0.01	0.01	0.01	0.01	0.01	0.01	0.01	0.01
6) ptmd_si_pt_5_shallow_ebb_t_gt_12	0.01	0.01	0.01	0.01	0.01	0.01	0.01	0.01	0.01	0.01
7) ptmd_sal_gt_1_si_pt_5	0.01	0.01	0.01	0.01	0.01	0.01	0.00	0.01	0.01	0.00
8) ptmd_sal_gt_1_h8_ebb_shallow_t_gt_18_acclim	0.01	0.01	0.01	0.01	0.01	0.01	0.01	0.01	0.01	0.01
9) tmd_sal_gt_1_ebb_shallow_t_gt_18	0.01	0.01	0.01	0.01	0.01	0.01	0.01	0.01	0.01	0.01
10) tmd_sal_gt_1_ptmd_prtmd_sd_pt_1_switch	0.01	0.01	0.01	0.01	0.02	0.02	0.02	0.02	0.01	0.02
SWP Salvage										
1) passive	#DIV/0!	#DIV/0!	#DIV/0!	#DIV/0!	#DIV/0!	#DIV/0!	#DIV/0!	#DIV/0!	#DIV/0!	#DIV/0!
2) turbidity_seeking	#DIV/0!	#DIV/0!	#DIV/0!	#DIV/0!	#DIV/0!	#DIV/0!	#DIV/0!	#DIV/0!	#DIV/0!	#DIV/0!
3) tmd	#DIV/0!	#DIV/0!	#DIV/0!	#DIV/0!	#DIV/0!	#DIV/0!	#DIV/0!	#DIV/0!	#DIV/0!	#DIV/0!
4) ptmd_sal_gt_1	#DIV/0!	#DIV/0!	#DIV/0!	#DIV/0!	#DIV/0!	#DIV/0!	#DIV/0!	#DIV/0!	#DIV/0!	#DIV/0!
5) ptmd_si_pt_5	#DIV/0!	#DIV/0!	#DIV/0!	#DIV/0!	#DIV/0!	#DIV/0!	#DIV/0!	#DIV/0!	#DIV/0!	#DIV/0!
6) ptmd_si_pt_5_shallow_ebb_t_gt_12	#DIV/0!	#DIV/0!	#DIV/0!	#DIV/0!	#DIV/0!	#DIV/0!	#DIV/0!	#DIV/0!	#DIV/0!	#DIV/0!
7) ptmd_sal_gt_1_si_pt_5	#DIV/0!	#DIV/0!	#DIV/0!	#DIV/0!	#DIV/0!	#DIV/0!	#DIV/0!	#DIV/0!	#DIV/0!	#DIV/0!
8) ptmd_sal_gt_1_h8_ebb_shallow_t_gt_18_acclim	#DIV/0!	#DIV/0!	#DIV/0!	#DIV/0!	#DIV/0!	#DIV/0!	#DIV/0!	#DIV/0!	#DIV/0!	#DIV/0!
9) tmd_sal_gt_1_ebb_shallow_t_gt_18	#DIV/0!	#DIV/0!	#DIV/0!	#DIV/0!	#DIV/0!	#DIV/0!	#DIV/0!	#DIV/0!	#DIV/0!	#DIV/0!
10) tmd_sal_gt_1_ptmd_prtmd_sd_pt_1_switch	#DIV/0!	#DIV/0!	#DIV/0!	#DIV/0!	#DIV/0!	#DIV/0!	#DIV/0!	#DIV/0!	#DIV/0!	#DIV/0!

Table A1. Con't.

j) 2D WY 2011 negative binomial error in SKT data ($\tau=10$)

Population model number	1	2	3	4	5	6	7	8	9	10
Salvage efficiency structure	const	const	const	const	~turb	~turb	~turb	~turb	const	~turb
Natural survival structure	S _c	S _{SKT}	S _a	S _w	S _c	S _{SKT}	S _a	S _w	S _a	S _a
SKT efficiency structure (θ_{c-SKT})	=1	=1	=1	=1	=1	=1	=1	=1	~Secchi	~Secchi
FMWT relative catch across regions										
1) passive	0.95	0.95	0.95	0.95	0.95	0.95	0.95	0.95	0.94	0.92
2) turbidity_seeking	0.90	0.90	0.90	0.90	0.90	0.90	0.90	0.90	0.87	0.86
3) tmd	0.97	0.97	1.00	0.97	0.97	0.97	0.97	0.97	0.97	0.97
4) ptmd_sal_gt_1	0.86	0.87	0.87	0.87	0.86	0.87	0.87	0.87	0.86	0.86
5) ptmd_si_pt_5	0.87	0.87	0.87	0.87	0.87	0.87	0.87	0.87	0.89	0.89
6) ptmd_si_pt_5_shallow_ebb_t_gt_12	0.90	0.90	0.90	0.90	0.90	0.91	0.99	0.91	0.91	0.90
7) ptmd_sal_gt_1_si_pt_5	0.84	0.84	0.84	0.85	0.84	0.84	0.84	0.84	0.83	0.87
8) ptmd_sal_gt_1_h8_ebb_shallow_t_gt_18_acclim	0.91	0.91	0.91	0.91	0.91	0.91	0.91	0.91	0.92	0.92
9) tmd_sal_gt_1_ebb_shallow_t_gt_18	0.84	0.84	0.84	0.84	0.84	0.84	0.84	0.84	0.84	0.90
10) tmd_sal_gt_1_ptmd_prtmd_sd_pt_1_switch	0.94	0.94	0.97	0.94	0.94	0.94	0.94	0.94	0.94	0.94
SKT catch by survey and region										
1) passive	0.63	0.63	0.62	0.62	0.63	0.63	0.62	0.62	0.57	0.61
2) turbidity_seeking	0.00	0.00	0.00	0.00	0.00	0.00	0.00	0.00	0.00	0.00
3) tmd	0.41	0.41	#DIV/0!	0.41	0.41	0.41	0.37	0.41	0.37	0.37
4) ptmd_sal_gt_1	0.07	0.08	0.07	0.07	0.07	0.08	0.07	0.07	0.07	0.07
5) ptmd_si_pt_5	0.23	0.23	0.23	0.23	0.23	0.23	0.23	0.23	0.19	0.21
6) ptmd_si_pt_5_shallow_ebb_t_gt_12	0.39	0.40	0.40	0.39	0.39	0.40	0.23	0.40	0.34	0.32
7) ptmd_sal_gt_1_si_pt_5	0.23	0.23	0.23	0.20	0.23	0.23	0.23	0.23	0.18	0.18
8) ptmd_sal_gt_1_h8_ebb_shallow_t_gt_18_acclim	0.30	0.32	0.30	0.30	0.30	0.32	0.30	0.30	0.30	0.30
9) tmd_sal_gt_1_ebb_shallow_t_gt_18	0.07	0.07	0.07	0.07	0.07	0.07	0.07	0.07	0.07	0.06
10) tmd_sal_gt_1_ptmd_prtmd_sd_pt_1_switch	0.21	0.19	0.04	0.20	0.21	0.19	0.20	0.19	0.21	0.21
CVP Salvage										
1) passive	0.01	0.01	0.01	0.01	0.01	0.01	0.01	0.01	0.01	0.01
2) turbidity_seeking	0.03	0.03	0.03	0.03	0.03	0.03	0.03	0.03	0.03	0.03
3) tmd	0.02	0.02	0.00	0.02	0.02	0.02	0.02	0.02	0.02	0.02
4) ptmd_sal_gt_1	0.01	0.01	0.01	0.01	0.01	0.01	0.00	0.00	0.01	0.00
5) ptmd_si_pt_5	0.01	0.01	0.01	0.01	0.01	0.01	0.01	0.01	0.01	0.01
6) ptmd_si_pt_5_shallow_ebb_t_gt_12	0.01	0.01	0.01	0.01	0.01	0.01	0.01	0.01	0.01	0.01
7) ptmd_sal_gt_1_si_pt_5	0.01	0.01	0.01	0.01	0.01	0.01	0.01	0.01	0.01	0.01
8) ptmd_sal_gt_1_h8_ebb_shallow_t_gt_18_acclim	0.01	0.01	0.01	0.01	0.01	0.01	0.01	0.01	0.01	0.01
9) tmd_sal_gt_1_ebb_shallow_t_gt_18	0.01	0.01	0.01	0.01	0.01	0.01	0.01	0.01	0.01	0.00
10) tmd_sal_gt_1_ptmd_prtmd_sd_pt_1_switch	0.01	0.01	0.01	0.01	0.01	0.01	0.01	0.01	0.01	0.01
SWP Salvage										
1) passive	#DIV/0!	#DIV/0!	#DIV/0!	#DIV/0!	#DIV/0!	#DIV/0!	#DIV/0!	#DIV/0!	#DIV/0!	#DIV/0!
2) turbidity_seeking	#DIV/0!	#DIV/0!	#DIV/0!	#DIV/0!	#DIV/0!	#DIV/0!	#DIV/0!	#DIV/0!	#DIV/0!	#DIV/0!
3) tmd	#DIV/0!	#DIV/0!	#DIV/0!	#DIV/0!	#DIV/0!	#DIV/0!	#DIV/0!	#DIV/0!	#DIV/0!	#DIV/0!
4) ptmd_sal_gt_1	#DIV/0!	#DIV/0!	#DIV/0!	#DIV/0!	#DIV/0!	#DIV/0!	#DIV/0!	#DIV/0!	#DIV/0!	#DIV/0!
5) ptmd_si_pt_5	#DIV/0!	#DIV/0!	#DIV/0!	#DIV/0!	#DIV/0!	#DIV/0!	#DIV/0!	#DIV/0!	#DIV/0!	#DIV/0!
6) ptmd_si_pt_5_shallow_ebb_t_gt_12	#DIV/0!	#DIV/0!	#DIV/0!	#DIV/0!	#DIV/0!	#DIV/0!	#DIV/0!	#DIV/0!	#DIV/0!	#DIV/0!
7) ptmd_sal_gt_1_si_pt_5	#DIV/0!	#DIV/0!	#DIV/0!	#DIV/0!	#DIV/0!	#DIV/0!	#DIV/0!	#DIV/0!	#DIV/0!	#DIV/0!
8) ptmd_sal_gt_1_h8_ebb_shallow_t_gt_18_acclim	#DIV/0!	#DIV/0!	#DIV/0!	#DIV/0!	#DIV/0!	#DIV/0!	#DIV/0!	#DIV/0!	#DIV/0!	#DIV/0!
9) tmd_sal_gt_1_ebb_shallow_t_gt_18	#DIV/0!	#DIV/0!	#DIV/0!	#DIV/0!	#DIV/0!	#DIV/0!	#DIV/0!	#DIV/0!	#DIV/0!	#DIV/0!
10) tmd_sal_gt_1_ptmd_prtmd_sd_pt_1_switch	#DIV/0!	#DIV/0!	#DIV/0!	#DIV/0!	#DIV/0!	#DIV/0!	#DIV/0!	#DIV/0!	#DIV/0!	#DIV/0!